Synthesis and Reactivity of Group 10 Silyl Pincer Complexes

by

Samuel J. Mitton

Submitted in partial fulfilment of the requirements
for the degree of Doctor of Philosophy

at

Dalhousie University
Halifax, Nova Scotia
August 2013

Table of Contents

List of Tables

List of Figures

List of Schemes

Abstract

In an effort to explore new metal mediated reactivity and further the versatility of metal pincer chemistry, research in the Turculet group has targeted the synthesis of novel bis(phosphino)silyl PSiP pincer complexes. In this context, the synthesis and reactivity of Group 10 complexes featuring [Cy-PSiP] ([Cy-PSiP] = [κ^3-(2-$Cy_2PC_6H_4)_2SiMe]^-$) ligation is described herein. The central silyl donor is anticipated to promote the formation of electron rich metal species capable of diverse and challenging reactivity.

In the course of this work, it was found that [Cy-PSiP] ligation supports the synthesis of square planar Pt^{II} alkyl complexes that can mediate Si-H and Si-Cl bond cleavage chemistry. A cationic Pt^{II} species was accessed by treatment of [Cy-PSiP]PtMe with $B(C_6F_5)_3$. The latter complex underwent B-C bond cleavage in the $[MeB(C_6F_5)_3]^-$ counteranion to produce [Cy-PSiP]Pt(C_6F_5). Examples of Si-C bond cleavage reactions at Pt^0 and Pt^{II} centers were also observed. Related alkyl complexes of Ni and Pd were observed to undergo rearrangement processes involving net Si-C(sp^2) and Si-C(sp^3) bond cleavage. In the case of Ni these Si-C bond cleavage steps are reversible on the NMR timescale. Attempts to prepare a terminal hydride complex of the type [Cy-PSiP]MH (M = Pd, Pt) resulted in the isolation of η^2-Si-H coordination complexes of the type [Cy-P*Si*(μ-H)P]*M*, which were shown to undergo insertion of CO_2 to form the corresponding formate species. In the presence of $B(C_6F_5)_3$, these η^2-Si-H complexes were capable of mediating the catalytic reduction of CO_2 to CH_4 using hydrosilanes as the reducing agent.

The synthesis and characterization of terminal, monomeric Pt hydroxide and alkoxide complexes of the type [Cy-PSiP]Pt(OR) (R= H, Ph, ^{t}Bu) was achieved, and these complexes were shown to readily deprotonate relatively acidic C-H bonds in phenylacetylene and acetonitrile. A rare example of hydrogenolysis of the Pt-OR linkage with H_2 was documented, as was an unusual example of Si-H addition across the Pt-OR bond to form Pt silyl species. While terminal anilido Pt complexes of the type [Cy-PSiP]Pt(NHAr) (Ar = Ph, 2,6-$Me_2C_6H_3$, 2,6-$^i Pr_2C_6H_3$) proved readily isolable, related Ni and Pd anilido species underwent rearrangement processes similar to those observed in their alkyl analogues. Terminal phosphido complexes supported by [Cy-PSiP] ligation were successfully isolated and characterized for all Group 10 metals. Lastly, the Pt and Pd coordination chemistry of a new PSiN pincer derivative was explored, and the amino donor arm of this pincer ligand was demonstrated to exhibit hemilabile coordination to the metal center.

List of Abbreviations and Symbols Used

acac = acetylacetonate
Anal. Calcd = Analysis Calculated
BDE = Bond Dissociation Energy
BQA = 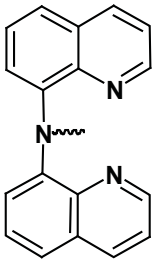

br = broad
COD = 1,5-cyclooctadiene
COSY = Homonuclear Shift *CO*rrelation *S*pectroscop*Y*
Cp = Cyclopentadienyl
Cp* = Pentamethylcyclopentadienyl
[Cy-PSiP] = 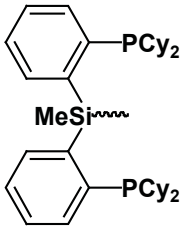

d = doublet
δ = chemical shift
dba = dibenzylideneacetone
DEPT = *D*istortionless *E*nhancement by *P*olarization *T*ransfer
dppe = 1,2-bis(diphenylphosphino)ethane
η = indicator of hapticity in π-bonding ligands
E = main group element
equiv = equivalents
EXAFS = *E*xtended *X*-ray *A*bsorption *F*ine *S*tructure
EXSY = *EX*change *S*pectroscop*Y*
h = hour
HMBC = *H*eteronuclear *M*ultiple *B*ond *C*orrelation
HSQC = *H*eteronuclear *S*ingle *Q*uantum *C*orrelation
IR = infrared
$^{n}J_{XX`}$ = n bond coupling constant between atom X and atom X`
κ = indicator of hapticity in σ-bonding ligands
L = neutral two electron donor ligand
μ = descriptor for a bridging ligand
m = multiplet

m = meta
M = generic transition metal *or* mol/L
mer = meridional
Mes = 2,4,6-trimethylphenyl
min = minutes
NMR = *N*uclear *M*agnetic *R*esonance
NSiN =

o = ortho
ORTEP = Oak Ridge Thermal Ellipsoid Plot
OTf = trifluoromethanesulfonate (triflate)
p = para
PCN =

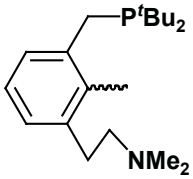

ppm = parts per million
[Ph-PSiP] =

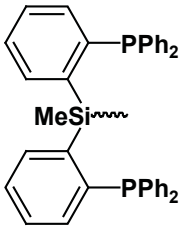

PNP =

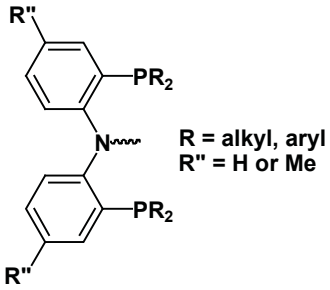

s = singlet
t = triplet
THF = tetrahydrofuran
TOF = Turn Over Frequency

TON = Turn Over Number
X = anionic donor ligand

Acknowledgments

The completion of a thesis is not done alone, and this one is no exception. I would first like to thank my supervisor Dr. Laura Turculet for her help and support throughout this process, not only in the preparation of this document but throughout my graduate studies. Her insights and guidance have been invaluable over the last five years. Working in her lab has been a privilege and has allowed me to grow as a chemist perhaps more than I thought possible. Thank you Laura, I appreciate it.

I would like to thank my supervisory committee, Drs. Jean Burnell, Jim Pincock and Mark Stradiotto for their support and guidance throughout my studies. Mike Lumsden and Kathy Robertson have been extremely helpful with various NMR experiments, and for this I am very thankful. I would also like to thank Drs. Robert McDonald and Mike Ferguson from the University of Alberta for X-ray crystallography experiments reported in this thesis. Further, the staff of the department of chemistry at Dalhousie University also need to be thanked for helping me with various problems I have encountered, both mechanical and logistical.

A big thank you to the Turculet group members (past and present) over the years. In particular, Erin Morgan for being a partner in crime from the beginning of this process to nearly the end, Morgan MacInnis for his guidance, insight and friendship, as well as Adam Ruddy for his humor and thoughts as well. Very special thank you to the Stradiotto group (past and present) for very helpful conversations and also allowing me to borrow seemingly anything from their lab.

Over the completion of my degree I have made several friends outside of the department who have helped me broaden my horizons, introduced me to several of my hobbies and have shown me the importance of a life outside the lab. While there are too many to name here, each has been very near and dear to me.

My family has always supported me troughout all of my endeavers, my graduate studies included. Without them I would have certainly not made it through this process, and for this and a million other reasons I continue to love them always. Erica Zirpolo also deserves a very special mention here. For a little over two years now she has helped me in so many ways. Her infinite support and care mean everything to me. Thank you.

CHAPTER 1: Introduction

1.1 Overview

The combination of an appropriately designed ancillary ligand set with a given transition metal can lead to highly reactive complexes that are able to facilitate challenging chemical reactions either stoichiometrically or catalytically. The importance of homogeneous transition metal complexes as catalysts in industrially relevant processes cannot be understated.[1] Of note are processes for the synthesis of commodity chemicals such as acetic acid, the majority of which is produced industrially via the carbonylation of methanol using a Rh-based (Monsanto process) or Ir-based catalyst.[1,2] Advances in homogeneous transition metal chemistry have also led to the development of new atom economical and/or highly selective synthetic transformations that are applicable to the synthesis of fine chemicals and pharmaceuticals, such as the catalytic cross-coupling of arenes,[3] and the asymmetric hydrogenation of alkenes.[4] To underscore the importance of transition metal catalysis, breakthroughs in asymmetric catalysis,[4-6] olefin metathesis,[7] and palladium-catalyzed cross coupling[8] were awarded the 2001, 2005, and 2010 Nobel Prize in Chemistry, respectively. Such advancements in synthetic methodology are rooted in fundamental research into transition metal chemistry and reactivity. In particular, investigations into the structure, bonding and stoichiometric reactivity of new transition metal complexes are essential to improving on known metal-catalyzed processes or discovering entirely new reactivity.

In this context, this thesis involves the synthesis and study of new Group 10 (Ni, Pd and Pt) transition metal silyl pincer complexes, with the goal of discovering highly reactive complexes that can mediate challenging bond cleavage reactions (e.g., C-H, N-

H, etc.) that are otherwise difficult to achieve under mild conditions. The long term goal of this work is to incorporate such reactivity into productive catalytic cycles. These studies build on the well-established role of Group 10 metal complexes as catalysts for reactions that involve E-H (E = main group element, e.g. C, Si) bond cleavage steps.[9] As ancillary ligand effects are known to play an important role in the structure and function of transition metal complexes, the ability of silyl pincer ligation to support unusual bonding and coordination geometries at the metal center was explored in this work, with the consideration that this may in turn lead to enhanced reactivity properties. Tuning of both the steric and electronic properties of the ancillary pincer ligand is anticipated to have a pronounced effect on the chemistry of the ensuing complexes.

In order to place this thesis into context, a brief introduction to the utility of Group 10 transition metal complexes in synthesis as well as a survey of recent advances in Group 10 metal pincer chemistry are provided in the following sections. In particular, Group 10 metal mediated C-H bond cleavage reactions are described, as are examples of unusual complexes supported by pincer ligation such as a terminal Pt oxo complex. Previous work involving silyl pincer-type ligation in Group 10 metal coordination chemistry will also be highlighted.

1.2 The Utility of Group 10 Metal Complexes in Synthesis

Transition metal complexes featuring Group 10 transition metals (Ni, Pd, Pt) have been shown to be useful catalysts for the synthesis of important organic targets. Their utility in C-C and C-N cross coupling catalysis,[3] as well as in catalyzing the hydrosilylation of unsaturated substrates[9c,9d] are well documented. In addition to these

processes, a reaction of particular note for platinum is the cleavage of C-H bonds in unactivated hydrocarbons such as benzene and alkanes.[9e-g] This reactivity holds tremendous promise for the selective functionalization of such unreactive substrates under relatively mild conditions and represents a central area of research in organometallic chemistry. Significant excitement about the role of platinum in such C-H bond cleavage chemistry came about due to the demonstration by Shilov and co-workers in the late 1960's of the catalytic conversion of methane to methanol and/or chloromethane mediated by platinum salts in aqueous solution (Scheme 1-1).[10] Unfortunately, the utility of this methane oxidation reaction was limited due to the high cost of the required stoichiometric oxidant $PtCl_6^{2-}$. Despite this drawback, this pioneering work established platinum organometallic complexes as key players in the development of hydrocarbon C-H bond cleavage chemistry. Organometallic platinum complexes have also found tremendous application in Si-H bond cleavage processes, namely as catalysts for alkene hydrosilylation reactions.[9c,d] Initial work by Speier and co-workers in the late 1950's showed that chloroplatinic acid (H_2PtCl_6) is a very active catalyst for alkene hydrosilylation.[11] Subsequently, the more active Karstedt's catalyst was developed by the reaction of divinyltetramethyldisiloxane with H_2PtCl_6 to form predominantly a Pt^0 complex of the type $Pt_2\{[(CH_2{=}CH)Me_2Si]_2O\}_3$ that is thought to contain both bridging and chelating divinyl ligands.[12]

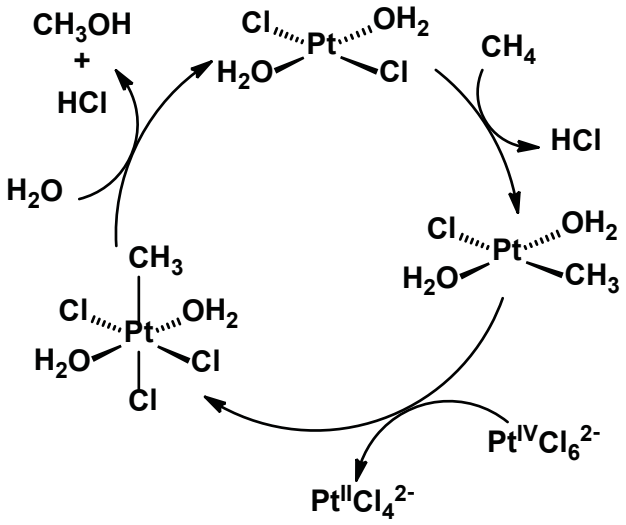

Scheme 1-1. Mechanism of catalytic methane oxidation to methanol in the Shilov system.

Palladium based catalysts have found numerous application in synthesis, particularly in the areas of C-C and C-N cross coupling.[3] Palladium catalyzed C-C cross coupling reactions such as Suzuki, Negishi, and Stille coupling reactions have become an essential tool in the cost-effective synthesis of pharmaceuticals, agrochemicals and other fine chemicals (Scheme 1-2).[13] The palladium catalyzed synthesis of amines via C-N cross coupling has also evolved as a reaction of tremendous utility in commercially important syntheses. Also known as Buchwald-Hartwig amination, this reaction features the coupling of a primary or secondary amine and an aryl halide in the presence of a base to form a C-N bond, with palladium acting as the catalytically active metal center in the presence of various phosphine-based ligands (Scheme 1-2).[14] Ligand modifications have led to the development of increasingly reactive and chemoselective catalysts for this amination reaction, including the development of catalyst systems that allow for the selective synthesis of primary aryl amines via the coupling of ammonia with aryl

halides.[15] This evolution emphasizes the importance of ligand design in the pursuit of unprecedented reactivity and selectivity.

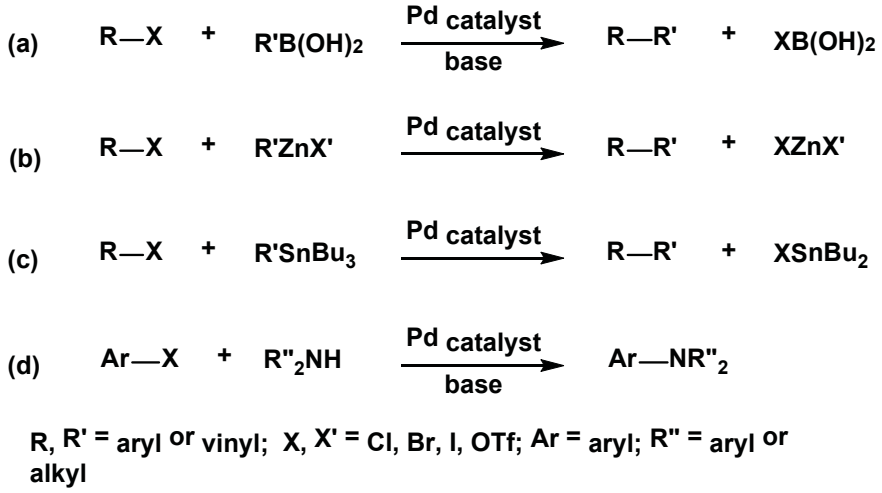

Scheme 1-2. Pd-catalyzed C-C and C-N coupling reactions: (a) Suzuki coupling; (b) Negishi coupling; (c) Stille coupling; and (d) Buchwald-Hartwig coupling.

The utility of organometallic nickel complexes in synthesis stems largely from the relatively lower cost of nickel as compared with palladium and platinum. As such, there is interest in developing Ni-catalyzed reactions that parallel related processes catalyzed by precious metals such as Pt and especially Pd. In this context, versions of many catalytic C-C cross-coupling processes feature organometallic Ni catalysts, including reactions such as Negishi, Kumada, and Suzuki couplings.[16,17] Industrially, organometallic Ni complexes are utilized as catalysts for two noteworthy processes: (i) the hydrocyanation of butadiene to form adiponitrile (Scheme 1-3), which is a key intermediate in the synthesis of nylon-6,6; and (ii) the oligomerization of ethylene to produce 1-alkenes of various lengths (e.g. C6 – C20) via the Shell higher-olefins process (SHOP; Scheme 1-3).[1,18]

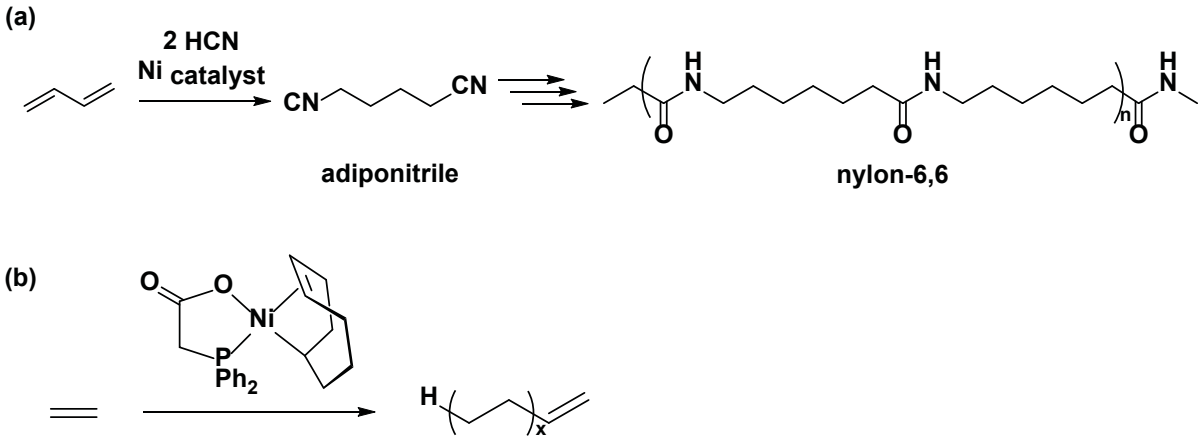

Scheme 1-3. Industrially relevant applications of organometallic Ni catalysts: (a) hydrocyanation of butadiene to adiponitrile for the synthesis of nylon-6,6; and (b) oligomerization of ethylene via the Shell higher-olefins process (SHOP).

1.3 Pincer-Type Ancillary Ligand Design for Tuning Transition Metal Reactivity

Ancillary ligand(s) can significantly influence the reactivity properties of a metal center via steric and electronic effects. As such, careful consideration and design must be implemented in choosing an ancillary ligand set for a particular application. With this in mind, typical ancillary ligand designs are most useful when they are modular, such that the ligand is easily altered in order to fine tune the reactive properties of the metal center. Furthermore, ancillary ligands should provide a stable platform to support reactive metal centers, all the while remaining intact during the course of reactivity even under harsh conditions.

In this regard, transition metal complexes supported by pincer-type ancillary ligands have been the subject of intense research in recent years,[19,20] owing to the remarkable stoichiometric and catalytic reactivity exhibited by such complexes, including

the first examples of Ir-catalyzed alkane dehydrogenation,[21] as well as the discovery of the Ru-catalyzed direct synthesis of amides from alcohols and amines.[22] Having the general form LXL (L = neutral donor; X = anionic donor), pincers are tridentate chelating ligands whose three donors atoms are linked by an organic backbone (Figure 1-1). Such ligands typically coordinate to a metal center in a *mer*-type configuration, and it has been demonstrated that due to their relatively rigid chelating framework, the ensuing metal pincer complexes exhibit relatively high thermal stability.[21] Thus, complexes such as [2,6-(^{t}Bu$_2$PCH$_2$)$_2$C$_6$H$_3$]Ir(H)Cl and [2,6-(^{t}Bu$_2$PCH$_2$)$_2$C$_6$H$_3$]Rh(H)Cl were found to sublime at 245–350 and 180–200 °C, respectively, without decomposition.[23b]

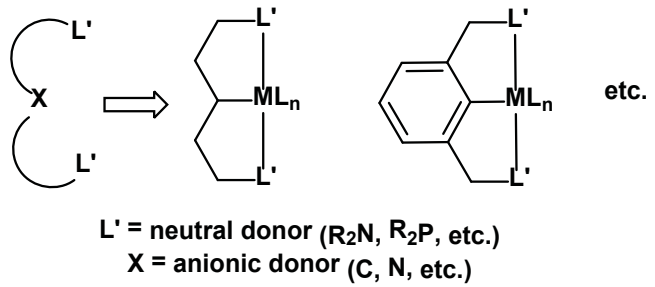

Figure 1-1. General form of pincer complexes and examples of LCL pincer coordination to a metal center.

Pincer ligation originated in the 1970's when Shaw and co-workers pioneered the synthesis of PCP-type pincer complexes of Rh, Ir, Pd and Pt via chelate-assisted C-H bond activation.[23] The peripheral phosphine donors of the pincer ligand can bind to the metal center, thus forcing an electronically and coordinatively unsaturated metal center in proximity to a C-H bond that can undergo a subsequent intramolecular C-H bond cleavage reaction to form the desired PCP-type pincer complex (Scheme 1-4). Since

these initial studies by Shaw and co-workers, pincers have evolved as useful ancillary ligands capable of supporting unusual and highly reactive transition metal complexes.

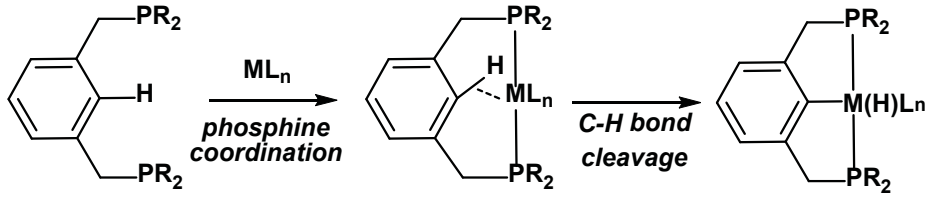

Scheme 1-4. Metalation of PCP-type pincer ligand precursors to a low-valent metal center via intramolecular C-H bond cleavage.

A large factor responsible for the utility of pincer-type ligands is their highly modular design. Several modification sites are readily accessible for fine tuning the properties of the ensuing pincer metal complexes. As such, the steric bulk can be easily altered by changing the substituents found on the peripheral neutral donors. Also, the rigidity of the backbone can be varied by substituting an aliphatic backbone for a more rigid aromatic linker. The choice of ligand backbone can also affect the electronic properties of the ensuing metal complex, as an aliphatic linker renders the donor atoms more electron donating, whereas an aromatic backbone can have an electron withdrawing effect.[20c] The identity of the donor atoms themselves also represents a point for modification of the pincer ligand. Both hard (e.g. amine) and soft (e.g. phosphine, thioether, N-heterocyclic carbene) neutral donors have been utilized in pincer ligands thus providing accommodation for a variety of transition metals in a range of oxidation states.[19,20] Besides providing steric protection, the substituents on these neutral donors are also capable of affecting the electronic properties of the metal center. Thus, alkyl substituents lead to increased electron donation to the metal center, whereas aromatic

substituents and substituents that feature electronegative atoms have an electron withdrawing effect.

With respect to the central anionic donor, the majority of research conducted with pincer complexes involves complexes where this donor is either carbon-[20a-c] or nitrogen-based.[20d] The design of ligands containing alternate central anionic donors has been relatively limited by comparison (*vide infra*). However, such modification can have a drastic effect on the electronic properties of the metal center and the structure of the ensuing complexes, depending on factors such as the electron releasing character of the central donor atom, the availability of additional lone pairs for π-bonding, and the *trans*-directing properties of the central donor relative to other ligands in the metal coordination sphere. In this context, a novel Ir pincer complex with a highly unusual central boryl donor was recently reported by Yamashita and co-workers.[24] The coordination of the strongly σ-donating boryl group in a PBP-type tridentate framework was achieved through metal mediated B-H bond cleavage. The work of Yamashita and co-workers follows extensive recent reports from the Turculet group involving the development and use of novel PSiP-type pincer ligands that feature a central silyl donor.[25] This thesis is focused on the chemistry of Group 10 metal complexes supported by such silyl pincer ligation.

1.4 Reactivity of Group 10 Metal Pincer Complexes

Most of the research reported to date involving Group 10 pincer complexes features pincer frameworks that contain an anionic carbon or nitrogen donor in the central position. Such complexes have been used to achieve challenging bond cleavage

processes such as C-H bond cleavage, as well as for the synthesis of unusual new coordination complexes that feature novel bonding motifs. Highlights from the recent literature featuring Group 10 metal pincer complexes are summarized below.

1.4.1 Pt^{II} Pincer complexes for arene C-H bond activation

The selective cleavage and functionalization of hydrocarbon C-H bonds is a long-standing goal in organometallic chemistry.[9e,26] Hydrocarbons are typically unreactive under standard reaction conditions, and reactions that do occur under harsh conditions (e.g. radical reactions at elevated temperatures) are typically not selective enough to be practical. Milder and more selective methodologies that utilize such an abundant and relatively inexpensive resource in a more efficient manner are thus highly desirable.

Electron-rich, coordinatively unsaturated late transition metal complexes have been documented to react with hydrocarbon substrates under relatively mild conditions to selectively cleave C-H bonds.[9e-g,21,26] However, the subsequent functionalization of such C-H bond activation products remains a challenging problem. One of the few examples of catalytic C-H bond functionalization is the previously mentioned Shilov system for methane oxidation (*vide supra*).[10] However, this process is not industrially viable, and as such significant effort is being dedicated to the discovery of alternative late metal complexes that can mediate the cleavage of C-H bonds and potentially the subsequent functionalization of the alkyl fragment. Due to the Shilov precedent, a large portion of these efforts are focused on Pt^{II} systems, and in recent years there has been increasing interest in the C-H bond activation profile of Pt^{II} complexes supported by chelating ancillary ligands.[9f]

In this context, two examples of Pt^{II} pincer complexes that can undergo arene C-H bond cleavage reactions have been reported recently.[27,28] A potential advantage of such pincer-mediated C-H bond activation chemistry is the well-documented thermal stability of pincer complexes,[21] which might prove advantageous for carrying out subsequent functionalization reactions. Peters and co-workers sought to use a thermally robust NNN-type Pt pincer system in order to cleave the C-H bonds of benzene.[27] A series of square planar Pt^{II} complexes supported by the bis(8-quinolinyl)amido ligand (BQA) were prepared and characterized, including (BQA)PtCl and (BQA)Pt(OTf) (Figure1-2).

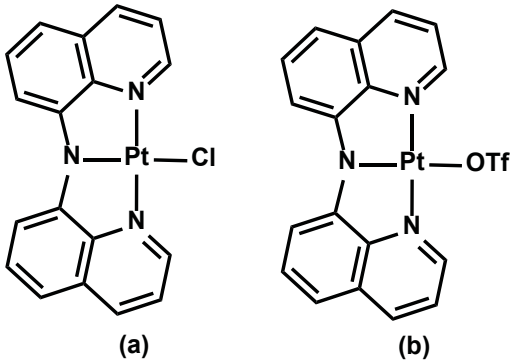

Figure 1-2. (BQA)Pt^{II} complexes reported by Peters and co-workers: (a) (BQA)PtCl; and (b) (BQA)Pt(OTf).

While heating of either (BQA)PtCl or (BQA)PtOTf at 150 °C in benzene solution did not produce a reaction, heating a benzene solution of the triflate complex at 150 °C in the presence of one equiv of N^iPr_2Et led to precipitation of $[HN^iPr_2Et][OTf]$ and ca. 90% (^{1}H NMR) conversion to the corresponding phenyl complex (BQA)PtPh (Scheme 1-5). By comparison, the chloride complex did not react with benzene even when heated in the presence of N^iPr_2Et.

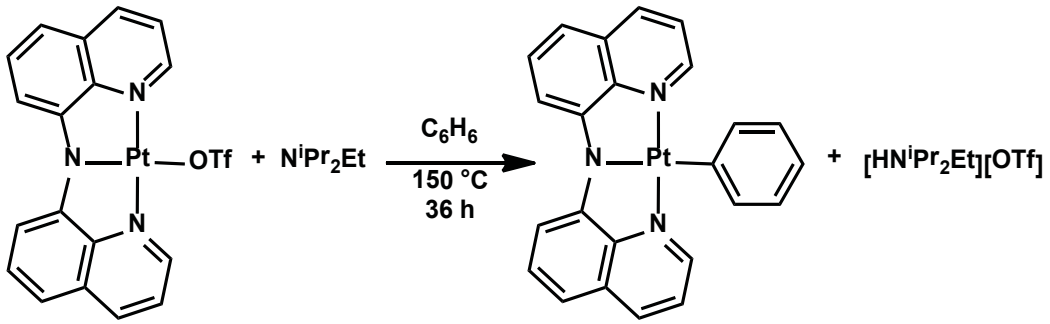

Scheme 1-5. Benzene C-H bond cleavage by (BQA)PtOTf to give (BQA)PtPh.

It is proposed that the heightened reactivity of (BQA)PtOTf relative to (BQA)PtCl is due to the enhanced ability of the triflate ligand as a leaving group. In this regard, the proposed reaction pathway that is preferred by Peters and co-workers involves associative displacement of the triflate ligand from the metal coordination sphere by a benzene C-H bond (Scheme 1-6). Subsequent oxidative addition of the C-H bond to the Pt center leads to the formation of a Pt^{IV} aryl hydride complex, which is then deprotonated by the N^{i}Pr$_2$Et base. Although no mechanistic studies were conducted to evaluate this proposed mechanism, this pathway is consistent with previous studies into the mechanism of C-H bond cleavage by Pt^{II}, which all indicate that at least one labile ligand in the Pt coordination sphere is necessary in order to allow for coordination of the C-H bond to the Pt center prior to the C-H bond cleavage step.

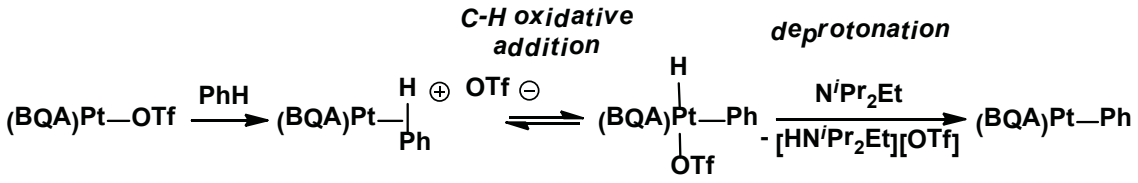

Scheme 1-6. Proposed mechanistic pathway for benzene C-H bond cleavage by (BQA)Pt(OTf).

A second related example of Pt pincer mediated C-H bond cleavage was recently reported by Liang and co-workers.[28] A series of square planar Pt^{II} complexes supported by the bis(2-diphenylphosphinophenyl)amide ligand (PNP) were prepared and characterized, including (PNP)PtCl, (PNP)Pt(OTf), and (PNP)PtMe (Figure 1-3).

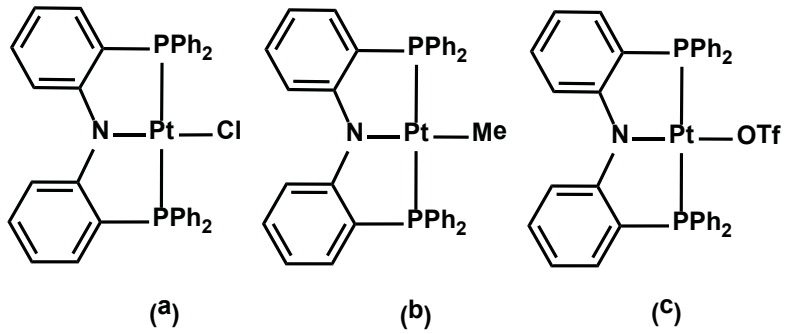

Figure 1-3. (PNP)Pt^{II} complexes reported by Liang and co-workers: (a) (PNP)PtCl; (b) (PNP)PtMe; and (c) (PNP)Pt(OTf).

The triflate complex showed significant lability of the triflate ligand, as indicated by the facile displacement of this ligand from the metal coordination sphere by either pyridine or acetonitrile. Much like the previous work from Peters and co-workers, heating a benzene solution of (PNP)PtOTf at 150 °C for 2.5 h in the presence of various of aliphatic amine bases (e.g. Et_3N) led to benzene C-H bond cleavage to form (PNP)PtPh quantitatively (^{31}P NMR, Scheme 1-7). As was previously observed by Peters

and co-workers, heating (PNP)Pt(OTf) in benzene solution in the absence of base did not lead to any observed reactivity.

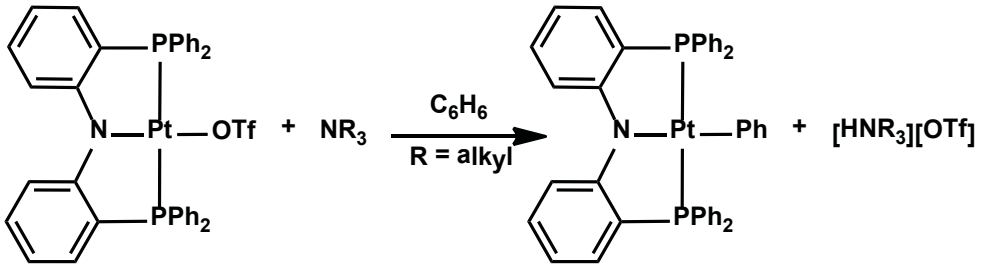

Scheme 1-7. Benzene C-H bond cleavage by (PNP)Pt(OTf).

Liang and co-workers also showed that treatment of a room temperature benzene solution of (PNP)PtMe with the strong Lewis acid $B(C_6F_5)_3$ led to the quantitative formation of (PNP)PtPh over the course of 31 h (Scheme 1-8). As $B(C_6F_5)_3$ mediated alkyl abstraction from transition metal alkyl complexes is well-precedented, it is likely that the reaction of (PNP)PtMe with this Lewis acid generates a highly reactive, coordinatively unsaturated intermediate of the type $[(PNP)Pt]^+$ that can readily coordinate a benzene C-H bond and undergo subsequent oxidative addition.

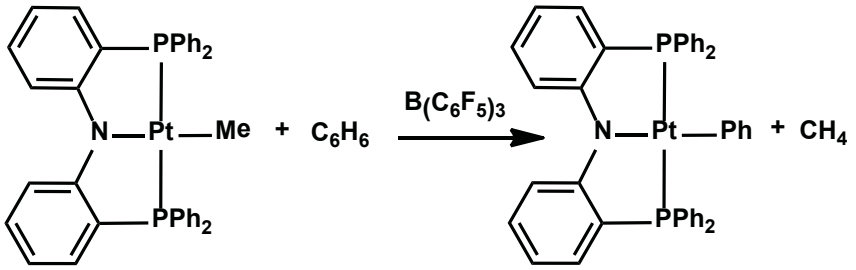

Scheme 1-8. Benzene C-H bond cleavage via methide abstraction from (PNP)PtMe by a strong Lewis acid.

In an effort to further explore the potential for cationic Pt species to mediate C-H bond activation chemistry, Ozerov and co workers synthesized Pt complexes supported by an isopropyl phosphino PNP derivative that also featured fluorine substitution in the *o*-phenylene backbone in order to provide a convenient ^{19}F NMR spectroscopic handle (Scheme 1-9).[29] Similar to the previous findings of Peters, a benzene solution of (^{F}PNP)Pt(OTf) undergoes slow aryl C-H bond cleavage to form the Pt aryl complex (^{F}PNP)PtPh after heating at 115 °C for seven days in the presence of NEt_3. In hopes of accessing a cationic (PNP)Pt^{II} complex, a benzene solution of (^{F}PNP)Pt(OTf) was treated with $K[B(C_6F_5)_4]$. Over the course of four days, arene C-H bond cleavage was observed, resulting in net addition of a benzene C-H bond across the Pt-N linkage to afford $[(^{F}PNHP)PtPh]^{+}[B(C_6F_5)_4]^{-}$. This unusual reaction is believed to be facilitated by the frustrated Lewis pair (FLP) character of the cationic Pt species, whereby the lone pair of the amide group in the PNP ligand backbone is orthogonal to the empty orbital at Pt, while steric bulk prevents dimerization, thus leading to a "frustrated" environment.

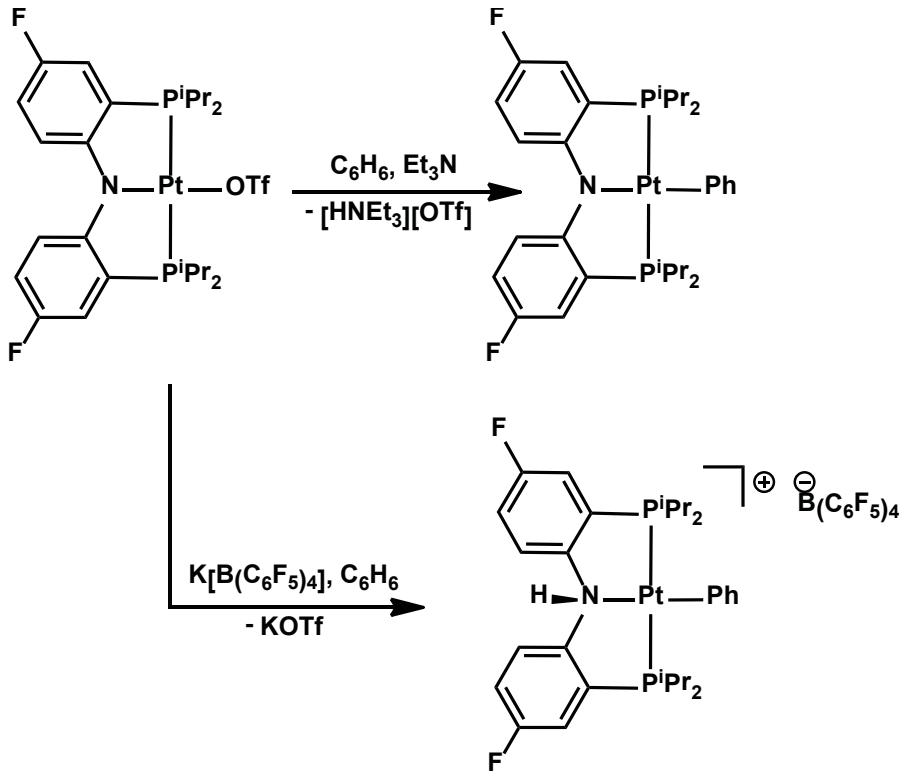

Scheme 1-9. Aryl C-H bond cleavage mediated by a cationic Pt^{II} pincer complex.

The previous work demonstrates that square planar Pt^{II} pincer complexes can readily undergo sp^2-C-H bond cleavage reactions, provided that a mechanism exits for making a coordination site available at the Pt center.[9f] This can be achieved either by taking advantage of labile ligands such as triflate, which can be readily displaced from the metal coordination sphere, or by utilizing non-coordinating anions such as $B(C_6F_5)_4^-$. Alternatively, this can also be achieved by alkyl abstraction using a strong Lewis acid such as $B(C_6F_5)_3$.

1.4.2 Synthesis and reactivity of a pincer supported Pt-oxo complex

Transition metal complexes that feature terminal oxo ligands play an important role in numerous biological and chemical processes.[30] Remarkably, very few terminal oxo metal complexes with five or more d-electrons have been isolated,[31] and of the handful of known examples, almost all are stabilized by strongly π-accepting ligands such as alkynes[32] or polytungstate ligands.[33] As the oxo ligand is a strong π-electron donor, it is thought that metal centers with five or more d-electrons cannot easily accommodate π-donation in the absence of additional π-acceptor ligands, thus leading to destabilization of the oxo ligand. However, it has been proposed that low valent oxo complexes lacking in electron withdrawing ligands may potentially exhibit interesting oxygen transfer reactivity properties.

In this regard, Milstein and co-workers recently found that reacting the cationic Pt^{II} species $(PCN)Pt^{+}$ (PCN = $C_6H_3[CH_2P(^tBu)_2][(CH_2)_2NMe_2]$) with dioxirane led to the elimination of acetone to afford a new complex formulated as a terminal, cationic Pt^{IV} oxo complex (Scheme 1-10).[34] This unusual Pt oxo complex was characterized via solution NMR experiments, as well as electrospray mass spectrometry, IR spectroscopy, and EXAFS. Density functional theory calculations were also carried out. All data and calculations proved consistent with a monomeric Pt^{IV} terminal oxo complex. Although an X-ray crystal structure of the oxo complex was not obtained, according to the calculations performed the optimized structure adopts a distorted square planar geometry with the oxygen atom being 35.3° out of the C–Pt–P plane. The calculated Pt–O bond length of 1.811 Å is significantly shorter than typical Pt^{IV}–OH single bonds (1.943 –

2.079 Å based on the Cambridge Structural Database). The non-planar geometry of the complex appears to decrease the overlap between Pt-O orbitals, thereby reducing the unfavorable occupation of the Pt-O π* molecular orbital. No π-backdonation from Pt to the PCN ligand backbone takes place due to the high energy of the vacant phenyl orbitals of the pincer ligand. As such, $[(PCN)Pt{=}O]^+$ appears to be the first example of a terminal Pt oxo complex that has no significant electron accepting ligand framework that can stabilize the oxo ligand.

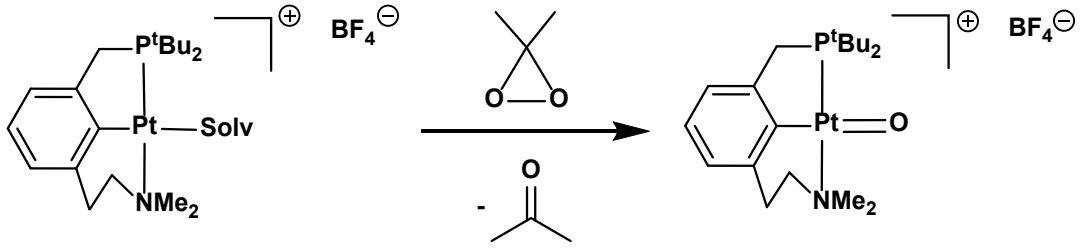

Scheme 1-10. Synthesis of a terminal, cationic Pt^{IV} oxo complex.

The diverse reactivity of this unique complex showed that $[(PCN)Pt{=}O]^+$ is an effective oxygen transfer reagent (Scheme 1-11). When treated with PPh_3, the oxo group was readily transferred to the phosphine to give $O{=}PPh_3$ and the corresponding Pt^{II} cation $[(PCN)Pt]^+$. Oxygen transfer to CO was also observed in the presence of 4 equiv of CO to form $[(PCN)Pt(CO)]^+$ and CO_2. Furthermore, in the presence of excess H_2 (5 atm) $[(PCN)Pt{=}O]^+$ reacted to form water, as well as the Pt^{II} cation $[(PCN)Pt]^+$. Intramolecular oxygen transfer, resulting in migration of the oxo ligand to the Pt-*P*, was observed if the Pt oxo complex remained in solution at room temperature for 7-10 h in the absence of an external oxygen acceptor (Scheme 1-11). The Pt oxo complex is also susceptible to

nucleophilic attack, as indicated by its reaction with KH to form (PCN)PtOH along with concomitant elimination of KBF_4.

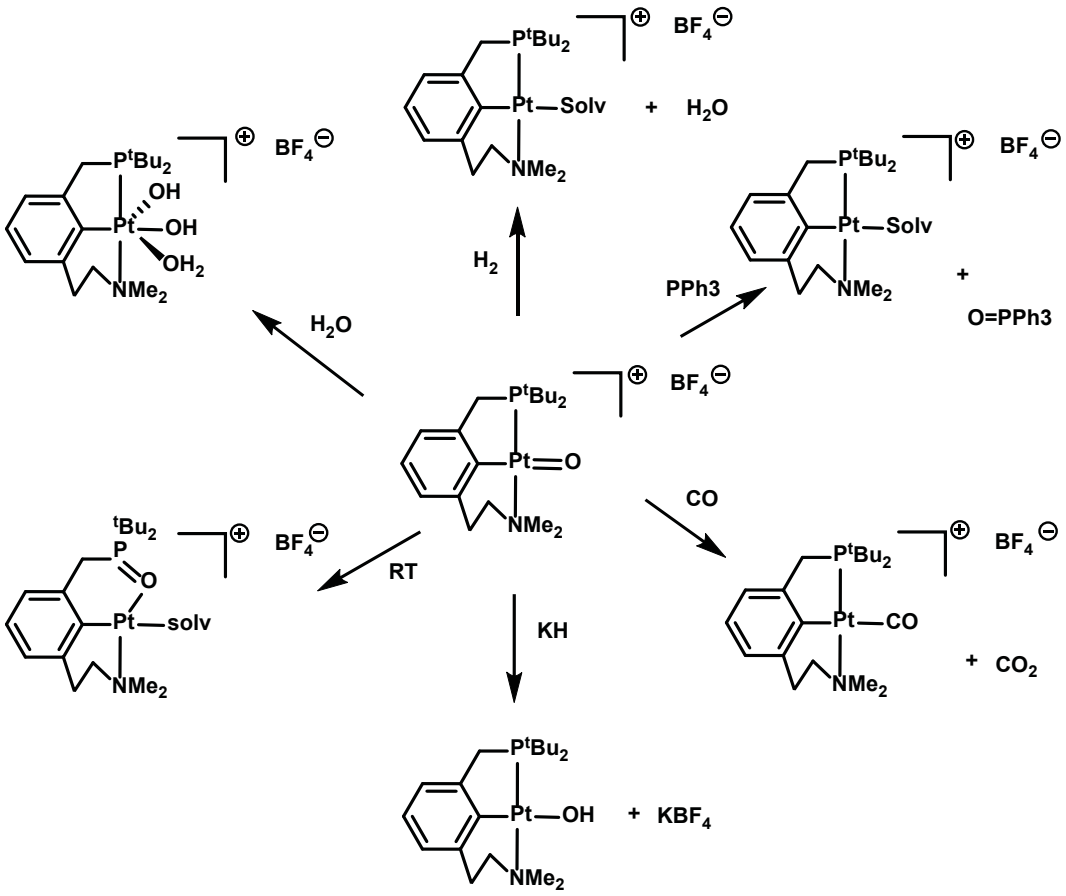

Scheme 1-11. Reactivity of $[(PNP)Pt{=}O]^{+}$ with H_2, PPh_3, CO, KH, H_2O and room temperature decomposition via intramolecular O transfer.

The reactivity of the cationic Pt oxo complex with water was also probed, as terminal oxo species have been implicated in the catalytic oxidation of water to O_2.[35] The mechanism of the latter process has been studied extensively and remains poorly understood in some portions. In the presence of excess H_2O, the Pt oxo species was

readily converted to a monomeric Pt^{IV} dihydroxo complex that also features a coordinated H_2O molecule (Scheme 1-11). This water activation reaction may be of relevance to both water oxidation catalysis as well as to the mechanism of alkane oxidation by O_2 to give alcohols, in which the oxidation of Pt^{II} to Pt^{IV} by O_2 in water to generate a Pt^{IV} dihydroxo complex has been proposed as a key step.[36]

Thus Milstein and co-workers were able to demonstrate that appropriately designed pincer-type frameworks are able to stabilize an unprecedented cationic Pt^{IV} terminal oxo complex. This work demonstrates the utility of pincer ligation for the stabilization of highly reactive and unusual transition metal complexes that have the potential to exhibit novel reactivity.

1.4.3 Intramolecular arene C-H bond activation mediated by (PNP)Ni species

The search for metal complexes that can perform selective hydrocarbon activation and functionalization chemistry has mainly been focused on complexes of the second and third row transition metals.[9e] Such research is motivated in part by the relatively stronger M-C and M-H bonds observed with the second and third row metals relative to the first row transition metals. Thus, Ni mediated C-H bond activation remains relatively unexplored in comparison to Pt and Pd. Due to the relatively high cost of Pt and Pd, exploring the reactive properties of less expensive Ni complexes is of benefit.

Previous work by Liang and co-workers had shown that $(PNP)Ni^{II}$ (PNP = $N(o\text{-}C_6H_4PR_2)_2^-$; R= ^{i}Pr, Cy, Ph) pincer complexes were effective towards C-X (X = Cl, Br, I) bond cleavage of halogenated hydrocarbons.[37] It was thus postulated that under appropriate reaction conditions, $(PNP)Ni^{II}$ mediated C-H bond cleavage may also be

observed. In an effort to obtain a highly reactive, coordinatively unsaturated Ni^{II} species that might participate in such C-H bond cleavage chemistry, (PNP)NiR' (R' = H, Me) was treated with one equiv. of the Lewis acid, $AlMe_3$.[38] Under these conditions, it was observed that at room temperature or upon mild heating in a benzene solution net arene C-H bond cleavage occurred to afford (PNP)NiPh (Scheme 1-12). In the case of (PNP)NiH, byproducts of this reaction also included methane and dimethylalane. Furthermore, it was shown that when the reaction was performed in a toluene solution, (PNP)Ni(*m*-tolyl) and (PNP)Ni(*p*-tolyl) were formed in a 2:1 ratio. The absence of an *ortho*-substituted tolyl product was attributed to the steric hindrance associated with *ortho*-C-H bond cleavage.

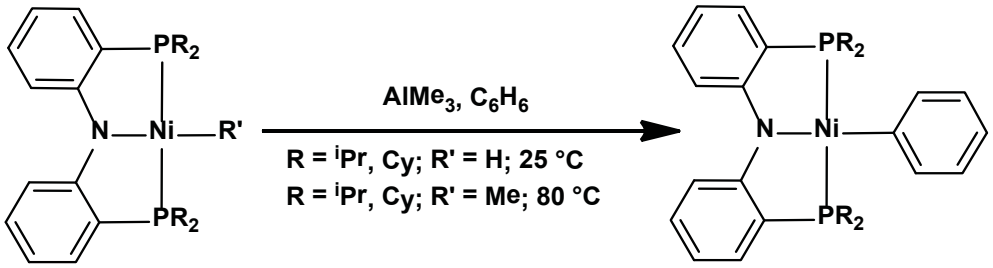

Scheme 1-12. Intermolecular benzene C-H bond cleavage mediated by $(PNP)Ni^{II}$.

The related (PNP)NiMe complex featuring phenyl substitution at the phosphine donors did not exhibit similar arene C-H bond cleavage reactivity, and it was proposed that phenyl substitution at phosphorus does not lead to a sufficiently electron-rich nickel center for arene C-H bond activation to occur. However, ineffective methide abstraction by $AlMe_3$ in the case of R = Ph cannot be ruled out as a possible hindrance to the reactivity of this phenylphosphino system.

To summarize, Liang and co-workers have demonstrated the first example of efficient intermolecular arene C-H bond cleavage mediated by Ni^{II} complexes. This work highlights the use pincer ligation for aggressive and unprecedented bond cleavage chemistry involving a first row transition metal.

1.4.4 Pd-mediated N-H and N-C bond cleavage reactions

Transition metal mediated processes involving N-H and C-N bond cleavage are implicated in numerous important catalytic reactions, including hydroamination of alkenes and alkynes[39] and hydrodenitrogenation of petroleum.[40] However, the oxidative addition of N-H[41] and C-N[42] bonds to late transition metal centers has not been widely demonstrated and studied. Investigations into such reactivity can provide insight into the kinetic and thermodynamic requirements of these processes, which can, in turn, guide the development of new and/or improved catalytic methodologies.

In this context, Ozerov and co-workers recently demonstrated the facile, chelate-assisted oxidative addition of both N-H and C-N bonds to a Pd^{II} center to form PNP-type pincer complexes.[43] Thus, the reaction of the secondary amine (2-$^{i}Pr_2$P-4-Me-$C_6H_3)_2$NH ((PNP)H) with (COD)$PdCl_2$ (COD = 1,5-cyclooctadiene) led to initial displacement of the COD ligand by the phosphine donors to form a κ^2-type [(*P*N*P*)H]$PdCl_2$ coordination complex that was observed in situ by ^{1}H and ^{31}P NMR spectroscopy (Scheme 1-13).[43c] Cleavage of the N-H bond in this bisphosphine κ^2-complex occurred upon exposing the compound to vacuum, which led to elimination of HCl and formation of the κ^3-pincer complex (PNP)PdCl (Scheme 1-13). The formation of (PNP)PdCl also occurred upon the addition of Et_3N to the bisphosphine κ^2-(*P*N*P*) intermediate. Furthermore, treatment

of (PNP)H with half an equiv of the Pd^0 reagent $Pd_2(DBA)_3$ (DBA = dibenzylideneacetone) also led to N-H bond cleavage to form (PNP)PdH, a rare example of N-H bond oxidative addition (Scheme 1-13).

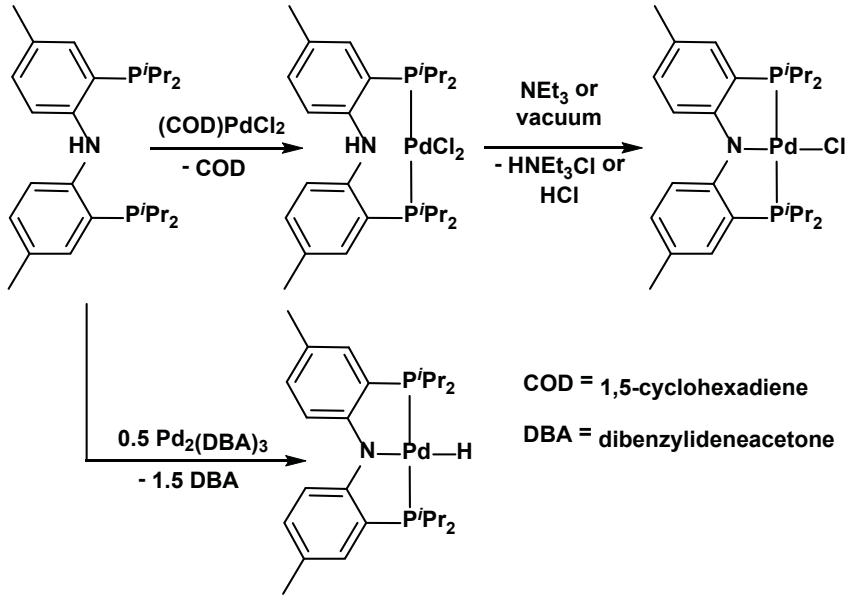

Scheme 1-13. Pd-mediated N-H bond cleavage to afford PNP-type pincer complexes.

The related tertiary amine (PNP)Me was also synthesized and upon its reaction with $Pd(COD)Cl_2$, N-Me bond cleavage was observed to form the pincer complex (PNP)PdCl with loss of MeCl (Scheme 1-14).[43b] This reaction was complete after heating for 1 h at 100 °C. The reaction proceeded via an observable intermediate that was characterized as the $\{[\kappa^3\text{-(PNP)Me}]PdCl\}^+Cl^-$ coordination complex in which COD has been displaced by the phosphine donors of the (PNP)Me ligand and a chloride ligand has moved to the outer coordination sphere to afford a four-coordinate Pd center (Scheme 1-14). This cationic complex is proposed to be in equilibrium with a neutral complex in which the chloride ligand is coordinated inner sphere; although the exact nature of this

neutral complex is unknown, a likely formulation is [κ^2-(*P*N*P*)Me]$PdCl_2$. Mechanistic studies of the C-N bond cleavage reaction indicated that the process is accelerated by decreasing the solvent polarity. Based on this observation, a mechanism for C-N cleavage involving C-N bond oxidative addition to the cationic intermediate {[κ^3-(*P*N*P*)Me]PdCl}$^+Cl^-$ is discounted. The authors propose that the C-N bond cleavage proceeds either via oxidative addition to the neutral species [κ^2-(*P*N*P*)Me]$PdCl_2$, or alternatively via a mechanism involving nucleophilic attack of X^- on the N-*Me* group. In a subsequent study, Ozerov and co-workers also investigated the oxidative addition of the N-Me linkage in (PNP)Me to Pd^0.[43a] Utilizing $Pd(PPh_3)_4$ as a commercially available source of Pd^0, the authors noted that ca. 30% conversion to (PNP)PdMe was attained upon heating of (PNP)Me and one equiv of $Pd(PPh_3)_4$ at 100 °C for 96 h (Scheme 1-14). No further increase in (PNP)PdMe concentration was detected by NMR spectroscopy after additional heating at this temperature. The incomplete conversion to the (PNP)PdMe product was attributed to inhibition of the reaction by free PPh_3 generated during the course of the reaction. These results constitute a rare example of the oxidative addition of an unstrained C-N bond to Pd^0. The observation that C-N bonds are readily cleaved by Pd^{II} is striking, especially considering the widespread use of Pd-based catalysts in C-N bond forming reactions, such as Buchwald-Hartwig amination reactions.

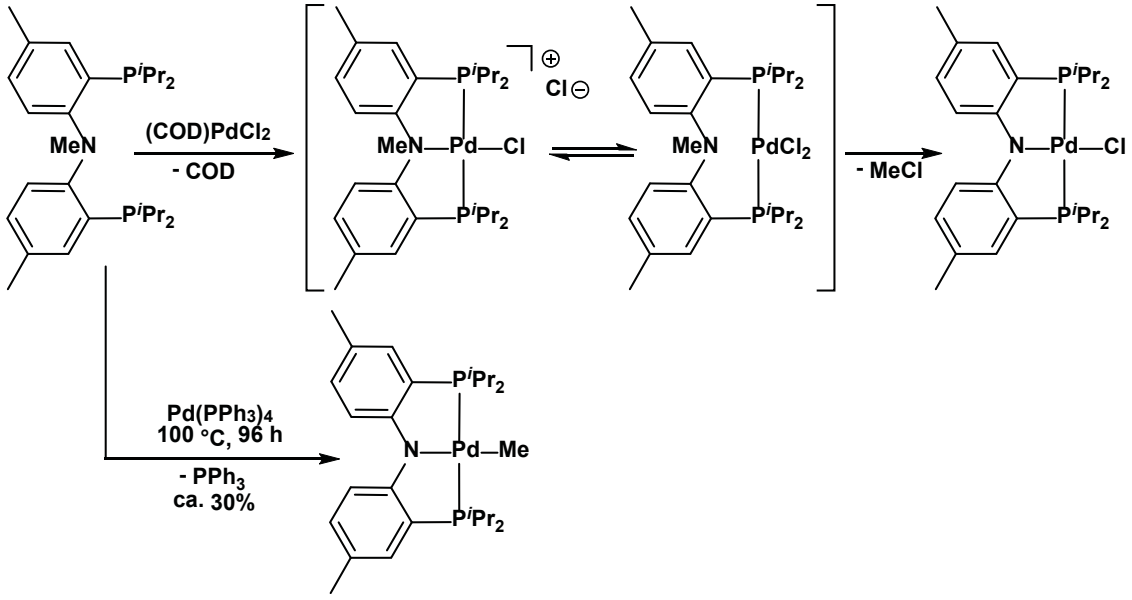

Scheme 1-14. Pd-mediated C-N bond cleavage.

1.4.5 Synthesis and reactivity of Pd^{II} hydride and hydroxide complexes

Late transition metal hydroxide and alkoxide complexes are considered to be important intermediates in various catalytic cycles such as olefin epoxidation[44] and water oxidation.[45] However, well characterized examples of monomeric, terminal hydroxide and alkoxide complexes of electron rich late metals are relatively scares. As such, the reactivity of such complexes has not been thoroughly investigated. The hydrogenation of late metal hydroxide and alkoxide species is a particularly intriguing reaction, as it has been implicated in several catalytic processes, including the generation of Stryker's reagent[46] and the generation of formic acid from the hydrogenation of CO_2.[47] Although very little is known about such hydrogenation processes, two recent examples of Pd^{II} hydroxides pincer complexes undergoing hydrogenolysis with molecular hydrogen have been reported.[48,49]

Goldberg and co-workers have demonstrated that the Pd^{II} hydroxide complex (^{tBu}PCP)Pd(OH) (^{tBu}PCP = 2,6-bis($^{t}Bu_2PCH_2$)C_6H_3) reacts with H_2 (7 atm) to form (^{tBu}PCP)PdH and water (Scheme 1-15).[48] Similar reactivity was observed when the methoxide species (^{tBu}PCP)Pd(OMe) was treated with H_2. Kinetic investigations into this reactivity involving the hydroxo Pd derivative indicated that a water-bridged dimeric species of the type $[(^{tBu}PCP)PdOH]_2 \bullet 4H_2O$ is present under the hydrogenolysis conditions and must dissociate to form the monomer prior to reaction with H_2.

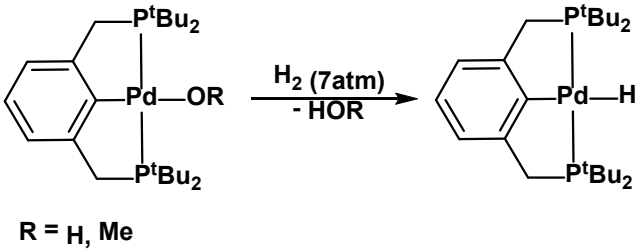

Scheme 1-15. Hydrogenolysis of (^{tBu}PCP)Pt^{II} hydroxide and methoxide complexes.

Several mechanisms for the hydrogenation of the Pd-OH linkage were considered (Scheme 1-16), including oxidative addition of H_2 followed by reductive elimination of water, a concerted process involving a four-centered transition state, as well as the formation of a Pd dihydrogen complex that could undergo subsequent deprotonation by OH^-. Computational analysis revealed that a concerted pathway featuring a four-centered transition state is preferred over one which includes oxidative addition and reductive elimination, as the kinetic barrier to a Pd^{IV} intermediate is too high.

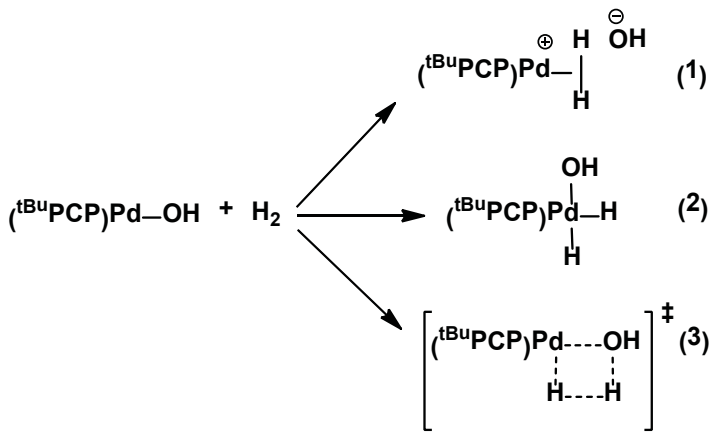

Scheme 1-16. Potential intermediates and transition states in the hydrogenolysis of (^{tBu}PCP)Pd(OH).

The Frech group recently reported on the synthesis of Pd^{II} hydroxo complexes supported by a PCP pincer ligand featuring an adamantylic core.[49] Treatment of (Cy-PAdP)PdH (Cy-PAdP = $[C_{10}H_{13}$-1,3-$(CH_2PCy_2)_2]^-$) with water resulted in the formation of the hydroxide complex (Cy-PAdP)Pd(OH) (Scheme 1-17). In the presence of excess water (50 to 100 equiv.) and 1 atm of H_2 the hydroxo complex was found to undergo rapid (15 min at 35 °C) hydrogenolysis to produce (Cy-PAdP)PdH.

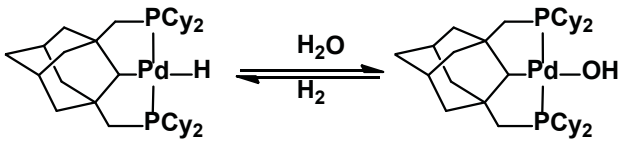

Scheme 1-17. Synthesis and reversible hydroxylation/hydrogenation of (Cy-PAdP)PdH and (Cy-PAdP)Pd(OH).

The unusual reactivity displayed by (Cy-PAdP)PdX (X = H, OH) species is attributed to the strong *trans*-influence of the adamantyl-derived central pincer donor. The authors propose that lengthening of the Pd-H linkage increases hydridic character

due to accumulation of negative charge at the H atom. This, in turn, leads to stronger dihydrogen bonding interactions of the type Pd-H···H-OR with protic species. Such interactions promote the formation of dihydrogen complexes and the subsequent liberation of H_2. The observed rate increase for the hydrogenolysis of the Pd-OH upon the addition of excess water supports a mechanism involving OH^- dissociation from Pd and the formation of a cationic dihydrogen complex that is subsequently deprotonated by OH^- (Scheme 1-18). This proposal differs from the concerted mechanism calculated for the hydrogenolysis of (^{t}Bu-PCP)Pd(OH), highlighting the profound effect that is brought about by changing the nature of the central pincer donor.

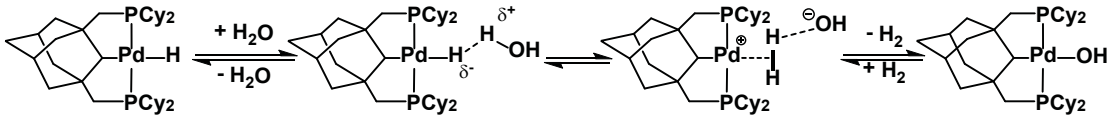

Scheme 1-18. Potential reaction mechanism for the reversible hydroxylation/hydrogenation of (Cy-PAdP)PdH and (Cy-PAdP)PdOH.

1.5 The Development of Group 10 Metal LSiL-type Pincer Complexes (L = N, P)

The examples highlighted thus far clearly indicate that pincer ligands have the ability to support a variety of Group 10 transition metal complexes. These complexes have exhibited a range of interesting reactivity, including C-H, N-H, and C-N bond cleavage. As well, pincer ligation has been shown to be particularly suited for the stabilization of highly unusual and reactive transition metal species, including an unprecedented terminal Pt-oxo species.

Despite the advances that have been highlighted in the previous sections, numerous opportunities for improvement and innovation still exist in transition metal pincer chemistry. In this context, alternative pincer ligand designs are of interest, as pincer ligand modification may facilitate the isolation of unusual and highly reactive complexes that are able to mediate new stoichiometric and catalytic transformations. In particular, the incorporation of elements into the ligand design that can engender electronic and coordinative unsaturation at the metal center is highly desirable. Such unsaturated Group 10 metal species have been shown to be intermediates in C-H bond activation chemistry of the type that has been described in the preceding sections. In addition, strongly electron-releasing donor groups are also desirable, as electron rich metal centers are more likely to engage in oxidative addition reactions that lead to the cleavage of E-H bonds (E = main group element, e.g. C, N, Si).

As described previously, there are many features of the pincer ligand design that can be modified in order to bring about desirable changes in the reaction chemistry of the corresponding metal complexes. While significant effort has been devoted to the synthesis of alternative pincer ligands, these efforts have focused almost exclusively on variation of the neutral (L) donor fragments and of the ancillary ligand backbone. By comparison, the central anionic donor (X) has largely been restricted to the elements C and N. In this context, the research described in this thesis targets the synthesis of Group 10 transition metal complexes supported by new PSiP-type ancillary pincer ligands that feature a central silyl (R_3Si^-) donor. It is anticipated that such novel ligands will impart unique reactivity properties to the ensuing complexes, leading to new applications in synthesis and catalysis. For example, the increased electron-donating character of Si

relative to C is anticipated to lead to a more electron-rich late metal center, thereby promoting the oxidative addition of typically unreactive substrates, such as hydrocarbons. In addition, the strong *trans*-labilizing ability of Si can better promote the generation of reactive, coordinatively unsaturated complexes.[42]

Relatively little attention has been given to the incorporation of silyl donor fragments into the framework of a preformed tridentate ancillary ligand. A notable exception is the work of Stobart and coworkers, who have reported late transition metal complexes featuring bi-, tri-, and tetradentate (phosphino)silyl ligands.[50] The tridentate bis(phosphino)silyl ligands reported by Stobart and co-workers featured relatively non-rigid aliphatic or benzylic backbones.[50b,c] Although several bis(phosphino)silyl Pt^{II} chloride complexes were synthesized (Figure 1-4), the organometallic reactivity of these complexes was not explored. As well, no exploration of Ni or Pd chemistry utilizing such PSiP ligation was reported.

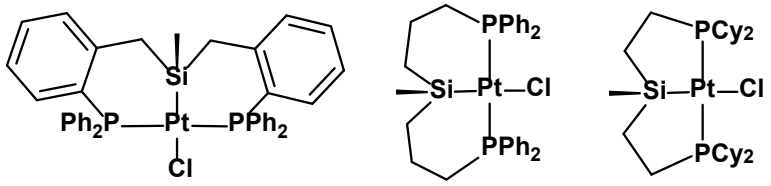

Figure 1-4. Examples of previously reported PSiP-type Pt^{II} pincer complexes.

In a more recent study, Tilley and coworkers reported a silyl pincer ligand featuring a bis(quinolyl) framework (bis(8-quinolyl)methylsilyl, NSiN), and demonstrated that a variety of (NSiN)Pt complexes are synthetically accessible.[51] The square planar Pt^{II} complex (NSiN)PtCl was prepared and structurally characterized, however, attempts to further derivatize this complex were generally unsuccessful.

Rather, NSiN ligation appears to be more compatible with the synthesis of Pt^{IV} complexes. Thus, (NSiN)PtCl underwent sluggish oxidative addition of H_2 to generate the octahedral Pt^{IV} complex (NSiN)Pt$(H)_2$Cl in low yield (Scheme 1-18). Related dimethyl Pt^{IV} complexes of the type (NSiN)PtMe_2X (X = I, OTf) were also prepared by utilizing the Pt^{IV} starting materials PtMe_3X in conjunction with (NSiN)H.

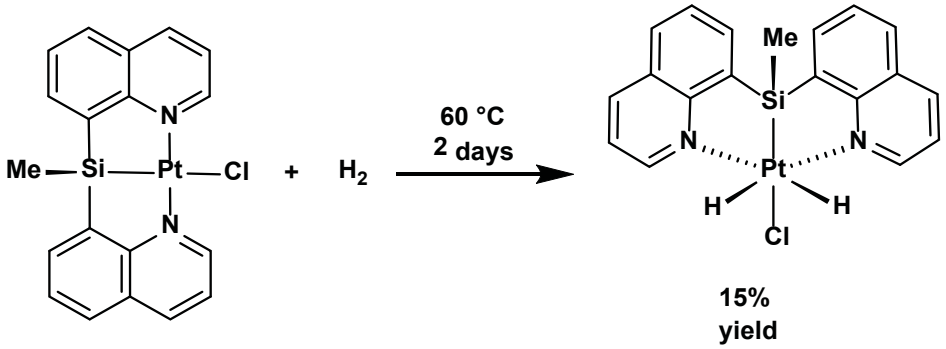

Scheme 1-18. Oxidative addition of H_2 to (NSiN)PtCl.

Treatment of the triflate derivative (NSiN)PtMe_2(OTf) with one equiv. of $(Et_2O)_3Li[B(C_6F_5)]_4$ led to formation of the unusual five-coordinate cationic species $[(NSiN)PtMe_2]^+$ upon elimination of LiOTf (Scheme 1-19). Although five-coordinate Pt^{IV} species are proposed as intermediates in bond activation chemistry,[9f] only a few X-ray structures of complexes of this type have been reported.[52] Remarkably, $[(NSiN)PtMe_2]^+$ is stable to ethane elimination as well as E-H bond activation chemistry, even upon extensive heating.[51]

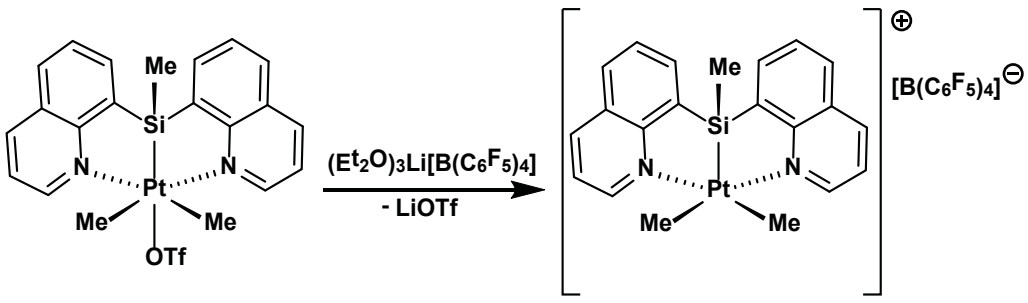

Scheme 1-19. Formation of the five-coordinate cationic complex $[(NSiN)PtMe_2]^+$

The relatively sluggish reactivity reported by Tilley and co-workers for NSiN-supported Pt complexes suggests that ligand modification might provide access to more reactive Pt species. Unfortunately, the synthesis of alternative NSiN derivatives is limited to varying the substitution on the quinolyl rings only, which can pose a synthetic challenge. Also, it appears that bis(quinolyl) ligation is not compatible with the synthesis of electron-rich Pt^{II} complexes of the type that might readily undergo oxidative addition reactions. No exploration of Ni or Pd chemistry utilizing such NSiN ligation has been reported.

1.6 Towards the Synthesis and Reactivity of Group 10 Pincer Complexes Featuring New Types of Phosphinosilyl Tridentate Ligands

This report documents in detail the synthesis and reactivity studies of new neutral and cationic Group 10 metal (Ni, Pd, Pt) pincer complexes supported by bis(phosphino)silyl ligands of the type $[\kappa^3\text{-}(2\text{-}Cy_2PC_6H_4)_2SiMe]^-$ ([Cy-PSiP], Figure 1-5). The work of Stobart and Tilley notwithstanding, the synthesis of silyl pincer M^{II} (M = Ni, Pd, Pt) organometallic species and the study of such complexes with respect to E-H bond activation had not been documented prior to the work detailed herein. By comparison

with the Stobart systems, it was anticipated that the reduced conformational flexibility and lack of β-hydrogens associated with the *ortho*-phenylene backbone of [Cy-PSiP] could provide enhanced stability and selectivity in metal-mediated reactivity. Furthermore, in comparison with the NSiN system studied by Tilley and co-workers, [R-PSiP] ligation offers the opportunity to readily tune the steric and electronic properties of the phosphino donors; the phosphino groups were also anticipated to be compatible with the preparation of electron-rich M^{II} derivatives of the type that might readily engage in E-H bond oxidative addition chemistry. What follows is a report of the work performed in this area to date in the context of my PhD research. The synthesis and isolation of neutral and cationic [Cy-PSiP]Pt^{II} complexes are described, as well as their application towards C-H, Si-H and Si-Cl bond cleavage reactions. In addition, the synthesis of [Cy-PSiP] ligated Pd^{II} and Ni^{II} complexes is detailed along with a description of an unusual rearrangement involving Si-C bond cleavage that was observed in the attempted isolation of alkyl derivates of these complexes. Notably, during the course of these studies Iwasawa and co-workers examined in detail the catalytic activity of related Pd complexes supported by [Ph-PSiP] (Ph-PSiP = $[\kappa^3$-(2-$Ph_2PC_6H_4)_2SiMe]^-$) ligation, including applications in the hydrocarboxylation of allenes and 1,3-dienes,[53] as well as the dehydrogenative borylation of alkenes and 1,3-dienes.[54]

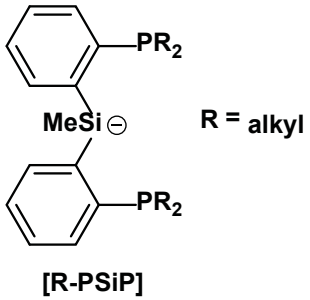

Figure 1-5. Bis(phosphino)silyl ligands under investigation by the Turculet group.

CHAPTER 2: Synthesis and Reactivity of Pt Bis(phosphino)silyl Pincer Complexes

2.1 Introduction

As previously described in the first chapter of this document, LNL- and LCL-type (L = neutral donor) late metal pincer complexes have been the focus of intense research recently. This class of complexes has shown remarkable stoichiometric and catalytic reactivity, as well as the ability to stabilize unusual structural motifs such as terminal anionic Pt^{II} oxo complexes.[19-22,34] Despite recent advances in these areas, alternative LXL-type (X = anionic donor) pincer frameworks that feature X donors other than C or N have received relatively little attention.[24] In this regard, research in the Turculet group has been focused on developing new classes of pincer-type complexes that feature heavier main group element X donors, in anticipation that such novel ligands will impart unique reactivity properties to the ensuing complexes.[25a-g] In particular, the work detailed in this thesis describes the synthesis and study of pincer-like metal complexes supported by new tridentate PSiP-type bis(phosphino)silyl ligands. The incorporation of strongly electron donating and *trans*-labilizing silyl groups into such multidentate ligands may promote the formation of electron-rich and coordinatively unsaturated complexes that exhibit novel reactivity with σ-bonds. In this context, this chapter details the synthesis and reactivity studies of new Pt complexes supported by bis(phosphino)silyl ligands of the type $[\kappa^3\text{-}(2\text{-}Cy_2PC_6H_4)_2SiMe]^-$ ([Cy-PSiP]). The utility of [Cy-PSiP]Pt^{II}

complexes in E-H (E = main group element) as well as Si-C(sp^3) bond cleavage reactions was investigated

2.2 Results and Discussion

2.2.1 Synthesis and characterization of [Cy-PSiP]PtX (X = Cl, OTf) complexes

A strategic starting point for the platinum silyl pincer chemistry was the formation of Pt^{II} chloride and triflate complexes, since they can be used as precursors for the synthesis of a wide variety of Pt^{II} species, including alkyl derivatives and cationic complexes. Treatment of $(Et_2S)_2PtCl_2$ with one equiv of the tertiary silane [Cy-PSiP]H in the presence of one equiv of Et_3N led to the formation of [Cy-PSiP]PtCl (**2-1**) upon heating at 65 °C for 30 h (Scheme 2-1). Complex **2-1** was isolated in 86% yield as an off-white solid. The related complex [Cy-PSiP]Pt(OTf) (**2-2**) was synthesized in 87% yield by treating **2-1** with one equiv of AgOTf in benzene solution (Scheme 2-1). Solution NMR spectroscopic data for **2-1** and **2-2** (benzene-d_6) are consistent with a C_s symmetric structure, as indicated by the presence of one ^{31}P NMR resonance at 59.4 (s with Pt satellites, $^1J_{PPt}$ = 2984 Hz) and 65.9 (s with Pt satellites, $^1J_{PPt}$ = 3055 Hz) ppm, respectively. The observation of ^{195}Pt satellites in both the ^{31}P and ^{29}Si NMR spectra (for **2-1**: 32.3 ppm, $^1J_{SiPt}$ = 1183 Hz; for **2-2**: 18.8 ppm, $^1J_{SiPt}$ = 1381 Hz) of these complexes is consistent with κ^3-coordination of the [Cy-PSiP] ligand. Contrary to the reactivity observed by Peters and co-workers[27] for (BQA)Pt(OTf) (BQA = bis(8-quinolinyl)amido), attempts to observe benzene C-H bond activation by heating of **2-1** or **2-2** in benzene

solution (several days at 100 °C) in the presence of amine bases such as Et_3N and $^{i}Pr_2MeN$ were not successful.

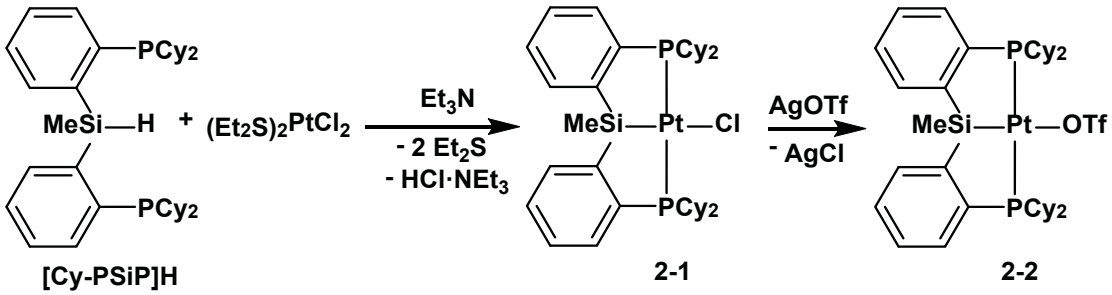

Scheme 2-1. Synthesis of [Cy-PSiP]PtCl (**2-1**) and [Cy-PSiP]Pt(OTf) (**2-2**).

2.2.2 Synthesis and characterization of [Cy-PSiP]Pt^{II} alkyl and hydride complexes

The synthesis of alkyl platinum derivatives of **2-1** was undertaken with the hopes of accessing Pt^{II} complexes that might exhibit increased reactivity towards E-H bonds (E = main group element) relative to **2-1** and **2-2**. Treatment of **2-1** with one equiv of MeLi (1.6 M in Et_2O) in THF solution led to the formation of the methyl complex [Cy-PSiP]PtMe (**2-3**), which was isolated in 55% yield (Scheme 2-2). Similarly, treatment of **2-1** with one equiv of PhLi (1.8 M in $^{n}Bu_2O$) in THF led to formation of the corresponding phenyl complex [Cy-PSiP]PtPh (**2-4**, Scheme 2-2), which was isolated as a yellow solid in 94% yield. Complexes **2-3** and **2-4** are among the first examples of Pt^{II} alkyl complexes supported by silyl pincer ligation.

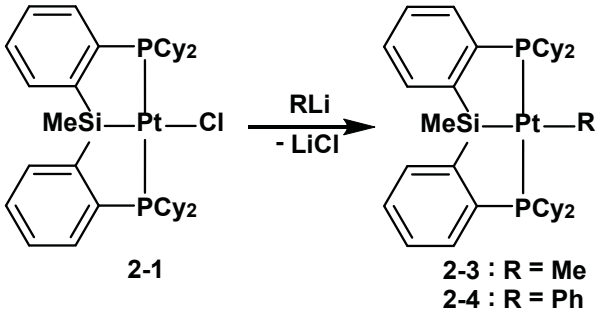

Scheme 2-2. Synthesis of [Cy-PSiP]PtMe (**2-3**) and [Cy-PSiP]PtPh (**2-4**).

Solution NMR data for both **2-3** and **2-4** (benzene-d_6) are consistent with the formation of C_s symmetric, square-planar complexes that feature tridentate coordination of the [Cy-PSiP] ligand with the Pt-Me and Pt-Ph ligands, respectively, occupying the coordination site *trans* to Si. Thus, the ^{31}P and ^{29}Si NMR spectra of both complexes feature a single resonance with Pt satellites (for **2-3**, ^{31}P NMR: 57.9 ppm, $^{1}J_{PPt}$ = 2938 Hz; ^{29}Si NMR: 63.9 ppm $^{1}J_{SiPt}$ = 696 Hz; for **2-4**, ^{31}P NMR: 56.2 ppm, $^{1}J_{PPt}$ = 2921 Hz; ^{29}Si NMR: 59.7 ppm, $^{1}J_{SiPt}$ = 646 Hz). The decreased values of $^{1}J_{SiPt}$ for both **2-3** and **2-4** relative to **2-1** and **2-2** are consistent with weakening of the Pt-Si bond due to the greater *trans*-influence of the methyl and phenyl ligands versus chloride and triflate. Indeed, a general trend of increasing δ ^{29}Si and decreasing $^{1}J_{SiPt}$ with increasing *trans*-influence of the ligand (X) positioned *trans* to Si is evident in the series of [Cy-PSiP]PtX complexes featured herein (Table 2-1). While the ^{1}H NMR resonance corresponding to the Pt-Me group in **2-3** is obscured by resonances for the cyclohexyl protons of the [Cy-PSiP] ligand, the ^{13}C{^{1}H} NMR spectrum of **2-3** contains a resonance at -1.6 ppm (apparent t, J = 8 Hz) that is assigned to the Pt-Me group, and which correlates to a ^{1}H NMR resonance at 1.25 ppm in a ^{1}H-^{13}C HSQC experiment.

Table 2-1. Comparison of ^{29}Si NMR data for square planar [R-PSiP]PtX complexes.[a]

Compound	Ligand *trans* to Si (X)	^{29}Si NMR δ	$^{1}J_{SiPt}$
2-2	OTf	18.8	1381
2-5	-	22.9	971
2-1	Cl	32.3	1183
2-6	C_6F_5	53.8	806
2-4	Ph	59.7	646
2-3	Me	63.9	696
2-9	$SiPh_2Cl$	74.9[b]	638[b]
2-8	SiH_2Ph	81.6[b]	650[b]

[a]In benzene-d_6. [b]For [Cy-PSiP] fragment.

X-Ray quality crystals were obtained from a concentrated Et_2O solution of **2-4**. The solid state structure of this complex (Figure 2-1, Table 2-2) features distorted square planar geometry at Pt, similar to that previously observed for [Ph-PSiP]PtBn,[25e] and is consistent with the solution NMR data obtained for **2-4**. This structure confirms that [Cy-PSiP] ligation can accommodate the formation of square-planar complexes that feature a strongly *trans*-labilizing ligand coordinated *trans* to Si despite the constraints imposed by sp^3-hybridization at Si and the rigid *o*-phenylene ligand backbone. The Pt-Si bond distance of 2.324(1) Å falls within the range characteristic of Pt-Si bond distances (2.255 – 1.444 Å).[52] The Pt-C2 bond distance of 2.139(2) Å is significantly longer than that reported for (BQA)PtPh (Pt-C_{Ph} = 2.023(4) Å),[27] which is in agreement with the strong *trans*-influence of Si relative to the central amido donor of the BQA ligand.

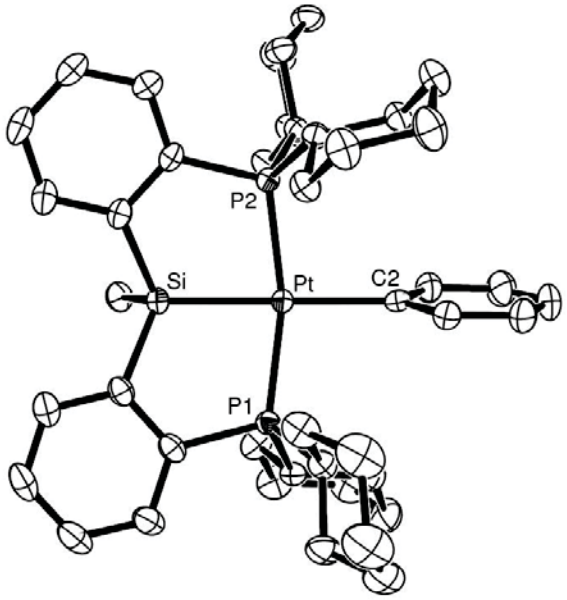

Figure 2-1. ORTEP diagram for **2-4**·OEt_2 shown with 50% displacement ellipsoids; all H-atoms, as well as the diethyl ether solvate, have been omitted for clarity

Table 2-2. Selected interatomic distances (Å) and angles (°) for **2-4**·OEt_2

Interatomic Distances (Å)			
Pt-P1	2.2776(7)	Pt-Si	2.324(1)
Pt-P2	2.2808(7)	Pt-C2	2.139(2)
Interatomic Angles (°)			
P1-Pt-P2	162.41(2)	P1-Pt-Si	83.58(2)
Si-Pt-C2	175.13(5)	P2-Pt-C2	96.63(5)

Complex **2-3** exhibited high thermal stability in benzene solution; no reaction was observed upon heating a benzene solution of **2-3** at 90 – 100 °C over the course of several days. Furthermore, **2-3** did not react with an atmosphere of H_2, even after heating in benzene solution for 2 days at 80 °C.

In an effort to access a cationic [Cy-PSiP]Pt^{II} complex that may exhibit enhanced reactivity with E-H bonds, **2-3** was treated with one equiv of $B(C_6F_5)_3$ in benzene solution. This reaction cleanly generated a new product (**2-5**) that was consistent with methide abstraction in **2-3** to form $\{[Cy\text{-}PSiP]Pt\}^+[MeB(C_6F_5)_3]^-$, as indicated by ^1H, ^{31}P and ^{11}B NMR spectroscopy of the reaction mixture (Scheme 2-3). Complex **2-5** was isolated in 87% yield and exhibits a characteristic, sharp $^{11}B\{^1H\}$ NMR resonance at -14.0 ppm (benzene-d_6) that is consistent with the $[MeB(C_6F_5)_3]^-$ anion. While the resonance for the B-*Me* protons is obscured by P-*Cy* resonances in the ^1H NMR spectrum of **2-5** (benzene-d_6), this signal was identified at 1.59 ppm by the use of ^1H-^{13}C HSQC correlation spectroscopy (the B-*Me* $^{13}C\{^1H\}$ NMR resonance was observed as a broad peak at 0.1 ppm in benzene-d_6). Both the ^{31}P (70.8 ppm, $^1J_{PPt}$ = 3038 Hz, benzene-d_6) and ^{29}Si (22.9 ppm, $^1J_{SiPt}$ = 971 Hz, benzene-d_6) NMR resonances of **2-5** are shifted substantially relative to **2-3**, and the increased value of $^1J_{SiPt}$ for **2-5** relative to **2-3** is in keeping with methide abstraction (Table 2-1).

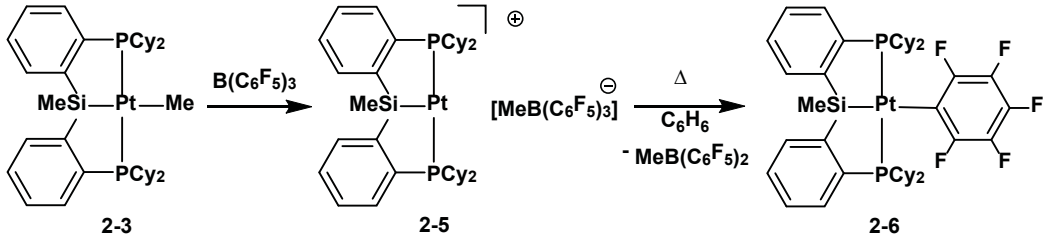

2-3 **2-5** **2-6**

Scheme 2-3. Synthesis of $\{[Cy\text{-}PSiP]Pt\}^+[MeB(C_6F_5)_3]^-$ (**2-5**) and [Cy-PSiP]Pt(C_6F_5) (**2-6**).

Heating a benzene solution of **2-5** at 100 °C for 48 h led quantitatively to a new product (**2-6**, Scheme 2-3). Compound **2-6** was identified on the basis of NMR spectroscopic studies as a neutral Pt-C_6F_5 derivative resulting from transfer of $C_6F_5^-$ from

B to Pt (Scheme 2-3). Consistent with this formulation, analysis of the crude reaction mixture by $^{11}B\{^{1}H\}$ NMR spectroscopy indicated a new broad resonance at 71.3 ppm (benzene-d_6) that corresponds to $MeB(C_6F_5)_2$, the anticipated side-product of this reaction.[55] Complex **2-6** was isolated in 86% yield, and features a ^{29}Si NMR resonance at 53.8 ppm that is shifted significantly down-field relative to **2-5**. Complex **2-6** also features a characteristic set of $^{19}F\{^{1}H\}$ NMR resonances (benzene-d_6, 25 °C; -110.8 (d with Pt satellites, 1 F, J_{FF} = 33 Hz, $^{3}J_{FPt}$ = 255 Hz), -112.1 (d with unresolved Pt satellites, 1 F, J_{FF} = 38 Hz), -162.0 (m, 1 F), -162.8 (m, 1 F), and -163.8 (m, 1 F) ppm) that correspond to the inequivalent *ortho*-, *para*-, and *meta*-fluorine substituents of the Pt-C_6F_5 group, in which rotation about the Pt-C bond is slow on the NMR timescale at 25 °C. As expected, isolated **2-6** does not exhibit a ^{11}B NMR resonance. While aryl transfer from $[RB(C_6F_5)_3]^-$ (R = alkyl) to cationic early transition metal centers is well established,[56,57] examples of similar reactivity involving late transition metal cations are not as common.[58] Liang and co-workers have reported a related example of $C_6F_5^-$ transfer from B to Ni for (PNP)Ni(μ-H)$B(C_6F_5)_3$ (PNP = $N(o\text{-}C_6H_4PR_2)_2^-$, R = ^{i}Pr, Cy) to form (PNP)Ni(C_6F_5).[38]

In an attempt to isolate a Pt^{II} hydride complex, a THF solution of **2-1** was treated with one equiv of $LiEt_3BH$ at room temperature. Quantitative conversion of **2-1** to a new product (**2-7**) was confirmed via ^{31}P NMR spectroscopy (76.6 ppm, s with Pt satellites, $^{1}J_{PPt}$ = 2908 Hz), and complex **2-7** was isolated in 92% yield following workup. Solution NMR data for isolated **2-7** support the identification of this complex as a C_s-symmetric bis(phosphino) Pt derivative of [Cy-PSiP]H that features η^2-Si-H coordination involving the tethered silicon fragment (Scheme 2-4).[59,60] In keeping with this formulation, the ^{1}H

NMR spectrum of **2-7** (benzene-d_6) features a characteristic resonance at 5.48 ppm (t with Pt satellites, 1 H, J_{HPt} = 921 Hz, J_{HP} = 19 Hz) that corresponds to the η^2-Si-*H* fragment. Notably, this resonance falls in the chemical shift region typically associated with Si-*H* resonances of free silanes or metal silyl species (ca. 3.0 – 6.0 ppm);[59] no resonance that could be attributed to a terminal Pt-*H* ligand was observed. The ^{29}Si NMR spectrum of **2-7** features a resonance with Pt satellites at 62.3 ppm (J_{SiPt} = 735 Hz, J_{SiH} = 52 Hz); this signal is shifted downfield relative to the ^{29}Si NMR resonance observed for [Cy-PSiP]H (-24.2 ppm, $^1J_{SiH}$ = 210 Hz, benzene-d_6)[25b] which supports the presence of a Pt-Si bonded interaction. The reduced J_{SiH} value (typical $^1J_{SiH}$ values in free silanes fall near 200 Hz, while $^1J_{SiH}$ values in metal silyl species range between ca. 140 - 220 Hz) observed for **2-7** falls in the range commonly associated with η^2-silane complexes.[59-61] Furthermore, in keeping with η^2-Si-H coordination to a metal center, the IR spectrum of **2-7** (film) exhibits a broad, intense band at 1808 cm^{-1}, a region characteristic of an η^2-Si-H metal species.[60c] Although the monomeric nature of **2-7** in solution cannot be unequivocally confirmed on the basis of the available NMR data, the steric demand of the chelating [Cy-PSiP] ligand would appear to preclude polynuclear variants of this complex.[62] Support for the monomeric structure of **2-7** was also obtained from a low resolution X-ray crystallographic analysis of this compound in which the Si-*H* position could not be located. A related complex of the type [Ph-P*Si*(μ-H)P]*Pd*PPh$_3$ has recently been crystallographically characterized by Iwasawa and co-workers, lending further support to the proposed formulation of **2-7**.[63]

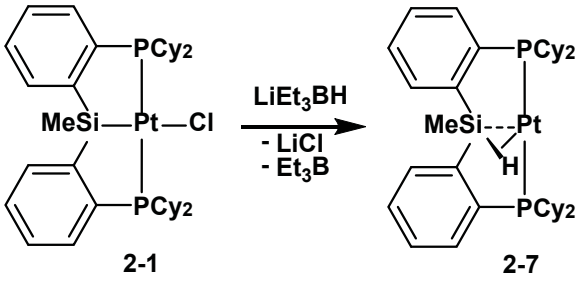

Scheme 2-4. Synthesis of [Cy-P*Si*(μ-H)P]*Pt* (**2-7**).

Complex **2-7** can be viewed as the product of "arrested" reductive elimination from the unobserved Pt^{II} hydrido silyl species [Cy-PSiP]PtH.[64] Given that direct reductive elimination from [Cy-PSiP]PtH to afford **2-7** is unlikely due to the *trans*-disposed Pt-Si and Pt-H groups, it is plausible that such Si-H elimination is preceded by Pt-P dissociation or a tetrahedral distortion in **2-7**, which would serve to bring the hydride ligand into the proximity of the Si in the [Cy-PSiP] ligand backbone. Such a distortion has previously been invoked for phosphine site exchange in *cis*-$(R_3P)_2Pt(ER_3)_2$ (E = Si or Sn) complexes.[65] Attempts to probe further the solution behavior of **2-7** by variable temperature ^1H and ^{31}P NMR spectroscopy (toluene-d_8) revealed no appreciable changes in spectroscopic features in the range of -80 – 90 °C.

2.2.3 Reactivity of [Cy-PSiP]Pt^{II} complexes with hydrosilanes

The reactivity of [Cy-PSiP]PtR (R = alkyl or aryl) complexes with hydrosilanes was explored in order to determine if such complexes could effectively cleave Si-H bonds. Although complex **2-3** did not react with an atmosphere of H_2 even under forcing conditions, treatment of **2-3** with one equiv of $PhSiH_3$ resulted in the rapid formation of the silyl complex [Cy-PSiP]PtSiH_2Ph (**2-8**, Scheme 2-5) with the concomitant evolution

of CH_4 (^{1}H NMR). The formation of **2-8** is quantitative as indicated by ^{31}P NMR spectroscopy of the reaction mixture, and the analytically pure complex was isolated in 96% yield. The ^{1}H NMR spectrum of isolated **2-8** features a resonance at 6.01 ppm (t with Pt and Si satellites, 2 H, $^1J_{SiH}$ = 152 Hz, $^2J_{HPt}$ = 33 Hz, $^3J_{HP}$ = 4 Hz) for the Si-H protons of the Pt-SiH_2Ph group. As expected, two ^{29}Si NMR resonances are observed for **2-8** (benzene-d_6) at 81.6 ($^1J_{SiPt}$ = 650 Hz) and 81.3 ($^1J_{SiPt}$ = 1067 Hz, $^1J_{SiH}$ = 152 Hz) ppm, corresponding to the [Cy-PSiP] and SiH_2Ph fragments, respectively. The IR spectrum of **2-8** features a medium-intensity Si-H stretch at 2018 cm^{-1} that corresponds to the Pt-*SiH*$_2$Ph group. On the basis of these data, complex **2-8** is assigned as a square planar bis(phosphino)silyl Pt^{II} phenylsilyl complex with the SiH_2Ph ligand coordinated *trans* to the [Cy-PSiP] ligand Si. Although phosphino Pt^{II} bis(silyl) complexes are known, most complexes of this type exhibit *cis*-coordination.[59] A rare example of a crystallographically characterized Pt^{II} complex featuring *trans*-disposed silyl ligands has been reported previously by Kim, Osakada, Yamamoto and co-workers.[66] In the case of **2-8** and the related [Ph-PSiP]Pt(SiH_2Ph) analogue that has also been reported by the Turculet group,[25e] the chelating nature of the [R-PSiP] ligand likely enforces this unusual geometry.

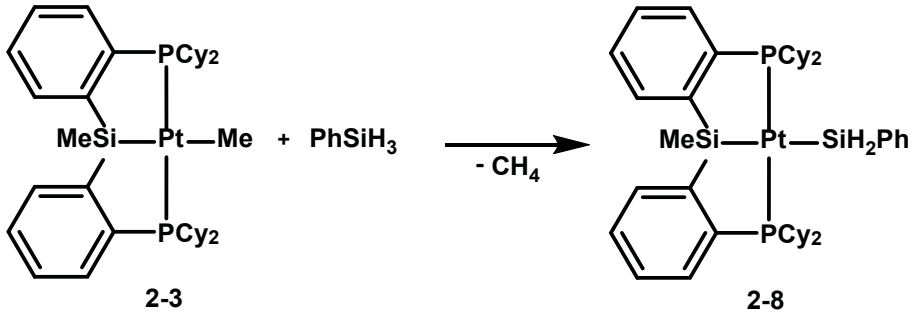

Scheme 2-5. Synthesis of [Cy-PSiP]PtSiH$_2$Ph (**2-8**) via Si-H bond activation in PhSiH$_3$.

The reactivity of **2-3** with hydrosilanes appears to be sensitive to steric effects, as bulkier secondary silanes such as Mes$_2$SiH$_2$ did not react with **2-3** even after prolonged heating (80°C, 2-3 days). Interestingly, when the scope of reactivity was expanded to include hydridochlorosilanes, divergent reactivity was observed. Thus, the reaction of **2-3** with one equiv of Ph$_2$SiHCl in benzene solution did not result in the elimination of CH$_4$ to form a new Pt silyl complex. Rather, the formation of [Cy-PSiP]PtCl (**2-1**) and concomitant evolution of Ph$_2$SiMeH were observed (Scheme 2-6). Within 10 minutes at room temperature, 25% conversion of **2-3** to **2-1** and Ph$_2$SiMeH was observed (^{1}H and ^{31}P NMR), and complete conversion was attained after heating the reaction mixture at 80 °C for 24 h. Complex **2-3** also reacted in a similar fashion with one equiv of ^{i}Pr$_2$SiHCl, generating **2-1** and ^{i}Pr$_2$SiMeH in benzene solution; 12% conversion of **2-3** to **2-1** was observed within 10 minutes at room temperature, and 90% conversion was attained after heating the reaction mixture at 80 °C for 7 days. In addition, **2-3** also reacted with one equiv of Me$_3$SiCl to form **2-1** and Me$_4$Si quantitatively (^{1}H and ^{31}P NMR) after heating at 80 °C for 7 days. No [Cy-PSiP]Pt-containing intermediates were observed by ^{31}P NMR spectroscopy during the course of these reactions. Whereas Si-H bond activation by electron rich metal centers is well-precedented,[59] Si-halide bond activation is

comparatively rare.[67] Although the mechanism for the conversion of **2-3** into **2-1** upon exposure to a chlorosilane has not been determined yet, a mechanism invoking direct Si-Cl oxidative addition followed by Si-C reductive elimination appears unlikely for the reactions involving hydridochlorosilanes, as Si-H oxidative addition to Pt^{II} is anticipated to be preferred.[67f] In this regard, previous studies involving the reaction of [Ph-PSiP]Pt(alkyl) complexes with hydridochlorosilanes showed that Si-H bond cleavage occurs to form a Pt^{II} silyl complex with evolution of the corresponding alkane.[25e] The divergent reactivity exhibited by **2-3** and [Ph-PSiP]Pt(alkyl) analogues towards hydridochlorosilanes reveals that changes in the substitution at phosphorus in the [R-PSiP] ligand can alter the course of reactions involving such substrates. Complex **2-4** also reacted with one equiv of either Ph_2SiHCl or $^{i}Pr_2SiHCl$ in benzene to generate **2-1**; however, these reactions were significantly slower, with the Ph_2SiHCl reaction reaching 40% conversion after 8 days at 80 °C and the $^{i}Pr_2SiHCl$ reaction reaching 23% conversion after 7 days at 80 °C (^1H and ^{31}P NMR).

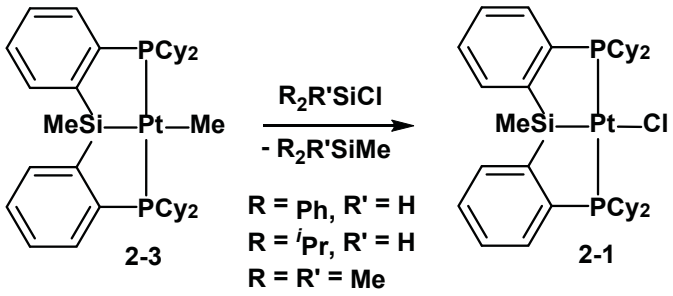

Scheme 2-6. Reactivity of [Cy-PSiP]PtMe (**2-3**) with chlorosilanes to give [Cy-PSiP]PtCl (**2-1**).

Interestingly the η^2-Si-H complex **2-7** reacted with one equiv of either $PhSiH_3$ or Ph_2SiHCl in benzene solution at room temperature to cleanly form the corresponding Pt

silyl complexes, [Cy-PSiP]PtSiH$_2$Ph (**2-8**) and [Cy-PSiP]PtSiPh$_2$Cl (**2-9**), with concomitant evolution of H_2 (Scheme 2-7). Complex **2-9** was isolated in 92% yield, and features ^{29}Si NMR resonances at 74.9 ($^1J_{SiPt}$ = 638 Hz) and 62.2 ($^1J_{SiPt}$ = 1357 Hz) ppm that correspond to the Pt-bound [Cy-PSiP] and SiPh$_2$Cl ligands, respectively. Complex **2-7** did not react with ^{i}Pr$_2$SiHCl upon heating at 80 °C for 3 days, but did react with one equiv of Me$_3$SiCl to form **2-1**, reaching approximately 80% conversion after 10 days of heating at 80 °C in benzene solution (^{1}H and ^{31}P NMR).

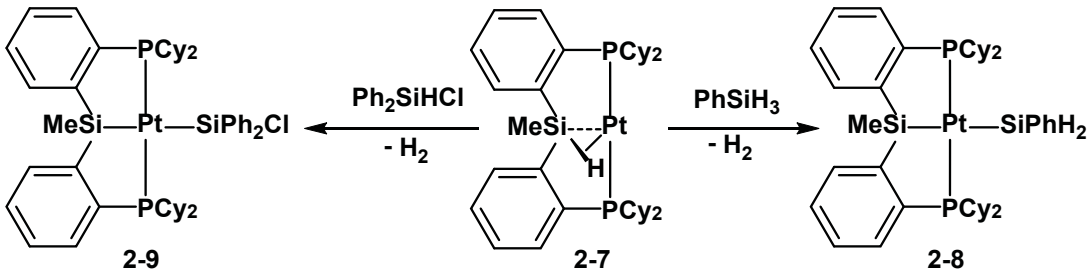

Scheme 2-7. Reactivity of [Cy-P*Si*(μ-H)P]*Pt* (**2-7**) towards hydrosilanes and hydrido-chlorosilanes.

2.2.4 Si-C(sp^3) bond activation at Pt^0

In this context, examples of Si-C(sp^3) bond activation by transition metals are exceedingly rare, [71,72] due in part to the high bond dissociation energy and low polarity associated with Si-C linkages. The study of metal complexes that readily undergo Si-C(sp^3) bond cleavage processes is anticipated to play an important role in furthering our understanding of Si-C bond activation and may have utility in the development of new metal catalyzed reactions for the functionalization of organosilanes.[9d] In an effort to observe Si-C bond cleavage mediated by Pt^0, the silane (2-Cy$_2$PC$_6$H$_4$)$_2$SiMe$_2$ (**2-10**) was

reacted with $Pt(PPh_3)_4$ (Scheme 2-8) at room temperature in benzene-d_6 solution and the reaction was monitored by use of ^1H and ^{31}P NMR spectroscopy. Over the course of 48 h, complete conversion to complex **2-3** was observed and the methyl complex was isolated in 86% yield from this reaction. No intermediates were observed by use of ^1H or ^{31}P NMR spectroscopy during the course of the reaction.

The mechanism of Si-C(sp^3) bond activation by Pt^0 complexes has been previously investigated. Hofmann and co-workers have demonstrated that Si-C bond activation of tetramethylsilane by (dtbpm)Pt^0 (dtbpm = $^tBu_2PCH_2P^tBu_2$) proceeds via an initial C-H bond activation of the silane, followed by a rearrangement to give the Si-C bond activation product.[68] As such, it is possible that the formation of **2-3** proceeds via an initial C-H bond activation of a Si*Me* group in **2-10**, which is followed by a rearrangement to provide **2-3** as the final product. However, there is no mechanistic data to favor this mechanism over direct insertion of the Pt center into a Si-C bond.

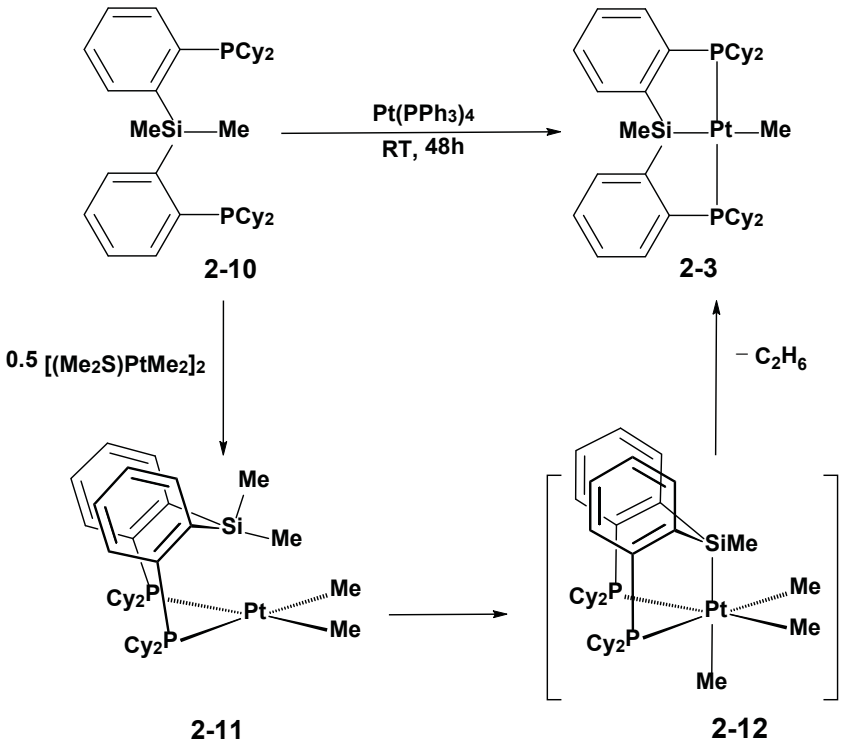

Scheme 2-8. Reaction of 2-10 with Pt^0, and Pt^{II} complexes.

2.2.5 Si-C(sp^3) bond activation involving Pt^{II}

The reactivity of **2-10** with $[(Me_2S)PtMe_2]_2$ was also investigated in order to determine if Si-C bond activation could also be achieved by use of Pt^{II} precursors. Thus, treatment of a benzene-d_6 solution of **2-10** with half an equiv. of $[(Me_2S)PtMe_2]_2$ led to the formation of three products (1:1:1 ratio by ^{31}P NMR) upon standing at room temperature for five days (Scheme 2-8). One of the three reaction products was identified as complex **2-3** on the basis of its ^{31}P NMR chemical shift (57.9 ppm, $^1J_{PPt}$ = 2938 Hz). A second product (**2-11**) features a ^{31}P NMR resonance at 27.7 ppm ($^1J_{PPt}$ = 2050 Hz), while the third species in solution (**2-12**) features a broad ^{31}P NMR resonance

at 23.1 ppm ($^1J_{PPt}$ = 934 Hz). The magnitude of the coupling constant observed for complex **2-12** suggests that this complex likely corresponds to a Pt^{IV} species.

Despite exhaustive efforts, thus far neither **2-11** nor **2-12** has been isolated in pure form; rather, mixtures of **2-3**, **2-11**, and **2-12** were invariably obtained. However, crystallization attempts enabled the collection of a minute quantity of crystalline material (from a Et_2O solution at -35 °C) that proved suitable for single crystal X-ray diffraction analysis. The crystallographically characterized material (Figure 2-2, Table 2-3) corresponds to [κ^2-(2-$Cy_2PC_6H_4)_2SiMe_2$]$PtMe_2$, the product of phosphine coordination in **2-10** to the $PtMe_2$ fragment. This compound is tentatively assigned as complex **2-11**, a putative intermediate in the formation of **2-3** via Si-C(sp^3) bond activation in **2-10** at a Pt^{II} center. The solid state structure of **2-11** features approximate square planar geometry at Pt, with *cis*-disposed phosphino groups (P1-Pt-P2 = 102.491(14) °). The eight-membered metallacycle resulting from coordination of the phosphino groups in **2-10** to Pt adopts a "boat-boat"-type configuration, such that a Si-*Me* group is oriented directly above the square plane defined by the Pt center (Pt···C(1) = 3.35 Å; Pt···Si = 3.53 Å). The structure of **2-11** is related to that of (bps)$PtMe_2$ (bps = bis(2-pyridyl)dimethylsilane), which adopts a similar orientation of a Si-Me substituent (Pt···Si = 3.25 Å).[69] Interestingly, the structurally related complex (bps)$PtMe_2$ has been reported to undergo Si-C(sp^3) bond cleavage only under oxidizing conditions to afford Pt^{IV} species of the type [κ^3*N*,*N*,*O*-(2-$C_5H_4N)_2$SiMeO]$PtMe_3$.[70] No Si-C bond activation was reported for (bps)$PtMe_2$ in the absence of oxidants such as oxygen, hydrogen peroxide, or dibenzoyl peroxide, in contrast to the system presented herein. Mechanistic studies in the

(bps)$PtMe_2$ system suggested that oxidation to Pt^{IV} preceded methyl transfer from Si to Pt.

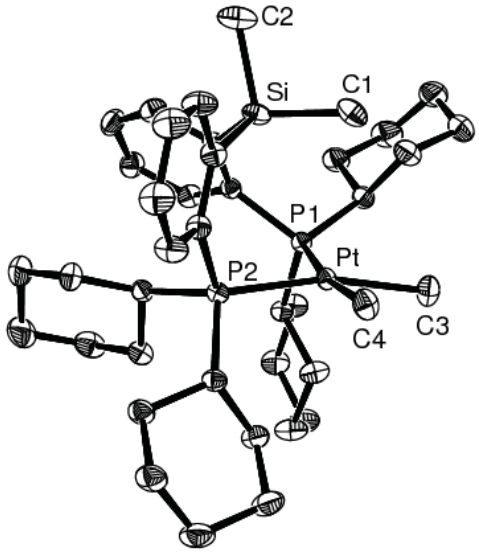

Figure 2-2. ORTEP diagram for **2-11** shown with 50% displacement ellipsoids; all H-atoms have been omitted for clarity.

Table 2-3. Selected interatomic distances (Å) and angles (°) for **2-11**

Interatomic Distances (Å)			
Pt-P1	2.3078(4)	Pt-C3	2.1032(16)
Pt-P2	2.3106(4)	Pt-C4	2.1051(16)
Pt···C(1)	3.35	Pt···Si	3.53
Interatomic Angles (°)			
P1-Pt-P2	102.491(14)	C3-Pt-C4	81.82(7)
P1-Pt-C4	170.50(5)	P2-Pt-C3	163.33(5)

In the case of Si-C activation in **2-10** involving an L_nPtMe_2 precursor, κ^2-coordination of **2-10** to Pt is proposed to occurs initially to form the bis(phosphino) complex **2-11**. In previously reported examples of Si-C(sp^3) activation at Pt^{II} centers, it has been proposed that such transformations proceed via an initial C-H bond activation step,[69,71] followed by a subsequent concerted migration process that leads to the formation of the net Si-C bond cleavage product.[69] Although such a mechanism is plausible in the case of **2-11**, a process involving direct insertion of Pt into a Si-C bond cannot be discounted. The product of such Si-C bond cleavage is the Pt^{IV} species (Cy-PSiP)$PtMe_3$, which is tentatively assigned as complex **2-12**, and which was observed in situ during the course of the formation of **2-3** (*vide supra*). Reductive elimination of ethane from the putative intermediate **2-12** would provide the final observed product of this reaction, complex **2-3**.[72] The ^{1}H NMR spectrum of the reaction mixture containing **2-11**, **2-12**, and **2-3** indeed indicates the evolution of ethane (0.80 ppm, benzene-d_6).

2.2.6 Attempted synthesis of a (Cy-PSiP)Pt^{IV} species

In an effort to synthesize a [Cy-PSiP]Pt^{IV} species that may serve as a model for the proposed Pt^{IV} intermediate (**2-12**) in the Si-C(sp^3) bond activation process observed for **2-10** at Pt^{II}, complex **2-3** was reacted with one equiv each of either MeI or I_2 (Scheme 2-9). No reaction was observed (by ^{31}P NMR) upon treatment of **2-3** with one equiv of MeI at room temperature in benzene-d_6 solution. Subsequent heating of the reaction mixture at 75 °C for 1 h resulted in quantitative (by ^{31}P NMR) formation of [Cy-PSiP]PtI (**2-13**; 58.9 ppm, $^1J_{PPt}$ = 2948 Hz), which was independently synthesized by the reaction of [Cy-PSiP]H with (COD)PtI_2 (COD = 1,5-cyclooctadiene) in the presence of Et_3N.

Treatment of **2-3** with one equiv of I_2 resulted in the immediate and quantitative (by ^{31}P NMR) formation of **2-13**. No intermediates were observed in the reaction of **2-10** with either MeI or I_2.

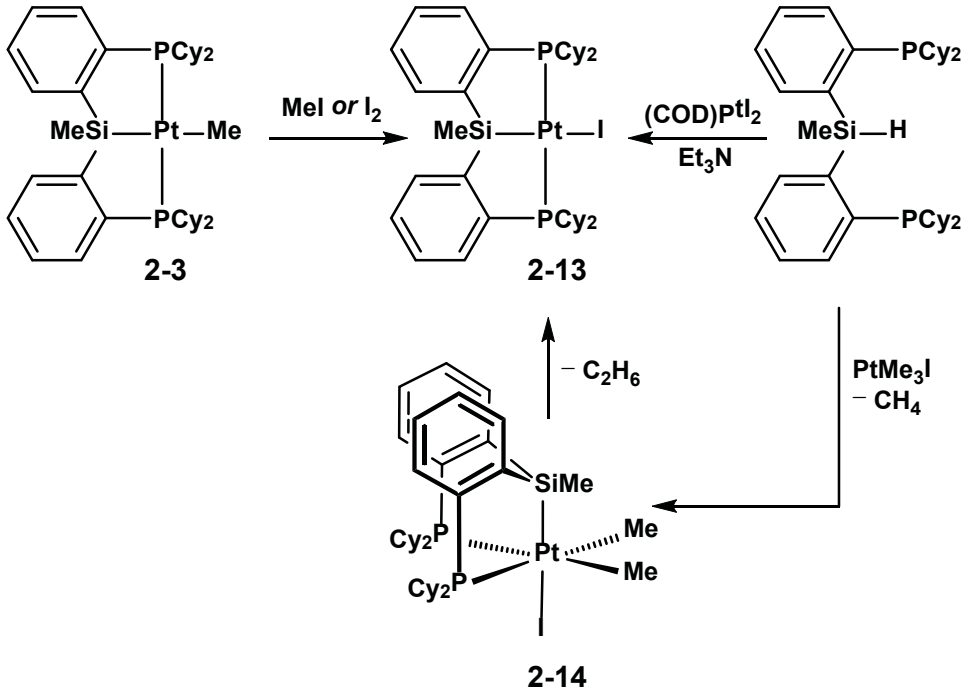

Scheme 2-9. Attempted synthesis of a [Cy-PSiP]Pt^{IV} species.

Alternatively, treatment of [Cy-PSiP]H with one equiv of $PtMe_3I$ in benzene-d_6 solution resulted in the formation of a mixture of two products (2:1 ratio by ^{31}P NMR) upon heating for 3.5 h at 75 °C. The major product (**2-14**) gives rise to a broad ^{31}P NMR resonance at 19.3 ppm ($^1J_{PPt}$ = 1187 Hz), while the minor product corresponds to the Pt^{II} iodo complex **2-13** (Scheme 2). The magnitude of the Pt-P one bond coupling in **2-14** is consistent with a Pt^{IV} species of the type [Cy-PSiP]$PtMe_2I$ (**2-14**; *cf.* $^1J_{PPt}$ = 1112 Hz for (dppe)$PtMe_3I$; dppe = $Ph_2PCH_2CH_2PPh_2$).[72b] The ^1H NMR spectrum of the reaction mixture features resonances for both methane (0.15 ppm) and ethane (0.80 ppm), which

is consistent with initial Si-H activation in [Cy-PSiP]H to liberate methane and form complex **2-14**, followed by C-C reductive elimination in **2-14** to give **2-13**. Further heating of the reaction mixture for 12 h at 95 °C resulted in the quantitative formation of **2-13**. Unfortunately, attempts to isolate the Pt^{IV} species **2-14** were not successful, as **2-13** was always observed as a contaminant. However, the in situ observation of putative **2-14** would appear to suggest that [Cy-PSiP]Pt^{IV} species of this type are synthetically accessible and readily undergo reductive elimination of ethane.

2.3 Conclusions

A new series of Group 10 metal complexes featuring the tridentate bis(phosphino)silyl ligands [κ^3-(2-$Cy_2PC_6H_4)_2Si$Me]$^-$ ([Cy-PSiP]) have been prepared and characterized, including some of the first examples of alkyl and silyl Pt^{II} complexes supported by silyl pincer ligation. Over the course of these studies [Cy-PSiP] ligation has been demonstrated to be an effective platform for the synthesis of a variety of square planar complexes that feature strongly electron-donating ligands, such as alkyl, aryl and silyl, coordinated *trans* to Si. Surprisingly, the reaction of **2-1** with $LiEt_3BH$ did not produce a terminal Pt-H, but rather resulted in the unexpected formation of the η^2-Si-H complex **2-7**. This complex can be viewed as the product of an "arrested" reductive elimination from the unobserved complex [Cy-PSiP]PtH. A cationic Pt^{II} species of the type {[Cy-PSiP]Pt}$^+$ was also prepared by alkyl anion abstraction. Despite the precedent for arene C-H activation by cationic Pt complexes, {[Cy-PSiP]Pt}$^+$ did not exhibit reactivity with benzene C-H bonds. Rather, B-C bond cleavage in the [$MeB(C_6F_5)_3$]$^-$ counteranion was observed to produce [Cy-PSiP]Pt(C_6F_5) and $MeB(C_6F_5)_2$. Heating of

[Cy-PSiP]PtX (X = Cl, OTf) complexes in benzene solution in the presence of amine bases also did not result in benzene C-H activation.

In an effort to further assess the reactivity of [Cy-PSiP]Pt(alkyl) species with respect to E-H bond activation, reactions with H_2 and hydrosilanes were also carried out. Although **2-3** did not react with an atmosphere of H_2 even under forcing conditions, it reacted readily with an equiv of $PhSiH_3$ to form the silane complex [Cy-PSiP]Pt(SiH_2Ph) with loss of CH_4. By comparison, **2-3** reacted with either Ph_2SiHCl, $^{i}Pr_2SiHCl$, or Me_3SiCl to form **2-1** with concomitant evolution of Ph_2SiMeH, $^{i}Pr_2SiMeH$, or Me_4Si, respectively. This reactivity is in stark contrast to that observed for analogous [Ph-PSiP]Pt(alkyl) complexes that reacted with hydridochlorosilanes to form the corresponding silyl complexes. Although the mechanism for the net Si-Cl bond cleavage reactions observed for **2-3** upon exposure to a chlorosilane has not been determined, the divergent reactivity observed for [Ph-PSiP]- versus [Cy-PSiP]Pt(alkyl) species reveals that modification of the steric and electronic properties of the [R-PSiP] ligand directs the outcome of reactions with hydridochlorosilanes towards either Si-H or net Si-Cl bond cleavage. Interestingly, **2-7** reacted with Ph_2SiHCl to produce the corresponding Pt silyl complex **2-9** with concomitant evolution of H_2.

Examples of Si-C(sp^3) bond activation in the silane $(2\text{-}Cy_2PC_6H_4)_2SiMe_2$ involving both Pt^0 and Pt^{II} precursors have also been described. In the case of Si-C cleavage involving Pt^0, [Cy-PSiP]Me reacted readily with $Pt(PPh_3)_4$ to form the Pt^{II} complex [Cy-PSiP]PtMe (**2-3**) with no evidence of intermediate species. The silane also reacted with $[(Me_2S)PtMe_2]_2$ to generate **2-3**. Two intermediate species were observed in situ during the course of the latter reaction. One intermediate was tentatively assigned as

the bis(phosphino) Pt^{II} species (κ^2-Cy-PSiP)$PtMe_2$, which was crystallographically characterized, and is structurally related to the bis(2-pyridyl) dimethylsilane complex (bps)$PtMe_2$. It is thought that Si-C(sp^3) cleavage in (κ^2-Cy-PSiP)$PtMe_2$ leads to the formation of the Pt^{IV} species [Cy-PSiP]$PtMe_3$, which undergoes subsequent elimination of ethane to generate **2-3**. The second intermediate observed in situ during the course of the reaction indeed appears to be a Pt^{IV} species. Unable to isolate the Pt^{IV} complex [Cy-PSiP]$PtMe_3$, attempts to prepare a model species that featured Cy-PSiP coordination to Pt^{IV} were undertaken. Indeed, the reaction of [Cy-PSiP]H with $PtMe_3I$ led to the formation of a Pt^{IV} complex, which was tentatively assigned as [Cy-PSiP]$PtMe_2I$ (**2-14**). The latter also undergoes relatively facile reductive elimination of ethane to generate [Cy-PSiP]PtI. Complex **2-14** features similar spectroscopic features (^{31}P NMR chemical shift and $^1J_{PPt}$) to the previously proposed intermediate [Cy-PSiP]$PtMe_3$. This data to provides indirect evidence for the viability of the intermediate (Cy-PSiP)$PtMe_3$ and for C-C reductive elimination to generate a Pt^{II} species.

2.4 Experimental Section

2.4.1 General considerations

All experiments were conducted under nitrogen in an MBraun glovebox or using standard Schlenk techniques. Dry, oxygen-free solvents were used unless otherwise indicated. Pentane, benzene and toluene were deoxygenated and dried by sparging with nitrogen and subsequent passage through a double-column solvent purification system purchased from MBraun Inc. Tetrahydrofuran and diethyl ether were purified by distillation from Na/benzophenone under N_2. All purified solvents were stored over 4 Å

molecular sieves. All deuterated solvents were degassed via three freeze-pump-thaw cycles and stored over 4 Å molecular sieves. $PtCl_2(SEt_2)_2$, was purchased from Strem Chemicals and used as received. Triethylamine was deoxygenated and dried by sparging with nitrogen and subsequent distillation from CaH_2. The compound (2-$Cy_2PC_6H_4)_2SiHMe$ ([Cy-PSiP]H) was prepared according to literature procedures.[25b] Silanes were purchased from Gelest, degassed via three freeze-pump-thaw cycles, and stored over 4 Å molecular sieves. All other reagents were purchased from Aldrich and used without further purification. Unless otherwise stated, ^{1}H, ^{13}C, ^{31}P, and ^{29}Si NMR characterization data were collected at 300K on a Bruker AV-500 spectrometer operating at 500.1, 125.8, 202.5, and 99.4 MHz (respectively) with chemical shifts reported in parts per million downfield of $SiMe_4$ (for ^{1}H, ^{13}C, and ^{29}Si) or 85% H_3PO_4 in D_2O (for ^{31}P). Unless otherwise stated, ^{19}F NMR characterization data were collected on a Bruker AC-250 spectrometer operating at 235.4 MHz with chemical shifts reported in parts per million relative to a standard sample of 0.5% $CF_3C_6H_5$ in chloroform-*d* at -63.7 ppm. Variable-temperature NMR data were collected on a Bruker AC-250 spectrometer. ^{1}H and ^{13}C NMR chemical shift assignments are based on data obtained from ^{13}C-DEPTQ, ^{1}H-^{1}H COSY, ^{1}H-^{13}C HSQC, and ^{1}H-^{13}C HMBC NMR experiments. ^{29}Si NMR assignments are based on ^{1}H-^{29}Si HMQC and ^{1}H-^{29}Si HMBC experiments. ^{1}H-^{29}Si coupling constants were determined by the use of ^{1}H-coupled ^{1}H-^{29}Si HMQC and ^{1}H-^{29}Si HMBC experiments. Elemental analyses were performed by Canadian Microanalytical Service Ltd. of Delta, British Columbia, Canada. Infrared spectra were recorded as thin films between NaCl plates using a Bruker VECTOR 22 FT-IR spectrometer at a resolution of 4 cm^{-1}.

2.4.2 Synthetic detail and characterization data

[Cy-PSiP]PtCl (2-1). A room temperature solution of [Cy-PSiP]H (0.34 g, 0.57 mmol) in 5 mL of benzene was added to a slurry of $PtCl_2(SEt_2)_2$ (0.25 g, 0.57 mmol) in 5 mL of benzene. The reaction mixture was then treated with Et_3N (0.080 mL, 0.058 g, 0.57 mmol), and the resulting solution was transferred to a thick-walled glass reaction vessel equipped with a Teflon stopcock. The pale yellow reaction mixture was subsequently heated at 65 °C for 30 h, over the course of which a white precipitate was observed. The reaction mixture was allowed to cool to room temperature and was filtered to afford a clear, pale-yellow solution. The volatile components of the filtrate solution were removed under vacuum to afford **2-1** as an off-white solid (0.41 g, 86% yield). ^{1}H NMR (500 MHz, benzene-d_6): δ 8.07 (d, 2 H, H_{arom}, J = 7 Hz), 7.46 (m, 2 H, H_{arom}), 7.29 (t, 2 H, H_{arom}, J = 7 Hz), 7.17 (t, 2 H, H_{arom}, J = 7 Hz), 3.32 (m, 2 H, PC*H*), 2.56 (m, 2 H, PC*H*), 2.36 (m, 2 H, P*Cy*), 2.28 (m, 2 H, P*Cy*), 2.09 (m, 2 H, P*Cy*), 1.76 – 1.32 (24 H, P*Cy*), 1.26 – 0.78 (10 H, P*Cy*), 0.72 (s with Pt satellites, 3 H, Si*Me*, $^3J_{HPt}$ = 26 Hz). ^{13}C{^{1}H} NMR (125.8 MHz, benzene-d_6): δ 156.6 (apparent t, J = 22 Hz, C_{arom}), 141.3 (apparent t, J = 26 Hz, C_{arom}), 133.3 (apparent t, J = 10 Hz, CH_{arom}), 131.7 (CH_{arom}), 130.7 (CH_{arom}), 129.3 (CH_{arom}), 37.3 (apparent t, CH_{Cy}, J = 14 Hz), 37.0 (apparent t, CH_{Cy}, J = 15 Hz), 30.2 (CH_{2Cy}), 29.9 (CH_{2Cy}), 29.2 (CH_{2Cy}), 28.0 (CH_{2Cy}), 27.4 (m, CH_{2Cy}), 27.1 (CH_{2Cy}), 26.3 (CH_{2Cy}), 8.2 (s with Pt satellites, $^2J_{CPt}$ = 56 Hz, Si*Me*). ^{31}P{^{1}H} NMR (202.5 MHz, benzene-d_6): δ 59.4 (s with Pt satellites, $^1J_{PPt}$ = 2984 Hz). ^{29}Si NMR (99.4 MHz, benzene-d_6): δ 32.3 (with Pt satellites, $^1J_{SiPt}$ = 1183 Hz). Anal. Calcd for $C_{37}H_{55}ClP_2PtSi$: C, 54.17; H, 6.76. Found: C, 54.09; H, 6.60.

[Cy-PSiP]Pt(OTf) (2-2). A room temperature solution of **2-1** (0.061 g, 0.074 mmol) in ca. 5 mL of benzene was treated with a slurry of AgOTf (0.019 g, 0.074 mmol) in ca. 3 mL of benzene. A white precipitate was observed upon mixing. The resulting reaction mixture was allowed to stir at room temperature for 45 min. The cloudy solution was then filtered through Celite to give a clear, colorless solution. The volatile components of the filtrate solution were removed under vacuum to afford **2-2** as a white solid (0.060 g, 87% yield). ^{1}H NMR (500 MHz, benzene-d_6): δ 7.89 (d, 2 H, H_{arom}, J = 7 Hz), 7.34 (m, 2 H, H_{arom}), 7.23 (t, 2 H, H_{arom}, J = 7 Hz), 7.13 (t, 2 H, H_{arom}, J = 7 Hz), 2.98 (m, 2 H, PC*H*), 2.81 (m, 2 H, PC*H*), 2.50 (m, 2 H, P*Cy*), 2.29 (m, 2 H, P*Cy*), 1.78 – 0.85 (36 H, P*Cy*), 0.71 (s with Pt satellites, 3 H, Si*Me*, $^{3}J_{HPt}$ = 24 Hz). ^{13}C{^{1}H} NMR (125.8 MHz, benzene-d_6): δ 153.9 (apparent t, J = 21 Hz, C_{arom}), 139.1 (apparent t, J = 26 Hz, C_{arom}), 132.8 (apparent t, J = 10 Hz, CH$_{arom}$), 132.2 (CH$_{arom}$), 131.0 (CH$_{arom}$), 129.6 (CH$_{arom}$), 36.9 (apparent t, CH$_{Cy}$, J = 15 Hz), 36.5 (apparent t, CH$_{Cy}$, J = 13 Hz), 31.0 (CH$_{2Cy}$), 29.8 (CH$_{2Cy}$), 29.6 (CH$_{2Cy}$), 29.4 (CH$_{2Cy}$), 27.8 (m, CH$_{2Cy}$), 27.5 – 27.1 (overlapping resonances, CH$_{2Cy}$), 26.4 (CH$_{2Cy}$), 7.6 (Si*Me*). ^{31}P{^{1}H} NMR (202.5 MHz, benzene-d_6): δ 65.9 (s with Pt satellites, $^{1}J_{PPt}$ = 3055 Hz). ^{29}Si NMR (99.4 MHz, benzene-d_6): δ 18.8 (with Pt satellites, $^{1}J_{SiPt}$ = 1381 Hz). ^{19}F{^{1}H} NMR (235.4 MHz, benzene-d_6): -77.9. Anal. Calcd for $C_{38}H_{55}F_3O_3P_2PtSSi$: C, 48.87; H, 5.94. Found: C, 49.03; H, 6.43.

[Cy-PSiP]PtMe (2-3). A pre-cooled (-30 °C) solution of **2-1** (0.18 g, 0.22 mmol) in ca. 5 mL of THF was treated with MeLi (1.6 M in Et_2O, 0.14 mL, 0.22 mmol). The resulting reaction mixture was allowed to stand at room temperature for 20 min. The volatile components of the reaction mixture were then removed under vacuum, and the

residue was extracted with ca. 10 mL of benzene. The benzene extracts were filtered through Celite and the filtrate was concentrated to dryness under vacuum. The remaining residue was washed with ca. 3 mL of cold (-30 °C) pentane and dried under vacuum to afford **2-3** as a pale yellow solid (0.096 g, 55% yield). ^{1}H NMR (500 MHz, benzene-d_6): δ 8.27 (d, 2 H, H_{arom}, J = 7 Hz), 7.57 (m, 2 H, H_{arom}), 7.34 (t, 2 H, H_{arom}, J = 7 Hz), 7.22 (t, 2 H, H_{arom}, J = 7 Hz), 2.83 (m, 2 H, P*C*H), 2.55 (m, 2 H, P*C*H), 2.27 (br d, 2 H, P*Cy*, J = 13 H), 2.06 (m, 2 H, P*Cy*), 1.78 – 0.83 (39 H, P*Cy* + Pt*Me*, overlapping resonances; the Pt*Me* resonance was identified at 1.25 ppm by the use of correlation spectroscopy), 0.74 (s with unresolved Pt satellites, 3 H, Si*Me*). ^{13}C{^{1}H} NMR (125.8 MHz, benzene-d_6): δ 160.3 (apparent t, J = 22 Hz, C_{arom}), 144.4 (apparent t, J = 26 Hz, C_{arom}), 134.1 (apparent t, J = 10 Hz, *C*H$_{arom}$), 131.4 (*C*H$_{arom}$), 130.3 (*C*H$_{arom}$), 128.9 (*C*H$_{arom}$), 38.0 (apparent t, *C*H$_{Cy}$, J = 13 Hz), 37.3 (apparent t, *C*H$_{Cy}$, J = 15 Hz), 30.3 (*C*H$_{2Cy}$), 29.6 (*C*H$_{2Cy}$), 29.2 (*C*H$_{2Cy}$), 28.1 – 27.0 (overlapping resonances, *C*H$_{2Cy}$), 26.5 (*C*H$_{2Cy}$), 9.2 (Si*Me*), -1.6 (t, $^{2}J_{CP}$ = 8 Hz, Pt*Me*). ^{31}P{^{1}H} NMR (202.5 MHz, benzene-d_6): δ 57.9 (s with Pt satellites, $^{1}J_{PPt}$ = 2938 Hz). ^{29}Si NMR (99.4 MHz, benzene-d_6): δ 63.9 (with Pt satellites, $^{1}J_{SiPt}$ = 696 Hz). Anal. Calcd for $C_{38}H_{58}P_2PtSi$: C, 57.05; H, 7.31. Found: C, 56.62; H, 7.34.

[Cy-PSiP]PtPh (2-4). A pre-cooled (-30 °C) solution of **2-1** (0.070 g, 0.085 mmol) in ca. 5 mL of THF was treated with PhLi (1.8 M in ^{n}Bu$_2$O, 47.4 μL, 0.085 mmol). The resulting reaction mixture was allowed to stand at room temperature for 20 min. The volatile components of the reaction mixture were then removed under vacuum, and the residue was extracted with ca. 10 mL of benzene. The benzene extracts were filtered through Celite and the filtrate was concentrated to dryness under vacuum to afford **2-4** as a yellow solid (0.069 g, 94% yield). ^{1}H NMR (500 MHz, benzene-d_6): δ

8.27 (d, 2 H, H_{arom}, J = 7 Hz), 7.96 (br d with Pt satellites, 2 H, Pt*Ph*$_{ortho}$, $^{3}J_{HPt}$ = 37 Hz), 7.55 – 7.47 (overlapping resonances, 4 H, H_{arom} + Pt*Ph*$_{meta}$), 7.33 (t, 2 H, H_{arom}, J = 7 Hz), 7.20 (t, 2 H, H_{arom}, J = 7 Hz), 7.13 (t, 1 H, Pt*Ph*$_{para}$, J = 7 Hz), 2.81 (m, 2 H, PC*H*), 2.44 (m, 2 H, PC*H*), 1.92 (m, 4 H, P*Cy*), 1.73 – 0.91 (36 H, P*Cy*), 0.71 (s with Pt satellites, 3 H, Si*Me*, $^{3}J_{HPt}$ = 11 Hz). $^{13}C\{^{1}H\}$ NMR (125.8 MHz, benzene-d_6): δ 177.8 (apparent t, J = 10 Hz, PtC_{ipso}), 159.7 (apparent t, J = 22 Hz, C_{arom}), 143.5 (apparent t, J = 26 Hz, C_{arom}), 142.2 (br s, Pt*Ph*$_{ortho}$), 134.0 (apparent t, J = 10 Hz, *C*H$_{arom}$), 131.5 (*C*H$_{arom}$), 130.5 (*C*H$_{arom}$), 128.7 (*C*H$_{arom}$), 127.9 (br s, Pt*Ph*$_{meta}$), 122.4 (Pt*Ph*$_{para}$), 37.9 (apparent t, *C*H$_{Cy}$, J = 14 Hz), 35.2 (apparent t, *C*H$_{Cy}$, J = 15 Hz), 30.6 (m, *C*H$_{2Cy}$), 29.8 (*C*H$_{2Cy}$), 28.7 – 27.4 (overlapping resonances, *C*H$_{2Cy}$), 26.8 (d, *C*H$_{2Cy}$, J = 8 Hz), 9.5 (s with Pt satellites, $^{2}J_{CPt}$ = 31 Hz, Si*Me*). $^{31}P\{^{1}H\}$ NMR (202.5 MHz, benzene-d_6): δ 56.2 (s with Pt satellites, $^{1}J_{PPt}$ = 2921 Hz). ^{29}Si NMR (99.4 MHz, benzene-d_6): δ 59.7 (with Pt satellites, $^{1}J_{SiPt}$ = 646 Hz). Anal. Calcd for $C_{43}H_{60}P_2PtSi$: C, 59.91; H, 7.02. Found: C, 59.97; H, 6.96. A crystal of **2-4·OEt$_2$** suitable for single-crystal X-ray diffraction studies was grown from a concentrated diethyl ether solution of **2-4** at -30 °C.

{[Cy-PSiP]Pt}$^{+}$[B(C$_6$F$_5$)$_3$Me]$^{-}$ (2-5). A room temperature solution of **2-3** (0.070 g, 0.088 mmol) in ca. 5 mL of benzene was treated with B(C_6F_5)$_3$ (0.045 g, 0.088 mmol). The resulting homogeneous yellow solution was allowed to stand at room temperature for 12 h. The volatile components were then removed under vacuum and the remaining residue was washed with 2 × 3 mL of cold (-30 °C) pentane and dried in vacuo to afford **2-5** as a yellow solid (0.10 g, 87% yield). ^{1}H NMR (500 MHz, benzene-d_6): δ 7.68 (d, 2 H, H_{arom}, J = 7 Hz), 7.17 – 7.12 (overlapping resonances, 4 H, H_{arom}), 7.07 (t, 2 H, H_{arom}, J = 7 Hz), 2.54 (m, 2 H, PC*H*), 2.32 (m, 2 H, PC*H*), 2.06 (br d, 2 H, P*Cy*, J = 11 Hz),

1.90 (br d, 2 H, P*Cy*, J = 11 Hz), 1.63 – 0.80 (37 H, P*Cy* + B*Me*, overlapping resonances; the B*Me* resonance was identified at 1.59 ppm by the use of correlation spectroscopy), 0.83 (m, 2 H, P*Cy*), 0.60 (s, 3 H, Si*Me*). $^{13}C\{^1H\}$ NMR (125.8 MHz, benzene-d_6): δ 150.4 (br m, C_{arom}), 136.6 (br m, C_{arom}), 132.5 (apparent t, J = 9 Hz, CH_{arom}), 132.3 (CH_{arom}), 131.7 (CH_{arom}), 130.4 (CH_{arom}), 37.5 – 37.2 (overlapping resonances, CH_{Cy}), 31.0 (CH_{2Cy}), 30.3 (CH_{2Cy}), 30.0 (CH_{2Cy}), 29.5 (CH_{2Cy}), 27.3 – 27.0 (overlapping resonances, CH_{2Cy}), 26.6 (CH_{2Cy}), 26.2 (CH_{2Cy}), 7.7 (Si*Me*), 0.1 (br, B*Me*). $^{31}P\{^1H\}$ NMR (202.5 MHz, benzene-d_6): δ 70.8 (s with Pt satellites, $^1J_{PPt}$ = 3038 Hz). ^{29}Si NMR (99.4 MHz, benzene-d_6): δ 22.9 (with Pt satellites, $^1J_{SiPt}$ = 971 Hz). $^{11}B\{^1H\}$ NMR (160.5 MHz, benzene-d_6): δ -14.0. $^{19}F\{^1H\}$ NMR (235.4 MHz, 25 °C, benzene-d_6): δ -132.3 (d, 6 F, J_{FF} = 20 Hz, C_6F_{5ortho}), -162.8 (apparent t, 3 F, J_{FF} = 22 Hz, C_6F_{5para}), -166.3 (apparent t, 6 F, J_{FF} = 21 Hz, C_6F_{5meta}). Anal. Calcd for $C_{56}H_{58}BF_{15}P_2PtSi$: C, 51.27; H, 4.46. Found: C, 50.50; H, 4.70.

[Cy-PSiP]Pt(C_6F_5) (2-6). A solution of **2-5** (0.051 g, 0.039 mmol) in ca. 5 mL of benzene was heated at 100 °C for 48 h. The volatile components were removed under vacuum. The remaining residue was washed with 2 × 3 mL of cold (-30 °C) pentane and dried in vacuo to afford **2-6** as an off-white solid (0.032 g, 86% yield). ^1H NMR (500 MHz, benzene-d_6): δ 8.14 (d, 2 H, H_{arom}, J = 7 Hz), 7.44 (m, 2 H, H_{arom}), 7.32 (t, 2 H, H_{arom}, J = 7 Hz), 7.18 (t, 2 H, H_{arom}, J = 7 Hz), 2.56 (m, 2 H, PC*H*), 2.37 (m, 2 H, PC*H*), 1.97 (br d, 2 H, P*Cy*, J = 14 Hz), 1.85 (br d, 2 H, P*Cy*, J = 14 Hz), 1.56 – 0.72 (36 H, P*Cy*), 0.57 (s with Pt satellites, 3 H, Si*Me*, $^3J_{HPt}$ = 16 Hz). $^{13}C\{^1H\}$ NMR (125.8 MHz, benzene-d_6): δ 158.1 (apparent t, J = 22 Hz, C_{arom}), 141.4 (apparent t, J = 26 Hz, C_{arom}),

133.7 (apparent t, J = 10 Hz, CH$_{arom}$), 131.5 (CH$_{arom}$), 131.1 (CH$_{arom}$), 129.1 (CH$_{arom}$), 37.8 – 37.5 (overlapping resonances, CH$_{Cy}$), 30.2 – 26.6 (overlapping resonances, CH$_{2Cy}$), 9.4 (Si*Me*). ^{31}P{^{1}H} NMR (202.5 MHz, benzene-d_6): δ 60.1 (s with Pt satellites, $^{1}J_{PPt}$ = 2919 Hz). ^{29}Si NMR (99.4 MHz, benzene-d_6): δ 53.8 (with Pt satellites, J_{SiPt} = 806 Hz). ^{19}F{^{1}H} NMR (470.8 MHz, 25 °C, benzene-d_6): δ -110.8 (d with Pt satellites, 1 F, J_{FF} = 33 Hz, $^{3}J_{FPt}$ = 255 Hz, C$_6F_{5ortho}$), -112.1 (d with unresolved Pt satellites, 1 F, J_{FF} = 38 Hz, C$_6F_{5ortho}$), -162.0 (m, 1 F, C$_6F_{5para}$), -162.8 (m, 1 F, C$_6F_{5meta}$), -163.8 (m, 1 F, C$_6F_{5meta}$).

[Cy-P*Si*(*μ*-H)P]*Pt* (2-7). A pre-cooled (-30 °C) solution of **2-1** (0.10 g, 0.12 mmol) in ca. 5 mL of THF was treated with LiEt$_3$BH (1.0 M in THF, 0.12 mL, 0.12 mmol). The resulting tan-colored reaction mixture was allowed to stand at room temperature for 20 min. The volatile components of the reaction mixture were then removed under vacuum, and the residue was extracted with ca. 10 mL of benzene. The benzene extracts were filtered through Celite and the filtrate was concentrated to dryness under vacuum to afford **2-7** as an off-white solid (0.087 g, 92% yield). ^{1}H NMR (500 MHz, benzene-d_6): δ 8.25 (d, 2 H, H_{arom}, J = 7 Hz), 7.47 (m, 2 H, H_{arom}), 7.33 (t, 2 H, H_{arom}, J = 7 Hz), 7.19 (t, 2 H, H_{arom}, J = 7 Hz), 5.48 (t with Pt satellites, 1 H, Pt-*H*-Si, J_{HPt} = 921 Hz, J_{HP} = 19 Hz), 2.63 (m, 2 H, P*Cy*), 2.39 (m, 2 H, P*Cy*), 2.30 – 2.23 (4 H, P*Cy*), 2.00 (br d, 2 H, J = 12 Hz, P*Cy*), 1.86 (br s, 4 H, P*Cy*), 1.65 – 0.75 (overlapping resonances, 33 H, P*Cy* + Si*Me*; the Si*Me* resonance was identified at 0.96 ppm by the use of correlation spectroscopy). ^{13}C{^{1}H} NMR (125.8 MHz, benzene-d_6): δ 160.0 (apparent t, J = 22 Hz, C_{arom}), 143.9 (apparent t, J = 22 Hz, C_{arom}), 134.5 (apparent t, J = 10 Hz, CH$_{arom}$), 131.3 (CH$_{arom}$), 130.5 (CH$_{arom}$), 128.7 (CH$_{arom}$), 38.7 (apparent t, CH$_{Cy}$, J = 13

Hz), 35.1 (apparent t, *C*H$_{Cy}$, *J* = 17 Hz), 32.3 (*C*H$_{2Cy}$), 29.6 (m, *C*H$_{2Cy}$), 29.0 – 27.1 (overlapping resonances, *C*H$_{2Cy}$), 26.6 (*C*H$_{2Cy}$), 9.1 (s with Pt satellites, $^{2}J_{CPt}$ = 33 Hz, Si*Me*). ^{31}P{^{1}H} NMR (202.5 MHz, benzene-d_6): δ 76.6 (s with Pt satellites, $^{1}J_{PPt}$ = 2908 Hz). ^{29}Si NMR (99.4 MHz, benzene-d_6): δ 62.3 (with Pt satellites, J_{SiPt} = 735 Hz, J_{SiH} = 52 Hz). IR (film, cm^{-1}): 1808 (br m, M-H). Anal. Calcd for $C_{37}H_{56}P_2PtSi$: C, 56.54; H, 7.18. Found: C, 56.35; H, 7.11.

[Cy-PSiP]Pt(SiH$_2$Ph) (2-8). A room temperature solution of **2-3** (0.050 g, 0.063 mmol) in ca. 5 mL of benzene was treated with $PhSiH_3$ (0.007 g, 7.7 μL, 0.063 mmol). The resulting reaction mixture was allowed to stand at room temperature for 18 h. The volatile components were then removed under vacuum to afford **2-8** as a pale yellow solid (0.054 g, 96% yield). ^{1}H NMR (500 MHz, benzene-d_6): δ 8.23 (d, 2 H, *H*$_{arom}$, *J* = 7 Hz), 8.04 (d, 2 H, Si*Ph*$_{ortho}$, *J* = 7 Hz), 7.56 (m, 2 H, *H*$_{arom}$), 7.33 (t, 2 H, *H*$_{arom}$, *J* = 7 Hz), 7.29 (t, 2 H, Si*Ph*$_{meta}$, *J* = 7 Hz), 7.21 (t, 2 H, *H*$_{arom}$, *J* = 7 Hz), 7.16 (t, 1 H, Si*Ph*$_{para}$, *J* = 7 Hz), 6.01 (t with Pt and Si satellites, 2 H, PtSi*H*$_2$Ph, $^{1}J_{SiH}$ = 152 Hz, $^{2}J_{HPt}$ = 33 Hz, $^{3}J_{HP}$ = 4 Hz), 2.85 (m, 2 H, PC*H*), 2.54 (m, 2 H, PC*H*), 2.08 – 2.01 (4 H, P*Cy*), 1.82 – 1.58 (6 H, P*Cy*), 1.58 – 0.78 (overlapping resonances, 30 H, P*Cy*), 0.69 (s, 3 H, Si*Me*). ^{13}C{^{1}H} NMR (125.8 MHz, benzene-d_6): δ 158.6 (apparent t, *J* = 22 Hz, *C*$_{arom}$), 148.4 (Si*Ph*$_{ipso}$), 144.5 (apparent t, *J* = 24 Hz, *C*$_{arom}$), 137.5 (Si*Ph*$_{ortho}$), 133.9 (apparent t, *J* = 10 Hz, *C*H$_{arom}$), 132.0 (*C*H$_{arom}$), 130.8 (*C*H$_{arom}$), 128.8 (*C*H$_{arom}$), 127.9 (Si*Ph*$_{meta}$), 127.0 (Si*Ph*$_{para}$), 39.1 (apparent t, *C*H$_{Cy}$, *J* = 17 Hz), 37.5 (apparent t, *C*H$_{Cy}$, *J* = 17 Hz), 31.2 (*C*H$_{2Cy}$), 30.1 – 29.3 (overlapping resonances, *C*H$_{2Cy}$), 27.8 – 27.2 (overlapping resonances, *C*H$_{2Cy}$), 26.6 (*C*H$_{2Cy}$), 9.9 (Si*Me*). ^{31}P{^{1}H} NMR (202.5 MHz, benzene-d_6): δ 66.4 (s with Pt satellites, $^{1}J_{PPt}$ = 2723 Hz). ^{29}Si NMR (99.4 MHz, benzene-d_6): δ 81.6

(with Pt satellites, $^{1}J_{SiPt}$ = 650 Hz, *Si*Me), 81.3 (with Pt satellites, $^{1}J_{SiPt}$ = 1067 Hz, $^{1}J_{SiH}$ = 152 Hz, *Si*H_2Ph). IR (film, cm^{-1}): 2018 (br m, Si-H). Anal. Calcd for $C_{43}H_{62}P_2PtSi_2$: C, 57.89; H, 7.00. Found: C, 57.78; H, 7.09.

[Cy-PSiP]Pt($SiPh_2Cl$) (2-9). A room temperature solution of **2-7** (0.10 g, 0.13 mmol) in ca. 5 mL of benzene was treated with Ph_2SiHCl (0.028 g, 24.9 μL, 0.13 mmol). The resulting reaction mixture was allowed to stand at room temperature for 16 h. The volatile components were then removed under vacuum to afford **2-9** as a pale yellow solid (0.12 g, 92% yield). ^{1}H NMR (500 MHz, benzene-d_6): δ 8.21 (d, 2 H, H_{arom}, J = 7 Hz), 8.13 (d, 4 H, Si*Ph*$_{ortho}$, J = 7 Hz), 7.53 (m, 2 H, H_{arom}, J = 7 Hz), 7.32 (t, 2 H, H_{arom}, J = 7 Hz), 7.26 (t, 4 H, Si*Ph*$_{meta}$, J = 7 Hz), 7.18 (t, 2 H, H_{arom}, J = 7 Hz), 7.13 (m, 2 H, Si*Ph*$_{para}$), 3.06 (m, 2 H, PC*H*), 2.30 (m, 2 H, PC*H*), 2.08 (m, 2 H, P*Cy*), 1.74 – 0.90 (overlapping resonances, 36 H, P*Cy*), 0.76 (s with unresolved Pt satellites, 3 H, Si*Me*), 0.72 (m, 2 H, P*Cy*). ^{13}C{^{1}H} NMR (125.8 MHz, benzene-d_6): δ 157.5 (apparent t, J = 22 Hz, C_{arom}), 151.7 (Si*Ph*$_{ipso}$), 143.3 (apparent t, J = 24 Hz, C_{arom}), 136.4 (Si*Ph*$_{ortho}$), 133.8 (apparent t, J = 10 Hz, CH$_{arom}$), 132.9 (CH$_{arom}$), 130.9 (CH$_{arom}$), 128.7 (CH$_{arom}$), 128.3 (Si*Ph*$_{para}$), 127.9 (Si*Ph*$_{meta}$), 39.8 (apparent t, J = 16 Hz, CH$_{Cy}$), 37.9 (apparent t, J = 14 Hz, CH$_{Cy}$), 32.3 (CH$_{2Cy}$), 30.5 – 30.0 (overlapping resonances, CH$_{2Cy}$), 27.9 – 26.1 (overlapping resonances, CH$_{2Cy}$), 9.7 (Si*Me*). ^{31}P{^{1}H} NMR (202.5 MHz, benzene-d_6): δ 65.8 (s with Pt satellites, $^{1}J_{PPt}$ = 2710 Hz). ^{29}Si NMR (99.4 MHz, benzene-d_6): δ 74.9 (with Pt satellites, $^{1}J_{SiPt}$ = 638 Hz, *Si*Me), 62.2 (with Pt satellites, $^{1}J_{SiPt}$ = 1357 Hz, *Si*Ph_2Cl). Anal. Calcd for $C_{49}H_{65}ClP_2PtSi_2$: C, 58.69; H, 6.53. Found: C, 58.53; H, 6.67.

(2-$Cy_2PC_6H_4$)$_2SiMe_2$ (2-10). A solution of 2-$Cy_2PC_6H_4Br$ (5.00 g, 14.2 mmol) in ca. 120 mL of pentane was cooled to -78 °C. ^{n}BuLi (8.85 mL, 1.6 M in hexanes, 14.2

mmol) was added dropwise to this solution. The reaction mixture was allowed to warm to room temperature and stir for an additional 18 h. The mixture was once again cooled to -78 °C and Cl_2SiMe_2 (0.86 mL, 7.1 mmol) was added via syringe. The resulting yellow reaction mixture was allowed to warm to room temperature and continue stirring for an additional 14 h at room temperature. The volatile components were then removed in vacuo and the remaining residue was extracted into ca. 50 mL of benzene. The benzene extracts were filtered through Celite and the benzene was removed in vacuo to afford a sticky yellow solid that was washed with cold (-30 °C) pentane (2 × 15 mL) to give (2-$Cy_2PC_6H_4)_2SiMe_2$ (3.13 g, 73%) as an off-white solid. ^{1}H NMR (500 MHz, benzene-d_6): δ 7.90 (m, 2 H, H_{arom}), 7.45 (m, 2 H, H_{arom}), 7.19 – 7.16 (4 H, H_{arom}), 1.91 (m, 4 H, P*Cy*), 1.76 – 1.69 (8 H, P*Cy*), 1.59 - 1.52 (8 H, P*Cy*), 1.46 (m, 4 H, P*Cy*), 1.31 – 1.18 (8 H, P*Cy*), 1.13 (t, 6 H, Si*Me*$_2$, J_{HP} = 2 Hz), 1.10 – 0.95 (12 H, P*Cy*). ^{13}C{^{1}H} NMR (125.8 MHz, benzene-d_6): δ 149.9 (d, C_{arom}, J_{CP} = 45 Hz), 144.5 (d, C_{arom}, J_{CP} = 18 Hz), 137.8 (d, CH_{arom}, J_{CP} = 15 Hz), 133.0 (CH_{arom}), 128.7 (CH_{arom}), 128.3 (CH_{arom}), 36.9 (d, CH_{Cy}, J_{CP} = 15 Hz), 31.4 (CH_{2Cy}), 31.3 (CH_{2Cy}), 28.1 (d, CH_{2Cy}, J_{CP} = 10 Hz), 27.9 (d, CH_{2Cy}, J_{CP} = 10 Hz), 27.2 (CH_{2Cy}), 5.9 (t, Si*Me*$_2$, J_{CP} = 13 Hz). ^{31}P{^{1}H} NMR (202.5 MHz, benzene-d_6): δ -6.6. ^{29}Si NMR (99.4 MHz, benzene-d_6): δ -7.4. Anal. Calcd for $C_{38}H_{58}P_2Si$: C, 75.45; H, 9.66. Found: C, 75.41; H, 9.71.

Synthesis of 2-3 via Si-C(sp^3) bond cleavage involving Pt^0. A solution of **2-10** (0.10 g, 0.17 mmol) in ca. 5 mL of benzene was added to $Pt(PPh_3)_4$ (0.21 g, 0.17 mmol). The resulting pale yellow solution was allowed to stand at room temperature over the course of 48 h. The volatile components of the reaction mixture were subsequently removed in vacuo and the remaining residue was washed with cold (-30 °C)

pentane (5 × 3 mL) and dried under vacuum to afford **2-3** as a pale yellow solid (0.12 g, 86% yield).

Generation of 2-3 via Si-C(sp^3) bond cleavage involving Pt^{II} A solution of **2-10** (0.030 g, 0.050 mmol) in ca. 1 mL of benzene-d_6 was added to $[Pt(SMe_2)Me_2]_2$ (0.014 g, 0.025 mmol). The resulting yellow solution was allowed to stand at room temperature over the course of five days and was monitored by ^{31}P and ^{1}H NMR spectroscopy. After standing at room temperature for 18 h, ^{31}P NMR analysis of the reaction mixture indicated 80% consumption of **2-10** and the formation of a product mixture consisting of **2-11** (27.7 ppm, $^{1}J_{PPt}$ = 2050 Hz) and **5** (23.1 ppm, br s, $^{1}J_{PPt}$ = 934 Hz) in a 1:3 ratio. After standing at room temperature for 5 days, ^{31}P NMR analysis of the reaction mixture indicated complete consumption of **2-10** and the formation of a product mixture consisting of **2-3** (57.9 ppm, $^{1}J_{PPt}$ = 2938 Hz), **2-11** (27.7 ppm, $^{1}J_{PPt}$ = 2050 Hz) and **2-12** (23.1 ppm, br s, $^{1}J_{PPt}$ = 934 Hz) in a 1:1:1 ratio. Although ^{1}H NMR analysis of the resulting product mixtures was complicated by the overlap of aryl and cyclohexyl proton resonances, a resonance at 0.80 ppm corresponding to ethane was observed.

[Cy-PSiP]PtI (2-13). A solution of [Cy-PSiP]H (0.10 g, 0.17 mmol) in. ca 2 mL of benzene was added to $(COD)PtI_2$ (0.095 g, 0.17 mmol). The resulting reaction mixture was treated with NEt_3 (0.026 mL, 0.19 mmol). The reaction mixture was subsequently allowed to stand at room temperature for 1 h, and was then filtered through Celite. The volatile components of the filtrate solution were removed under vacuum. The remaining yellow residue was washed with ca. 3 mL of cold (-30 ˚C) pentane and dried under vacuum to afford **2-13** as a pale yellow solid (0.15 g, 96% yield). The spectroscopic data obtained for **2-13** are in good agreement with the previously reported analogous

complexes [Cy-PSiP]PtCl and [Cy-PSiP]PtOTf [5]. ^{1}H NMR (500 MHz, benzene-d_6): δ 8.07 (d, 2 H, H_{arom}, J = 7 Hz), 7.51 (m, 2 H, H_{arom}), 7.31 (t, 2 H, H_{arom}, J = 7 Hz), 7.19 (t, 2 H, H_{arom}, J = 7 Hz), 3.43 (m, 2 H, PC*H*), 2.77 (m, 2 H, PC*H*), 2.40 (m, 2 H, PC*y*), 2.24 – 2.09 (overlapping resonances, 6 H, PC*y*), 1.75 - 0.82 (overlapping resonances, 32 H, PC*y*), 0.68 (s with Pt satellites, 3 H, Si*Me*, $^{3}J_{HPt}$ = 26 Hz). ^{13}C{^{1}H} NMR (125.8 MHz, benzene-d_6): δ 156.4 (apparent t, $C_{arom,}$ J = 22 Hz), 141.1 (apparent t, $C_{arom,}$ J = 25 Hz), 133.3 (CH$_{arom}$), 131.8 (CH$_{arom}$), 130.9 (CH$_{arom}$), 129.4 (CH$_{arom}$), 39.5 (apparent t, CH$_{Cy}$, J = 15 Hz), 37.9 (apparent t, CH$_{Cy}$, J = 13 Hz), 31.6 - 26.3 (overlapping resonances, CH$_{2Cy}$), 8.4 (Si*Me*). ^{31}P {^{1}H} NMR (202.5 MHz, benzene-d_6): δ 59.0 (s with Pt satellites, $^{1}J_{PPt}$ = 2948 Hz). ^{29}Si NMR (99.4 MHz, benzene-d_6): δ 39.8 (s with Pt satellites, $^{1}J_{SiPt}$ = 1155 Hz).

Generation of 2-13 via the reaction of 2-3 with MeI. A solution of **2-3** (0.015 g, 0.019 mmol) in ca. 1 mL of benzene-d_6 was treated with MeI (1.2 μl, 0.019 mmol). The resulting pale yellow reaction mixture was heated at 75 °C for 1 h, at which point ^{31}P NMR analysis indicated quantitative conversion to **2-13**.

Generation of 2-13 via the reaction of 2-3 with I_2. A solution of **2-3** (0.010 g, 0.013 mmol) in ca. 1 mL of benzene-d_6 was treated with I_2 (0.003 g, 0.013 mmol). The resulting purple reaction mixture was allowed to stand at room temperature over the course of 10 minutes, at which point ^{31}P NMR analysis indicated quantitative conversion to **2-13**.

Generation of 2-4 via $PtMe_3I$ A solution of [Cy-PSiP]H (0.015 g, 0.025 mol) in ca. 1 mL of benzene-d_6 was added to $PtMe_3I$ (0.009 g, 0.025 mmol). The reaction mixture was subsequently heated at 75 °C over the course of 3.5 h, at which

point ^{31}P NMR analysis indicated complete consumption of [Cy-PSiP]H and the formation of a product mixture consisting of **2-13** and **2-14** (19.3 ppm, br s, $^{1}J_{PPt}$ = 1187 Hz) in a 1:2 ratio. Subsequent heating of the reaction mixture at 95 °C for 12 h resulted in the quantitative formation of **2-13**. ^{1}H NMR (500 MHz) analysis of the reaction mixture after heating at 75 °C for 3.5 h revealed several resonances that could be unambiguously assigned to **2-14** (as well as the formation of ethane and methane): δ 7.65 (d, 2 H, H_{arom}, J = 7 Hz). 7.46 (m, 2 H, H_{arom}), 7.12 (t, 2 H, H_{arom}, J = 7 Hz), 7.03 (t, 2 H, H_{arom}, J = 7 Hz), 0.35 – 0.86 (overlapping resonances corresponding to P*Cy* and Pt*Me* protons in **2-13** and **2-14**), 0.61 (s with Pt satellites, 3 H, Si*Me*, $^{3}J_{HPt}$ = 17 Hz).

2.4.3 Crystallographic solution and refinement details

Crystallographic data for each of **2-4**·OEt_2 and **2-11** were obtained at 173(±2) K on a Bruker D8/APEX II CCD diffractometer using graphite-monochromated Mo Kα (λ = 0.71073 Å) radiation, employing a sample that was mounted in inert oil and transferred to a cold gas stream on the diffractometer. Programs for diffractometer operation, data collection, and data reduction (including SAINT) were supplied by Bruker. Gaussian integration (face-indexed) was employed as the absorption correction method in each case. All structures were solved by use of the Patterson search/structure expansion and were refined by use of full-matrix least-squares procedures (on F^2) with R_1 based on $F_o^2 \geq 2\sigma(F_o^2)$ and wR_2 based on $F_o^2 \geq -3\sigma(F_o^2)$. During the structure solution process for **2-4**·OEt_2, one equivalent of diethyl ether was located in the asymmetric unit and refined in a satisfactory manner. Anisotropic displacement parameters were employed for all the non-hydrogen atoms in **2-4**·OEt_2 and **2-11**. Hydrogen atoms were added at calculated

positions and refined by use of a riding model employing isotropic displacement parameters based on the isotropic displacement parameters of the attached atoms. Additional crystallographic information for **2-4** and **2-11** is provided in Appendix A.

CHAPTER 3: Synthesis and Reactivity of [Cy-PSiP]M^{II} (M = Ni, Pd) Complexes

3.1 Introduction

In the course of extending the previously observed [Cy-PSiP]Pt^{II} chemistry to Ni and Pd, an unusual ligand rearrangement was observed which resulted in facile Si-C(sp^2) and Si-C(sp^3) bond cleavage. [68,69,71, 73,74] Notably, for M = Ni these Si-C bond activation processes are reversible on the NMR timescale in solution. Although Si-C(sp^2) bond activation is well documented,[73] examples of unstrained Si-C(sp^3) bond cleavage within the coordination sphere of a mononuclear metal complex are extremely rare,[68,69,71,74] and are unprecedented for Ni.[75] Remarkably, this ligand rearrangement was not observed in our [Cy-PSiP]Pt^{II} chemistry.

3.2 Results and Discussion

3.2.1 Synthesis and characterization of [Cy-PSiP]MCl (M = Ni, Pd) complexes.

As an entry point into the chemistry of [Cy-PSiP]M (M = Ni, Pd) complexes, metal chloride species of the type [Cy-PSiP]MCl were targeted. Towards this end, treatment of [Cy-PSiP]H with one equiv each of $(PPh_3)_2NiCl_2$ and NEt_3 in benzene solution at room temperature resulted in the formation of [Cy-PSiP]NiCl (**3-1**) with concomitant elimination of $HCl{\cdot}NEt_3$. Analytically pure **3-1** was isolated as a yellow solid in 97% yield. The solution NMR data for isolated **3-1** (benzene-d_6) are consistent with the formation of a diamagnetic C_s-symmetric complex featuring tridentate

coordination of the [Cy-PSiP] ligand to the Ni center. The solid state structure of **3-1** was confirmed by single crystal X-ray diffraction analysis (Figure 3-1,Table 3-1). Complex **3-1** exhibits square planar geometry at Ni in the solid state with a Ni-Cl bond distance of 2.242(1) Å.

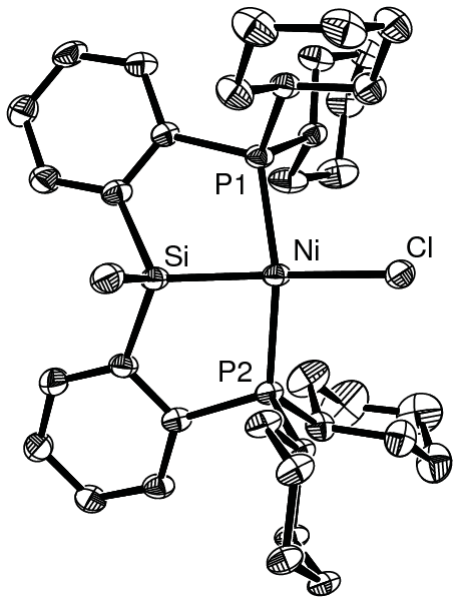

Figure 3-1. ORTEP diagram for **3-1** shown with 50% displacement ellipsoids; hydrogen atoms have been removed for clarity.

Table 3-1. Selected interatomic distances (Å) and angles (°) for **3-1**.

Interatomic Distances (Å)			
Ni-P1	2.1977(11)	Ni-Si	2.2136(12)
Ni-P2	2.1908(11)	Ni-Cl	2.2419(12)
Interatomic Angles (°)			
P1-Ni-P2	160.86(4)	P1-Ni-Si	83.87(4)
Si-Ni-Cl	170.70(5)	P2-Ni-Cl	94.86(4)

Similarly, the Pd analogue [Cy-PSiP]PdCl (**3-2**) was synthesized by reacting [Cy-PSiP]H with half an equiv of $[(\eta^3\text{-}C_3H_5)PdCl]_2$ in benzene solution at room temperature (Scheme 2-8). Complex **3-2** was isolated as an off white solid in 78% yield. As in the case of **3-1**, the solution NMR data for isolated **3-2** (benzene-d_6) are consistent with the formation of a C_s-symmetric, square planar complex.

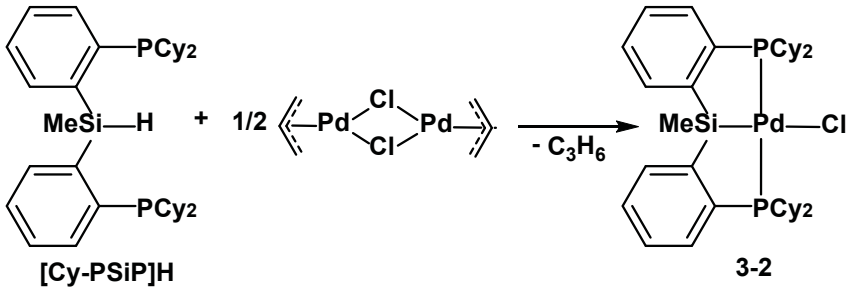

Scheme 3-1. Synthesis of [Cy-PSiP]PdCl (**3-2**).

3.2.2 Synthesis and reactivity of [Cy-PSiP]M(alkyl) complexes (M = Ni, Pd): observation of Si-C(sp^2) and Si-C(sp^3) bond cleavage chemistry

In the pursuit of new Ni and Pd alkyl complexes, **3-1** and **3-2** were treated with alkyl lithium and Grignard reagents. In the case of **3-2**, treatment with one equiv of MeLi led to the formation of [Cy-PSiP]PdMe (**3-3**), which was isolated in 78% yield (Scheme 3-2). The NMR spectra of isolated **3-3** (benzene-d_6) are consistent with a C_s-symmetric complex, as indicated by the presence of a single ^{31}P NMR resonance at 60.5 ppm. The ^{1}H NMR spectrum of **3-3** features a singlet at 0.72 ppm that corresponds to the Si*Me* protons of the pincer ligand, as well as a triplet at 0.56 ppm ($^3J_{HP}$ = 4 Hz) that corresponds to the Pd*Me* group. Interestingly, upon standing at room temperature ^{31}P NMR analysis of a benzene solution of **3-3** revealed the appearance of a new species (**3-4**) that features inequivalent phosphorous environments, as indicated by two new ^{31}P resonances at 68.3 (d, $^2J_{PP}$ = 19 Hz) and -39.2 (d, $^2J_{PP}$ = 19 Hz) ppm. Quantitative conversion to **3-4** was attained after heating (65 °C, 7 h), and complex **3-4** was isolated in 90% yield. The ^{1}H NMR spectrum of isolated **3-4** features a doublet at 1.01 ppm (6 H, $^4J_{HP}$ = 3 Hz) that correlates to a ^{29}Si NMR resonance at 34.4 ppm (d, $^2J_{SiP}$ = 157 Hz) in a ^{1}H-^{29}Si HMBC experiment. On the basis of these data, **3-4** was formulated as a complex featuring *cis*-phosphine ligands, as well as a Pd-Si*Me*$_2$R substituent in which the silyl group is positioned *trans* to a phosphine. It was envisioned that such a species could arise via rearrangement of **3-3** involving net transfer of the Pd*Me* group to Si and cleavage of a Si-C(sp^2) bond in the pincer ligand backbone to yield a four-membered Pd-C-C-P metallacycle (Scheme 3-2).[68-69,71,74] The solid-state structure of **3-4** (Figure 3-2,

Table 3-2) was confirmed by single-crystal X-ray diffraction analysis, and is consistent with this formulation.

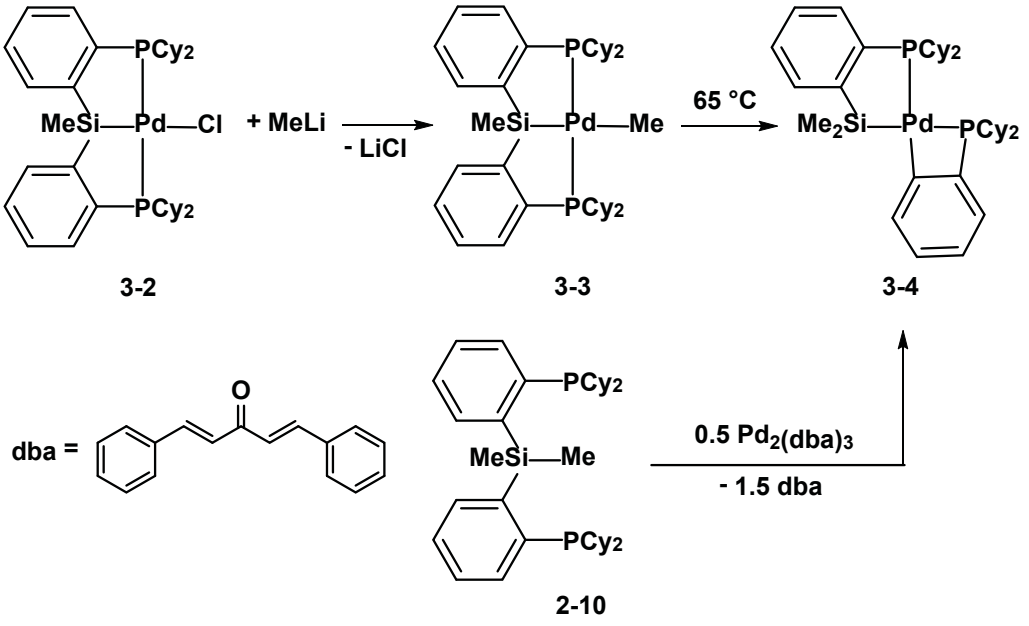

Scheme 3-2. Synthesis of [Cy-PSiP]PdMe (**3-3**) and subsequent rearrangement via Si-C(sp^2) bond cleavage to form **3-4**.

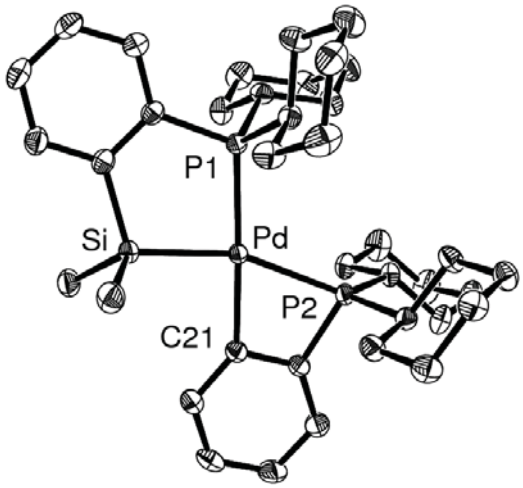

Figure 3-2. ORTEP diagram for **3-4** shown with 50% displacement ellipsoids; hydrogen atoms have been removed for clarity.

Table 3-2. Selected interatomic distances (Å) and angles (°) for **3-4**.

Interatomic Distances (Å)			
Pd-P1	2.2992(4)	Pd-Si	2.3037(4)
Pd-P2	2.4433(4)	Pd-C21	2.0867(14)
Interatomic Angles (°)			
P1-Pd-P2	113.262(13)	P1-Pd-Si	84.963(14)
Si-Pd-C21	93.44(4)	P2-Pd-C21	68.44(4)

While alternative pathways can be envisioned, a possible mechanism for the formation of **3-4** could involve the intermediacy of a Pd^0 species (**3-5**), which undergoes Si-C(sp^2) oxidative addition (Scheme 3-3). Given that direct reductive elimination from **3-3** to afford **3-5** is unlikely due to the *trans*-disposed Pd-Si and Pd-Me groups, it is plausible that Si-C(sp^3) bond formation is preceded by Pd-P dissociation or a tetrahedral distortion in **3-3**. Support for the viability of a Pd^0 species such as **3-5** undergoing Si-C(sp^2) oxidative addition to form **3-4** was obtained by the quantitative generation of **3-4** from the reaction of $(2\text{-}Cy_2PC_6H_4)_2SiMe_2$ (**2-10**) with half an equiv of the Pd^0 species $Pd_2(dba)_3$ (dba = dibenzylideneacetone; Scheme 3-2). Surprisingly, Si-C bond activation in **2-10** involving Pd^0 differs from the reaction of **2-10** with $Pt(PPh)_4$, which also proceeds quantitatively in room temperature benzene-d_6 solution to provide, the product of Si-C(sp^3) bond cleavage as in the case of the $Pd_2(dba)_3$ reaction, no intermediates were observed by use of ^1H or ^{31}P NMR spectroscopy during the course of this reaction. [25f] Thus it appears that the choice of metal influences the outcome of Si-C bond cleavage in

this system, such that Pt favors the formation of products resulting from Si-C(sp^3) bond cleavage, while Pd favors the formation of products resulting from Si-C(sp^2) bond cleavage, and Ni is able to access both types of products in a reversible fashion (*vide infra)*.

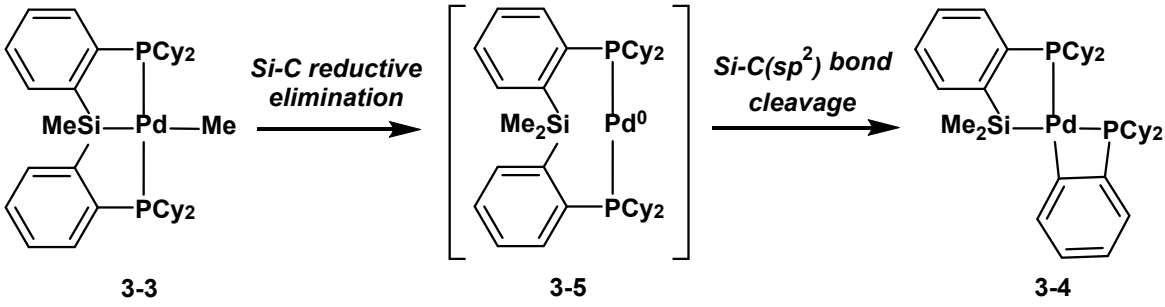

3-3 **3-5** **3-4**

Scheme 3-3. Proposed mechanism for Si-C(sp2) bond cleavage in [Cy-PSiP]PdMe (**3-3**) via a Pd^0 intermediate (**3-5**)

Intrigued by the unusual rearrangement of **3-3** to **3-4**, the preparation of a Ni*Me* derivative analogous to **3-3** was sought. Treatment of **3-1** with one equiv of MeMgBr resulted in the quantitative consumption of **3-1** and the clean formation of two new products, **3-6** and **3-7** (1:2 ratio, ^{31}P NMR; Scheme 3-4). Complex **3-6** gives rise to a single ^{31}P NMR resonance at 60.0 ppm, while complex **3-7** exhibits two ^{31}P NMR resonances at 68.4 (d, 1 P, J_{PP} = 9 Hz) and -32.8 (d, 1 P, J_{PP} = 9 Hz) ppm. Repeated attempts to alkylate **3-1** with MeMgBr under modified conditions led to reaction mixtures with an identical ratio of **3-6**:**3-7**, and heating of these reaction mixtures (up to 100 °C) did not result in increased conversion to either product. Attempts to separate **3-6** and **3-7** by precipitation or crystallization were not successful. ^{1}H NMR analysis of this product mixture indicates two Si*Me* resonances at 1.02 (d, J_{HP} = 2 Hz) and 0.69 ppm that

correlate to ^{29}Si NMR resonances at 35.0 (d, $^{2}J_{SiP}$ = 132 Hz) and 65.2 ppm, respectively, in a ^{1}H-^{29}Si HMBC experiment, as well as a resonance at 0.43 ppm (t, $^{3}J_{HP}$ = 6 Hz) that corresponds to a terminal Ni*Me* group. By analogy with the NMR features observed for **3-3** and **3-4**, compound **3-6** is assigned as the C_S-symmetric complex [Cy-PSiP]NiMe, while **3-7** is formulated as the Ni analogue of **3-4** (Scheme 3-4). Unlike the clean formation of **3-3** en route to **3-4**, in the case of Ni it appears that either **3-6** and **3-7** are formed independently, or that by analogy with the Pd system, **3-6** is the first-formed product that in turn establishes an equilibrium with **3-7**.

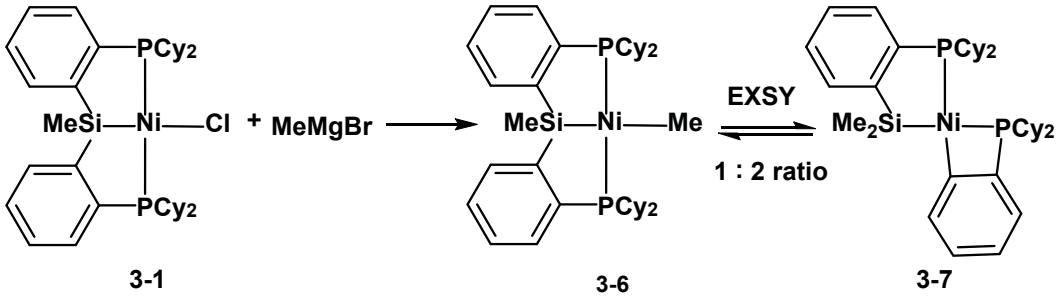

Scheme 3-4. Attempted methylation of [Cy-PSiP]NiCl (**3-1**) leading to a mixture of [Cy-PSiP]NiMe (**3-6**) and the rearrangement product **3-7**. The interconversion of **3-6** and **3-7** was observed by EXSY NMR spectroscopy.

In an effort to probe the interconversion of **3-6** and **3-7**, variable temperature ^{1}H and ^{31}P NMR studies of this mixture were performed (toluene-d_8); no appreciable changes in the ratio of **3-6** to **3-7** were observed in the range of -80 to 90 °C. However, ^{31}P-^{31}P EXSY NMR spectra of the **3-6**/**3-7** mixture (70 °C; mixing times = 0.75 and 1.5 s; Figure 3-3) revealed chemical exchange between the magnetically non-equivalent phosphorus environments in **3-7** (in keeping with reversible Si-C(sp^2) bond cleavage), as well as off-diagonal cross-peaks indicative of exchange involving **3-6** and **3-7** (in keeping with reversible Si-C(sp^3) bond cleavage). Under similar conditions, no chemical

exchange between the magnetically non-equivalent phosphorus environments in **3-4** was observed. The interconversion of **3-6** and **3-7** (possibly via a Ni^0 intermediate **3-8** analogous to **3-5**) was further confirmed by ^1H-^1H EXSY NMR experiments (70 °C; mixing times = 0.75 and 1.5 s; Figure 3-4), which revealed chemical exchange between the Si*Me* and Ni*Me* environments in **3-6** and **3-7**.[76] Given the rarity of well-documented Si-C(sp^3) bond activation processes involving first row transition metals,[68-69,71,74] the facile and reversible Ni-mediated Si-C(sp^3) bond cleavage reaction required for the interconversion of **3-6** and **3-7** is remarkable,[75] especially in light of the robust nature of the Si-C(sp^3) linkage (BDE of ca. 90 kcal mol^{-1}). The observed transformation of **3-3** into **3-4**, and the direct formation of a **3-6**/**3-7** mixture are in stark contrast to [Cy-PSiP]PtMe, which does not undergo a similar rearrangement (*see Chapter 2*). In light of the heightened propensity of Pt for σ-bond activation (relative to Pd and Ni), it is possible that the divergent reactivity observed for these species may correlate with the barrier to accessing **3-5** and **3-8** from related [Cy-PSiP]MMe precursors (M = Pd, Ni). Indeed, given the previously observed reaction of **2-10** with $Pt(PPh_3)_4$ to form [Cy-PsiP]PtMe, it appears that the barrier to accessing species of the type $[\kappa^2\text{-}(2\text{-}Cy_2PC_6H_4)_2SiMe]M^0$ from [Cy-PSiP]Me is much higher for M = Pt then for M = Pd or Ni.

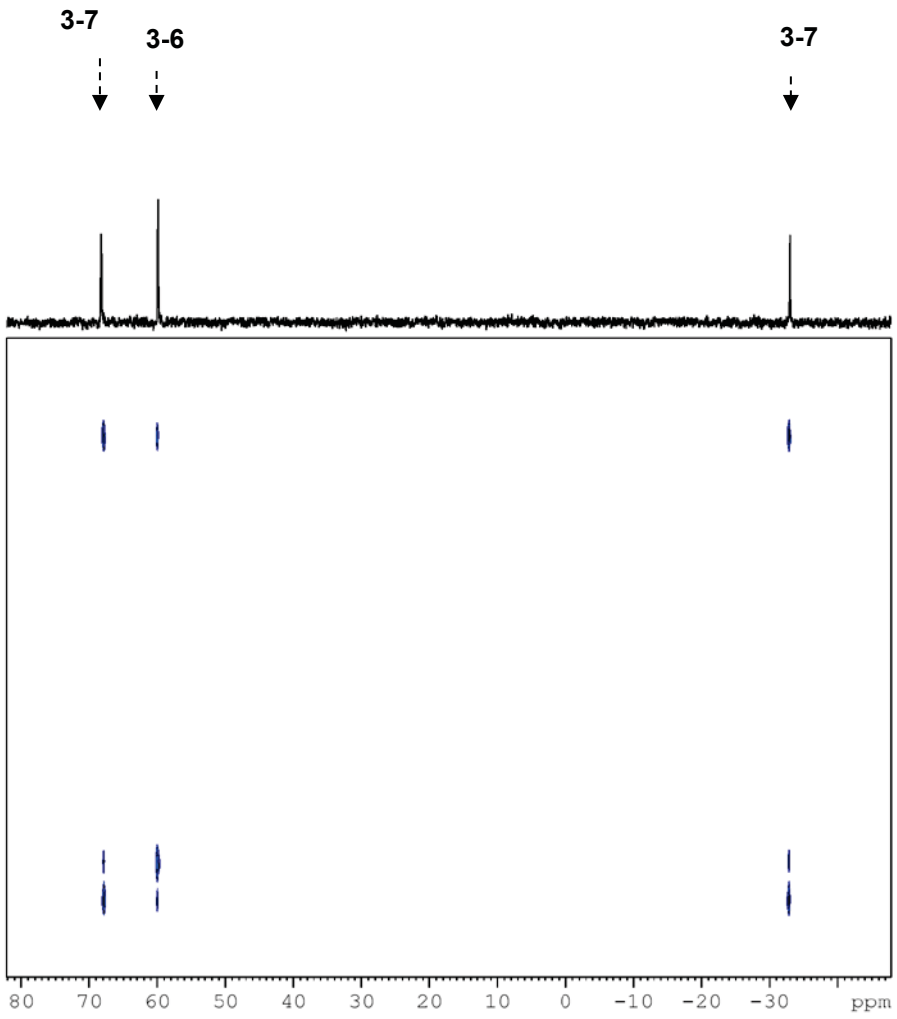

Figure 3-3. Representative ^{31}P-^{31}P EXSY NMR spectrum of the **3-6**/**3-7** product mixture (70 °C, toluene-d_8, 1.5 s mixing time). The off-diagonal cross-peaks are of the same phase as the signals on the diagonal in keeping with chemical exchange involving the magnetically nonequivalent phosphorus environments in **3-6** (60.0 ppm) and **3-7** (68.4 and -32.8 ppm).

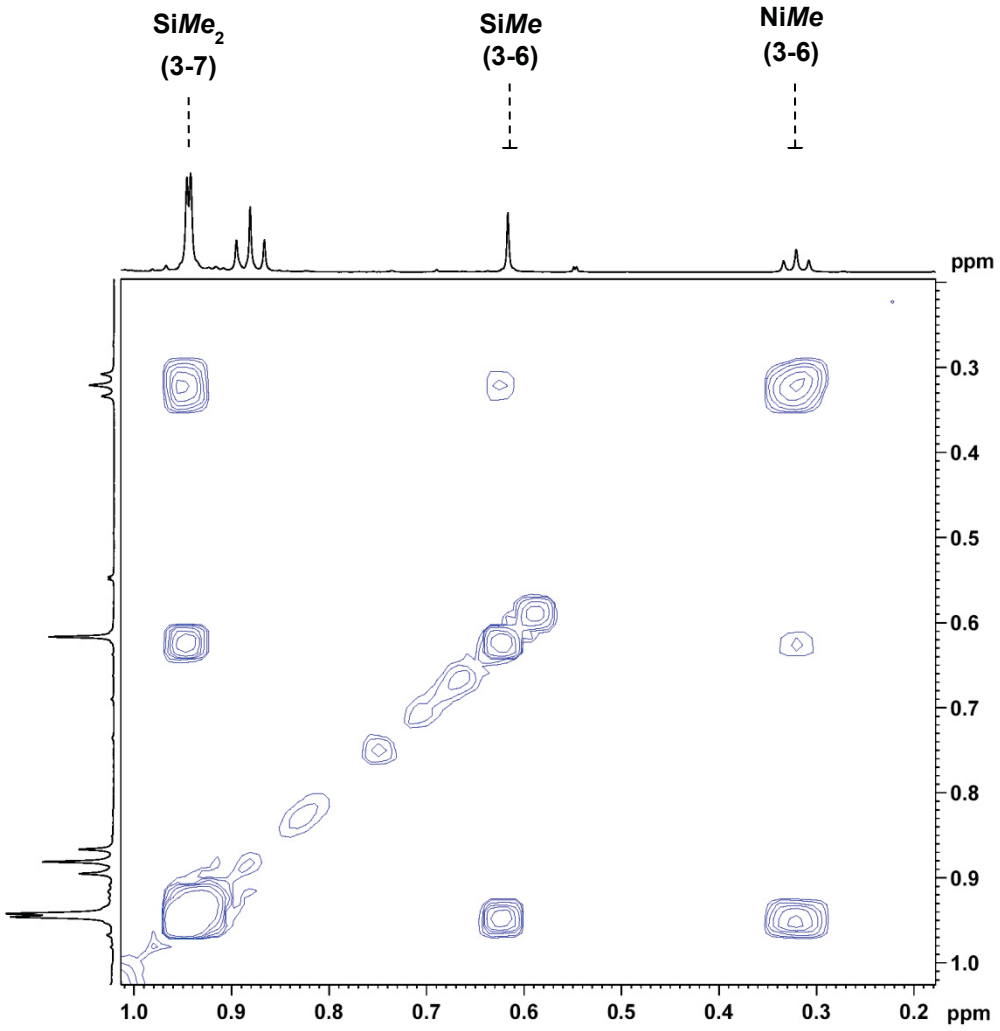

Figure 3-4. Representative ^{1}H-^{1}H EXSY NMR spectrum of the **3-6**/**3-7** product mixture (70 °C, toluene-d_8, 1.5 s mixing time). The off-diagonal cross-peaks are of the same phase as the signals on the diagonal in keeping with chemical exchange involving the Si*Me* and Ni*Me* environments in **3-6** (0.62 and 0.32 ppm) and **3-7** (0.94 ppm); * = pentane.

The reactivity of **3-3**, **3-4** and **3-6**/**3-7** was probed in order to gain further understanding of the possible interconversion of the terminal methyl complexes **3-3** and

3-6 with the rearrangement products **3-4** and **3-7** (Scheme 3-5). Treatment of isolated **3-3** with one equiv of Ph_2SiH_2 led to the formation of [Cy-PSiP]Pd($SiHPh_2$) (**3-9**). The X-ray crystal structure of **3-9** (Figure 3-5, Table 3-3) is consistent with distorted square planar coordination geometry at Pd in which the $SiHPh_2$ ligand is coordinated *trans* to the pincer Si donor. No reaction was observed upon heating of isolated **3-9** (100 °C, 24 h; ^{31}P NMR). Compound **3-3** also reacted with one equiv of Ph_2SiHCl to form [Cy-PSiP]PdCl (**3-2**) and Ph_2SiHMe (^1H and ^{31}P NMR; Scheme 3-5). Surprisingly, treatment of **3-4** with one equiv of Ph_2SiH_2 resulted in 50% conversion to **3-9** after heating in benzene solution (96 h, 100 °C; ^1H, ^{31}P and ^{29}Si NMR; Scheme 3-5). Similarly, exposure of **3-4** to one equiv of Ph_2SiHCl led to quantitative formation of **3-2** and Ph_2SiHMe after heating in benzene (96 h, 100 °C; ^1H and ^{31}P NMR; Scheme 3-5). Throughout the course of these reactions, no evidence of **3-3** was observed (^{31}P NMR). While the conversion of **3-3** to **3-2** and **3-9** can be viewed as proceeding with retention of connectivity within the [Cy-PSiP] ligand, the conversion of **3-4** to **3-2** and **3-9** requires cleavage of a Si-C(sp^3) linkage within the rearranged species **3-4** in order to reform the [Cy-PSiP] framework. From a mechanistic perspective, the possibility that **3-3** and **3-4** may traverse independent reaction pathways en route to each of **3-2** and **3-9** cannot be ruled out. It is possible that **3-4** transiently regenerates the terminal methyl complex **3-3** under the reaction conditions and/or that **3-3** and **3-4** access a common reactive intermediate such as **3-5** in these transformations. A similar rationale may apply in the Ni system, where the **3-6**/**3-7** product mixture is cleanly transformed into [Cy-PSiP]NiCl (**3-1**) with loss of Ph_2SiHMe upon exposure to one equiv of Ph_2SiHCl (25 °C, 12 h); the possible intermediacy of **3-3** is supported by ^{31}P-^{31}P EXSY NMR data (*vide supra*). Monitoring of this transformation

did not provide evidence for intermediates, and the ratio of **3-6**:**3-7** did not vary during the reaction (^{31}P NMR).

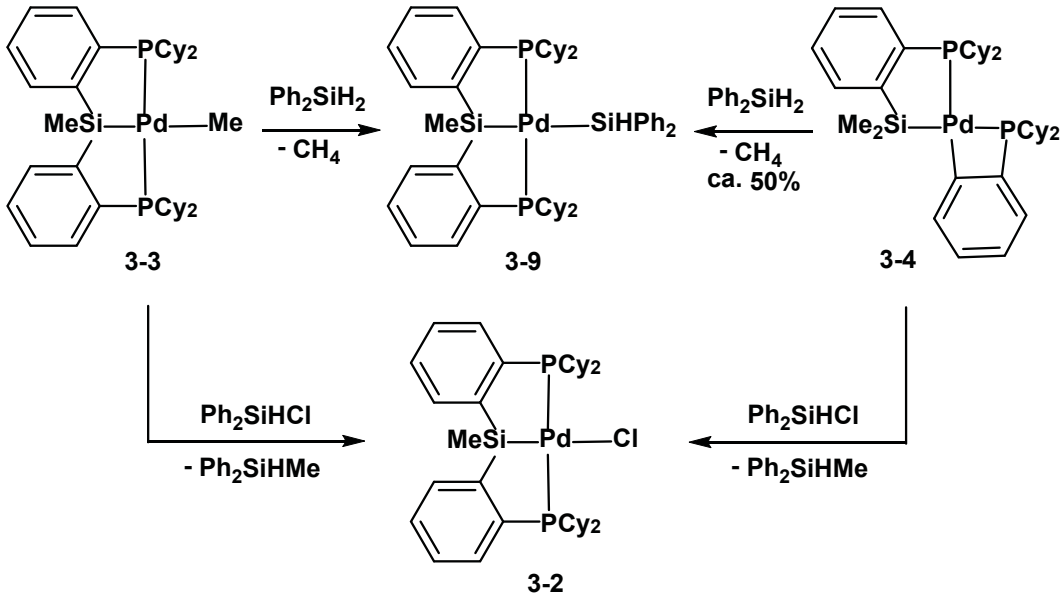

Scheme 3-5. Reactivity of **3-3** and **3-4** with hydrosilanes and hydridochlorosilanes

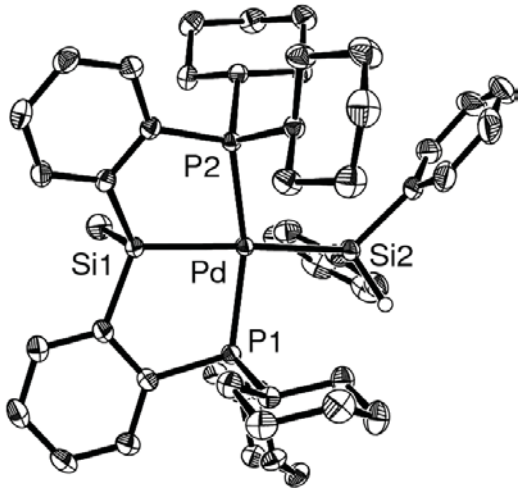

Figure 3-5. ORTEP diagram for **3-9** shown with 50% displacement ellipsoids; hydrogen atoms have been removed for clarity

Table 3-3. Selected interatomic distances (Å) and angles (°) for **3-9**

Interatomic Distances (Å)			
Pd-P1	2.2928(3)	Pd-Si1	2.3211(4)
Pd-P2	2.3079(3)	Pd-Si2	2.4721(4)
Interatomic Angles (°)			
P1-Pd-P2	154.937(13)	P1-Pd-Si1	82.358(13)
Si1-Pd-Si2	163.070(14)	P2-Pd-Si2	105.458(13)

In order to further survey the scope of these unusual Si-C bond activation processes, the synthesis of Ni and Pd allyl complexes was also attempted. Treatment of **3-1** with one equiv of (C_3H_5)MgBr led to the formation of [Cy-PSiP]Ni(η^3-C_3H_5) (**3-10**, 94%;Scheme 3-4).[77] Complex **3-10** features C_1 symmetry in solution (27 °C, benzene-d_6), as evidenced by an AB pattern centered at 49.2 ppm in the $^{31}P\{^1H\}$ NMR spectrum; the X-ray structure of **3-10**·OEt_2 is consistent with the room temperature NMR data for this complex (Figure 3-6, Table 3-4). No reaction was observed upon heating of isolated **3-10** (100 °C, 96 h; ^{31}P NMR). By comparison, treatment of **3-2** with one equiv of (C_3H_5)MgBr led to the formation of the C_s-symmetric complex [Cy-PSiP]Pd(η^1-C_3H_5) (**3-11**, 88%; Scheme 3-6), which features a ^{31}P NMR resonance at 59.1 ppm. The η^1-coordination of the allyl ligand is invoked on the basis of the allyl ^{13}C NMR resonances observed at 135.2, 87.3, and 25.3 ppm (27 °C, benzene-d_6).[67] Upon heating at 70 °C for 40 minutes, 66% conversion of **3-11** to **3-12** was observed (^{1}H, ^{13}C, ^{31}P and ^{29}Si NMR), where **3-12** is proposed as an analog of **3-4** in which a Si*Me* fragment is replaced by an

allyl group (Scheme 3-6). Decomposition of **3-12** was observed upon additional heating at this temperature. The relatively facile rearrangement observed for **3-11** relative to the η^3-allyl Ni complex **3-10** suggests that allyl η^3-coordination confers stability to the latter complex.

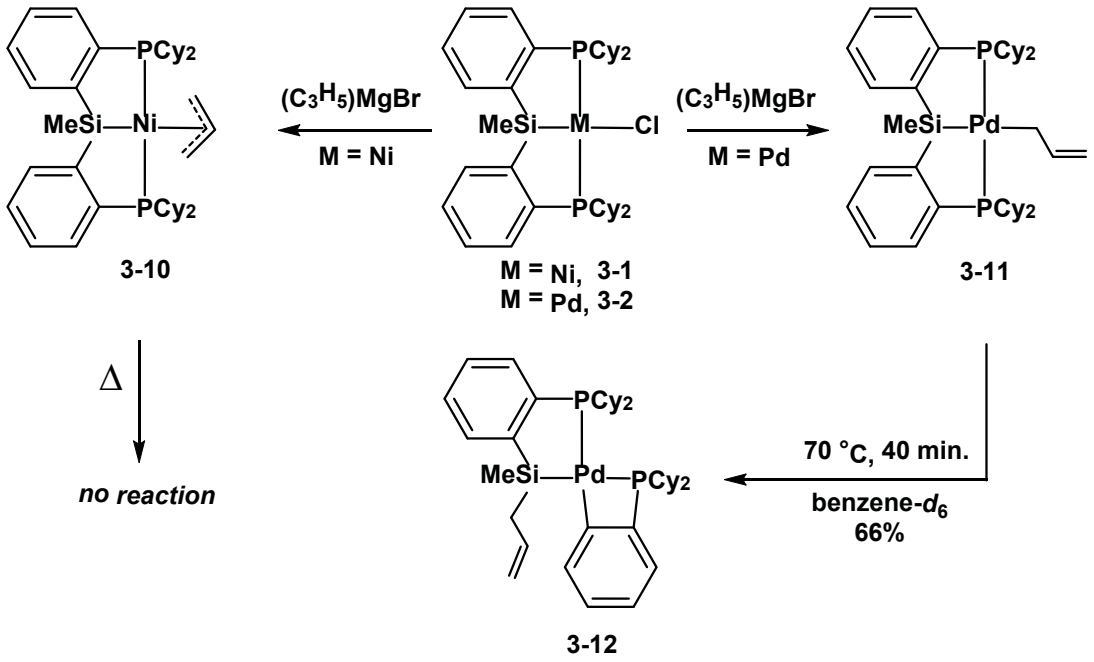

Scheme 3-6. Synthesis and divergent reactivity of [Cy-PSiP]M(allyl) complexes (M = Ni, **3-10**; M = Pd, **3-11**).

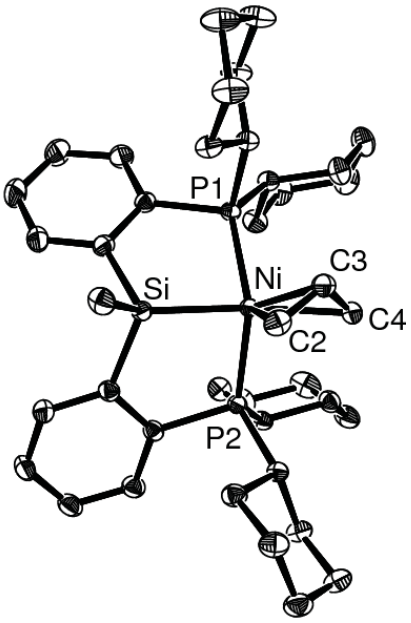

Figure 3-6. ORTEP diagram for **3-10**·OEt_2 shown with 50% displacement ellipsoids; hydrogen atoms and the diethyl ether solvate have been removed for clarity.

Table 3-4. Selected interatomic distances (Å) and angles (°) for **3-10**·OEt_2.

Interatomic Distances (Å)			
Ni-P1	2.2206(3)	Ni-Si	2.2344(4)
Ni-P2	2.2061(3)	Ni-C2	2.1228(13)
Ni-C3	2.0152(12)	Ni-C4	2.1020(13)
Interatomic Angles (°)			
P1-Ni-P2	130.802(13)	C2-Ni-Si	93.13(4)
C4-Ni-Si	163.45(4)	P1-Ni-C2	123.15(4)

3.3 Conclusions

In conjunction with Ni and Pd, the [Cy-PSiP] ligand underwent an unusual rearrangement involving reversible and remarkably facile Si-C(sp^2) and Si-C(sp^3) bond cleavage steps. In the case of Ni these Si-C bond activation processes are reversible on the NMR timescale in solution. Such examples of metal-mediated cleavage of an unstrained Si-C(sp^3) bond are extremely rare, and are unprecedented for Ni. Preliminary investigations of the scope of this reaction have indicated that the rearrangement is most facile for [Cy-PSiP]M(η^1-alkyl) (M = Ni, Pd) species, with no reactivity of this type observed for [Cy-PSiP]Ni(η^3-C_3H_5) or [Cy-PSiP]PdSiHPh$_2$. While these rearrangements are certainly relevant to silyl pincer systems, ancillary ligand reactivity of this type may also play a role in the chemistry of alternative classes of pincer-like tridentate ligands that feature *o*-phenylene backbone fragments.

3.4 Experimental Section

3.4.1 General Considerations.

All experiments were conducted under nitrogen in an MBraun glovebox or using standard Schlenk techniques. Dry, oxygen-free solvents were used unless otherwise indicated. Benzene, pentane and toluene were deoxygenated and dried by sparging with nitrogen and subsequent passage through a double-column solvent purification system purchased from MBraun Inc. Tetrahydrofuran and diethyl ether were purified by distillation from Na/benzophenone under N_2. All purified solvents were stored over 4 Å molecular sieves. All deuterated solvents were degassed via three freeze-pump-thaw

cycles and stored over 4 Å molecular sieves. The compounds $[(\eta^3\text{-}C_3H_5)PdCl]_2$, $Pd_2(dba)_3$ and $(PPh_3)NiCl_2$ were purchased from Strem Chemicals and used as received. Triethylamine was deoxygenated and dried by sparging with nitrogen and subsequent distillation from CaH_2. The compound $(2\text{-}Cy_2PC_6H_4)_2SiHMe$ ([Cy-PSiP]H) was prepared according to literature procedures.[25b] Silanes were purchased from Gelest, degassed via three freeze-pump-thaw cycles, and stored over 4 Å molecular sieves. All other reagents were purchased from Aldrich and used without further purification. Unless otherwise stated, ^1H, ^{13}C, ^{31}P, and ^{29}Si NMR characterization data were collected at 300K on a Bruker AV-500 spectrometer operating at 500.1, 125.8, 202.5, and 99.4 MHz (respectively) with chemical shifts reported in parts per million downfield of $SiMe_4$ (for ^1H, ^{13}C, and ^{29}Si) or 85% H_3PO_4 in D_2O (for ^{31}P). ^1H and ^{13}C NMR chemical shift assignments are based on data obtained from ^{13}C-DEPTQ, ^1H-^1H COSY, ^1H-^{13}C HSQC, and ^1H-^{13}C HMBC NMR experiments. ^{29}Si NMR assignments are based on ^1H-^{29}Si HMQC and ^1H-^{29}Si HMBC experiments. ^1H-^{29}Si coupling constants were determined by the use of ^1H-coupled ^1H-^{29}Si HMQC and ^1H-^{29}Si HMBC experiments. Elemental analyses were performed by Canadian Microanalytical Service Ltd. of Delta, British Columbia, Canada. Infrared spectra were recorded as thin films between NaCl plates using a Bruker VECTOR 22 FT-IR spectrometer at a resolution of 4 cm^{-1}.

3.4.2 Synthetic detail and characterization data

[Cy-PSiP]NiCl (3-1). A room-temperature solution of [Cy-PSiP]H (0.30 g, 0.51 mmol) in 5 mL of benzene was added to a slurry of $(PPh_3)_2NiCl_2$ (0.33 g, 0.51 mmol) in 5 mL of benzene. The reaction mixture was treated with Et_3N (0.052 g, 0.071 mL, 0.51

mmol), and the resulting solution was allowed to stir at room temperature for 18 h, over the course of which a white precipitate was observed. The reaction mixture was filtered through Celite to afford a clear, pale-yellow solution. The volatile components of the filtrate solution were removed under vacuum and the remaining residue was washed with cold (-30 °C) pentane (3 × 5 mL) and dried under vacuum to give **3-1** (0.34 g, 97%) as a pale yellow solid. ^{1}H NMR (500 MHz, benzene-d_6): δ 7.96 (d, 2 H, H_{arom}, J = 7 Hz), 7.44 (br d, 2 H, H_{arom}, J = 7 Hz), 7.29 (t, 2 H, H_{arom}, J = 7 Hz), 7.20 (t, 2 H, H_{arom}, J = 7 Hz), 2.61 (m, 4 H, PC*H*), 2.52 (br d, 2 H, P*Cy*, J = 12 Hz), 2.30 (br d, 2 H, P*Cy*, J = 13 Hz), 2.09 (m, 2 H, P*Cy*), 1.83 – 1.44 (22 H, P*Cy*), 1.29 – 1.09 (10 H, P*Cy*), 0.92 (m, 2 H, P*Cy*), 0.73 (s, 3 H, Si*Me*). ^{13}C{^{1}H} NMR (125.8 MHz, benzene-d_6): δ 157.6 (apparent t, C_{arom}, J = 26 Hz), 142.1 (apparent t, C_{arom}, J = 22 Hz), 132.6 (apparent t, CH$_{arom}$, J = 10 Hz), 131.4 (CH$_{arom}$), 130.6 (CH$_{arom}$), 129.3 (CH$_{arom}$), 37.6 (apparent t, CH$_{Cy}$, J = 10 Hz), 35.7 (apparent t, CH$_{Cy}$, J = 10 Hz), 31.3 (CH$_{2Cy}$), 30.1 (CH$_{2Cy}$), 29.6 (CH$_{2Cy}$), 28.1 – 27.8 (overlapping resonances, CH$_{2Cy}$), 27.2 (CH$_{2Cy}$), 26.7 (CH$_{2Cy}$), 8.5 (Si*Me*). ^{31}P{^{1}H} NMR (202.5 MHz, benzene-d_6): δ 52.8. ^{29}Si NMR (99.4 MHz, benzene-d_6): δ 54.4. Anal. Calcd for $C_{37}H_{55}ClP_2SiNi$: C, 64.97; H, 8.10. Found: C, 65.30; H, 7.88. A single crystal of **3-1** suitable for X-ray diffraction analysis was grown from a concentrated diethyl ether solution at -30 °C.

[Cy-PSiP]PdCl (3-2). A room-temperature solution of [Cy-PSiP]H (0.40 g, 0.68 mmol) in 5 mL of benzene was added to a solution of [(η^3-C_3H_5)PdCl]$_2$ (0.12 g, 0.34 mmol) in 5 mL of benzene. The reaction mixture was allowed to stand at room temperature for 18 h. The volatile components of the reaction mixture were subsequently removed under vacuum and the remaining residue was washed with cold (-30 °C)

pentane (3 × 5 mL) and dried under vacuum to give **3-2** (0.48 g, 96%) as an off white solid. ^{1}H NMR (500 MHz, benzene-d_6): δ 8.01 (d, 2 H, H_{arom}, J = 7 Hz), 7.43 (m, 2 H, H_{arom}), 7.30 (t, 2 H, H_{arom}, J = 7 Hz), 7.19 (t, 2 H, H_{arom}, J = 7 Hz), 3.06 (m, 2H, PC*H*), 2.39 (m, 2 H, PC*H*), 2.33 (br d, 2 H, P*Cy*, J = 13 Hz), 2.22 (br d, 2 H, P*Cy*, J = 13 Hz), 2.06 (m, 2 H, P*Cy*), 1.72 – 0.87 (34 H, P*Cy*), 0.72 (s, 3 H, Si*Me*). ^{13}C{^{1}H} NMR (125.8 MHz, benzene-d_6): δ 156.9 (apparent t, C_{arom}, J = 26 Hz), 141.0 (apparent t, C_{arom}, J = 20 Hz), 133.4 (apparent t, CH$_{arom}$, J = 12 Hz), 131.9 (CH$_{arom}$), 130.8 (CH$_{arom}$), 129.5 (CH$_{arom}$), 37.4 (apparent t, CH$_{Cy}$, J = 11 Hz), 36.7 (apparent t, CH$_{Cy}$, J = 11 Hz), 30.4 (CH$_{2Cy}$), 29.4 (CH$_{2Cy}$), 27.9 – 27.5 (overlapping resonances, CH$_{2Cy}$), 27.1 (CH$_{2Cy}$), 26.4 (CH$_{2Cy}$), 9.7 (Si*Me*). ^{31}P{^{1}H} NMR (202.5 MHz, benzene-d_6): δ 56.6 (s). ^{29}Si NMR (99.4 MHz, benzene-d_6): δ 53.8. Anal. Calcd for $C_{37}H_{55}ClP_2SiPd$: C, 60.73; H, 7.58. Found: C, 60.33; H, 7.46.

[Cy-PSiP]PdMe (3-3). A room-temperature solution of **3-2** (0.10 g, 0.14 mmol) in ca. 5 mL of benzene was treated with MeLi (1.6 M in Et_2O, 0.088 mL, 0.14 mmol). The reaction mixture was allowed to stand at room temperature for 40 minutes and was subsequently concentrated to dryness under vacuum. The residue was redissolved in benzene and filtered through Celite. The filtrate was concentrated to dryness under vacuum and the remaining residue was washed with ca. 3 mL of cold (-30 °C) pentane and dried under vacuum to afford **3-3** (0.076 g, 78%) as an off white solid. ^{1}H NMR (500 MHz, benzene-d_6): δ 8.22 (d, 2 H, H_{arom}, J = 7 Hz), 7.56 (m, 2 H, H_{arom}), 7.35 (t, 2 H, H_{arom}, J = 7 Hz), 7.24 (t, 2 H, H_{arom}, J = 7 Hz), 2.63 (t, 2 H, PC*H*, J = 12 Hz), 2.40 (t, 2 H, PC*H*, J = 12 Hz), 2.25 (br d, 2 H, P*Cy*, J = 12 Hz), 2.01 (br d, 2 H, P*Cy*, J = 13 Hz), 1.78 - 1.03 (34 H, P*Cy*), 0.86 (m, 2 H, P*Cy*), 0.72 (s, 3 H, Si*Me*), 0.56 (t, 3 H, Pd*Me,* $^{3}J_{HP}$

= 4 Hz). $^{13}C\{^{1}H\}$ NMR (125.8 MHz, benzene-d_6): δ 159.5 (apparent t, C_{arom}, J = 26 Hz), 144.3 (apparent t, C_{arom}, J = 20 Hz), 134.0 (apparent t, CH_{arom}, J = 11 Hz), 131.5 (CH_{arom}), 130.3 (CH_{arom}), 128.7 (CH_{arom}), 37.9 (apparent t, CH_{Cy}, J = 11 Hz), 37.6 (apparent t, CH_{Cy}, J = 11 Hz), 30.8 (CH_{2Cy}), 30.4 (CH_{2Cy}), 30.2 (CH_{2Cy}), 29.3 (CH_{2Cy}), 28.0 - 27.7 (overlapping resonances, CH_{2Cy}), 27.2 (CH_{2Cy}), 26.5 (CH_{2Cy}), 9.4 (Si*Me*), -7.9 (t, Pd*Me*, $^{2}J_{CP}$ = 12 Hz). $^{31}P\{^{1}H\}$ NMR (202.5 MHz, benzene-d_6): δ 60.5. ^{29}Si NMR (99.4 MHz, benzene-d_6): δ 64.5. Anal. Calcd for $C_{38}H_{58}P_2SiPd$: C, 64.16; H, 8.22. Found: C, 64.12; H, 8.13.

[(κ^2–$Cy_2PC_6H_4SiMe_2$)Pd(κ^2–$Cy_2PC_6H_4$)] (3-4). ***Method 1:*** A solution of **3-3** (0.10 g, 0.14 mmol**)** in ca. 5 mL of benzene was heated at 65 ˚C for 7 h. The reaction mixture was subsequently concentrated to dryness under vacuum. The remaining residue was washed with ca. 3 mL of cold (-30 °C) pentane and dried under vacuum to afford **3-4** (0.090 g, 90%) as an off white solid. ***Method 2:*** A solution of $(2\text{-}Cy_2PC_6H_4)_2SiMe_2$ (**2-10**, 0.010 g, 0.017 mmol) in ca. 0.4 mL of benzene-d_6 was added to a slurry of $Pd_2(dba)_3$ (0.008 g, 0.009 mmol) in ca. 0.4 mL of benzene-d_6. The resulting dark purple reaction mixture was allowed to stand at room temperature for 10 h, over the course of which the color of the solution changed to clear yellow. ^{31}P and ^{1}H NMR analysis of the reaction mixture indicated the quantitative formation of **3-4**. ^{1}H NMR (500 MHz, benzene-d_6): δ 8.27 (m, 1 H, H_{arom}), 7.77 (d, 1 H, H_{arom}, J = 7 Hz), 7.43 - 7.40 (overlapping resonances, 2 H, H_{arom}), 7.30 (m, 1 H, H_{arom}), 7.22 - 7.17 (overlapping resonances, 3 H, H_{arom}), 2.23 - 2.02 (8 H, P*Cy*), 1.85 (br d, 2 H, P*Cy*, J = 13 Hz), 1.72 (br d, 2 H, P*Cy*, J = 11 Hz), 1.69 – 1.53 (14 H, P*Cy*), 1.48 – 1.02 (18 H, P*Cy*), 1.01 (d, 6 H, Si*Me*$_2$, $^{4}J_{HP}$ = 3 Hz). $^{13}C\{^{1}H\}$ NMR (125.8 MHz, benzene-d_6): δ 169.5 (d, C_{arom}, J = 110 Hz), 163.6 (d, C_{arom}, J = 61

Hz), 150.3 (d, C_{arom}, J = 35 Hz), 139.2 (d, C_{arom}, J = 42 Hz), 136.0 (d, CH_{arom}, J = 22 Hz), 133.9 (d, CH_{arom}, J = 24 Hz), 130.7 (CH_{arom}), 130.5 (CH_{arom}), 130.1 (d, CH_{arom}, J = 8 Hz), 129.7 (m, CH_{arom}), 124.7 (d, CH_{arom}, J = 5 Hz), 36.0 (d, CH_{Cy}, J = 17 Hz), 33.1 (CH_{Cy}), 30.9 (CH_{2Cy}), 30.8 (CH_{2Cy}), 30.0 (CH_{2Cy}), 29.3 (CH_{2Cy}), 28.1 - 27.7 (overlapping resonances, CH_{2Cy}), 27.1 (CH_{2Cy}), 26.9 (CH_{2Cy}), 5.8 (d, SiMe_2, $^3J_{CP}$ = 8 Hz). $^{31}P\{^1H\}$ NMR (202.5 MHz, benzene-d_6): δ 68.3 (d, 1 P, $^2J_{PPcis}$ = 19 Hz), -39.2 (d, 1 P, $^2J_{PPcis}$ = 19 Hz). ^{29}Si NMR (99.4 MHz, benzene-d_6): δ 34.4 (d, $^2J_{SiP}$ = 157 Hz). Anal. Calcd for $C_{38}H_{58}P_2SiPd$: C, 64.16; H 8.22. Found: C, 64.01; H, 8.09. A single crystal of **3-4** suitable for X-ray diffraction analysis was grown from diethyl ether at -30 °C.

[Cy-PSiP]NiMe (3-6) + [(κ^2–Cy$_2$*P*C$_6$H$_4$*Si*Me$_2$)Ni(κ^2–Cy$_2$*P*C$_6$H$_4$)] (3-7). A room-temperature solution of **3-1** (0.35 g, 0.51 mmol**)** in ca. 8 mL of benzene was treated with MeMgBr (3.0 M in Et_2O, 0.17 mL, 0.51 mmol). The dark colored reaction mixture was allowed to stand at room temperature for 40 minutes and was subsequently concentrated to dryness under vacuum. The residue was redissolved in benzene and filtered through Celite. The filtrate was concentrated to dryness under vacuum and the remaining green/brown residue was washed with ca. 3 mL of cold (-30 °C) pentane and dried under vacuum to afford a 1:2 mixture (^{31}P NMR) of **3-6** and **3-7** (0.31 g, 92%). ^{1}H NMR (500 MHz, benzene-d_6; the integrations provided are relative to **3-7**, whereby the high frequency resonance at 8.24 ppm is assigned an integral value of 1 H): δ 8.24 (m, 1 H, H_{arom} in **3-7**), 8.16 (d, 1 H, H_{arom} in **3-6**, J = 7 Hz), 7.77 (d, 1 H, H_{arom} in **3-7**, J = 7 Hz), 7.55 (br d, 1 H, H_{arom} in **3-6**, J = 7 Hz), 7.48- 7.04 (overlapping resonances, 8 H, H_{arom} in **3-6** + **3-7**), 2.53 - 1.05 (66 H, P*Cy* in **3-6** + **3-7**, 1.02 (d, 6 H, Si*Me* in **3-7**, $^4J_{HP}$ = 2 Hz), 0.69 (s, 1.5 H, Si*Me* in **3-6**), 0.43 (t, 1.5 H, Ni*Me* in **3-6**, $^3J_{HP}$ = 6 Hz). $^{13}C\{^1H\}$

NMR (125.8 MHz, benzene-d_6): δ 167.2 (d, C_{arom}, J = 67 Hz), 164.2 (d, C_{arom}, J = 59 Hz), 159.6 (apparent t, C_{arom}, J = 27 Hz), 148.2 (d, C_{arom}, J = 34 Hz), 145.3 (apparent t, C_{arom}, J = 22 Hz), 140.3 (d, C_{arom}, J = 45 Hz), 137.2 (d, CH_{arom}, J = 24 Hz), 133.2 (d, CH_{arom}, J = 23 Hz), 133.0 (apparent t, CH_{arom}, J = 11 Hz), 131.3 (CH_{arom}), 130.7 (CH_{arom}), 130.2 (CH_{arom}), 130.0 (CH_{arom}), 129.2 (m, CH_{arom}), 128.9-128.7 (overlapping resonances, CH_{arom}), 125.4 (d, CH_{arom}, J = 6 Hz), 38.4 (apparent t, CH_{Cy}, J = 10 Hz), 36.5 (apparent t, CH_{Cy}, J = 10 Hz), 35.9 (d, CH_{Cy}, J = 17 Hz), 33.2 (d, CH_{Cy}, J = 6 Hz), 32.0 (CH_{2Cy}), 31.1 (CH_{2Cy}), 31.0 (CH_{2Cy}), 30.3 (CH_{2Cy}), 30.1 (CH_{2Cy}), 29.8 (CH_{2Cy}), 29.3 (CH_{2Cy}), 28.4 - 26.8 (overlapping resonances, CH_{2Cy}), 8.1 (Si*Me* in **3-6**), 6.1 (d, SiMe_2 in **3-7**, $^3J_{CP}$ = 6 Hz), -5.1 (t, Ni*Me* in **3-6**, $^2J_{CP}$ = 14 Hz). $^{31}P\{^1H\}$ NMR (202.5 MHz, benzene-d_6): δ 68.4 (d, 1 P in **3-7**, $^2J_{PPcis}$ = 9 Hz), 60.0 (s, **3-6**), -32.8 (d, 1 P in **3-7**, $^2J_{PPcis}$ = 9 Hz). ^{29}Si NMR (99.4 MHz, benzene-d_6): δ 35.0 (d, **3-7**, $^2J_{SiP}$ = 132 Hz), 65.2 (**3-6**). Anal. Calcd for $C_{38}H_{58}P_2SiNi$: C, 68.78; H 8.81. Found: C, 68.60; H, 8.46.

[Cy-PSiP]Pd(SiHPh$_2$) (3-9). A room-temperature solution of **3-3** (0.032 g, 0.045 mmol) in. ca. 5 mL of benzene was treated with Ph_2SiH_2 (0.008 g, 8.4 μL, 0.045 mmol). The reaction mixture was allowed to stand at room temperature for 48 h and was subsequently concentrated to dryness under vacuum. The remaining yellow residue was washed with ca. 2 mL of cold (-30 °C) pentane and dried under vacuum to afford **3-9** (0.030 g, 76%) as a yellow solid. ^{1}H NMR (500 MHz, benzene-d_6): δ 8.19 (d, 2 H, H_{arom}, J = 7 Hz), 8.02 (d, 4 H, SiPh_{ortho}, J = 7 Hz), 7.53 (br d, 2 H, H_{arom}, J = 7 Hz), 7.36 (t, 2 H, H_{arom}, J = 7 Hz), 7.30 (t, 4 H, SiPh_{meta}, J = 7 Hz), 7.23 (t, 2 H, H_{arom}, J = 7 Hz), 7.19 (t, 2 H, SiPh_{para}, J = 7 Hz), 5.92 (t with Si satellites, 1 H, Si*H*, $^3J_{HP}$ = 6 Hz, $^1J_{SiH}$ = 142 Hz), 2.72 (t, 2 H, P*CH*, J = 12 Hz), 2.36 (t, 2 H, P*CH*, J = 12 Hz), 2.18 - 0.93 (overlapping

resonances, 40 H, P*Cy*), 0.55 (s, 3 H, Si*Me*). $^{13}C\{^{1}H\}$ NMR (125.8 MHz, benzene-d_6): δ 157.7 (apparent t, C_{arom}, J = 25 Hz), 149.4 (SiPh_{ipso}),143.6 (apparent t, C_{arom}, J = 19 Hz), 138.3 (SiPh_{ortho}), 133.7 (apparent t, CH_{arom}, J = 12 Hz), 132.0 (CH_{arom}), 130.7 (CH_{arom}), 129.0 (CH_{arom}), 127.8 (SiPh_{meta}), 127.0 (SiPh_{para}), 38.2 (apparent t, CH_{Cy}, J = 12 Hz), 37.9 (apparent t, CH_{Cy}, J = 12 Hz), 30.7 (CH_{2Cy}), 30.5 (CH_{2Cy}), 30.3 (CH_{2Cy}), 29.4 (CH_{2Cy}), 27.8 - 26.9 (overlapping resonances, CH_{2Cy}), 26.4 (CH_{2Cy}), 9.8 (Si*Me*). $^{31}P\{^{1}H\}$ NMR (202.5 MHz, benzene-d_6): δ 66.9. ^{29}Si NMR (99.4 MHz, benzene-d_6): δ 72.2 (P*Si*P), 94.1 (Pd*Si*HPh$_2$, $^{1}J_{SiH}$ = 142 Hz). A single crystal of **3-9** suitable for X-ray diffraction analysis was grown from a concentrated pentane solution at -30 °C.

[Cy-PSiP]Ni(η^3-C_3H_5) (3-10). A cold (-30 °C) solution of **3-1** (0.15 g, 0.22 mmol) in ca. 5 mL of THF was treated with (C_3H_5)MgBr (2.0 M in THF, 0.11 mL, 0.22 mmol). The reaction mixture was allowed to warm to room temperature over the course of 30 minutes and was subsequently concentrated to dryness under vacuum. The residue was redissolved in benzene and filtered through Celite. The filtrate was concentrated to dryness under vacuum and the remaining residue was washed with ca. 3 mL of cold (-30 °C) pentane and dried under vacuum to afford **3-10** (0.14 g, 94%). ^{1}H NMR (500 MHz, benzene-d_6): δ 8.02 (br s, 1 H, H_{arom}), 7.87 (br s, 1 H, H_{arom}), 7.33 (br m, 2 H, H_{arom}), 7.23 – 7.05 (br overlapping resonances, 4 H, H_{arom}), 4.67 (m, 1 H, NiC$_3H_5$), 3.26 (br s, 1 H, NiC$_3H_5$), 3.11 (d, 1 H, NiC$_3H_5$, J = 6 Hz), 2.66 (m, 1 H, NiC$_3H_5$), 2.28 – 2.13 (3 H, NiC$_3H_5$ + PC*H*), 2.05 (m, 1 H, PC*H*), 1.80 – 0.95 (overlapping resonances, 40 H, P*Cy* + Si*Me*; the Si-*Me* resonance was identified at 1.05 ppm by the use of correlation spectroscopy), 0.82 (m, 2 H, P*Cy*), 0.65 (m, 1 H, P*Cy*), 0.48 (m, 1 H, P*Cy*). $^{3}C\{^{1}H\}$ NMR (125.8 MHz, benzene-d_6): δ 133.2 (d, CH_{arom}, J = 18 Hz), 132.7 (d, CH_{arom}, J = 23

Hz), 129.7 (br, CH_{arom}), 129.2 (br, CH_{arom}), 128.7 (CH_{arom}), 127.5 (CH_{arom}), 127.4 (CH_{arom}), 95.2 ($NiCH_2CHCH_2$), 49.5 (m, $NiCH_2CHCH_2$), 41.5 ($NiCH_2CHCH_2$), 38.0 (br, CH_{Cy}), 35.9 (br, CH_{Cy}), 30.7 (CH_{2Cy}), 30.0 (CH_{2Cy}), 29.9 (CH_{2Cy}), 29.4 (CH_{2Cy}), 28.8 (CH_{2Cy}), 28.7 (CH_{2Cy}), 28.2 – 27.9 (overlapping resonances, CH_{2Cy}), 27.4 (CH_{2Cy}), 27.2 (CH_{2Cy}), 26.9 (CH_{2Cy}), 25.7 (CH_{2Cy}), 6.7 (Si*Me*). $^{31}P\{^1H\}$ NMR (202.5 MHz, benzene-d_6): δ 49.2 (AB pattern; apparent doublets at 53.3 and 45.1 ppm each exhibiting $^2J_{PP}$ = 113 Hz). ^{29}Si NMR (99.4 MHz, benzene-d_6): δ 54.6. Anal. Calcd for $C_{40}H_{60}P_2SiNi$: C, 69.66; H 8.77. Found: C, 69.35; H, 8.42. A single crystal of **3-10·OEt₂** suitable for X-ray diffraction analysis was grown from a concentrated diethyl ether solution at -30 °C.

[Cy-PSiP]Pd(η^1-C_3H_5) (3-11). A cold (-30 °C) solution of **3-2** (0.15 g, 0.20 mmol) in ca. 5 mL of THF was treated with $(C_3H_5)MgBr$ (2.0 M in THF, 0.10 mL, 0.20 mmol). The reaction mixture was allowed to warm to room temperature over the course of 30 minutes and was subsequently concentrated to dryness under vacuum. The residue was redissolved in benzene and filtered through Celite. The filtrate was concentrated to dryness under vacuum and the remaining residue was washed with ca. 3 mL of cold (-30 °C) pentane and dried under vacuum to afford **3-11** (0.13 g, 88%) as an off white solid. ^1H NMR (500 MHz, benzene-d_6): δ 8.13 (d, 2 H, H_{arom}, J = 7 Hz), 7.47 (br d, 2 H, H_{arom}, J = 7 Hz), 7.30 (t, 2 H, H_{arom}, J = 7 Hz), 7.19 (t, 2 H, H_{arom}, J = 7 Hz), 6.48 (apparent quint, 1 H, $PdCH_2CH{=}CH_2$, J = 11 Hz), 4.46 – 4.34 (2 H, $PdCH_2CH{=}CH_2$), 2.90 (br s, 2 H, $PdCH_2CH{=}CH_2$), 2.45 (m, 2 H, P*CH*), 2.29 – 2.24 (4 H, P*Cy* + P*CH*), 1.97 (br d, 2 H, P*Cy*, J = 13 Hz), 1.88 – 1.72 (6 H, P*Cy*), 1.61 – 1.04 (28 H, P*Cy*), 0.96 (s, 3 H, Si*Me*), 0.85 (m, 2 H, P*Cy*). $^{13}C\{^1H\}$ NMR (125.8 MHz, benzene-d_6): δ 158.9 (apparent t, C_{arom}, J = 28 Hz), 143.6 (apparent t, C_{arom}, J = 19 Hz), 135.2 ($PdCH_2CH{=}CH_2$), 133.5 (apparent

t, CH_{arom}, J = 11 Hz), 131.1 (CH_{arom}), 130.1 (CH_{arom}), 128.7 (CH_{arom}), 87.3 (br, $PdCH_2CH{=}CH_2$), 37.4 (apparent t, CH_{Cy}, J = 10 Hz), 37.2 (apparent t, CH_{Cy}, J = 9 Hz), 31.3 (CH_{2Cy}), 29.8 (CH_{2Cy}), 29.5 (CH_{2Cy}), 28.9 (CH_{2Cy}), 28.0 – 27.6 (overlapping resonances, CH_{2Cy}), 27.3 (CH_{2Cy}), 26.8 (CH_{2Cy}), 25.3 (br, $PdCH_2CH{=}CH_2$), 10.1 (Si*Me*). $^{31}P\{^1H\}$ NMR (202.5 MHz, benzene-d_6): δ 59.1. ^{29}Si NMR (99.4 MHz, benzene-d_6): δ 63.7. Anal. Calcd for $C_{40}H_{60}P_2SiPd$: C, 65.16; H 8.20. Found: C, 65.51; H, 8.46.

Generation of [(κ^2–$Cy_2PC_6H_4Si(C_3H_5)Me$)Pd(κ^2–$Cy_2PC_6H_4$)] (3-12). A solution of **3-11** (0.010 g, 0.014 mmol) in ca. 0.8 mL of benzene-d_6 was heated at 70 °C for 40 minutes, at which point ^1H and ^{31}P NMR analysis of the reaction mixture indicated 66% conversion to **3-12**. Further heating at this temperature resulted in the formation of multiple unidentified products and no additional conversion to **3-12**. Characteristic NMR data for **3-12** are provided; selected aromatic and all PCy_2 resonances could not be unequivocally assigned due to overlap with **3-11**. ^1H NMR (500 MHz, benzene-d_6): δ 8.26 (m, 1 H, H_{arom}), 7.82 (d, 1 H, H_{arom}, J = 7 Hz), 6.17 (m, 1 H, $SiCH_2CH{=}CH_2$), 4.92 (m, 1 H, $SiCH_2CH{=}CH_2$), 4.81 (m, 1 H, $SiCH_2CH{=}CH_2$), 2.61 (d, 1 H, $SiCH_2CH{=}CH_2$, J = 8 Hz), 2.49 (1 H, $SiCH_2CH{=}CH_2$, overlapping with P*Cy*), 1.00 (d, 6 H, $SiMe_2$, $^4J_{HP}$ = 3 Hz). $^{13}C\{^1H\}$ NMR (125.8 MHz, benzene-d_6): δ 139.1 ($SiCH_2CH{=}CH_2$), 135.7 (CH_{arom}), 134.4 (CH_{arom}), 124.9 (CH_{arom}), 111.4 ($SiCH_2CH{=}CH_2$), 30.0 ($SiCH_2CH{=}CH_2$), 3.4 (Si*Me*). $^{31}P\{^1H\}$ NMR (202.5 MHz, benzene-d_6): δ 67.9 (d, 1 P, $^2J_{PPcis}$ = 18 Hz), -40.0 (d, 1 P, $^2J_{PPcis}$ = 18 Hz). ^{29}Si NMR (99.4 MHz, benzene-d_6): δ 36.0 (d, $^2J_{SiP}$ = 166 Hz).

3.4.3 Crystallographic solution and refinement details

Crystallographic data for each of **3-1**, **3-4**, **3-9**, and **3-10**·OEt_2 were obtained at 173(±2) K on a Bruker D8/APEX II CCD diffractometer using graphite-monochromated Mo Kα (λ = 0.71073 Å) radiation, employing a sample that was mounted in inert oil and transferred to a cold gas stream on the diffractometer. Programs for diffractometer operation, data collection, and data reduction (including SAINT) were supplied by Bruker. Gaussian integration (face-indexed) was employed as the absorption correction method in each case. All structures were solved by use of the Patterson search/structure expansion and were refined by use of full-matrix least-squares procedures (on F^2) with R_1 based on $F_o^2 \geq 2\sigma(F_o^2)$ and wR_2 based on $F_o^2 \geq -3\sigma(F_o^2)$. Anisotropic displacement parameters were employed for all the non-hydrogen atoms in **3-1**, **3-4** and **3-9**. During the structure solution process for **3-10**·OEt_2 an equiv of Et_2O was located in the asymmetric unit. Disorder involving this solvent molecule was identified during refinement. The non-hydrogen atoms of the disordered Et_2O solvate were refined over two positions, where O1SA and C1SA – C4SA were refined anisotropically with an occupancy factor of 0.75, while O1SB and C1SB – C4SB were refined isotropically with and occupancy factor of 0.25. Anisotropic displacement parameters were employed for all remaining non-hydrogen atoms in **3-10**·OEt_2. The Si-*H* in **3-9** was located in the difference map and refined isotropically. Otherwise, all hydrogen-atoms were added at calculated positions and refined by use of a riding model employing isotropic displacement parameters based on the isotropic displacement parameter of the attached

atom. Additional crystallographic information for **3-1**, **3-4**, **3-9** and **3-10** is provided in Appendix A.

CHAPTER 4: Catalytic Reduction of CO_2 Mediated by Group 10 Silyl Pincer Complexes

4.1 Introduction

The large-scale combustion of fossil fuels (coal, petroleum, natural gas) has led to a significant and alarming rise in levels of atmospheric CO_2 over the past several decades, and this trend is anticipated to continue.[78] As a greenhouse gas, CO_2 is a significant contributor to global warming, and thus the current high level of anthropogenic CO_2 in the atmosphere is of great concern. [78] Although efforts to capture and sequester CO_2 are being pursued, such efforts have so far proven relatively costly and remain in their infancy.[79] A complementary strategy for addressing both the high levels of atmospheric CO_2 and the dwindling supply of fossil fuels available to meet our energy needs is the recycling of CO_2 via conversion into a hydrocarbon fuel that is suitable for use in our current energy infrastructure. As such, there is significant interest in the development of efficient methodologies for the reduction of CO_2 to methanol and/or methane, with the ultimate goal of achieving a carbon-neutral catalytic process.[78b,80,81]

In this context, the pursuit of homogeneous catalysts for the conversion of CO_2 to methanol and/or methane is an area of growing interest, [47,81-85] and to date, only a handful of such catalyst systems have been developed.[86-91,] With respect to methanol formation, Milstein and co-workers recently demonstrated the facile hydrogenation of CO_2-derived organic carbonates, carbamates, and formates to methanol utilizing PNN pincer Ru complexes as catalysts.[87] Building on this pioneering work, Sanford and co-workers reported a three component cascade catalysis route for the hydrogenation of CO_2 to form

methanol,[86d] and Leitner and co-workers demonstrated that a single Ru phosphine catalyst is also effective in this transformation.[86e] There has also been significant interest in the development of efficient reduction pathways that do not rely on hydrogen for the reduction of CO_2 to the methoxide level. Utilizing a POCOP pincer Ni^{II} hydride catalyst, Guan and co-workers demonstrated the hydroboration of CO_2 with catecholborane to give methoxyboryl species with a relatively high turnover frequency. [89] Furthermore, while the Ir-catalyzed hydrosilylation of CO_2 to form methoxysilane species was initially reported over twenty years ago, albeit with low efficiency,[90a] more recently Ying and co-workers reported a metal-free N-heterocyclic carbene catalyzed process for the reduction of CO_2 with diphenylsilane to form the corresponding methoxysilane with significantly improved turnover numbers and turnover frequencies.[90b,c]

Focusing on the complete reduction of CO_2 to methane, prior to the work reported in this chapter, only three examples of such homogeneous catalyst systems had been reported. [91] Matsuo and Kawaguchi showed that the use of bis(phenoxo) Zr alkyl complexes, in conjunction with the highly Lewis acidic borane $B(C_6F_5)_3$, catalyzed the reaction of CO_2 with hydrosilanes to form methane.[91a] Piers and co-workers subsequently disclosed a catalyst system based on the frustrated Lewis pair (FLP) 2,2,6,6-tetramethylpiperidine (TMP)/$B(C_6F_5)_3$, which reacts with CO_2 and Et_3SiH to form a formatoborate species that is subsequently hydrosilylated in the presence of excess $B(C_6F_5)_3$ to form methane.[91c] Lastly, Wehmschulte and co-workers recently reported that the highly reactive Lewis acid Et_2Al^+ catalyzes the conversion of CO_2 to methane as well as other hydrocarbons upon reaction with hydrosilanes, albeit at elevated temperatures and long reaction times.[91d]

In an effort to diversify the catalyst portfolio available for the reduction of CO_2 to methane, we became interested in identifying a complementary late metal catalyst system for this transformation. It was envisioned that a platinum group metal catalyst might offer increased stability and decreased sensitivity to protic impurities relative to a d^0 metal alkyl or a cationic Group 13 alkyl species, while still achieving suitable activity in CO_2 reduction chemistry. The utility of such late metal species in the reduction of CO_2 to methanol is encouraging, and the identification of an appropriately configured late metal catalyst could provide an entry point towards complementary processes leading to formation of methane. The catalytic activity of Group 10 (Pd, Pt) silyl pincer complexes, in combination with $B(C_6F_5)_3$, the conversion of CO_2 to methane using tertiary silanes as the reductant is detailed herein. While this work was in progress, Brookhart and co-workers reported a related Ir pincer complex that is an active catalyst for CO_2 hydrosilation.[91b]

4.2. Results and Discussion

4.2.1 Mild reduction of carbon dioxide to methane with tertiary silanes catalyzed by platinum and palladium silyl pincer complexes

The synthesis, structural features and bond activation reactivity of a variety of platinum group metal pincer complexes supported by tridentate phosphinosilyl ligands of the type $(\kappa^3\text{-}(2\text{-}R_2PC_6H_4)_2SiMe)^-$ (R-PSiP, R = alkyl, aryl) have been previously reported,[25a-d] including the synthesis of square planar group 10 (Ni, Pd, Pt) complexes that undergo facile cleavage of Si-H, Si-Cl and Si-C(sp^2 and sp^3) bonds.[25e-g] Furthermore, [Ph-PSiP]Pd^{II} complexes have been shown to be useful in the catalytic

hydrocarboxylation of allenes and 1,3-dienes with CO_2 under mild conditions as well as in the synthesis of diborylalkenes via dehydrogenative borylation.[53-54] Efforts to prepare a Pt^{II} hydride complex of the type [Cy-PSiP]PtH led to the formation of [Cy-P*Si*(μ-H)P]*Pt* (**2-7**), which was identified on the basis of NMR and IR spectroscopic data as a bis(phosphino) Pt derivative of [Cy-PSiP]H that features η^2-Si-H coordination involving the tethered silicon fragment (Scheme 4-1).[25e] The Pd analogue (**4-1**) of **2-7** was prepared by a similar route involving treatment of [Cy-PSiP]PdCl with $LiEt_3BH$ and exibits spectroscopic features analgous to **2-7** including a ^{1}H NMR shift of 1.28 ppm for the μ-Si-H proton. (Scheme 4-1). Subsequent to this work, Hazari and co-workers reported the X-ray crysal structure of **4-1**, which was tentatively assigned as a terminal hydride complex in the solid state.[142] It is certainly possible that **4-1** exists in equilibrium with a terminal hydride isomer, and that the terminal hydride is the predominant structure in the solid state.

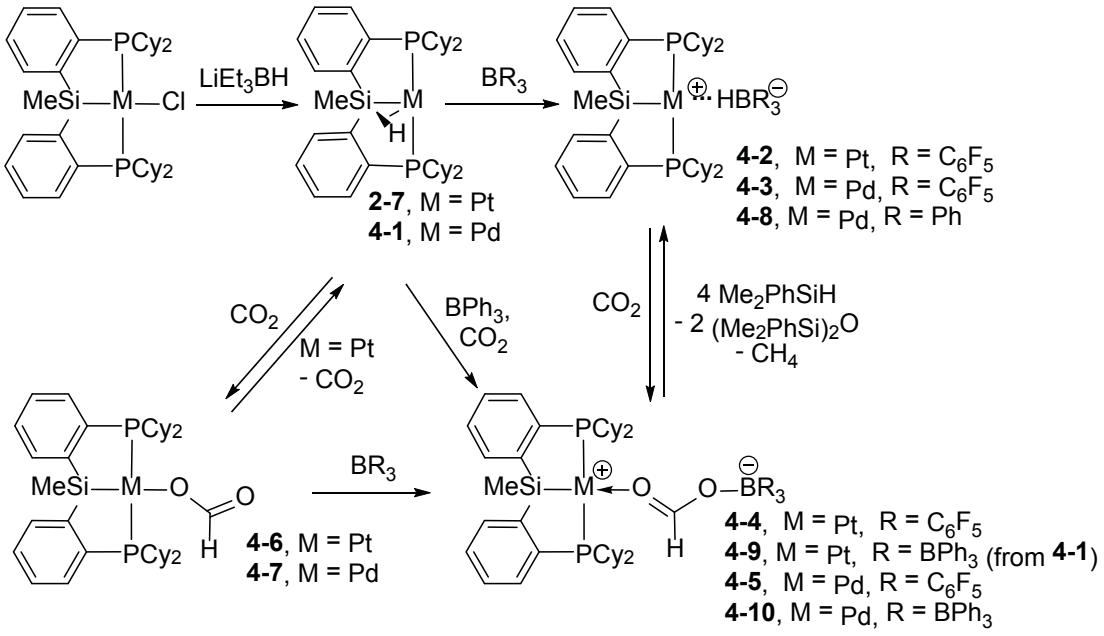

Scheme 4-1. Synthesis of [Cy-PSiP]Pt and Pd Complexes (only one resonance structure is shown for formatoborate complexes **4-4**, **4-5**, **4-9** and **4-10**).

In an effort to further explore the reactivity of these unusual η^2-Si-H complexes, their ability to provide access to cationic species via hydride abstraction was investigated. Interestingly, treatment of complexes **2-7** and **4-1**, respectively, with the strong Lewis acid $B(C_6F_5)_3$ afforded the hydride abstracted products **4-2** and **4-3** (Scheme 4-1), as evidenced by the appearance of a sharp ^{11}B NMR resonance in each case (for **4-2**: -25.4 ppm, d, $^1J_{BH}$ = 92 Hz, THF-d_8; for **4-3**: -23.3 ppm, d, $^1J_{BH}$ = 77 Hz, benzene-d_6) that featured B-H coupling. It was considered that complexes **4-2** and **4-3** offered an intriguing entry point for studying CO_2 fixation due to parallels between these complexes and the FLP-derived salt $[TMPH][HB(C_6F_5)_3]$, which reacts with CO_2 to form a formatoborate species that has been implicated in the stoichiometric hydrogenation of

CO_2 to methanol as well as the catalytic formation of methane upon reaction with excess $B(C_6F_5)_3$ and Et_3SiH.[91c]

Treatment of a benzene solution of either complex **4-2** or **4-3** with CO_2 gas (ca. 1 atm) resulted in the immediate formation of the corresponding Pt and Pd formatoborate complexes (Scheme 4-1; M = Pt, **4-4**; M = Pd, **4-5**). The ^{1}H NMR spectra of complexes **4-4** and **4-5** each contain a diagnostic formate resonance at 8.65 and 8.49 ppm, respectively, while the ^{13}C NMR spectra of these complexes feature a resonance at 171.7 and 170.8 ppm, respectively, corresponding to the formate carbon. The formatoborate complexes **4-4** and **4-5** were readily distinguished from the corresponding Pt and Pd formate species (Scheme 4-1; M = Pt, **4-6**; M = Pd, **4-7**) on the basis of their ^{1}H, ^{13}C and ^{31}P NMR spectroscopic features (e.g., the ^{1}H NMR resonance corresponding to the formate proton for **4-6** = 9.81 ppm, s with Pt satellites, $^3J_{HPt}$ = 40 Hz; for **4-7** = 9.20 ppm). Furthermore, unlike complex **4-4**, which was isolated in 87% yield, the Pt formate complex **4-8** was only observed under a CO_2 atmosphere and reformed **2-7** upon removal of CO_2 (Scheme 4-). While the Pd formate complex **4-7** proved isolable, treatment of **4-7** with an equiv. of $B(C_6F_5)_3$ resulted in quantitative (by ^{1}H and ^{31}P NMR) conversion to **4-5** (Scheme 4-1). Similar insertion of CO_2 into a hydroborate B-H bond has previously been observed for main group fragments involving FLPs.[88c,91c] Few related examples of formatoborate complexes involving transition metal species have been reported, and all previously reported examples appear to result exclusively from the initial formation of a metal formyl species that subsequently forms a formate-borane adduct.[92] Furthermore, Bercaw and Labinger have reported that in the case of $[HNi(dmpe)_2]^+$, while trialkyl boranes facilitate the formation of formate-borane adducts upon reaction with CO_2,

$B(C_6F_5)_3$ exhibited only hydride transfer from Ni to B and no CO_2 reduction.[92] Thus, it appears that the facile reduction of CO_2 by **4-2** and **4-3** to form formatoborate species is unprecedented.

In an effort to determine if less Lewis acidic boranes would facilitate similar stoichiometric CO_2 reduction chemistry, complexes **2-7** and **4-1** were each treated with one equiv of BPh_3. While **2-7** did not appear to undergo a reaction with BPh_3, complex **4-1** reacted readily at room temperature to quantitatively (by ^{31}P NMR) afford **4-8**, the BPh_3 analogue of **4-3**, which was isolated in 95% yield (Scheme 4-1). Treatment of **4-8** with CO_2 (1 atm) resulted in the formation of the desired formatoborate complex **4-10**, which features a characteristic formate ^1H NMR resonance at 8.85 ppm (benzene-d_6), as well as a ^{13}C NMR resonance at 173.3 ppm corresponding to the formate carbon (Scheme 4-). Complex **4-10** was also accessed by the reaction of the Pd formate species **4-7** with one equiv of BPh_3. While a BPh_3 analogue of **4-2** was not available, it proved possible to access related platinum formatoborate complex (**4-8**) by treating of a mixture of **2-7** and BPh_3 with CO_2 (Scheme 4-1). Complex **4-9** was isolated in 90% yield and, like **4-10**, features both ^1H and ^{13}C NMR resonances consistent with a formate group. It was postulated that **4-9** forms via the in situ formation of **4-6**, which can subsequently react with BPh_3 to form the observed formatoborate complex.

Treatment of a benzene-d_6 solution of either **4-4** or **4-5** with four equiv of Me_2PhSiH resulted in the quantitative (by ^{31}P NMR) formation of **4-2** or **4-3**, respectively, with the concomitant evolution of methane and $(Me_2PhSi)_2O$ (Scheme 4-1), which were observed in the ^1H NMR spectra of the reaction mixtures at 0.14 and 0.32 ppm, respectively. Having thus observed the stoichiometric reduction of CO_2 to

methane, a catalytic variant of this reaction was pursued using in situ generated **4-2** or **4-3** (from treatment of **2-7** or **4-1** with one equiv of $B(C_6F_5)_3$) (Table 4-1). Using Me_2PhSiH as the reductant, catalytic reactions were carried in fluorobenzene at 65 °C, 1 atm of CO_2, and a catalyst loading of 0.065 mol % relative to silane. The amount of $(Me_2PhSi)_2O$ produced was determined on the basis of calibrated GC data and turnover numbers were determined based on mol of silane reacted per mol of catalyst. Using **4-2** as the catalyst afforded 1063 turnovers after 4 h, while the Pd analogue at the same loading resulted in 469 turnovers with heating at 85 °C (Table 4-1, entries 1 and 6). In the case of the more active Pt based catalyst **4-2**, the turnover frequency (TOF) after 0.5 h at 65 °C was determined to be 956 h^{-1}. As expected, the TOF was observed to decrease over the course of the reaction (TOF = 616 h^{-1} after 1 h and 266 h^{-1} after 4 h). Notably, the use of BPh_3 in place of $B(C_6F_5)_3$ under comparable conditions afforded no catalytic turnover.

In an effort to assess the lifetime of the catalyst (0.016 mol % **4-2** relative to the starting amount of silane), experiments where a fresh charge of CO_2 (1 atm) was reintroduced to the reaction vessel after an initial run of 4 h at 65 °C was carried out. Subsequent heating for an additional 4 h at the same temperature resulted in a TON of 1781 after a total of 8 h heating (entry 2). After two additional rounds of reintroducing CO_2, (16 h total heating at 65 °C), a TON of 2156 was achieved, indicating that catalyst activity does diminish with time (entry 3). The bulkier silane Et_3SiH led to significantly lowered activity (entry 4). Control experiments carried out in the absence of CO_2 confirmed that the observed silyl ether formation cannot be attributed to side reactions involving, for example, adventitious water (entry 5). Further control experiments confirmed the key role of both the platinum group metal complex and $B(C_6F_5)_3$ in

achieving the efficient catalytic reduction of CO_2 (entries 7-10). Notably, the catalytic productivity (TON) and rates (TOF) exhibited by **4-2** are comparable in magnitude to those observed by Brookhart and co-workers in their recently reported cationic (POCOP)Ir^{III} system.[91b]

Table 4-1. Reduction of CO_2 with trialkylsilanes.[a]

Entry	Catalyst	Mol % of catalyst	Silane	Time (h)	$(R_3Si)_2O$ (mmol)[b]	TON[c]
1	**4-2**	0.065	Me_2PhSiH	4	3.4	1063[d]
2[e]	**4-2**	0.016	Me_2PhSiH	8	5.7	1781
3[f]	**4-2**	0.016	Me_2PhSiH	16	6.9	2156
4	**4-2**	0.065	Et_3SiH	4	0.07	22
5[g]	**4-2**	0.065	Me_2PhSiH	4	0	0
6[h]	**4-3**	0.065	Me_2PhSiH	4	1.5	469
7[i]	$NaH/B(C_6F_5)_3$/15-c-5	0.4	Me_2PhSiH	4	1.2	57
8	$LiEt_3BH/B(C_6F_5)_3$	0.1	Me_2PhSiH	4	0.1	16
9	**2-7**	0.0065	Me_2PhSiH	4	0	0
10	**4-1**	0.0065	Me_2PhSiH	4	0	0

[a] Reaction conditions: 2 mL C_6H_5F, 1 atm CO_2, 9.78 mmol silane, 65 °C. [b] Determined on the basis of calibrated GC data. [c] Calculated based on mol of Si-H reacted per mol of catalyst. [d] TOF of 956 h^{-1} (0.5 h) and 616 h^{-1} (1 h).and 266 h^{-1} (4 h). [e] Reaction carried out using 39.16 mmol of silane; CO_2 (1 atm) was reintroduced to the reaction mixture after 4 h at 65 °C. [f] Reaction carried out using 39.16 mmol of silane; CO_2 (1 atm) was reintroduced to the reaction mixture after 4, 8 and 12 h at 65 °C. [g] Reaction conducted in absence of CO_2. [h] Reaction carried out at 85 °C. [i] 15-c-5 = 15-Crown-5.

A proposed catalytic cycle for the reduction of CO_2 utilizing complexes such as **4-2** and **4-3** and tertiary silanes is shown in Scheme 4-2. Based on the observed stoichiometric reactivity, we postulate that the abstracted hydride species **4-2** and **4-3**

initially react with CO_2 to form the corresponding formatoborate complexes **4-4** and **4-5**, respectively, which subsequently react with 2 equiv of silane to reform **4-2** and **4-3** and generate an equivalent of $CH_2(OSiR_3)_2$. Evidence for the intermediacy of the bis(silyl)acetal species was observed from the reaction of complexes **4-4** and **4-5** with one equivalent of either Me_2PhSiH or Et_3SiH. In both cases, this reaction resulted in the complete consumption of silane and afforded ca. 50% conversion (by ^{31}P NMR) to the abstracted hydride species **4-2** and **4-3**. The corresponding bis(silyl)acetal was also observed in the reaction mixture by ^{1}H NMR spectroscopy (5.0 ppm, s, C*H*$_2$(OSiR$_3$)). The subsequent reduction of the bis(silyl)acetal to form methane and the corresponding bis(silyl)ether is most likely achieved by the previously reported route involving $B(C_6F_5)_3$ mediated hydrosilylation.[91a,c,93] Support for this latter series of steps is drawn from the observation that the replacement of $B(C_6F_5)_3$ with the less Lewis acidic borane BPh_3 does not lead to the formation of methane and bis(silyl)ether. Rather, upon the reaction of **4-9** or **4-10** with 4 equiv of Me_2PhSiH, only the formation of $CH_2(OSiPhMe_2)_2$ was observed. Dissociation of $B(C_6F_5)_3$ from and of **4-2**-**4-5** may provide a significant (catalytic) amount of borane in solution to facilitate the hydrosilation steps. Interestingly, the addition of excess $B(C_6F_5)_3$ (2 equiv) to the catalysis reaction mixture led to a decrease in catalytic activity, which suggests that excess borane must somehow inhibit reactivity. This phenomenon remains to be investigated.

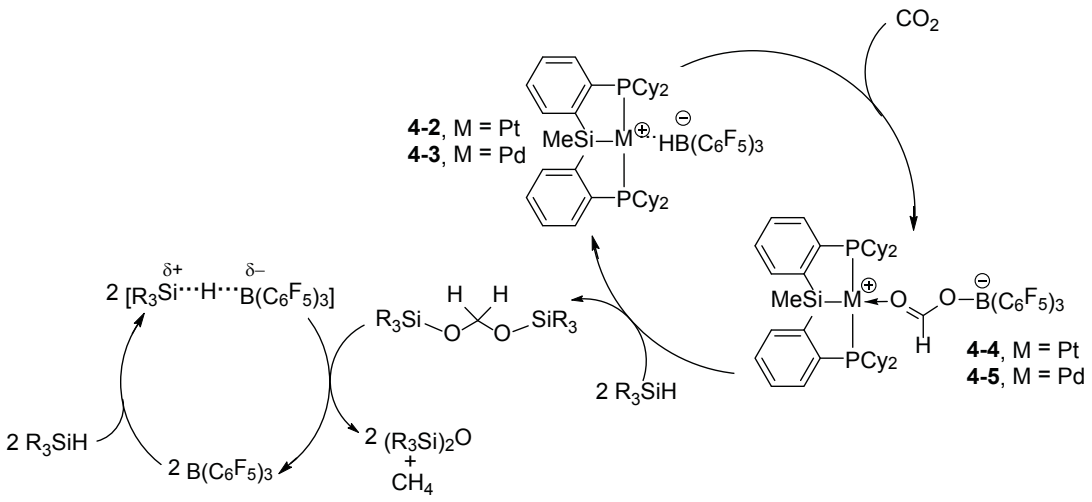

Scheme 4-2. Proposed catalytic cycle for the reduction of CO_2 to CH_4.

4.3 Conclusions

In summary, it has been demonstrated that Group 10 (Pd, Pt) silyl pincer complexes in combination with $B(C_6F_5)_3$ can facilitate the efficient catalytic conversion of CO_2 to methane using a tertiary silane as the reductant under mild conditions. The reduction involves the formation of Pd and Pt formatoborate complexes, which have been isolated and characterized. This reactivity represents a rare example of transition metal catalyzed CO_2 reduction to methane.

4.4. Experimental Section

4.4.1 General considerations

All experiments were conducted under nitrogen in an MBraun glovebox or using standard Schlenk techniques. Dry, oxygen-free solvents were used unless otherwise indicated. Tetrahydrofuran was purified by distillation from Na/benzophenone ketyl. All

other non-deuterated solvents were deoxygenated and dried by sparging with nitrogen and subsequent passage through a double-column solvent purification system purchased from MBraun Inc. All purified solvents were stored over 4 Å molecular sieves. Benzene-d_6, THF-d_8, and bromobenzene-d_5 were degassed via three freeze-pump-thaw cycles and stored over 4 Å molecular sieves. All other reagents were purchased from commercial supliers and used without further purification. Unless otherwise stated, ^{1}H, ^{13}C, ^{31}P, ^{11}B and ^{29}Si NMR characterization data were collected at 300 K on a Bruker AV-500 spectrometer operating at 500.1, 125.8, 202.5, 160.5 and 99.4 MHz (respectively) with chemical shifts reported in parts per million downfield of $SiMe_4$ (for ^{1}H, ^{13}C, and ^{29}Si), $BF_3{\cdot}OEt_2$ (for ^{11}B), or 85% H_3PO_4 in D_2O (for ^{31}P). ^{19}F NMR characterization data were collected at 300 K on a Bruker AV-300 spectrometer operating at 282.4 MHz with chemical shifts reported in parts per million relative to a standard sample of 0.5% $CF_3C_6H_5$ in chloroform-*d* at -63.7 ppm. ^{1}H and ^{13}C NMR chemical shift assignments are based on data obtained from ^{13}C-DEPTQ, ^{1}H-^{1}H COSY, ^{1}H-^{13}C HSQC, and ^{1}H-^{13}C HMBC NMR experiments. ^{29}Si NMR assignments are based on ^{1}H-^{29}Si HMBC experiments. In some cases, fewer than expected unique ^{13}C NMR resonances were observed, despite prolonged acquisition times. Infrared spectra were recorded as thin films between NaCl plates using a Bruker TENSOR 27 FT-IR spectrometer at a resolution of 4 cm^{-1}. Elemental analyses were performed by Canadian Microanalytical Service Ltd. of Delta, British Columbia, Canada and Midwest Microlab of Indianapolis, Indiana.

4.2.2 Typical procedure for the catalytic reduction of CO_2 with hydrosilanes

All catalytic runs were conducted under a nitrogen atmosphere in 50 mL resealable glass reaction cells containing a magnetic stirbar and fitted with a gas-tight PTFE stopcock. Dodecane (0.50 mL) was added to a solution of **2-7** (0.005 g, 0.0064 mmol) and $B(C_6F_5)_3$ (0.003 g, 0.0064 mmol) in 2 mL of C_6H_5F. The solution was transferred to a reaction cell and was degassed via two freeze-pump-thaw cycles. CO_2 (1 atm) was introduced. Under a purge of CO_2, neat Me_2PhSiH (1.50 mL, 9.78 mmol) was added to the reaction mixture via syringe. The sealed reaction cell was subsequently heated for 4 h at 65 °C. Once the reaction was complete the cell was submerged in a room temperature water bath and quickly exposed to vacuum and refilled with N_2 gas. In the glove box, the reaction mixture was filtered through a silica plug and was subsequently analyzed by use of gas chromatographic methods.

4.4.3 Synthetic detail and characterization data.

[Cy-P*Si*(μ-H)P]*Pd* (4-1). A cold (-30 °C) solution of **3-2** (0.15 g, 0.21 mmol) in ca. 5 mL of THF was treated with $LiEt_3BH$ (1.0 M in THF, 0.21 μL, 0.21 mmol). The resulting reaction mixture was allowed to stand at room temperature for 20 min. The volatile components of the reaction mixture were then removed under vacuum, and the residue was extracted with ca. 10 mL of benzene. The benzene extracts were filtered through Celite and the filtrate was concentrated to dryness under vacuum to afford **4-1** as an off white solid (0.13 g, 89% yield). ^{1}H NMR (500 MHz, benzene-d_6): δ 8.19 (d, 2 H, H_{arom}, J = 7 Hz), 7.47 (m, 2 H, H_{arom}), 7.33 (t, 2 H, H_{arom}, J = 7 Hz), 7.21 (t, 2 H, H_{arom}, J

= 7 Hz), 2.63 (m, 2 H, PC*y*), 2.37 (m, 2 H, PC*H*), 2.22 – 2.11 (overlapping resonances, 4 H, CH_{2Cy} + PC*H*), 1.96 (m, 2 H, CH_{2Cy}), 1.86 (m, 4 H, CH_{2Cy}), 1.62 – 0.98 (overlapping resonances, 31 H, CH_{2Cy} + Pd*H*; the Pd*H* resonance was identified at 1.28 ppm by the use of correlation spectroscopy), 0.92 (s, 3 H, Si*Me*). $^{13}C\{^1H\}$ NMR (125.8 MHz, benzene-d_6): δ 159.5 (apparent t, J = 26 Hz, C_{arom}), 144.1 (apparent t, J = 20 Hz, C_{arom}), 134.4 (apparent t, J = 11 Hz, CH$_{arom}$), 131.3 (CH$_{arom}$), 130.4 (CH$_{arom}$), 128.7 (CH$_{arom}$), 37.9 (apparent t, J = 11 Hz, P*C*H), 35.5 (apparent t, J = 13 Hz, P*C*H), 32.4 (CH$_{2Cy}$), 29.6 (CH$_{2Cy}$), 29.1 (CH$_{2Cy}$), 28.7 (CH$_{2Cy}$), 28.0 - 27.2 (overlapping resonances, CH$_{2Cy}$), 26.6 (CH$_{2Cy}$), 8.9 (s, Si*Me*). $^{31}P\{^1H\}$ NMR (202.5 MHz, benzene-d_6): δ 78.4 (s). ^{29}Si NMR (99.4 MHz, benzene-d_6): δ 62.5 (J_{SiH} = 47 Hz). IR (film, cm^{-1}): 1623 (br m, M-H). Anal. Calcd for $C_{37}H_{56}P_2SiPd$: C, 63.73; H, 8.09. Found: C, 63.65; H, 7.88.

{[Cy-PSiP]Pt}{HB(C$_6$F$_5$)$_3$} (4-2). A solution of **2-7** (0.10 g, 0.13 mmol) in. ca. 5 mL of benzene was treated with B(C_6F_5)$_3$ (0.065 g, 0.13 mmol). The resulting reaction mixture was allowed to stand at room temperature for 2 h. The volatile components of the reaction mixture were then removed under vacuum. The remaining residue was washed with ca. 3 mL of pentane and dried under vacuum to afford **4-2** as an off white solid (0.16 g, 95% yield). ^{1}H NMR(500 MHz, THF-d_8): δ 8.20 (m, 2 H, H_{arom}), 7.83 (m, 2 H, H_{arom}), 7.61 (m, 4 H, H_{arom}), 3.73 (br m, resonance obscured by residual THF, 1 H, B-*H*), 2.78 (m, 2 H, PC*H*), 2.61 (m, 2 H, PC*H*), 2.29 - 2.01 (overlapping resonances, 4 H, CH_{2Cy}), 1.96 - 1.07 (overlapping resonances, 36 H, CH_{2Cy}), 0.51 (s with Pt satellites, 3 H, Si*Me*, $^3J_{HPt}$ = 32 Hz). $^{13}C\{^1H\}$ NMR (125.8 MHz, THF-d_8): δ 150.3 (m, C_{arom}), 148.5 (m, C_{arom}), 139.7 (m, C_{arom}), 138.3 (m, C_{arom}), 136.3 (m, C_{arom}), 133.5 (m, CH$_{arom}$), 132.9 (m, CH$_{arom}$), 132.3 (m, CH$_{arom}$), 131.0 (CH$_{arom}$), 37.8 (br, P*C*H), 31.2 - 26.4 (overlapping

resonances, CH_{2Cy}), 7.5 (s, Si*Me*). ^{31}P {^{1}H} NMR (202.5 MHz, THF-d_8): δ 66.8 (s with Pt satellites, $^{1}J_{PPt}$ = 3055 Hz). ^{29}Si NMR (99.4 MHz, THF-d_8): δ 18.1 ($^{1}J_{SiPt}$ = 1271 Hz). ^{11}B NMR (160.5 MHz, THF-d_8): δ - 25.4 (d, $^{1}J_{BH}$ = 92 Hz). ^{19}F NMR (282.4 MHz, THF-d_8): δ -132.2 (br s, 6 F, *o*-C_6F_5), -163.0 (t, 3 F, $^{3}J_{FF}$ = 20 Hz, *p*-C_6F_5), -166.2 (m, 6 F, *m*-C_6F_5). Anal. Calcd for $C_{55}H_{56}BF_{15}P_2SiPt$: C, 50.90; H, 4.35. Found: C, 50.62; H, 4.47.

{[Cy-PSiP]Pd}{HB(C_6F_5)$_3$} (4-3). A solution of **4-1** (0.098 g, 0.14 mmol) in ca. 5 mL of benzene was treated with B(C_6F_5)$_3$ (0.072 g, 0.14 mmol). The resulting reaction mixture was allowed to stand at room temperature for 2 h. The volatile components of the reaction mixture were then removed under vacuum. The remaining residue was washed with ca. 3 mL of pentane and dried under vacuum to afford **4-3** as an off white solid (0.15 g, 89% yield). ^{1}H NMR (500 MHz, benzene-d_6): δ 7.66 (d, 2 H, H_{arom}, J = 7 Hz), 7.23 (t, 2 H, H_{arom}, J = 7 Hz), 7.18 - 7.09 (overlapping resonances, 4 H, H_{arom}), 4.06 (br m, 1 H, B-*H*), 2.17 (m, 2 H, PC*H*), 1.91 (m, 2 H, PC*H*), 1.80 (m, 4 H, CH_{2Cy}), 1.65 – 0.98 (overlapping resonances, 36 H, CH_{2Cy}), 0.71 (s, 3 H, Si*Me*). ^{13}C{^{1}H} NMR (125.8 MHz, benzene-d_6): δ 152.1 (apparent t, J = 26 Hz, C_{arom}), 150.4 (m, C_{arom}), 148.4 (m, C_{arom}), 138.6 (m, C_{arom}), 136.8 (m, C_{arom}), 136.1 (m, C_{arom}), 133.2 (apparent t, J = 11 Hz, CH_{arom}), 132.3 (CH_{arom}), 132.1 (CH_{arom}), 130.8 (CH_{arom}), 36.4 (apparent t, J = 13 Hz, P*C*H), 35.7 (apparent t, J = 15 Hz, P*C*H), 31.0 - 26.1 (overlapping resonances, CH_{2Cy}), 9.5 (s, Si*Me*). ^{31}P {^{1}H} NMR (202.5 MHz, benzene-d_6): δ 56.9 (s). ^{29}Si NMR (99.4 MHz, benzene-d_6): δ 55.8. ^{11}B NMR (160.5 MHz, benzene-d_6): δ -23.3 (d, $^{1}J_{BH}$ = 77 Hz). ^{19}F NMR (282.4 MHz, benzene-d_6): δ -133.1 (br s, 6 F, *o*-C_6F_5), -162.0 (t, 3 F, $^{3}J_{FF}$

= 17 Hz, *p*-C_6F_5), -165.8 (m, 6 F, *m*-C_6F_5). Anal. Calcd for $C_{55}H_{56}BF_{15}P_2SiPd$: C, 54.63; H 4.67. Found: C, 54.34; H, 4.61.

{[Cy-PSiP]Pt}{(HCO_2)B(C_6F_5)$_3$} (4-4). A solution of **4-2** (0.10 g, 0.077 mmol) in ca. 5 mL of benzene was placed in a 250 mL round bottom Schlenk flask. The solution was subsequently sparged with CO_2 gas (ca. 1 atm.) for 1 min. The resulting reaction mixture was allowed to stand at room temperature under a CO_2 atmosphere for 2 h. The volatile components of the reaction mixture were then removed under vacuum. The remaining residue was washed with ca. 3 mL of pentane and dried under vacuum to afford **4-4** as an off white solid (0.091 g, 88% yield). ^{1}H NMR (500 MHz, THF-d_8): δ 8.68 (s, 1 H, *H*CO_2), 8.01 (d, 2 H, H_{arom}, J = 7 Hz), 7.59 (m, 2 H, H_{arom}), 7.39 (t, 2 H, H_{arom}, J = 7 Hz), 7.32 (t, 2 H, H_{arom}, J = 7 Hz), 2.78 (m, 2 H, P*CH*), 2.15 – 1.97 (overlapping resonances, 4 H, PC*H* + CH_{2Cy}), 1.78 – 0.71 (overlapping resonances, 38 H, CH_{2Cy}), 0.44 (s, 3 H, Si*Me*). ^{13}C{^{1}H} NMR (125.8 MHz, bromobenzene-d_5): δ 170.8 (s, HCO_2), 149.5 (m, C_{arom}), 147.5 (m, C_{arom}), 138.4 (m, C_{arom}), 136.2 (m, C_{arom}),132.8 (*C*H$_{arom}$), 128.6 (*C*H$_{arom}$), 36.4 (m, P*C*H), 30.4 (*C*H$_{2Cy}$), 29.2 (*C*H$_{2Cy}$), 28.6 (*C*H$_{2Cy}$), 27.9 (*C*H$_{2Cy}$), 27.3 - 26.7 (overlapping resonances, *C*H$_{2Cy}$), 26.0 (*C*H$_{2Cy}$),, 6.6 (Si*Me*). ^{31}P{^{1}H} NMR (202.5 MHz, THF-d_8): δ 64.1 (s with Pt satellites, $^1J_{PtP}$ = 3079 Hz). ^{29}Si NMR (99.4 MHz, THF-d_8): δ 20.8. ^{11}B NMR (160.5 MHz, THF-d_8): -3.93. ^{19}F NMR (282.4 MHz, THF-d_8): -133.2 (d, 6 F, *o*-C_6F_5, $^3J_{FF}$ = 23 Hz), -158.1 (t, 3 F, *p*-C_6F_5 $^3J_{FF}$ = 20 Hz), -164.4 (m, 6 F, *m*-C_6F_5). Anal. Calcd for $C_{56}H_{56}BF_{15}O_2P_2SiPt$: C, 50.12; H, 4.21. Found: C, 50.26; H, 4.47.

{[Cy-PSiP]Pd}{(HCO_2)B(C_6F_5)$_3$} (4-5). A solution of **4-7** (0.083 g, 0.11 mmol) in ca. 5 mL of benzene was treated with B(C_6F_5)$_3$ (0.058 g, 0.11 mmol). The resulting

reaction mixture was allowed to stand at room temperature for 2 h. The volatile components of the reaction mixture were then removed under vacuum. The remaining residue was washed with ca. 3 mL of pentane and dried under vacuum to afford **4-5** as an off white solid (0.13 g, 94% yield). ^{1}H NMR (500 MHz, benzene-d_6): δ 8.49 (s, 1 H, HCO_2), 7.80 (d, 2 H, H_{arom}, J = 7 Hz), 7.23-7.19 (overlapping resonances, 4 H, H_{arom}), 7.11 (t, 2 H, H_{arom}, J = 7 Hz), 2.36 (m, 2 H, P*CH*), 2.60 (overlapping resonances, 4 H, P*CH* + CH_{2Cy}), 1.91 (m, 2 H, CH_{2Cy}), 1.89 (m, 2 H, CH_{2Cy}), 1.77 – 0.90 (overlapping resonances, 32 H, CH_{2Cy}), 0.87 – 0.72 (overlapping resonances, 5 H, Si*Me* + CH_{2Cy}; the Si*Me* resonance was identified at 0.80 ppm by the use of correlation spectroscopy). ^{13}C{^{1}H} NMR (125.8 MHz, benzene-d_6): δ 171.7 (s, HCO_2), 155.0 (apparent t, J = 25 Hz, C_{arom}), 150.1 (C_{arom}), 148.2 (m, C_{arom}), 138.9 (m, C_{arom}), 138.2 (apparent t, J = 21 Hz, C_{arom}), 136.9 (m, C_{arom}),133.3 (apparent t, J = 22 Hz, CH_{arom}), 131.7 (CH_{arom}), 131.4 (CH_{arom}), 129.9 (CH_{arom}), 36.1(P*C*H), 30.9 (CH_{2Cy}), 30.1 (CH_{2Cy}), 28.9 (CH_{2Cy}), 28.8 (CH_{2Cy}), 27.6 - 26.9 (overlapping resonances, CH_{2Cy}), 26.1 (CH_{2Cy}), 8.8 (Si*Me*). ^{31}P {^{1}H} NMR (202.5 MHz, benzene-d_6): δ 56.4. ^{29}Si NMR (99.4 MHz, benzene-d_6): δ 51.9. ^{19}F NMR (282.4 MHz, benzene-d_6): δ -132.2 (m, 6 F, *o*-C_6F_5), -157.7 (m, 3 F, *p*-C_6F_5), -163.7 (m, 6 F, *m*-C_6F_5). Anal. Calcd for $C_{54}H_{56}BF_{15}O_2P_2SiPd$: C, 53.67; H, 4.50. Found: C, 53.57; H, 4.28.

[Cy-PSiP]Pt(HCO$_2$) (4-6). A solution of (Cy-P*Si*(μ-H)P)*Pt* (**2-7**) (0.010 g, 0.013 mmol) in. ca. 0.6 mL of benzene-d_6 was placed in a J. Young NMR tube and degassed via three freeze-pump-thaw cycles. CO_2 gas (ca. 1 atm) was introduced into the tube. The resulting reaction mixture was allowed to stand at room temperature for 15 minutes and was subsequently characterized *in situ*. ^{1}H NMR (500 MHz, benzene-d_6): δ 9.81 (s

with Pt satellites, 1 H, *H*CO_2, $^3J_{HPt}$ = 40 Hz), 8.04 (d, 2 H, H_{arom}, J = 7 Hz), 7.40 (m, 2 H, H_{arom}), 7.27 (t, 2 H, H_{arom}, J = 7 Hz), 7.15 (m, 2 H, H_{arom}), 2.90 (m, 2 H, PC*H*), 2.62 (m, 2 H, PC*H*), 2.48 (m, 2 H, CH_{2Cy}), 2.21 (m, 2 H, CH_{2Cy}), 1.81 (m, 2 H, CH_{2Cy}), 1.72 – 0.84 (overlapping resonances, 34 H, CH_{2Cy}), 0.80 (s with Pt satellites, 3 H, Si*Me*, $^3J_{HPt}$ = 26 Hz). $^{13}C\{^1H\}$ NMR (125.8 MHz,benzene-d_6): δ 166.9 (HCO_2), 155.7 (apparent t, J = 21 Hz, C_{arom}), 140.0 (apparent t, J = 26 Hz, C_{arom}), 132.5 (apparent t, J = 10 Hz, CH$_{arom}$), 130.9 (CH$_{arom}$), 129.9 (CH$_{arom}$), 128.4 (CH$_{arom}$), 36.9 (apparent t, J = 14 Hz, P*C*H), 35.8 (apparent t, J = 14 Hz, P*C*H), 29.7 (CH$_{2Cy}$), 29.0 (CH$_{2Cy}$), 28.6 (CH$_{2Cy}$), 28.2 (CH$_{2Cy}$), 27.3 – 26.9 (overlapping resonances, CH$_{2Cy}$), 26.4 (CH$_{2Cy}$), 25.8 (CH$_{2Cy}$), 6.8 (Si*Me*). $^{31}P\{^1H\}$ NMR (202.5 MHz, C_6D_5Br): δ 62.1 (s with Pt satellites, $^1J_{PPt}$ = 3101 Hz).

[Cy-PSiP]Pd(HCO$_2$) (4-7). A thick-walled Schlenk tube fitted with a Teflon stopcock was charged with a solution of **4-1** (0.11 g, 0.16 mmol) in. ca 5 mL of benzene. The solution was degassed via three freeze-pump-thaw cycles and CO_2 gas (ca. 1 atm) was introduced into the reaction vessel. The resulting reaction mixture was allowed to stand at room temperature under a CO_2 atmosphere for 30 minutes. The volatile components of the reaction mixture were then removed under vacuum. The remaining residue was washed with ca. 3 mL of pentane and dried under vacuum to afford **4-7** as an off white solid (0.10 g, 84% yield). ^1H NMR (500 MHz, benzene-d_6): δ 9.20 (s, 1 H, *H*CO_2), 7.93 (d, 2 H, H_{arom}, J = 7 Hz), 7.33 (m, 2 H, H_{arom}) 7.26 (t, 2 H, H_{arom}, J = 7 Hz), 7.15 (m, 2 H, H_{arom}), 2.60 (m, 2 H, P*CH*), 2.40 – 2.32 (overlapping resonances , 4 H, P*CH* + CH_{2Cy}), 2.11 (m, 2 H, CH_{2Cy}), 1.78 (m, 2 H, CH_{2Cy}), 1.67 – 1.04 (overlapping resonances, 34 H, CH_{2Cy}), 0.76 (s, 3 H, Si*Me*,). $^{13}C\{^1H\}$ NMR (125.8 MHz, benzene-d_6): δ 170.3 (HCO_2), 156.8 (apparent t, J = 26 Hz, C_{arom}), 140.3 (apparent t, J = 20 Hz, C_{arom}),

133.5 (apparent t, J = 8 Hz, CH$_{arom}$), 131.9 (CH$_{arom}$), 131.1 (CH$_{arom}$), 129.6 (CH$_{arom}$), 36.8 (PCH), 30.7 (CH$_{2Cy}$), 29.9 - 27.8 (overlapping resonances, CH$_{2Cy}$), 27.2 (CH$_{2Cy}$), 26.7 (CH$_{2Cy}$), 9.4 (SiMe). ^{31}P{^{1}H} NMR (202.5 MHz, benzene-d_6): δ 56.8. ^{29}Si NMR (99.4 MHz, benzene-d_6): δ 51.1. Anal. Calcd for $C_{38}H_{56}O_2P_2SiPd$: C, 61.57; H, 7.61. Found: C, 61.19; H, 7.54.

{[Cy-PSiP]Pd}{HBPh$_3$} (4-8). A solution of **4-1** (0.10 g, 0.14 mmol) in. ca 5 mL of benzene was treated with BPh$_3$ (0.035 g, 0.14 mmol). The resulting reaction mixture was allowed to stand at room temperature for 2 h. The volatile components of the reaction mixture were then removed under vacuum. The remaining residue was washed with ca. 3 mL of pentane and dried under vacuum to afford **4-8** as an off white solid (0.12 g, 91% yield). ^{1}H NMR (500 MHz, benzene-d_6): δ 8.10 (br m, 6 H, o-BPh_3), 7.94 (d, 2 H, H_{arom}, J = 7 Hz), 7. 36 (t, 6 H, m-BPh_3, J = 7 Hz), 7.27 – 7.21 (overlapping resonances, 7 H, p-BPh_3 + H_{arom}), 7.13 (t, 2 H, H_{arom}, J = 7 Hz), 2.29 (m, 4 H, PCH), 1.60 – 1.01 (overlapping resonances, 38 H, CH_{2Cy}), 0.85 (s, 3 H, SiMe), 0.73 (m, 2 H, CH_{2Cy}). ^{13}C{^{1}H} NMR (125.8 MHz, benzene-d_6): δ 154.8 (apparent t, J = 24 Hz, C_{arom}), 140.1 (apparent t, J = 21 Hz, C_{arom}), 137.3 (o-BPh_3), 133.2 (apparent t, J = 11 Hz, CH$_{arom}$), 132.4 (CH$_{arom}$), 131.1 (CH$_{arom}$), 129.6 (CH$_{arom}$), 127.4 (m-BPh_3), 125.3 (br, p-BPh_3), 35.9 (m, PCH), 31.0 (CH$_{2Cy}$), 29.9 – 27.1 (overlapping resonances, CH$_{2Cy}$), 26.3 (CH$_{2Cy}$), 9.9 (SiMe). ^{31}P {^{1}H} NMR (202.5 MHz, benzene-d_6): δ 58.8. ^{29}Si NMR (99.4 MHz, benzene-d_6): δ 58.3. ^{11}B NMR (160.5 MHz, benzene-d_6): δ 3.13 (br s). Anal. Calcd for $C_{55}H_{71}BP_2SiPd$: C, 70.32; H, 7.62. Found: C, 69.88; H, 7.67.

{[Cy-PSiP]Pt}{(HCO$_2$)BPh$_3$} (4-9). A solution of [Cy-PSi(μ-H)P]Pt (**2-7**) (0.046 g, 0.059 mmol) in ca. 5 mL of benzene was placed in a 250 mL round bottom

Schlenk flask and was treated with BPh_3 (0.014 g, 0.059 mmol). The solution was sparged with CO_2 (1 atm) for 1 min. The resulting reaction mixture was allowed to stand at room temperature under a CO_2 atmosphere for 2 h. The volatile components of the reaction mixture were then removed under vacuum. The remaining residue was washed with ca. 3 mL of pentane and dried under vacuum to afford **4-9** as an off-white solid (0.057 g, 90% yield). ^{1}H NMR (500 MHz, benzene-d_6): δ 9.06 (s, 1 H, *H*CO_2), 7.94 (d, 2 H, H_{arom}, J = 7 Hz), 7.82 (m, 6 H, *o*-B*Ph*$_3$), 7.37 (m, 6 H, *m*-B*Ph*$_3$), 7.27 - 7.21 (overlapping resonances, 7 H, *p*-B*Ph*$_3$ + H_{arom}), 7.11 (t, 2 H, H_{arom}, J = 7 Hz), 2.67 (m, 2 H, P*CH*), 2.28 - 2.20 (overlapping resonances, 4 H, PC*H* + CH_{2Cy}), 2.00 (m, 2 H, CH_{2Cy}), 1.64 - 0.88 (overlapping resonances, 37 H, CH_{2Cy} + Si*Me*; the Si*Me* resonance was identified at 0.88 ppm by the use of correlation spectroscopy), 0.72 (m, 2 H, CH_{2Cy}). ^{13}C{^{1}H} NMR (125.8 MHz, benzene-d_6): δ 173.6 (H*C*O_2), 154.9 (apparent t, J = 21 Hz, C_{arom}), 139.2 (apparent t, J = 28 Hz, C_{arom}), 135.1 (*o*-B*Ph*$_3$), 133.1 (apparent t, J = 10 Hz, *C*H$_{arom}$), 131.8 (*C*H$_{arom}$), 131.5 (*C*H$_{arom}$), 130.6 (*C*H$_{arom}$), 127.5 (*m*-B*Ph*$_3$), 125.5 (*p*-B*Ph*$_3$), 37.0 (apparent t, J = 14 Hz, P*C*H), 36.3(apparent t, J = 15 Hz, P*C*H), 30.7 (*C*H$_{2Cy}$), 29.3-26.6 (overlapping resonances, *C*H$_{2Cy}$), 25.9 (*C*H$_{2Cy}$), 7.0 (Si*Me*). ^{31}P{^{1}H} NMR (202.5 MHz, benzene-d_6): δ 62.6 (s with Pt satellites, $^1J_{PPt}$ = 3059 Hz). ^{29}Si NMR (99.4 MHz, benzene-d_6): δ 21.1 ($^1J_{SiPt}$ = 1307 Hz). ^{11}B NMR (160.5 MHz, benzene-d_6): δ 8.01 (br s). Anal. Calcd for $C_{56}H_{71}BO_2P_2SiPt$: C, 62.74; H, 6.68. Found: C, 63.01; H, 6.60.

{[Cy-PSiP]Pd}{(HCO$_2$)BPh$_3$} (4-10). A solution of **4-8** (0.080 g, 0.085 mmol) in. ca 5 mL of benzene was placed in a 250 mL round bottom Schlenk flask. The solution was sparged with CO_2 gas (1 atm) for 1 minute. The resulting reaction mixture

was allowed to stand at room temperature under a CO_2 atmosphere for 2 h. The volatile components of the reaction mixture were then removed under vacuum. The remaining residue was washed with ca. 3 mL of pentane and dried under vacuum to afford **4-10** as an off white solid (0.064 g, 77% yield). ^{1}H NMR (500 MHz, benzene-d_6): δ 8.85 (s, 1 H, *H*CO_2), 7.89 (d, 2 H, H_{arom}, J = 7 Hz), 7.83 (d, 6 H, *o*-B*Ph*$_3$, J = 7 Hz), 7.37 (t, 6 H, *m*-B*Ph*$_3$, J = 7 Hz), 7.27 - 7.23 (overlapping resonances, 7 H, H_{arom} + *p*-B*Ph*$_3$),7.11 (t, 2 H, H_{arom}, J = 7 Hz), 2.4 (m, 2 H, P*CH*), 2.18 - 2.08 (overlapping resonances, 4 H, PC*H* + CH_{2Cy}), 1.97 (m, 2 H, CH_{2Cy}) 1.65 - 0.98 (overlapping resonances, 34 H, CH_{2Cy}), 0.93 (s, 3 H, Si*Me*), 0.71 (m, 2 H, CH_{2Cy}). ^{13}C{^{1}H} NMR (125.8 MHz, benzene-d_6): δ 173.3 (H*C*O_2), 156.1(br s, C_{arom}), 155.8 (apparent t, J = 26 Hz, C_{arom}), 139.0 (apparent t, J = 20 Hz, C_{arom}), 135.1 (*o*-B*Ph*$_3$), 133.3 (apparent t, J = 11 Hz, *C*H$_{arom}$), 131.6 (*C*H$_{arom}$), 131.2 (*C*H$_{arom}$), 129.7 (*C*H$_{arom}$), 127.5 (*m*-B*Ph*$_3$), 125.3 (*p*-B*Ph*$_3$), 36.1 (P*C*H), 30.8 (*C*H$_{2Cy}$), 29.7 (*C*H$_{2Cy}$), 29.2 (*C*H$_{2Cy}$), 29.1 (*C*H$_{2Cy}$), 27.7 – 26.8 (overlapping resonances, *C*H$_{2Cy}$), 25.9 (*C*H$_{2Cy}$), 9.1 (Si*Me*). ^{31}P {^{1}H} NMR (202.5 MHz, benzene-d_6): δ 56.6. ^{29}Si NMR (99.4 MHz, benzene-d_6): δ 51.1. ^{11}B NMR (160.5 MHz, benzene-d_6): δ 5.9 (br s). Anal. Calcd for $C_{56}H_{71}BO_2P_2SiPd$: C, 68.39; H, 7.28. Found: C, 68.22; H, 7.37.

CHAPTER 5: Synthesis and Reactivity of [Cy-PSiP]Pt^{II} Hydroxo and Alkoxo Complexes: Si-H, C-H, and H-H Bond Activation Chemistry

5.1 Introduction

Late metal complexes featuring terminal, non-dative heteroatomic ligands (e.g. -OR, $-NR_2$) represent an important class of compounds that have received a considerable amount of attention in recent years, due in part to their involvement in important catalytic processes,[39a,39e,45,94] as well as their potential as highly reactive species due to the disruption of ligand to metal π-donation and the polar nature of the metal-heteroatom bond.[95] Despite their significance, well documented examples of such complexes have been relatively rare,[95b] especially in comparison to late metal alkyl and hydrido complexes.

From the perspective of stoichiometric reactivity, there has been significant recent interest in developing E-H (E = main group element, e.g. H, C, Si) bond activation processes that involve the addition of an E-H bond across a late metal-heteroatom linkage.[96] A handful of examples of H-H and C-H bond activation involving late metal amido, alkoxo, and hydroxo complexes have been reported thus far. Periana and co-workers have recently shown that Ir^{III} hydroxo and methoxide complexes are capable of heterolytic C-H bond activation. It was shown that heating a benzene solution of (acac-O,O)$_2$Ir(OR)(Py) (acac-O,O = κ^2-*O,O*-acetylacetonate, Py = pyridine, R = H, Me) resulted in formation of (acac-O,O)$_2$Ir(Ph)(Py) and HOR via an initial dissociation of the pyridine ligand followed by coordination of benzene and subsequent metathesis-like C-H

bond cleavage.[97] Similarly, Gunnoe and co-workers have shown net C-H activation by Ru^{II} hydroxide, phenoxide and anilido complexes. Heating of a benzene-d_6 solution of $TpRu(PMe_3)_2(X)$ (Tp = hydridotris(pyrazolyl)borate, X = OH, OPh, NHPh) resulted in reversible H/D exchange both at the non dative ligand X, as well as the Tp ligand. It is believed that the reaction involving H/D exchange at the ligand X proceeds by initial dissociation of PMe_3 followed by coordination of benzene then 1,2-addition of a C-H/D bond across the Ru-heteroatom moiety.[98] Goldberg and co-workers have also shown C-H bond cleavage by Rh^{I} hydroxide and trifluoroethoxide species. This was achieved by heating a benzene solution of (PNP)Rh(X) (PNP = 2,6-($^{t}Bu_2PCH_2)_2C_5H_3N$, X = OH, OCH_2CF_3) to afford (PNP)Rh(Ph).[99] It is noteworthy, in this instance, that no ancillary ligand dissociation was necessary to achieve C-H activation. The incorporation of such C-H bond activation processes into a catalytic cycle could provide routes for the production of heteroatom functionalized products from hydrocarbons, which is a highly desirable type of reactivity. In this regard, the development of alternative systems that can undergo such E-H bond addition steps across a late metal heteroatom linkage is an important goal, as it can further the understanding of this type of reactivity and may provide a platform for potential catalytic applications.

In this context, the synthesis of silyl pincer supported, monomeric Pt^{II} hydroxo and alkoxo complexes of the type [Cy-PSiP]Pt(OR) ([Cy-PSiP] = [κ^3-(2-$Cy_2PC_6H_4)_2SiMe]^-$, R = H, alkyl) was pursued, with the goal of studying the E-H bond activation reactivity of such species. Although many Pt^{II} alkoxo and hydroxo species are known to form dimers via coordination of the available lone pair on oxygen to an

adjacent metal center,[94a,95a,100] the chelating tridentate coordination of [Cy-PSiP] to Pt^{II} is anticipated to promote the isolation of monomeric, square planar complexes.

5.2 Results and Discussion

5.2.1 Synthesis of [Cy-PSiP]Pt(OR) (R = H, Ph, ^{t}Bu)

The most general synthetic approach developed for the preparation of [Cy-PSiP]Pt^{II} alkoxo and hydroxo complexes involved treatment of the Pt^{II} amido complex [Cy-PSiP]Pt(NH^{t}Bu) (**5-1**) with an alcohol or water to generate H_2N^tBu and the corresponding alkoxo or hydroxo complex, respectively (Scheme 5-1). In turn, complex **5-1** proved readily accessible by treatment of [Cy-PSiP]PtCl (**2-1**) with one equiv of LiNH^{t}Bu (Scheme 5-1). The ^{1}H NMR spectrum (benzene-d_6) of **5-1** features a characteristic *tert*-butyl resonance at 1.71 ppm (s) as well as a resonance at 1.30 ppm that was assigned as the N*H* proton on the basis of ^{1}H-^{15}N HMQC correlation spectroscopy. The N-H stretch is observed as a weak signal at 3206 cm^{-1}. Interestingly, although complexes of the type [Cy-PSiP]M(alkyl) (M = Ni, Pd) have been shown to undergo intramolecular rearrangement processes involving Si-C bond cleavage in the pincer backbone and transfer of the alkyl ligand to Si (Chapter 3)[25f], complex **5-1** does not appear to undergo such reactivity, despite the high anticipated strength of the Si-N linkage that would result.

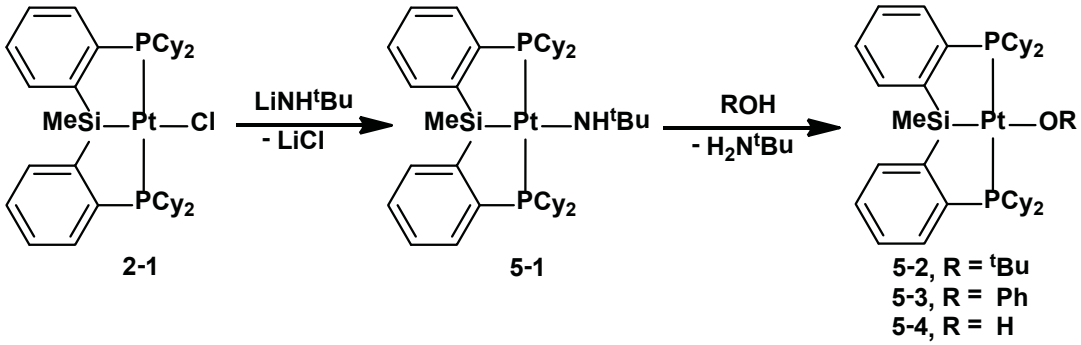

Scheme 5-1. Synthesis of amido and alkoxo [Cy-PSiP]Pt^{II} complexes.

Treatment of **5-1** with an excess (6.6 equiv.) of ^{t}BuOH led to formation of the C_s-symmetric complex [Cy-PSiP]Pt(O^{t}Bu) (**5-2**) with the concomitant formation of $H_2N^{t}Bu$ (Scheme 5-1). Given the anticipated highly basic nature of the Pt-*NH^{t}Bu* group,[96a] this type of reaction is likely best described as a Bronsted acid/base type of process involving deprotonation of the alcohol by the Pt-amido ligand.[94a,101] Complex **5-2** was readily isolated in 97% yield and gives rise to a new *tert*-butyl ^{1}H NMR resonance associated with the O*^{t}Bu* ligand at 1.76 ppm in the ^{1}H NMR spectrum (benzene-d_6). The solid state structure of **5-2** was determined using single crystal X-ray diffraction techniques (Figure 5-1, Table 5-1). The monomeric alkoxide complex exhibits distorted square planar geometry in the solid state (P1-Pt-P2 angle of 156.15(4)º and Si-Pt-O angle of 177.03(8)º), with the O^{t}Bu ligand coordinated *trans*- to Si. The Pt-O bond distance of 2.132(2) Å is relatively long in comparison with previously reported terminal Pt-alkoxide complexes, which show a range of Pt-O distances of 1.99 - 2.07 Å.[94a] This phenomenon likely reflects the strong *trans*-influence of the silyl group in the pincer ligand backbone, as well as possibly the steric crowding around the metal center. The Pt-O-C2 bond angle of 124.1(2)º is significantly bent.

Treatment of **5-1** with one equiv of PhOH resulted in the formation of [Cy-PSiP]Pt(OPh) (**5-3**), which was isolated in 72% yield (Scheme 5-1). The solution (benzene-d_6) NMR data for **5-3** is in agreement with the formulation of this complex as a C_s-symmetric terminal phenoxide species, as indicated by a single ^{31}P NMR resonance at 60.9 ppm ($^1J_{PPt}$ = 3052 Hz), as well as the presence of three additional aromatic ^{1}H NMR resonances (relative to **5-1**) at 7.45, 7.35, and 6.79 ppm that correspond to the *meta*-, *ortho*-, and *para*-phenoxide protons, respectively. Similarly, treatment of **5-1** with a large excess (ca. 230 equiv) of degassed water afforded the hydroxo complex [Cy-PSiP]Pt(OH) (**5-4**) in 84% isolated yield (Scheme 5-1). The ^{1}H NMR spectrum of **5-4** (benzene-d_6) no longer features a *tert*-butyl resonance and instead exhibits a sharp resonance at 3.69 ppm (1 H) that is attributed to the Pt-O*H*. This assignment was confirmed by the reaction of **5-1** with D_2O to give [Cy-PSiP]Pt(OD) (**5-4-*d*$_1$**), which gives rise to a ^{1}H NMR spectrum similar to that of **5-4** with the only exception being the absence of the resonance at 3.69 ppm. The ^{2}H NMR spectrum of **5-4-*d*$_1$** (benzene) contains a broad resonance centered at 4.13 ppm, which is assigned to the Pt-O*D* group in **5-4-*d*$_1$**. The O-H stretch in **5-4** is observed in the IR spectrum as a broad signal at 3227 cm^{-1}.

The solid state structure of **5-4** was confirmed using X-ray diffraction techniques, which confirmed the monomeric nature of this complex (Figure 5-1,Table 5-1). Similar to **5-2,** the geometry at Pt can best be described as distorted square planar (P1-Pt-P2 angle of 164.71(3)º and Si-Pt-O angle of 178.84(8)º) with the hydroxide ligand positioned *trans* to the silyl donor. The Pt-O distance of 2.126(3)Å is somewhat long in comparison to previous crystallographically characterized Pt^{II} terminal hydroxo complexes (2.03 Å – 2.194 Å),[102] and is comparable to the Pt-O bond observed for **5-2** (2.132(2) Å). As in the

case of **5-2**, this relatively long bond distance can be attributed to the strong *trans*-influence of the silyl group. Complex **5-4** thus represents a relatively rare example of a terminal, monomeric Pt^{II} hydroxo complex. [102-103]

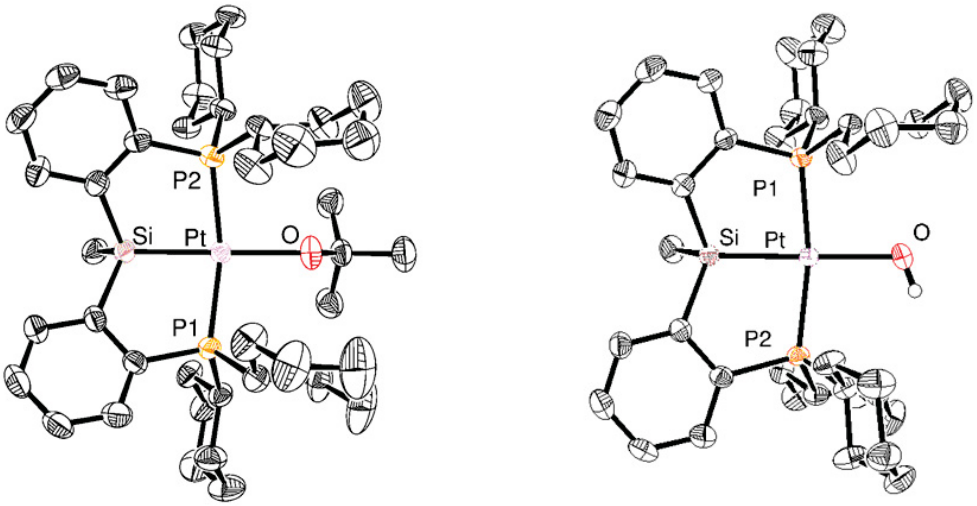

5-2 **5-4**

Figure 5-1. ORTEP diagrams for **5-2** and **5-4** shown with 50% displacement ellipsoids; selected H atoms have been omitted for clarity.

Table 5-1. Selected interatomic distances (Å) and angles (°) for **5-2** and **5-4**.

Interatomic Distances (Å)		
	5-2	**5-4**
Si-Pt	2.2818(10)	2.2782(10)
Pt-O	2.131(2)	2.126(3)
Interatomic Angles (°)		
	5-2	**5-4**
P1-Pt-P2	156.15(4)	164.71(3)
Si-Pt-O	177.03(8)	178.84(8)

5.2.2 Reactivity of [Cy-PSiP]Pt^{II} alkoxo and hydroxo complexes with E-H bonds

Having successfully prepared a variety of terminal Pt^{II} alkoxo and hydroxo complexes supported by Cy-PSiP ligation, the reactivity of such complexes towards a variety of E-H bonds was explored. Having noted that complexes **5-2** - **5-4** are stable indefinitely in benzene solution, even upon heating (80 ºC, 72 h), the reactivity of more readily activated E-H bonds was pursued. Molecules containing relatively acidic C-H bonds were targeted initially, as terminal Pt^{II} alkoxo and hydroxo complexes are anticipated to be strongly basic, and may thus activate acidic C-H bonds via Bronsted acid/base processes.[104] Thus, each of **5-2**, **5-3**, and **5-4** was treated with one equiv of phenylacetylene (pKa = 28.8,[105]). In all three cases rapid and quantitative (^{31}P NMR) formation of the acetylide complex [Cy-PSiP]Pt(C≡CPh) (**5-5**) was observed. The solution ^{1}H NMR spectrum of isolated **5-5** features three characteristic aryl resonances at

7.79, 7.23 and 7.01 ppm corresponding to the *ortho*-, *meta*-, and *para*-protons, respectively, of the phenylacetylide ligand. The IR spectrum of **5-5** contains a distinct acetylide C-C stretch at 2087 cm^{-1}. The solid state structure of **5-5** was determined using single crystal X-ray diffraction techniques (Figure 5-2, Table 5-2). The geometry about the metal center is slightly distorted square planar with a P1-Pt-P2 angle of 162.87(2)º and a Si-Pt-C2 angle of 175.77(7)º. The acetylide ligand is approximately linear, with a Pt-C2-C3 angle of 175.0(2)º and a C2-C3-C4 angle of 177.1(3)º. The Pt-C2 bond length of 2.064(2) Å is slightly longer than previously isolated Pt^{II} arylacetylide complexe (1.96 Å – 1.98 Å)[106] , likely due to the strong *trans*-influence of the silyl group.

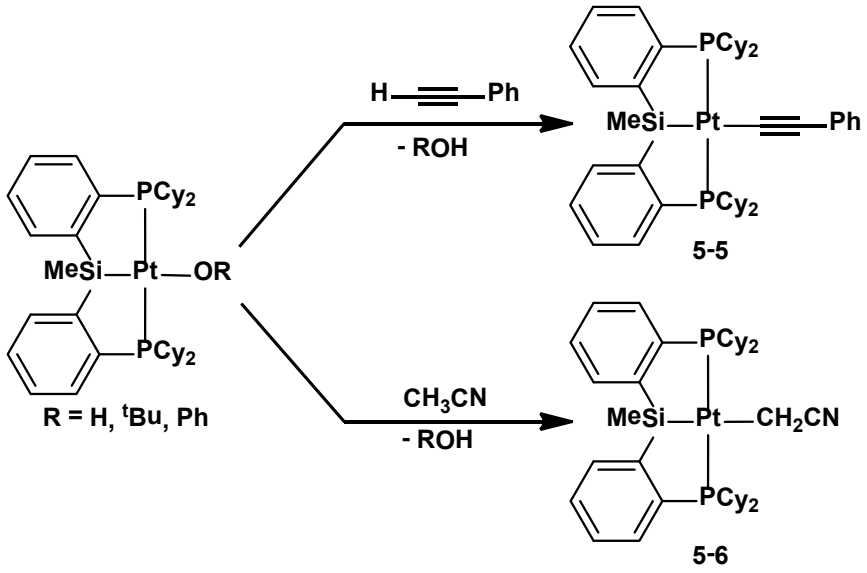

Scheme 5-2. Reactivity of [Cy-PSiP]Pt^{II} alkoxo and hydroxo complexes with acidic C-H bonds.

In a similar fashion, **5-2**, **5-3**, and **5-4** were each reacted with excess (ca. 15 equiv) acetonitrile (pKa = 31.3)[105] to quantitatively (^{31}P NMR) produce the cyanomethyl complex [Cy-PSiP]Pt(CH_2CN) (**5-6**). The ^{1}H NMR spectrum of isolated **5-6** (benzene-d_6)

features a resonance at 2.22 ppm ($^{2}J_{HPt}$ = 10 Hz) that corresponds to the cyanomethyl ligand protons and correlates to a ^{13}C NMR resonance at -9.1 ppm ($^{1}J_{CPt}$ = 396 Hz) in a ^{1}H-^{13}C HSQC experiment. The quaternary cyano carbon gives rise to a resonance at 131.2 ppm in the ^{13}C NMR spectrum of **5-6**. Furthermore, the IR spectrum of **5-6** features a characteristic nitrile stretch at 2178 cm^{-1}. An X-ray crystal structure of **5-6** was obtained, however the cyanomethyl complex was found to co-crystallize with another complex that refined as [Cy-PSiP]PtCl. Nonetheless, the crystal structure appears to confirm the connectivity in **5-6** (Figure 5-2).

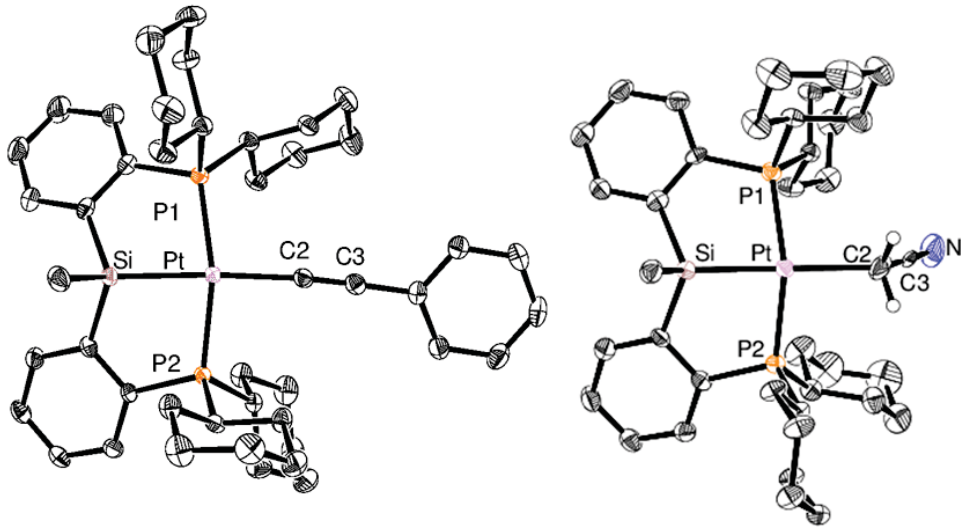

5-5 **5-6**

Figure 5-2. ORTEP diagrams for **5-5** and **5-6** shown with 50% displacement ellipsoids; selected H atoms have been omitted for clarity.

Table 5-2. Selected interatomic distances (Å) and angles (º) for **5-5**.

Interatomic Distances (Å)			
Pt-P1	2.2814(6)	Pt-Si	2.324(1)
Pt-P2	2.2838(6)	Pt-C2	2.064(2)
Interatomic Angles (°)			
P1-Pt-P2	162.87(2)	P1-Pt-Si	83.71(2)
Si-Pt-C2	175.77(7)	P2-Pt-C2	93.22(7)

The reactivity of **5-2**, **5-3** and **5-4** with alternative main group species was also explored. The addition of one equiv of NH_3BH_3 to a THF solution of either **5-2**, **5-3** or **5-4** resulted in gas evolution and the appearance of a white precipitate. In all cases, ^{31}P NMR spectroscopy indicated the quantitative formation of [Cy-PSi(μ-H)P]Pt (**2-7**). The $^{11}B\{^1H\}$ NMR spectrum of the reaction mixture featured multiple resonances between 2.6 and -15 ppm, which is consistent with the formation of mono-dehydrogenated cyclic $[H_2NBH_2]_n$ (n = 1,2,3) oligomers.[107] The reaction of such alkoxo and hydroxo Pt species with NH_3BH_3 may follow a similar path to that reported for the reaction of the related complex [Cy-PSiP]Ru(O^tBu) with NH_3BH_3, which involves intramolecular deprotonation of ammonia and subsequent borane B–H bond oxidative addition to produce the aminoborane NH_2BH_2 that can subsequently oligomerize or undergo further dehydrogenation steps.[107]

In an effort to further develop the E-H bond activation chemistry of Pt alkoxo and hydroxo species, the reactivity of non-acidic H-H and Si-H bonds was also investigated

(Scheme 5-3). Towards these ends, a degassed benzene solution of **5-4** was exposed to H_2 gas (ca. 1 atm) and the reaction mixture was subsequently heated at 75 ºC. Over the course of 28 h, quantitative formation of the previously isolated complex [Cy-PSi(μ-H)P]Pt (**2-7**) was observed using ^{1}H and ^{31}P NMR spectroscopy. No intermediates were observed spectroscopically during the course of this reaction. To the best of our knowledge this represents the first example of the hydrogenation of a Pt^{II} hydroxide complex. A related example involving the net hydrogenation of a Pt-NHPh linkage was reported by Gunnoe and co-workers, and mechanistic studies suggested that this process is catalyzed by $Pt_{(s)}$. Addition of mercury to the hydrogenation reaction of **5-4** to **2-7** did not alter the rate of the reaction, which suggest that $Pt_{(s)}$ does not catalyse the hydrogenation. Goldberg and co-workers have also reported on the hydrogenation of (PCP)Pd(OR) species (PCP = 2,6-($^{t}Bu_2PCH_2$)C_6H_3; R = H, alkyl or aryl).[48]

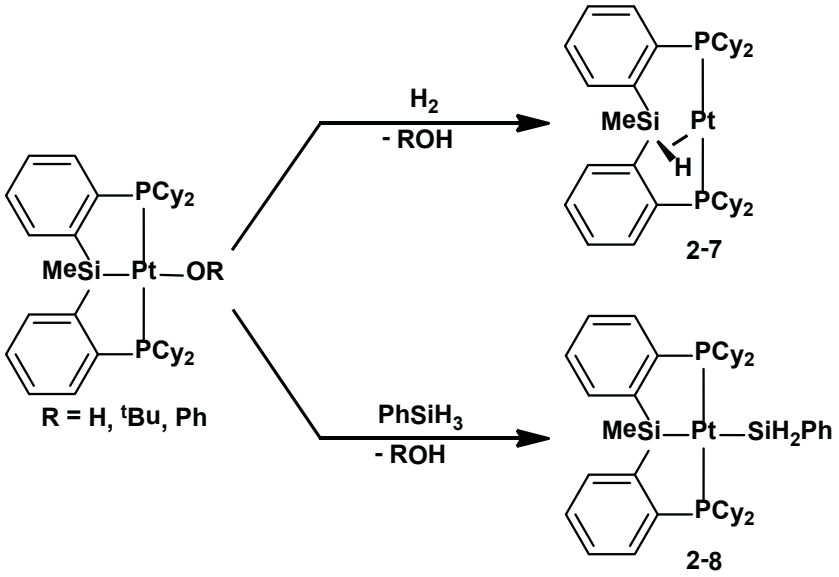

Scheme 5-3. Reactivity of alkoxo and hydroxo [Cy-PSiP]Pt^{II} species with Si-H and H-H bonds.

Although such hydrogenation steps have been invoked in the context of numerous catalytic processes,[82b,108] very little is known about the mechanistic details of H_2 addition across metal-heteroatom bonds. While Gunnoe and co-workers proposed a process involving a heterogeneous catalyst for the hydrogenation of a Pt-amido linkage,[98] Goldberg and co-workers proposed a concerted mechanism involving a four-center Pd-H-H-O transition state, wherein a proton is transferred intramolecularly from coordinated H_2 to the oxygen atom (Scheme 5-4, Path B).[97a,109] This latter mechanistic proposal was based on DFT calculations that indicated the four-center transition state is ca. 15 kcal mol^{-1} lower in energy than a Pd^{IV} dihydride species that would result from oxidative addition of H_2 (Scheme 5-4, Path A). Since no intermediates were observed in the hydrogenation of **5-4**, it is difficult to differentiate experimentally between such a concerted mechanism or one involving oxidative addition of H_2 and subsequent reductive elimination of H_2O. DFT calculations aimed at elucidating the mechanism of H_2 addition

to **5-4** are on-going (in collaboration with Dr. Felix Kannemann). Preliminary results support a concerted mechanism analogous to that reported by Goldberg and co-workers.

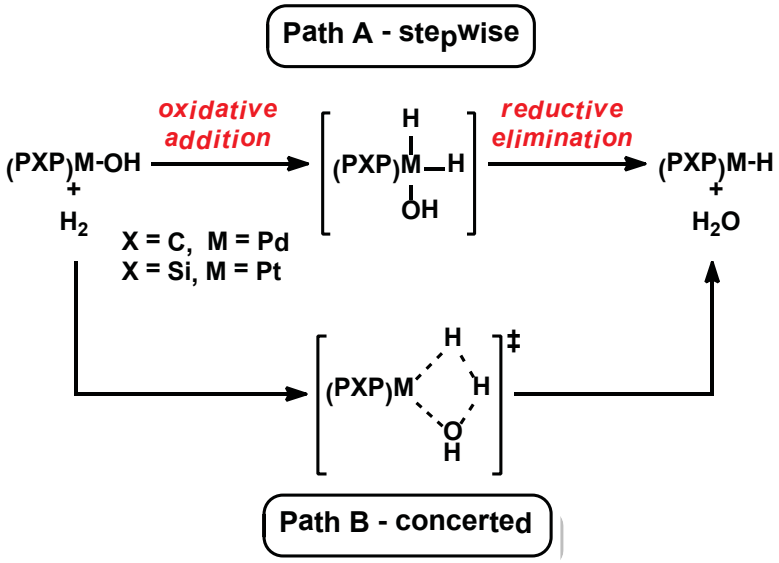

Scheme 5-4. Two possible mechanisms for addition of H_2 across M-OH bond (M = Pd, Pt).

Similar hydrogenolysis involving **5-2** was observed upon treatment of the alkoxide complex with 1 atm of H_2 in benzene solution (Scheme 5-3). Quantitative formation of **2-7** was observed after heating the reaction mixture at 75 °C for 24 h. ^{1}H NMR analysis of the reaction mixture also indicated the formation of HO^{t}Bu. Under identical reaction conditions, the hydrogenolysis of the phenoxide complex **5-3** reached a maximum of 25% conversion to **2-7** after 18 h at 75 ºC. The apparent decreased reactivity in the case of **5-3** is attributed to the back-reaction of **2-7** with phenol formed during the course of the hydrogenolysis process, which reforms the starting complex **5-3**. Similar reactivity was reported for (PCP)Pd(OPh) (PCP = 2,6-(^{t}Bu$_2$PCH$_2$)C$_6$H$_3$) by Goldberg and

co-workers. Indeed, treatment of a benzene solution of **2-7** with one equiv of phenol resulted in the quantitative (^{31}P NMR) formation of **5-3**.

Having observed facile H_2 addition across Pt-O bonds, related reactions involving hydrosilanes were also pursued (Scheme 5-3). As such, each of **5-2**, **5-3** and **5-4** was treated with one equiv of $PhSiH_3$. In all three cases, quantitative (^{31}P NMR) formation of the Pt silyl complex [Cy-PSiP]Pt(SiH_2Ph) (**2-8**) was observed upon mixing, with concomitant formation of the corresponding alcohol. No intermediate Pt-containing species were observed spectroscopically during the course of these reactions. These results are surprising given the thermodynamic preference for the formation of Si-O bonds, which would result in formation of a metal hydride species such as **2-7**. Indeed, a related example involving the reaction of Cp*(Et_3P)Ni(OMe) and Cp*(Et_3P)Ni(NHTol) with $HSiMe_3$ to form Cp*(Et_3P)Ni(H) was previously reported by Bergman and co-workers.[110,111] As such, the observed reactivity of **5-2** - **5-4** with $PhSiH_3$ appears to be more closely related to benzene C-H bond activation by late metal hydroxo and amido complexes, which has been shown to lead to the formation of metal-phenyl derivatives, as well as water or amine, respectively.[97-99] DFT studies exploring the mechanism of this unusual reactivity with $PhSiH_3$ are on-going (in collaboration with Dr. Felix Kannemann). Preliminary results involving **5-4** suggest that the hydroxo ligand may actually deprotonate $PhSiH_3$, as elongation of the Pt-OH bond appears to precede hydrogen atom transfer from Si to O. This deprotonation step is followed by rapid formation of the Pt-Si bond. This would represent an unusual example of Si-H deprontonation.[112]

5.3 Conclusions

In conclusion, a series of silyl pincer supported, terminal Pt hydroxo and alkoxo complexes were successfully synthesized. These complexes undergo Bronsted acid/base reactivity with acidic C-H bonds in molecules such as phenylacetylene and acetonitrile to afford the corresponding Pt-alkynyl and -cyanomethyl products with loss of alcohol. Dehydrogenation of NH_3BH_3 to form $[NH_2BH_2]_n$ oligomers was also observed. Surprisingly, facile hydrogenolysis of the Pt-O linkage was observed for [Cy-PSiP]Pt(OH) and [Cy-PSiP]Pt(O^tBu) upon reaction with H_2. This represents a rare example of hydrogenolysis of a late metal-heteroatom bond, and may proceed via a concerted pathway. Related reactivity involving $PhSiH_3$ addition to Pt hydroxo and alkoxo species resulted in formation of the Pt silyl complex [Cy-PSiP]Pt(SiH_2Ph) rather than the expected Pt hydride species. This reactivity mirrors that of late metal hydroxo, alkoxo, and amido species with benzene C-H bonds to form metal phenyl derivatives. DFT studies to elucidate the mechanism of this transformation are on-going.

5.4 Experimental Section

5.4.1 General considerations

All experiments were conducted under nitrogen in an MBraun glovebox or using standard Schlenk techniques. Dry, oxygen-free solvents were used unless otherwise indicated. Benzene and pentane were deoxygenated and dried by sparging with nitrogen and subsequent passage through a double-column solvent purification system provided by

MBraun Inc. Tetrahydrofuran and diethyl ether were sparged with nitrogen and distilled from Na/benzophenone. All purified solvents were stored over 4 Å molecular sieves. Benzene-d_6, was degassed via three freeze-pump-thaw cycles and stored over 4 Å molecular sieves. Distilled water was deoxygenated by sparging with argon. The compound $LiNH^tBu$ was prepared by treating $^tBuNH_2$ with ^nBuLi in hexanes at -35 ºC. All other reagents were purchased and used without further purification. Unless otherwise stated, ^1H, ^{13}C, ^{31}P, ^{29}Si and ^{11}B NMR characterization data were collected at 300K on a Bruker AV-500 spectrometer operating at 500.1, 125.8, 202.5, 99.4 and 160.5 MHz (respectively) with chemical shifts reported in parts per million downfield of $SiMe_4$ (for ^1H, ^{13}C, and ^{29}Si), 85% H_3PO_4 in D_2O (for ^{31}P) or $BF_3{\cdot}Et_2O$ 15% in $CDCl_3$ (for ^{11}B). ^1H and ^{13}C NMR chemical shift assignments are based on data obtained from ^{13}C-DEPT, ^1H-^1H COSY, ^1H-^{13}C HSQC, and ^1H-^{13}C HMBC NMR experiments. ^{29}Si NMR assignments are based on ^1H-^{29}Si HMBC experiments. In some cases, fewer than expected unique ^{13}C NMR resonances were observed, despite prolonged acquisition times. Infrared spectra were recorded as thin films or Nujol mulls between NaCl plates using a Bruker Tensor 27 Ft-IR spectrometer at a resolution of 4 cm^{-1}.

5.4.2 Synthetic detail and characterization data

[Cy-PSiP]Pt(NH^tBu) (5-1). A solution of **2-1** (0.10 g, 0.12 mmol) in ca. 5 mL of benzene was treated with $LiNH^tBu$ (0.009 g, 0.12 mmol). The resulting reaction mixture was allowed to stand at room temperature for 18 h. A gradual color change from pale yellow to orange was observed. The volatile components of the reaction mixture were then removed under vacuum, and the residue was extracted with ca. 10 mL of pentane.

The pentane extracts were filtered through Celite and the filtrate was concentrated to dryness under vacuum to afford **5-1** as an orange solid (0.070 g, 67% yield). ^{1}H NMR (500 MHz, benzene-d_6): δ 8.17 (d, 2 H, H_{arom}, J = 7 Hz), 7.51 (m, 2 H, H_{arom}, J = 7 Hz), 7.28 (t, 2 H, H_{arom}, J = 7 Hz), 7.17 (t, 2 H, H_{arom}, J = 7 Hz), 2.86 (m, 2 H, PC*H*), 2.69 (m, 2 H, PC*H*), 2.36 (m, 2 H, P*Cy*), 2.04 - 1.96 (overlapping resonances, 4 H, PC*y*), 1.86 (m, 3 H, P*Cy*), 1.71 (s, 9 H, N^{t}*Bu*), 1.68 – 1.58 (overlapping resonances, 10 H, P*Cy*), 1.45 (m, 6 H, P*Cy*), 1.34 - 1.18 (overlapping resonances, 9 H, P*Cy*), 1.30 (N*H*, found through correlation spectroscopy), 1.06 – 0.97 (overlapping resonances, 6 H, P*Cy*), 0.83 (s with Pt satellites, 3 H, Si*Me*, $^{3}J_{HPt}$ = 15 Hz). ^{13}C{^{1}H} NMR (125.8 MHz, benzene-d_6): δ 158.0 (apparent t, $C_{arom,}$ J = 22 Hz), 143.3 (apparent t, $C_{arom,}$ J = 26 Hz), 133.3 (apparent t, CH$_{arom}$, J = 9 Hz), 131.4 (CH$_{arom}$), 130.1 (CH$_{arom}$), 128.9 (CH$_{arom}$), 56.3 (NCMe$_3$), 39.0 (NCMe_3), 36.6 (m, CH$_{Cy}$), 31.6 (CH$_{2Cy}$), 29.4 (m, CH$_{2Cy}$), 28.8 (CH$_{2Cy}$), 28.0 (m, CH$_{2Cy}$), 27.3 (CH$_{2Cy}$), 26.8 (CH$_{2Cy}$), 7.5 (Si*Me*). ^{31}P {^{1}H} NMR (202.5 MHz, benzene-d_6): δ 56.9 (s with Pt satellites, $^{1}J_{PPt}$ = 3102 Hz). ^{29}Si{^{1}H} NMR (99.4 MHz, benzene-d_6): δ 45.3 ($^{1}J_{SiPt}$ = 832 Hz). IR (film, cm^{-1}): 3206 (br m, ν_{NH})

[Cy-PSiP]Pt(O^{t}Bu) (5-2). A solution of **5-1** (0.10 g, 0.12 mmol) in ca. 5 mL of THF was treated with ^{t}BuOH (0.070 mL, 0.79 mmol). The resulting reaction mixture was allowed to stand at room temperature for 15 min. The volatile components of the reaction mixture were then removed under vacuum. The remaining residue was washed with ca. 3 mL of cold (-30 ºC) pentane and dried under vacuum to afford **5-2** as an off white solid (0.096 g, 97% yield). ^{1}H NMR (500 MHz, benzene-d_6): δ 8.10 (d, 2 H, H_{arom}, J = 7 Hz), 7.44 (m, 2 H, H_{arom}), 7.26 (t, 2 H, H_{arom}, J = 7 Hz), 7.15 (t, 2 H, H_{arom}, J = 7 Hz), 3.50 (m, 2 H, P*Cy*), 2.95 (m, 2 H, P*CH*), 2.67 (t, 2 H, P*CH*, J = 12 Hz), 2.38 (m, 2 H, P*Cy*), 1.96

(m, 8 H, P*Cy*), 1.76 (s, 9 H, O^t*Bu*), 1.69 – 1.41 (overlapping resonances, 16 H, P*Cy*), 1.30 – 0.94 (overlapping resonances, 16 H, P*Cy*), 0.82 (s with Pt satellites, 3 H, Si*Me*, $^3J_{HPt}$ = 20 Hz). $^{13}C\{^1H\}$ NMR (125.8 MHz, benzene-d_6): δ 157.4 (apparent t, $C_{arom,}$ J = 22 Hz), 141.9 (apparent t, $C_{arom,}$ J = 26 Hz), 133.1 (apparent t, CH_{arom}, J = 10 Hz), 131.8 (apparent t, CH_{arom}, J = 17 Hz), 130.2 (CH_{arom}), 128.7 (CH_{arom}), 72.2 (OCMe$_3$), 37.4 (s, OCMe_3), 36.5 (apparent t, CH_{Cy}, J = 15 Hz), 36.1 (apparent t, CH_{Cy}, J = 12 Hz), 31.9 (CH_{2Cy}), 29.3 (CH_{2Cy}), 29.1 (CH_{2Cy}), 28.0 – 27.9 (overlapping resonances, CH_{2Cy}), 27.2 (CH_{2Cy}), 26.7 (CH_{2Cy}), 7.0 (Si*Me*). ^{31}P $\{^1H\}$ NMR (202.5 MHz, benzene-d_6): δ 57.7 (s with Pt satellites, $^1J_{PPt}$ = 3139 Hz). $^{29}Si\{^1H\}$ NMR (99.4 MHz, benzene-d_6): δ 30.8 (s with Pt satellites, $^1J_{SiPt}$ = 1020 Hz. X-ray quality crystals of **5-2**•Et_2O were obtained from a concentrated Et_2O solution at -30 ºC.

[Cy-PSiP]Pt(OPh) (5-3). A solution of **5-1** (0.11 g, 0.13 mmol) in ca. 5 mL of THF was treated with PhOH (0.012 g, 0.13 mmol). The resulting reaction mixture was allowed to stand at room temperature for 2 h. The volatile components of the reaction mixture were then removed under vacuum. The remaining residue was washed with ca. 3 mL of cold (-30 ºC) pentane and dried under vacuum to afford **5-3** as a white solid (0.074 g, 72% yield). ^1H NMR (500 MHz, benzene-d_6): δ 8.04 (d, 2 H, H_{arom}, J = 7 Hz), 7.45 (m, 2 H, OPh_{meta}, J = 7 Hz), 7.38 - 7.33 (overlapping resonances, 4 H, H_{arom} + OPh_{ortho}), 7.26 (t, 2 H, H_{arom}, J = 7 Hz), 6.79 (t, 1 H, OPh_{para}, J = 7 Hz), 2.85 (m, 2 H, P*CH*), 2.31 - 2.18 (overlapping resonances, 6 H, PC*H* + P*Cy*), 2.00 (m, 2 H, P*Cy*), 1.83 - 0.89 (overlapping resonances, 34 H, P*Cy*), 0.73 (s, 3 H, Si*Me*, $^3J_{HPt}$ = 10 Hz). $^{13}C\{^1H\}$ NMR (125.8 MHz, benzene-d_6): δ 173.0 (OPh_{ipso}), 157.0 (apparent t, $C_{arom,}$ J = 22 Hz), 141.1 (apparent t, $C_{arom,}$ J = 26 Hz), 133.4 (apparent t, CH_{arom}, J = 10 Hz), 131.8 (apparent t, CH_{arom}, J = 22

Hz), 130.7 (CH$_{arom}$), 129.7 (OPh_{meta}), 129.2 (CH$_{arom}$), 120.7 (OPh_{ortho}), 113.1 (OPh_{para}), 37.6 (apparent t, CH$_{Cy}$, J = 13 Hz), 36.3 (apparent t, CH$_{Cy}$, J = 15 Hz), 30.7 (CH$_{2Cy}$), 29.7(CH$_{2Cy}$), 29.3 (CH$_{2Cy}$), 28.1 – 27.9 (overlapping resonances, CH$_{2Cy}$), 27.6 (m, CH$_{2Cy}$), 27.3 (CH$_{2Cy}$), 26.8 (CH$_{2Cy}$), 5.3 (Si*Me*). ^{31}P{^{1}H} NMR (202.5 MHz, benzene-d_6): δ 60.9 (s with Pt satellites, $^{1}J_{PPt}$ = 3052 Hz). ^{29}Si{^{1}H} NMR (99.4 MHz, benzene-d_6): δ 25.9 (s with Pt satellites, $^{1}J_{SiPt}$ = 1274 Hz).

[Cy-PSiP]Pt(OH) (5-4). A solution of **5-1** (0.10 g, 0.12 mmol) in ca. 10 mL of THF was treated with degassed H_2O (0.40 mL, 27.7 mmol). The volatile components of the reaction mixture were removed under vacuum immediately after addition. The remaining residue was washed with ca. 3 mL of cold (-30 ºC) pentane and dried under vacuum to afford **5-4** as an off white solid (0.078 g, 84% yield). ^{1}H NMR (500 MHz, benzene-d_6): δ 8.12 (d, 2 H, H_{arom}, J = 7 Hz), 7.41 (m, 2 H, H_{arom}), 7.28 (t, 2 H, H_{arom}, J = 7 Hz), 7.17 (t, 2 H, H_{arom}, J = 7 Hz), 3.69 (s, 1 H, O*H*), 2.96 (m, 2 H, P*CH*), 2.40 (m, 2 H, P*CH*), 2.29 (d, 2 H, P*Cy*, J = 13 Hz), 2.23 (d, 2 H, P*Cy*, J = 13 Hz), 2.07 (m, 2 H, P*Cy*), 1.77 - 0.97 (overlapping resonances, 34 H, P*Cy*), 0.76 (s with Pt satellites, 3 H, Si*Me*, $^{3}J_{HPt}$ = 19 Hz). ^{13}C{^{1}H} NMR (125.8 MHz, benzene-d_6): δ 158.3 (apparent t, $C_{arom,}$ J = 22 Hz), 142.0 (apparent t, $C_{arom,}$ J = 27 Hz), 133.5 (apparent t, CH$_{arom}$, J = 10 Hz), 131.3 (apparent t, CH$_{arom}$, J = 17 Hz), 130.3 (CH$_{arom}$), 128.8 (CH$_{arom}$), 37.2 (apparent t, CH$_{Cy}$, J = 13 Hz), 36.6 (apparent t, CH$_{Cy}$, J = 14 Hz), 30.1 (CH$_{2Cy}$), 29.9 (CH$_{2Cy}$), 29.1 (CH$_{2Cy}$), 28.0 – 27.7 (overlapping resonances, CH$_{2Cy}$), 27.5 – 27.3 (overlapping resonances, CH$_{2Cy}$), 27.2 (CH$_{2Cy}$), 26.3 (CH$_{2Cy}$), 7.8 (Si*Me*). ^{31}P{^{1}H} NMR (202.5 MHz, benzene-d_6): δ 58.6 (s with Pt satellites, $^{1}J_{PPt}$ = 3045 Hz). ^{29}Si{^{1}H} NMR (99.4 MHz, benzene-d_6): δ

30.5 (s with Pt satellites, $^{1}J_{SiPt}$ = 1022 Hz). IR (Nujol mull, cm^{-1}): 3227 (br, ν_{OH}). X-ray quality crystals of **5-4** were obtained from a concentrated Et_2O solution at -30 ºC

[Cy-PSiP]Pt(C≡CPh) (5-5). A solution of **5-4** (0.080 g, 0.093 mmol) in ca. 5 mL of benzene was treated with phenyl acetylene (0.011 mL, 0.10 mmol). The resulting reaction mixture was allowed to stand at room temperature for 1 h. The volatile components of the reaction mixture were then removed under vacuum. The remaining residue was washed with ca. 3 mL of cold (-30 ºC) pentane and dried under vacuum to afford **5-** as an off white solid (0.072 g, 77% yield). ^{1}H NMR (500 MHz, benzene-d_6): δ 8.17 (d, 2 H, H_{arom}, J = 7 Hz), 7.79 (d, 2 H, CPh_{ortho}), 7.50 (m, 2 H, H_{arom}, J = 7 Hz), 7.32 (m, 2 H, H_{arom}, J = 7 Hz), *7*.23 (m, 2 H, CPh_{meta}), 7.19 (d, 2 H, H_{arom}, J = 7 Hz), 7.01 (t, 1 H, CPh_{para}, J = 7 Hz), 3.22 (m, 2 H, P*CH*), 2.47 (m, 2 H, P*CH*), 2.34 (d, 2 H, P*Cy*, J = 13 Hz), 2.15 (d, 2 H, P*Cy*, J = 13 Hz), 2.02 – 1.91 (overlapping resonances, 4 H, P*Cy*) 1.76 – 1.37 (overlapping resonances, 24 H, PCy), 1.22- 1.17 (overlapping resonances, 5 H, PCy), 1.10 – 1.01 (overlapping resonances, 4 H, *PCy*), 0.90 – 0.85 (overlapping resonances, 3 H, P*Cy*), 0.76 (s with Pt satellites, 3 H, Si*Me*, $^{3}J_{HPt}$ = 15 Hz). ^{13}C{^{1}H} NMR (125.8 MHz, benzene-d_6): δ 158.8 (apparent t, $C_{arom,}$ J = 21 Hz), 142.7 (apparent t, $C_{arom,}$ J = 26 Hz), 134.0 (apparent t, *C*H$_{arom}$, J = 10 Hz), 131.3 (*C*H$_{arom}$), 131.2 (CPh_{ortho}), 130.8 (*C*H$_{arom}$), 129.3 (CPh_{meta}), 128.9 (*C*H$_{arom}$), 125.3 (CPh_{para}), 122.3 (CPh_{ipso}), 38.1 – 37.9 (overlapping resonances, *C*H$_{Cy}$), 30.7 (*C*H$_{2Cy}$), 30.2 (apparent t, *C*H$_{2Cy}$, J = 8 Hz), 29.1 (*C*H$_{2Cy}$), 29.0 (*C*H$_{2Cy}$), 28.1 (m, *C*H$_{2Cy}$), 27.8 (apparent t, *C*H$_{2Cy}$, J = 5 Hz), 27.5 – 27.4 (overlapping resonances, *C*H$_{2Cy}$), 27.1 (*C*H$_{2Cy}$), 26.4 (*C*H$_{2Cy}$), 8.9 (Si*Me*). ^{31}P{^{1}H} NMR (202.5 MHz, benzene-d_6): δ 60.4 (s with Pt satellites, $^{1}J_{PPt}$ = 2850 Hz). ^{29}Si{^{1}H} NMR (99.4 MHz, benzene-d_6): δ 55.2 (s with Pt satellites $^{1}J_{SiPt}$ = 778 Hz). IR (film, cm^{-1})

2087 (w, $\nu_{C\equiv C}$). X-ray quality crystals of **5-5**•C_6H_6 were obtained from a concentrated benzene solution.

[Cy-PSiP]Pt(CH_2CN) (5-6). A solution of **5-4** (0.10 g, 0.13 mmol) in ca. 10 mL of benzene was treated with CH_3CN (0.10 mL, 1.9 mmol). The resulting reaction mixture was allowed to stand at room temperature for 2 h. The volatile components of the reaction mixture were then removed under vacuum. The remaining residue was washed with ca. 3 mL of cold (-30 ºC) pentane and dried under vacuum to afford **5-** as an off white solid (0.087 g, 82% yield). ^{1}H NMR (500 MHz, benzene-d_6): δ 8.16 (d, 2 H, H_{arom}, J = 7 Hz), 7.48 (m, 2 H, H_{arom}), 7.30 (t, 2 H, H_{arom}, J = 7 Hz), 7.18 (t, 2 H, H_{arom}, J = 7 Hz), 2.81 (m, 2 H, P*CH*), 2.69 (m, 2 H, P*CH*), 2.27 (d, 2 H, P*Cy*, J = 14 Hz), 2.22 (s with Pt satellites, 2 H, CH_2CN, $^2J_{HPt}$ = 10 Hz), 2.12 (d, 2 H, P*Cy*, J = 14 Hz), 1.66 - 1.37 (overlapping resonances, 20 H, P*Cy*), 1.28 – 1.07 (overlapping resonances, 16 H, P*Cy*), 0.67 (s with Pt satellites, 3 H, Si*Me*, $^3J_{HPt}$ = 16 Hz). ^{13}C{^{1}H} NMR (125.8 MHz, benzene-d_6): δ 158.1 (apparent t, $C_{arom,}$ J = 23 Hz), 142.5 (apparent t, $C_{arom,}$ J = 25 Hz), 133.6 (apparent t, CH$_{arom}$, J = 10 Hz), 131.6 (apparent t, CH$_{arom}$, J = 19 Hz), 131.2 (apparent t, CH$_2C$N, $^2J_{PtP}$ = 19 Hz), 130.7 (CH$_{arom}$), 129.0 (CH$_{arom}$), 37.7 – 37.3 (overlapping resonances, CH$_{Cy}$), 30.7 (CH$_{2Cy}$), 30.0 (CH$_{2Cy}$), 29.8 (CH$_{2Cy}$), 29.3 (CH$_{2Cy}$), 27.8 (CH$_{2Cy}$), 27.5 – 27.3 (overlapping resonances, CH$_{2Cy}$), 27.0 (CH$_{2Cy}$), 26.5 (CH$_{2Cy}$), 8.9 (Si*Me*), -9.1 (s with Pt satellites, CH$_2$CN, $^1J_{PtC}$ = 396 Hz). ^{31}P{^{1}H} NMR (202.5 MHz, benzene-d_6): δ 57.4 (s with Pt satellites, $^1J_{PPt}$ = 2915 Hz). ^{29}Si{^{1}H} NMR (99.4 MHz, benzene-d_6): δ 55.2 (s with Pt satellites, $^1J_{SiPt}$ = 800 Hz). IR (film, cm^{-1}) 2178 (s, m, ν_{CN}). X-ray quality crystals of **5-6** were obtained from a concentrated Et_2O solution at -30 ºC.

5.4.3 Crystallographic solution and refinement details

Crystallographic data for **5-2**•OEt_2 and **5-5**•C_6H_6 were obtained at 223(±2) K and 173(±2) K, respectively, on a Bruker PLATFORM/APEX II CCD diffractometer using graphite-monochromated Mo Kα (λ = 0.71073 Å) radiation, employing a sample that was mounted in inert oil and transferred to a cold gas stream on the diffractometer. Crystallographic data for **5-4**•OEt_2 and **5-6** were obtained at 173(±2) K on a Bruker D8/APEX II CCD diffractometer using graphite-monochromated Mo Kα (λ = 0.71073 Å) radiation, employing a sample that was mounted in inert oil and transferred to a cold gas stream on the diffractometer. Programs for diffractometer operation, data collection, and data reduction (including SAINT) were supplied by Bruker. Gaussian integration (face-indexed) was employed as the absorption correction method in each case. All structures were solved by use of the Patterson search/structure expansion except for **5-4**•OEt_2, which was solved by direct methods. All structures were refined by use of full-matrix least-squares procedures (on F^2) with R_1 based on $F_o^2 \geq 2\sigma(F_o^2)$ and wR_2 based on $F_o^2 \geq -3\sigma(F_o^2)$. Unless otherwise stated, anisotropic displacement parameters were employed throughout for non-hydrogen atoms. During the structure solution process for **5-2**•OEt_2, one equivalent of diethyl ether was located in the asymmetric unit. The non-hydrogen atoms of the disordered diethyl ether solvate were refined with a common isotropic displacement parameter over two positions, where O1SA and C1SA - C4SA were refined with an occupancy factor of 0.55, while O1Sb and C1SB - C4SB were refined with an occupancy factor of 0.45. During the structure solution process for **5-4**•OEt_2, one equivalent of diethyl ether was located in the asymmetric unit and refined in a

satisfactory manner. During the structure solution process for **5-5**•C_6H_6, one equivalent of benzene was located in the asymmetric unit and refined in a satisfactory manner. During the solution and refinement process for **5-6**, significant electron density in the region of C2 suggested that this sample exists as a co-crystal involving a secondary [Cy-PSiP]PtX species. Assignment of X = Cl with an occupancy factor of 0.35 relative to X = CH_2CN (occupancy factor of 0.65 for N, C2, C3, and the hydrogens attached to C2) afforded optimal refinement statistics. All hydrogen-atoms were added at calculated positions and refined by use of a riding model employing isotropic displacement parameters based on the isotropic displacement parameter of the attached atom. All relevant crystal data for **5-2**•OEt_2, **5-4**•OEt_2, **5-5**•C_6H_6, and **5-6** are provided in Appendix A.

CHAPTER 6: Synthesis and Reactivity of Group 10 [Cy-PSiP]M^{II} (M = Ni, Pd, Pt) Anilido and Phosphido Complexes

6.1 Introduction

The synthesis and reactivity of Group 10 amido and phosphido complexes remains relatively unexplored by comparison with that of related alkyl and hydrido derivatives. Anilido complexes in particular are proposed intermediates in a number of important catalytic processes,[39e,113] including Pd-catalyzed C-N cross-coupling,[39e,113] and thus a fundamental understanding of the structure and reactivity properties of such complexes is anticipated to aid in the development of further breakthroughs in amination catalysis. Metal phosphido complexes have similarly been implicated in element-phosphorus bond forming processes.[39c,114] In the context of electron-rich late transition metal complexes that feature a high d-electron count at the metal centre, such nondative heteroatomic ligands are proposed to be nucleophilic and strongly basic due to disruption of ligand-to-metal π-bonding.[95c,96a,115]

Group 10 anilido species have the potential to form bridging dimers via the lone pair on nitrogen. Terminal, monomeric anilido complexes have been invoked as intermediates in catalytic C-N coupling reactions. Hartwig and co-workers, have demonstrated thermally induced reductive elimination of $C(sp^3)$-N bonds from a Pd^{II} anilido complex (scheme 6-1), an important step in catalytic C-N cross coupling.[116] Gunnoe and co-workers reported the synthesis of monomeric Pt^{II} anilido complexes of the type, (^{t}bpy)Pt(Me)(NHPh) (^{t}bpy = 4,4'-di-tertbutyl-2,2'dipyridyl). These Pt anilido species exhibited Bronsted base-like reactivity, as indicated by their reactivity with a

variety of protic E-H (E = O, C) bonds. Hydrogenolysis of the Pt-N linkage was also observed. Liang and co-workers have also isolated a terminal Ni^{II} anilido complex of the type [Ph-PNP-^{i}Pr]Ni(NHPh) [Ph-NPN-^{i}Pr] = [N(*o*-$C_6H_4PPh_2$)(*o*-$C_6H_4P^{i}Pr_2$)]$^-$) via the salt metathesis reaction of [Ph-NPN-^{i}Pr]NiCl with LiNHPh. The Ni anilido complex was capable of deprotonating weakly acidic substrates such as acetonitrile, and also undewent CO insertion.[117]

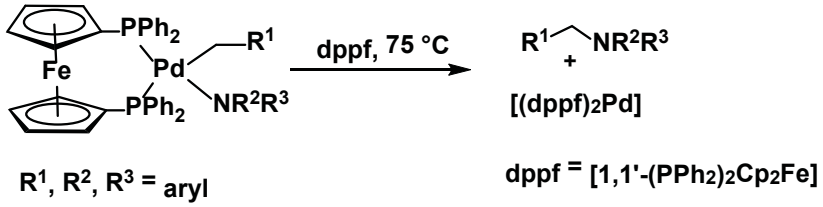

Scheme 6-1. Reductive elimination of C(sp^3)-N from a Pd^{II} center.

While phosphido (PR_2) derivatives of Group 10 metals most commonly exhibit bridging between two metal centers,[118] the study of comparatively more reactive terminal phosphido complexes may lead to breakthroughs in phosphorous - element bond formation reactions. The synthesis of Group 10 phosphido complexes is most commonly achieved through two synthetic strategies: (i) salt metathesis via the use of alkali metalphosphido reagents with Group 10 metal halide complexes; (ii) coordination of a primary or secondary phosphine to a metal halide or cationic complex, followed by deprotonation with an appropriate base.[118] van Koten and co-workers isolated and characterized a terminal monomeric Pt^{II} phosphido complex via coordination of diphenyl phosphine ($PHPh_2$) to the cationic platinum pincer complex (NCN)Pt(H_2O)(X) (NCN = [2,6-$(CH_2NMe_2)_2C_6H_3$]$^-$, X = BF_4, OTf) and subsequent deprotonation with ^{n}BuLi to afford (NCN)Pt(PPh_2).[119] Hillhouse and co-workers isolated the Ni^{I} phosphido complex

(dtbpe)Ni(P^tBu_2) (dtbpe = $^tBu_2PCH_2CH_2P^tBu_2$) via a salt metathesis reaction of the Ni^I dimer [(dtbpe)Ni(μ-Cl)]$_2$ with LiP^tBu_2.[120]

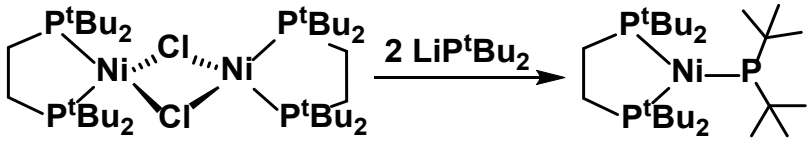

Scheme 6-2. Synthesis of a termianl Ni^I phosphido complex.

6.2 Results and Discussion

6.2.1 [Cy-PSiP]Pt^{II} anilido complexes

A series of [Cy-PSiP]Pt^{II} anilido complexes were synthesized via salt metathesis reactions that involved the treatment of [Cy-PSiP]PtCl (**2-1**) with the appropriate lithium anilide reagent (Scheme 6-1). The reaction of a THF solution of **2-1** with one equiv of LiNHPh resulted in the quantitative (^{31}P NMR) formation of the C_s-symmetric complex [Cy-PSiP]Pt(NHPh) (**6-1**), as indicated by the appearance of a new ^{31}P NMR resonance at 58.0 ppm ($^1J_{PPt}$ = 3000 Hz). The ^{1}H NMR spectrum (benzene-d_6) of isolated **6-1** features three aryl resonances at 7.34 (t, 2 H, N*Ph*$_{meta}$), 6.93 (d, 2 H, N*Ph*$_{ortho}$), and 6.59 ppm (t, 1 H, N*Ph*$_{para}$) belonging to the phenyl substituent of the anilido ligand, as well as an N*H* resonance at 2.53 ppm. The related anilido complex [Cy-PSiP]Pt{NH(2,6-$Me_2C_6H_3$)} (**6-2**) was prepared in a similar fashion, by treating **2-1** with LiNH(2,6-$Me_2C_6H_3$). The room temperature ^{1}H NMR spectrum of **6-2** (benzene-d_6) features two aryl resonances at 7.29 and 7.21 ppm corresponding to the *meta*- and *para*-hydrogens, respectively, of the anilido ligand. ^{1}H NMR resonances observed at 3.20 and 2.52 ppm correspond to inequivalent *ortho*-methyl groups in **6-2**, consistent in part with restricted rotation about the C-N bond

on the NMR timescale. No coalescence of these resonances was observed in the ^{1}H NMR spectrum of **6-2** upon heating up to 80 °C (toluene-d_8). Furthermore, a ^{1}H NMR resonance at 2.15 ppm is assigned to the N*H* of the anilido ligand. Similarly, treatment of **2-1** with one equiv of LiNH(2,6-^{i}Pr$_2$C$_6$H$_3$) led to the formation of [Cy-PSiP]Pt{NH(2,6-^{i}Pr$_2$C$_6$H$_3$)} (**6-3**). The ^{1}H NMR spectrum of **6-3** features two aryl resonances belonging to the anilido ligand at 7.26 (*meta*) and 6.71 ppm (*para*), as well as two distinct sets of isopropyl resonances, which once again indicates hindered rotation about the C-N bond. It was observed that these resonances begin to coalesce at 90 ºC (toluene-d_8). The N-H resonance is observed as a singlet at 2.36 ppm.

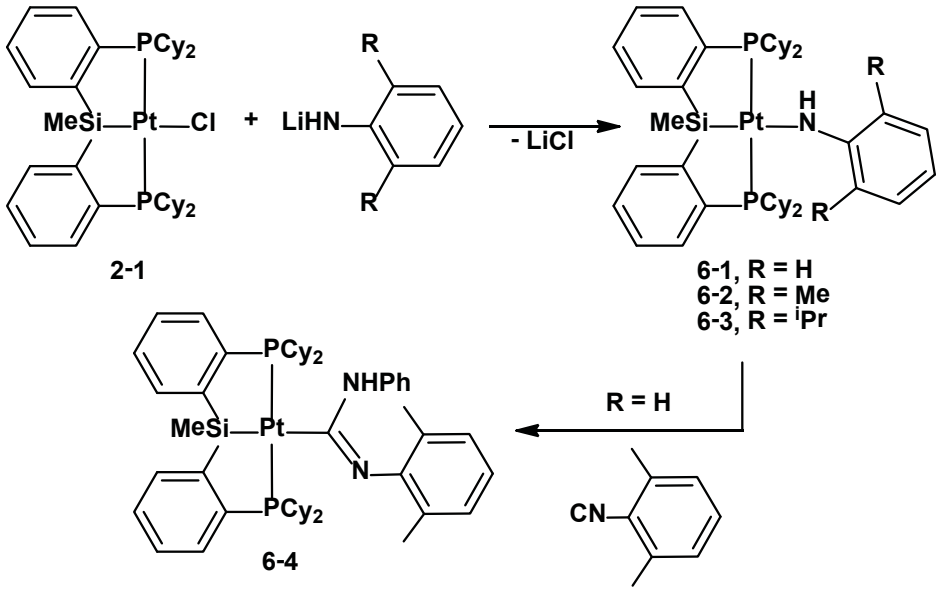

Scheme 6-3. Synthesis of [Cy-PSiP]Pt^{II} anilido complexes.

The solid state structure of **6-3** was determined using single crystal X-ray diffraction techniques (Figure 6-1, Table 6-1). The geometry at Pt is best described as distorted square planar with a P1-Pt-P2 bond angle of 153.17(2)° and Si-Pt-N bond angle

of 175.18(6)°. The Pt-N bond distance of 2.204(2) Å is longer than that reported for previously isolated Pt^{II} anilido complexes. (e.g. The Pt-N bond in (^{t}bpy)Pt(Me)(NHPh) = 2.005(2) Å). We attribute the longer Pt-N bond distance to the strong *trans*-influence of the silyl group in the pincer backbone. Consistent with this, Trogler and co-workers reported a relatively long Pt-N bond distance of 2.125(5) Å in *trans*-$(PEt_2)_2Pt(H)(NHPh)$.[121]

In an effort to probe the reactivity of the Pt-N bond, a benzene solution of **6-1** was reacted with one equiv. of 2,6-dimethylphenyl isocyanide, resulting in the quantitative formation (^{31}P NMR) of a new C_s-symmetric product (**6-4**) that gives rise to a ^{31}P NMR resonance at 56.0 ppm. Complex **6-4** is formulated as the product of 2,6-dimethylphenyl isocyanide insertion into the Pt-N linkage (Scheme 6-1). The ^{1}H NMR spectrum (benzene-d_6) of isolated **6-4** features a resonance at 2.65 ppm (s, 6 H) that corresponds to the xylyl methyl substituents, while the ^{13}C NMR spectrum features a quaternary carbon resonance at 195.4 ppm (m) that has been assigned to the Pt-*C*=N of the isocyanide insertion product. The solid state structure of **6-4** was determined using single crystal X-ray diffraction techniques (Figure 6-1, Table 6-1), and confirmed the connectivity in the insertion product. The geometry around Pt is best described as distorted square planar with P1-Pt-P2 and Si-Pt-C2 bond angles of 158.76(6)° and 177.60(17)° respectively. The sum of the bond angles of 360.1º about C2 indicates a trigonal planar geometry. The N1-C2 bond length of 1.285(8) Å is considerably shorter than the N2-C2 bond length (1.403(8) Å), consistent with the presence of a C-N double bond. Bergman and co-workers also observed similar isocyanide insertion into a late metal amido bond by treatment of an Ir azametallacyclobutane complex $(Cp)(PMe_3)Ir(CH_2CMe_2NH)$ with *tert*-

butyl isocyanide.[122] By comparison, a parent amido Ir^{III} complex $(Cp^*)(PMe_3)Ir(NH_2)(Ph)$ reacted with 2,6-dimethylphenyl isocyanide to lose NH_3 and generate an unusual η^4-tetramethylfulvene complex.[123]

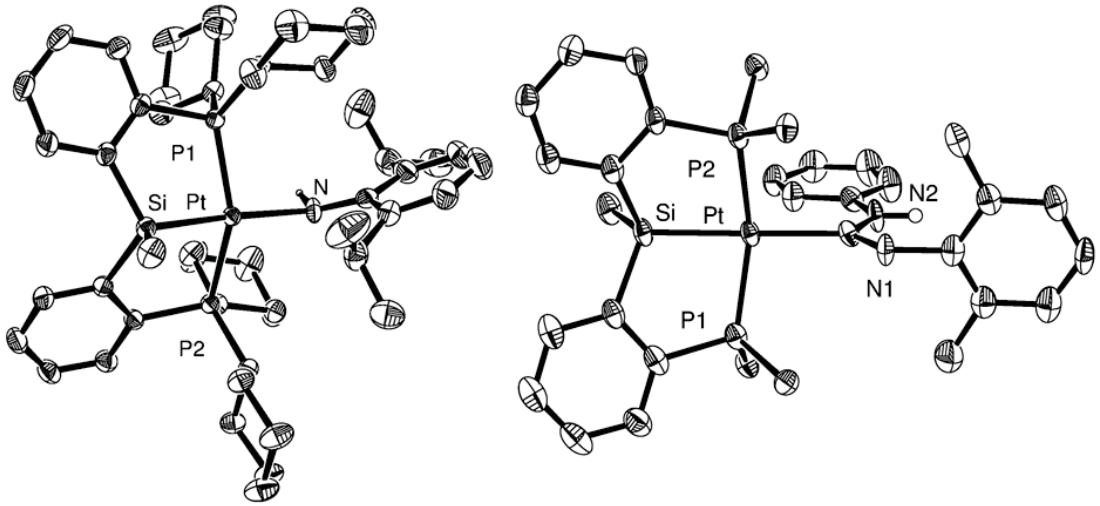

6-3 **6-4**

Figure 6-1. ORTEP diagrams of **6-3** and **6-4** shown with 50% displacement ellipsoids; selected carbon and hydrogen atoms have been removed for clarity.

Table 6-1. Selected interatomic distances (Å) and angles (º) for **6-3** and **6-4**.

Interatomic Distances (Å)		
	6-3	**6-4**
Si-Pt	2.2913(7)	2.3217(17)
Pt-X (X = N, C2)	2.204(2)	2.159(6)
Interatomic Angles (°)		
	6-3	**6-4**
P1-Pt-P2	153.17(2)	158.76(6)
Si-Pt-X (X = N, C2)	175.18(6)	177.60(17)

Complex **6-2** was also treated with 1-hexene and styrene. However, despite prolonged heating at 70 ºC, no reaction was observed either case. In an effort to assess the relative basicity of **6-1**, treatment with excess (>100 equiv) H_2O resulted in quantitative formation of [Cy-PSiP]PtOH (**5-4**). Similarly, addition of 1 equiv of PhOH to **6-1** resulted in quantitative formation of [Cy-PSiP]PtOPh (**5-3**).

6.2.2 [Cy-PSiP]M^{II} (M = Ni, Pd) anilido complexes

Having successfully synthesized a series of Pt^{II} anilido complexes supported by silyl pincer ligation, the isolation of Ni and Pd analogues was also undertaken. As rearrangements involving Si-C(sp^2) and Si-C(sp^3) bond cleavage in the ligand backbone were previously observed for Ni and Pd alkyl species supported by Cy-PSiP ligation,[25f] the possibility of such rearrangement processes for related anilido complexes must also be considered. In this context, treatment of a benzene solution of [Cy-PSiP]PdCl (**3-2**) with one equiv of LiNHPh led to quantitative (^{31}P NMR) conversion to a new [Cy-

PSiP]Pd species (**6-5**, Scheme 6-4) that is tentatively assigned as the terminal Pd anilido complex [Cy-PSiP]Pd(NHPh). The ^{31}P NMR spectrum of **6-5** features a singlet at 56.5 ppm, which is consistent with the proposed formulation for this complex. As well, the ^{1}H NMR (benzene-d_6) spectrum of isolated **6-5** features resonances at 7.14, 6.73 and 6.33 ppm that correspond to the *meta*-, *ortho*-, and *para*-protons, respectively, of the anilido ligand, while a resonance at 2.10 ppm corresponds to the N*H* proton. Upon heating a benzene solution of **6-5** at 75 ºC for 18 h, ^{31}P{^{1}H} NMR analysis revealed quantitative conversion to a new C_1-symmetric complex (**6-6**), as evidenced by the appearance of two resonances at 69.2 (d, $^{2}J_{PPcis}$ = 20 Hz) and -39.6 (d, $^{2}J_{PPcis}$ = 20 Hz) ppm in a ratio of 1:1. Complex **6-6** also gives rise to a ^{29}Si NMR resonance at 29.2 ppm, which is shifted considerably relative to the starting complex **6-5** (55.6 ppm). These spectroscopic features are consistent with the formulation of **6-6** as a C_1-symmetric complex featuring *cis*-phosphino ligands that is analogous to complex **3-4** (Scheme 6-4). As was previously determined for [Cy-PSiP]PdMe (**3-3**), such a species could arise via a rearrangement of **6-5** involving net transfer of the anilido group to Si with concommitant Si-C(sp^2) bond cleavage in the ligand backbone and Pd-C bond formation leading to a four-membered Pd-C-C-P metallacycle. No intermediates were observed spectroscopically (^{31}P NMR) in the rearragement of **6-5**.

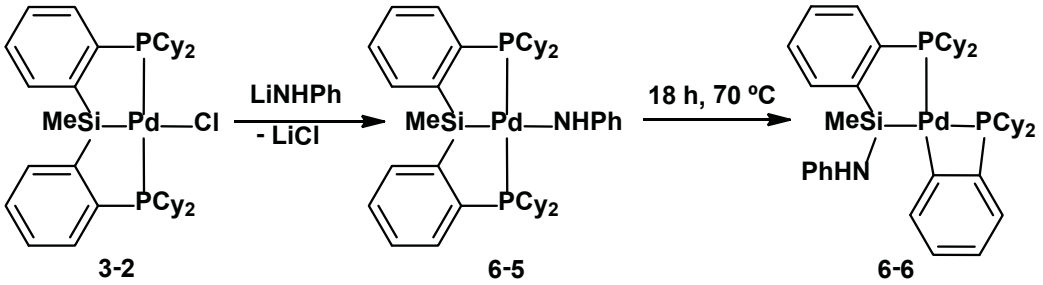

Scheme 6-4. Synthesis and intramolecular rearrangement of a [Cy-PSiP]Pd^{II} anilido complex.

Treatment of [Cy-PSiP]NiCl (**3-1**) with one equiv. of LiNHPh resulted in the quantitative (^{31}P NMR) formation of two new products (**6-7** and **6-8**) in a 2:1 ratio. Complex **(6-7** gives rise to a single ^{31}P NMR resonance at 49.1 ppm, while complex **6-8** gives rise to two doublets observed at 68.7 and -33.6 ppm, respectively, each exhibiting *cis*-PP coupling (J_{PP} = 10 Hz). By analogy with complex **6-6**, complex **6-8** is assigned as a rearranged species resulting from net transfer of the anilido ligand in the terminal anilido complex **6-7a** to Si, with concommitant Si-C(sp^2) bond cleavage in the ligand backbone and Ni-C bond formation leading to a four-membered Ni-C-C-P metallacycle (Scheme 6-4). ^{1}H and ^{29}Si NMR data for complex **6-7** (benzene-d_6) are consistent with a square planar (κ^3-PSiP)Ni^{II} species. Two possible formulations for this complex are: (i) [Cy-PSiP]Ni(NHPh) (**6-7a**) or (ii) a complex where the anilido ligand has been transferred to Si and net Si-C(sp^3) bond cleavage has occurred to transfer the methyl ligand to Ni (**6-7b**, Scheme 6-4). Complex **6-7b** can be envisioned to result from Si-C(sp^2) reductive elimination in **6-8**, followed by net Si-C(sp^3) oxidative addition of the Si-Me bond to provide the proposed Ni-Me species. It is anticipated that insertion of the Ni center into the Si-C linkage would be more facile that insertion into a Si-N linkage,

which is what would be required if the formation of **6-8** from **6-7a** was reversible. Treatment of the reaction mixture containing **6-7** and **6-8** with Ph_2SiH_2 led to the evolution of methane (^{1}H NMR), which suggests that the two species observed in solution are in fact **6-7b** and **6-8**. The facile interconversion of **6-7b** and **6-8** was confirmed by ^{31}P-^{31}P EXSY NMR experiments (70 °C; toluene-d_8, mixing times = 0.75 and 1.5 s), which revealed chemical exchange between the *trans*-*P*Ni*P* environment in **6-8** and the *cis*-*P*Ni*P* environment in **6-7b** (Figure 6-2). This exchange process is analogous to that observed for [Cy-PSiP]NiMe (**3-6**) and the rearranged species [(κ^2–$Cy_2PC_6H_4SiMe_2$)Ni(κ^2–$Cy_2PC_6H_4$)] (**3-7**).

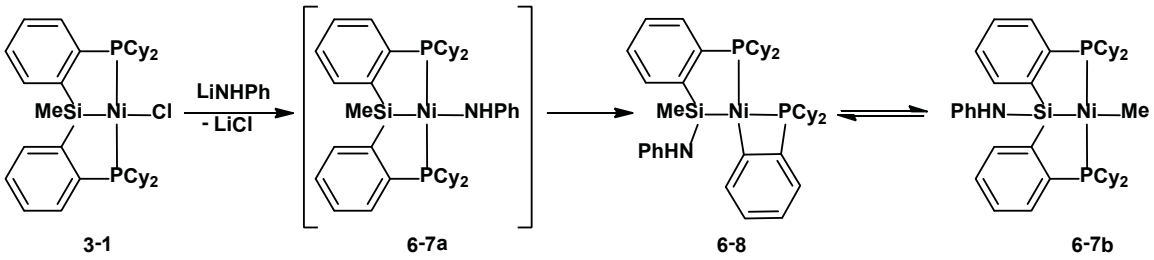

Scheme 6-5. Intramolecular rearrangements involving a proposed [Cy-PSiP]Ni^{II} anilido complex.

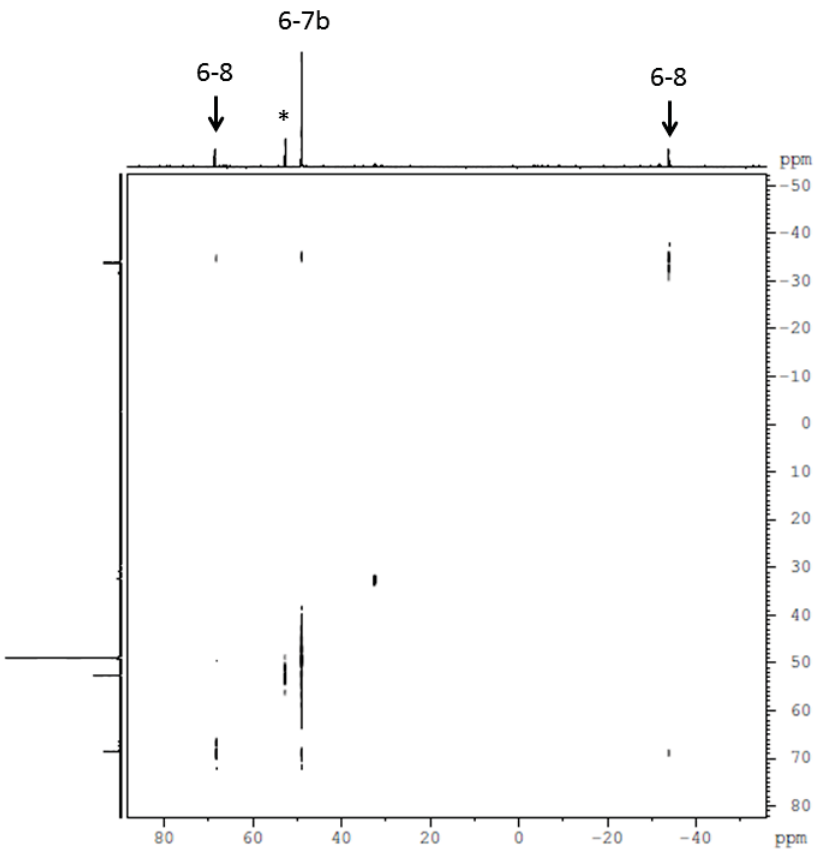

Figure 6-2. Representative ^{31}P-^{31}P EXSY spectrum of the **6-8**/**6-7b** product mixture (70ºC, toluene-d_8, 1.5 s mixing time). The off-diagonal cross peaks are of the same phase as the signals on the diagonal in keeping with chemical exchange involving the magnetically nonequivalent phosphorous environment in **6-8** and **6-7b** (* = impurity).

6.2.3 [Cy-PSiP]Pt^{II} phosphido complexes

Having shown that [Cy-PSiP]Pt^{II} anilido complexes are synthetically accessible, the synthesis of related phosphido species was undertaken. Treatment of a THF solution of **2-1** with one equiv. of LiPHMes (Mes = 1,3,6-trimethylbenzene) resulted in the quantitative (^{31}P NMR) formation of the C_s-symmetric complex [Cy-PSiP]Pt(PHMes) (**6-9**), which was isolated in 91% yield (Scheme 6-6). The $^{31}P\{^1H\}$ NMR spectrum of **6-9** features two resonances at 62.6 (s, $^1J_{PPt}$ = 2906 Hz) and -112.7 (s, $^1J_{PPt}$ = 536 Hz) ppm

corresponding to the pincer phosphine donors and the phosphido ligand, respectively. Coupling between the phosphino and phosphido ligand phosphorus nuclei was not observed. The ^{1}H NMR spectrum (benzene-d_6) of **6-9** features a characteristic Pt-P*H* resonance at 4.23 ppm (dt, $^{2}J_{PtH}$ = 47 Hz, $^{3}J_{PH}$ = 7 Hz, $^{1}J_{PH}$ = 195 Hz). Interestingly, unlike the related anilido complex **6-2**, which featured inequivalent *ortho*-Me groups on the NMR timescale at room temperature, the *ortho*-Me substituents of the phosphido ligand in **6-9** are equivalent, giving rise to a single ^{1}H NMR resonance at 2.99 ppm (s, 6 H). It is likely that the hindered rotation about the C-N bond observed for **6-2** is alleviated in the phosphido analogue due to the anticipated longer Pt-P and C-P distances (relative to Pt-N and C-N distances in **6-2**).

The solid state structure of complex **6-9** was determined by use of single crystal X-ray diffraction techniques (Figure 6-3, Table 6-2). The geometry around Pt is distorted square planar with a P1-Pt-P2 angle of 154.39(3)º and a P3-Pt-Si bond angle of 164.49(3)º. The sum of the bond angles about the phosphido phosphorus donor is 302.8º, which indicates a pyramidal phosphorus center and suggests that there is no interaction between the phosphorous lone pair and the Pt metal center.[124] This is further confirmed by the Pt-P3 bond distance of 2.4567(8) Å, which is slightly lengthend in comparison to 2.372(4) Å found for the Pt-P distant Pt((R,R)-Me-Duphos)(Me)(PPh^{i}Bu),[125] and 2.378(5) Å found for the Pt-P distance in Pt(dppe)(Me)(PHMes*).[126] both of which feature pyramidal geometry at the phosphido donor and no π-bonding involving the phosphorous lone pair.

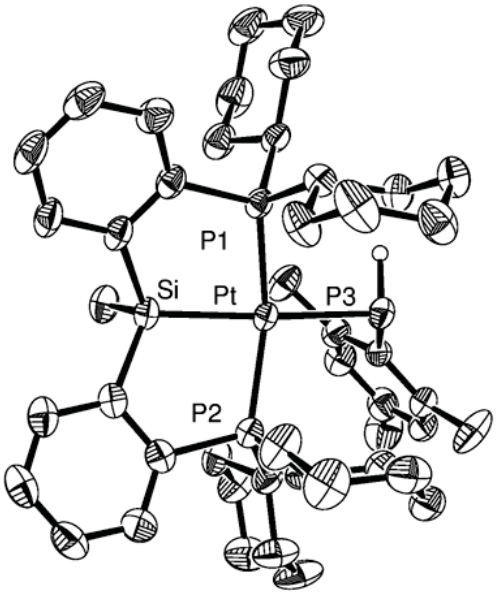

Figure 6-3. ORTEP diagram of **6-9** shown with 50% displacement ellipsoids; selected hydrogen atoms have been removed for clarity

Table 6-2. Selected interatomic distances (Å) and angles (º) for **6-9**.

Interatomic Distances (Å)			
Pt-P1	2.2902(8)	Pt-Si	2.3167(8)
Pt-P2	2.2839(8)	Pt-P3	2.4567(8)
Interatomic Angles (°)			
P1-Pt-P2	154.39(3)	P1-Pt-Si	83.56(3)
Si-Pt-P3	164.49(3)	P2-Pt-P3	100.67(3)

The reaction of **2-1** with one equiv. of LiP^{i}Pr$_2$ also afforded the C_s-symmetric phosphido complex [Cy-PSiP]Pt(P^{i}Pr$_2$) (**6-10**) in 66% isolated yield (Scheme 6-6). The ^{31}P{^{1}H} NMR spectrum of **6-10** features a resonance corresponding to the phosphido donor at -25.8 ppm (s, $^{1}J_{PtP}$ = 711 Hz), as well as a resonance 56.2 ppm (s, $^{1}J_{PtP}$ = 2948

Hz) that is assigned to the pincer ligand phosphino groups. As in the case of complex **6-9**, coupling between the phosphino and phosphido ligand phosphorus nuclei was not observed.

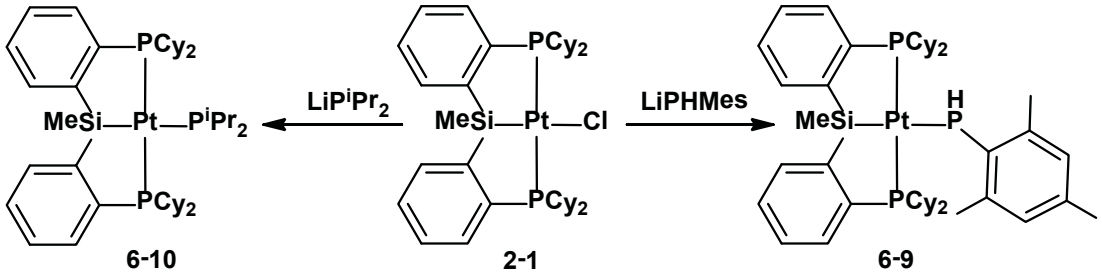

Scheme 6-6. Synthesis of [Cy-PSiP]Pt^{II} phosphido complexes.

6.2.4 Synthesis of a [Cy-PSiP]Pd^{II} phosphido complex

Examples of Pd^{II} phosphido complexes are quite rare. Glueck and co-workers successfully isolated a dinuclear bridging phosphido Pd^{II} complex of the type $Pd_2I_2(\mu$-dppf)(μ-H)(μ-PPh_2).[127] Cyclometalated Pd^{II} terminal phosphido complexes of the type Pd(dppe)($CH_2C_6H_2Me_2P$(Mes)) (dppe = $PPh_2PCH_2CH_2PPh_2$) have also been isolated by this group.[128] To date, the isolation of a monomeric Pd^{II} phosphido complex remains elusive. Encouraged by the isolation of terminal [Cy-PSiP]Pt^{II} phosphido species (*vide supra*), related Pd analogues were targeted. Toward these ends, treatment of a THF solution of **3-2** with one equiv. of LiPHMes afforded the corresponding C_s-symmetric phosphido complex [Cy-PSiP]Pd(PHMes) (**6-11**) in 75% isolated yield. The phosphido group in **6-11** gives rise to a $^{31}P\{^1H\}$ NMR resonance at -129.9 ppm (s), while the neutral phosphino donors give rise to a resonance at 62.1 ppm (s). As was previously observed in the case of square planar [Cy-PSiP]Pt^{II} phosphido complexes, no P-P coupling was

detected by $^{31}P\{^{1}H\}$ NMR spectroscopy. The ^{1}H NMR spectrum of **6-11** (benzene-d_6) features at P*H* resonance at 3.60 ppm (dt, $^{1}J_{PH}$ = 187 Hz, $^{3}J_{PH}$ = 4 Hz), as well as equivalent *ortho*-Me groups that give rise to a singlet at 2.86 ppm (6 H). These spectroscopic features are consistent with a monomeric, square planar structure for complex **6-11** that is likely enforced by the tridentate silyl pincer ligation. Heating **6-11** in a benzene solution did not lead to any reactivity or rearrangement similar to that previously observed for the Pd anilido derivative **6-5.**

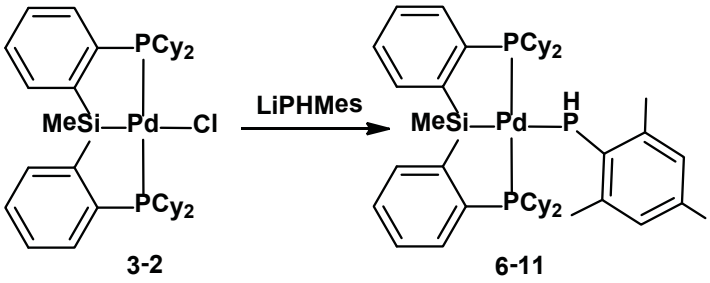

3-2 **6-11**

Scheme 6-7. Synthesis of [Cy-PSiP]Pd**(**PHMes**)**.

6.2.5 Synthesis of a [Cy-PSiP]Ni^{II} phosphido complex

Having succeeded in preparing an isolable, monomeric Pd^{II} phosphido complex supported by Cy-PSiP ligation, an analogous Ni^{II} phosphido complex was also targeted. Following the strategy previously employed for the synthesis of Pt and Pd phosphido species supported by Cy-PSiP ligation, treatment of a THF solution of **3-1** with one equiv of LiPHMes afforded the C_s-symmetric Ni^{II} phosphido complex [Cy-PSiP]Ni(PHMes) (**6-12**) in high yield (Scheme 6-8). The $^{31}P\{^{1}H\}$ NMR spectrum of **6-12** features a resonance at -55.5 ppm (s) that corresponds to the phosphido donor, as well as a resonance at 63.3 ppm (s) that corresponds to the pincer ligand phosphino donors. As was

previously determined for the related phosphido complexes **6-9 - 6-11**, no P-P coupling was observed in the ^{31}P NMR spectrum of **6-12**. The ^{1}H NMR spectrum of **6-12** (benzene-d_6) exhibits a P*H* resonance at 4.35 ppm (dt, $^{1}J_{PH}$ = 216 Hz, $^{3}J_{PH}$ = 9 Hz), as well as a resonance at 2.85 ppm (s, 6 H) that corresponds to equivalent *ortho*-Me substituents in the P*Mes* group on the NMR timescale at room temperature.

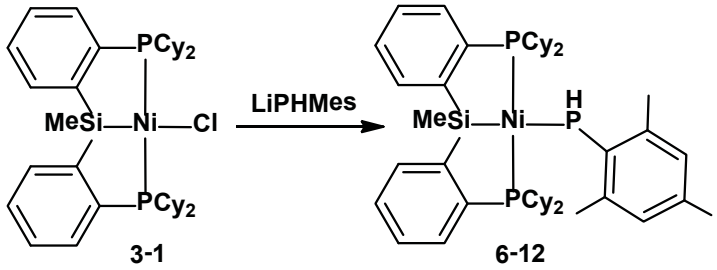

Scheme 6-8. Synthesis of [Cy-PSiP]Ni(PHMes).

The solid state structure of **6-12** was determined by use of single crystal X-ray diffraction techniques (Figure 6-4, Table 6-3). The coordination geometry at the Ni center is strongly distorted from square planarity, with a P1-Ni-P2 bond angle of 148.78(2)° and a Si-Ni-P3 bond angle of 148.98(2)°. This distortion is consistent with previous observations that Ni^{II} complexes can more readily undergo the distortion away from square planar geometry.[1] To date, no ligand rearrangement with a [Cy-PSiP]Pt^{II} complex has been observed, indicative of the rigid square planar geometry at Pt^{II}. The sum of the bond angles at the phosphido phosphorous is 342.8º, which is significantly deviated from pyramidal geometry (*cf*. 302.8º in **6-9**) and suggests the possibility of some degree of interaction between the lone pair of the phosphido donor and the Ni center. An interatomic distance of 2.2009(5) Å between Ni and the phosphido donor is observed. Although there are very few examples of crystallographically characterized terminal Ni

phosphido complexes, the metrical parameters observed for **6-12** are very similar to those reported for the terminal Ni^{I} phosphido complex (dtbpe)Ni(P^tBu_2) (dtbe = $^tBu_2PCH_2CH_2P^tBu_2$), which features a Ni-phosphido distance of 2.2077(12) Å and a sum of bond angles at the phosphido phosphorus of 344º.[120]

Unlike the related anilido complex **6-7a**, complex **6-12** is stable at room temperature in solution and does not appear to undergo intramolecular rearrangements involving Ni-P/Si-C bond cleavage. Heating a benzene solution (70 ºC) of **6-12** also did not result in such rearrangement process. The possible interaction of the phosphido lone pair with the Ni center may afford extra stability to **6-12** and may thus discourage Si-C bond cleavage processes of the type observed for related anilido and alkyl Ni derivatives.

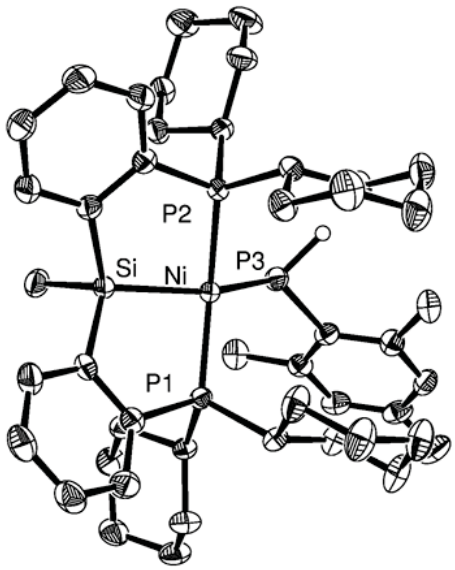

Figure 6-4. ORTEP diagram of **6-12** shown with 50% displacement ellipsoids; selected hydrogen atoms have been removed for clarity.

Table 6-3. Selected interatomic distances and angles for **6-12**.

Interatomic Distances (Å)			
Ni-P1	2.1732(4)	Ni-Si	2.2511(5)
Ni-P2	2.1964(5)	Ni-P3	2.2009(5)
Interatomic Angles (°)			
P1-Ni-P2	148.78(2)	P1-Ni-Si	84.580(17)
Si-Ni-P3	148.98(2)	P2-Ni-P3	96.587(18)

6.3 Conclusions

In summary, a variety of substituted [Cy-PSiP]Pt^{II} anilido complexes were successfuly isolated and characterized. The reactivity of such complexes with unsaturated substrates was probed, and the insertion of xylyl isocyanide into the Pt-N bond was documented. Although a [Cy-PSiP]Pd^{II} anilido complex was observed and characterized in situ, this complex underwent an intramolecular rearrangement similar to what has previously been observed for [Cy-PSiP]PdMe, where the ligand *trans* to the silyl group is transferred to Si and net Si-C(sp^2) bond cleavage occurs to provide a Pd-C-C-P metallacycle. Attempts to access a [Cy-PSiP]Ni^{II} anilido complex resulted in the observation of related rearrangements, where an equilibrium mixture of Ni-N/Si-C bond cleavage products was accessed at room temperature.

Examples of terminal [Cy-PSiP]Pt^{II} phosphido complexes were also synthesized and crystallographically characterized. The complex [Cy-PSiP]Pt(PHMes) features a substantially pyramidalized phosphido donor in the solid state. Relatively rare examples of terminal Pd^{II} and Ni^{II} phosphido complexes were also successfully isolated. In contrast

to the observed aptitude of Pd and Ni anilido species to undergo rearrangement processes that transfer the anilido group to Si, no analogous rearrangement processes involving phosphido species was observed. The monomeric nature of such Cy-PSiP supported phosphido complexes is likely enforced by the chelating pincer ligand. The complex [Cy-PSiP]Ni(PHMes) was crystallographically characterized and exhibits significant distortion from square planarity in the solid state. The phosphido donor is substantially more planar in the Ni complex than it is in the Pt analogue, which suggests that some amount of Ni-P π-interaction may be occurring.

6.4 Experimental Section

6.4.1 General considerations

All experiments were conducted under nitrogen in an MBraun glovebox or using standard Schlenk techniques. Dry, oxygen-free solvents were used unless otherwise indicated. Tetrahydrofuran and diethyl ether were purified by distillation from Na/benzophenone ketyl. All other non-deuterated solvents were deoxygenated and dried by sparging with nitrogen and subsequent passage through a double-column solvent purification system purchased from MBraun Inc. All purified solvents were stored over 4 Å molecular sieves. All deuterated solvents were degassed via three freeze-pump-thaw cycles and stored over 4 Å molecular sieves. LiNHPh, LiNH(2,6-$Me_2C_6H_3$) and LiNH(2,6-$^{i}Pr_2C_6H_3$) were obtained by reacting equimolar amounts of the corresponding aniline and ^{n}BuLi in cold pentane. Similarly, LiPHMes and Li$P^{i}Pr_2$ were obtained by reacting equimolar amounts of the corresponding phosphine and ^{n}BuLi in cold pentane. All other reagents were purchased from Aldrich and used without further purification.

Unless otherwise stated, ^{1}H, ^{13}C, ^{31}P, and ^{29}Si NMR characterization data were collected at 300K on a Bruker AV-500 spectrometer operating at 500.1, 125.8, 202.5, and 99.4 MHz (respectively) with chemical shifts reported in parts per million downfield of $SiMe_4$ (for ^{1}H, ^{13}C, and ^{29}Si) or 85% H_3PO_4 in D_2O (for ^{31}P). Variable-temperature NMR data were collected on a Bruker AV-300 MHz spectrometer. ^{1}H and ^{13}C NMR chemical shift assignments are based on data obtained from ^{13}C-DEPTQ, ^{1}H-^{1}H COSY, ^{1}H-^{13}C HSQC, and ^{1}H-^{13}C HMBC NMR experiments. ^{29}Si NMR assignments are based on ^{1}H-^{29}Si HMBC experiments. In some cases, despite prolonged acquisition times, not every ^{13}C resonance was observed.

6.4.2 Synthetic detail and characterization data

[Cy-PSiP]Pt(NHPh) (6-1). A pre-cooled (-30 °C) solution of **2-1** (0.10 g, 0.12 mmol) in ca. 5 mL of THF was treated with LiNHPh (0.012 g, 0.12 mmol). The resulting reaction mixture was allowed to stand at room temperature for 2 h. The volatile components of the reaction mixture were then removed under vacuum, and the residue was extracted with ca. 10 mL of benzene. The benzene extracts were filtered through Celite and the filtrate was concentrated to dryness under vacuum. The remaining residue was washed with ca. 3 mL of cold (-30 °C) pentane and dried under vacuum to afford **6-1** as a yellow solid (0.083 g, 78% yield). ^{1}H NMR (500 MHz, benzene-d_6): δ 8.12 (d, 2 H, H_{arom}, J = 7 Hz), 7.42 (m, 2 H, H_{arom}, J = 7 Hz), 7.34 (t, 2 H, NPh_{meta}, J = 7 Hz), 7.29 (d, 2 H, H_{arom}, J = 7 Hz), 7.15 (t, 2 H, H_{arom}, J = 7 Hz), 6.93 (d, 2 H, NPh_{ortho}, J = 7 Hz), 6.59 (t, 1 H, NPh_{para}, J = 7 Hz), 2.73 (m, 2 H, PC*H*), 2.53 (t, 1 H, N*H*, J = 16 Hz), 2.36 (m, 2 H, PC*H*), 2.27 (d, 2 H, P*Cy*, J = 13 Hz), 2.00 (d, 2H, P*Cy*), 1.70-0.94 (overlapping

resonances, 36 H, P*Cy*), 0.74 (s with Pt satellites, 3 H, Si*Me*, $^{3}J_{HPt}$ = 18 Hz). $^{13}C\{^{1}H\}$ NMR (125.8 MHz, benzene-d_6): δ 163.7 (N*Ph*$_{ipso}$), 158.0 (apparent t, $C_{arom,}$ J = 22 Hz), 141.7 (apparent t, $C_{arom,}$ J = 26 Hz), 133.5 (apparent t, *C*H$_{arom}$, J = 10 Hz), 131.5 (apparent t, *C*H$_{arom}$, J = 21 Hz), 130.5 (*C*H$_{arom}$), 129.6 (N*Ph*$_{meta}$), 128.9 (*C*H$_{arom}$), 116.4 (apparent t, N*Ph*$_{ortho}$, J = 12 Hz), 109.8 (N*Ph*$_{para}$), 38.1 (apparent t, *C*H$_{Cy}$, J = 13 Hz), 35.9 (apparent t, *C*H$_{Cy}$, J = 15 Hz), 30.2 (*C*H$_{2Cy}$), 30.0 (*C*H$_{2Cy}$), 29.2 (t, *C*H$_{2Cy}$, J = 13 Hz), 28.6 (*C*H$_{2Cy}$), 27.8 – 27.7 (overlapping resonances, *C*H$_{2Cy}$), 27.6 – 27.3 (*C*H$_{2Cy}$), 26.7 (*C*H$_{2Cy}$), 8.2 (s, Si*Me*). $^{31}P\{^{1}H\}$ NMR (202.5 MHz, benzene-d_6): δ 58.0 (s with Pt satellites, $^{1}J_{PPt}$ = 3000 Hz). $^{29}Si\{^{1}H\}$ NMR (99.4 MHz, benzene-d_6): δ 38.6 (s with Pt satellites, $^{1}J_{SiPt}$ = 967 Hz).

[Cy-PSiP]Pt{NH(2,6-Me$_2$C$_6$H$_3$} (6-2). A a pre-cooled (-30 °C) solution of **2-1** (0.10 g, 0.12 mmol) in ca. 5 mL of THF was treated with LiNH(2,6-Me$_2$C$_6$H$_3$) (0.015 g, 0.12 mmol). The resulting reaction mixture was allowed to stand at room temperature for 2 h. The volatile components of the reaction mixture were then removed under vacuum, and the residue was extracted with ca. 10 mL of benzene. The benzene extracts were filtered through Celite and the filtrate was concentrated to dryness under vacuum. The remaining residue was washed with ca. 3 mL of cold (-30 °C) pentane and dried under vacuum to afford **6-2** as a yellow solid (0.090 g, 83% yield). ^{1}H NMR (500 MHz, benzene-d_6): δ 8.11 (d, 2 H, *H*$_{arom}$, J = 7 Hz), 7.42 (m, 2 H, *H*$_{arom}$, J = 7 Hz), 7.29 (t, 2 H, N*Ar*$_{meta}$, J = 7 Hz), 7.21 (d, 1 H, N*Ar*$_{para}$, J = 7 Hz), 7.17 (t, 2 H, *H*$_{arom}$, J = 7 Hz), 6.53 (t, 2 H, *H*$_{arom}$, J = 7 Hz), 3.20 (s, 3 H, C*Me*) 2.77 (m, 2 H, PC*H*), 2.52 (s, 3 H, C*Me*), 2.35 (m, 2 H, PC*H*), 2.15 (s, 1 H, N*H*), 2.15 (m, 2 H, P*Cy*), 2.02 (m, 2 H, P*Cy*), 1.62 - 1.01 (overlapping resonances, 36 H, P*Cy*), 0.65 (s with Pt satellites, 3 H, Si*Me*, $^{3}J_{HPt}$ = 18 Hz).

$^{13}C\{^{1}H\}$ NMR (125.8 MHz, benzene-d_6): δ 161.6 (N*Ar*$_{ipso}$), 157.6 (apparent t, *C*$_{arom,}$ *J* = 22 Hz), 141.7 (apparent t, *C*$_{arom,}$ *J* = 26 Hz), 133.5 (apparent t, *C*H$_{arom}$, *J* = 10 Hz), 131.4 (apparent t, *C*H$_{arom}$, *J* = 21 Hz), 130.5 (*C*H$_{arom}$), 130.2 (N*Ar*$_{meta}$), 128.9 (*C*H$_{arom}$), 128.7 (N*Ar*$_{para}$), 110.1 (*C*H$_{arom}$), 37.0 (apparent t, *C*H$_{Cy}$, *J* = 13 Hz), 35.6 (apparent t, *C*H$_{Cy}$, *J* = 15 Hz), 29.5 (*C*H$_{2Cy}$), 29.4 (*C*H$_{2Cy}$), 29.3 (*C*H$_{2Cy}$), 29.2 (*C*H$_{2Cy}$), 28.6 (*C*H$_{2Cy}$), 28.0 (*C*H$_{2Cy}$), 27.7 – 27.4 (overlapping resonances, *C*H$_{2Cy}$), 27.2 (*C*H$_{2Cy}$), 26.7 (*C*H$_{2Cy}$), 22.6 (C*Me*), 20.8 (C*Me*), 7.9 (Si*Me*). $^{31}P\{^{1}H\}$ NMR (202.5 MHz, benzene-d_6): δ 55.5 (s with Pt satellites, $^{1}J_{PPt}$ = 3074 Hz). ^{29}Si NMR$\{^{1}H\}$ (99.4 MHz, benzene-d_6): δ 36.7 (s with Pt satellites, $^{1}J_{SiPt}$ = 953 Hz).

[Cy-PSiP]Pt{NH(2,6-^{i}Pr$_2$C$_6$H$_3$} (6-3). A pre-cooled (-30 °C) solution of **2-1** (0.10 g, 0.12 mmol) in ca. 5 mL of THF was treated with LiNH(2,6-^{i}Pr$_2$C$_6$H$_3$) (0.022 g, 0.12 mmol). The resulting reaction mixture was allowed to stand at room temperature for 2 h. The volatile components of the reaction mixture were then removed under vacuum, and the residue was extracted with ca. 10 mL of benzene. The benzene extracts were filtered through Celite and the filtrate was concentrated to dryness under vacuum. The remaining residue was washed with ca. 3 mL of cold (-30 °C) pentane and dried under vacuum to afford **6-3** as a yellow solid (0.096 g, 82% yield). ^{1}H NMR (500 MHz, benzene-d_6): δ 8.11 (d, 2 H, *H*$_{arom}$, *J* = 7 Hz), 7.41 (m, 2 H, *H*$_{arom}$, *J* = 7 Hz), 7.30 (d, 1 H, N*Ar*$_{meta}$, *J* = 7 Hz), 7.27 (t, 2 H, *H*$_{arom}$, *J* = 7 Hz), 7.20 (d, 1 H, N*Ar*$_{meta}$, *J* = 7 Hz), 7.15 (t, 2 H, *H*$_{arom}$, *J* = 7 Hz), 6.71 (t, 1 H, N*Ar*$_{para}$, *J* = 7 Hz), 4.92 (m, 1 H, CC*H*Me$_2$), 3.46 (m, 1 H, CC*H*Me$_2$), 2.73 (m, 2 H, P*CH*), 2.41 - 2.36 (overlapping resonances, 3 H, N*H* + P*CH*; the N*H* resonance was identified at 2.36 ppm), 2.12 (d, 2 H, P*Cy*, *J* = 13 Hz), 1.88 (m, 4 H, P*Cy*), 1.69 - 0.94 (overlapping resonances, 48 H, CCH*Me*$_2$ + P*Cy*; the CCH*Me*$_2$

resonances were identified at 1.58 (d, J = 7 Hz) and 1.49 (d, J = 7 Hz) ppm by the use of correlation spectroscopy), 0.74 (s with Pt satellites, 3 H, Si*Me*, $^{3}J_{HPt}$ = 8 Hz). $^{13}C\{^{1}H\}$ NMR (125.8 MHz, benzene-d_6): δ 161.6 (NAr_{ortho}), 157.0 (apparent t, $C_{arom,}$ J = 22 Hz), 141.7 (apparent t, $C_{arom,}$ J = 26 Hz), 133.3 (apparent t, CH$_{arom}$, J = 10 Hz), 131.0 (CH$_{arom}$), 130.5 (CH$_{arom}$), 128.4 (CH$_{arom}$), 123.3 (NAr_{meta}), 122.3 (NAr_{meta}), 111.7 (NAr_{para}), 37.0 (apparent t, CH$_{Cy}$, J = 13 Hz), 35.6 (apparent t, CH$_{Cy}$, J = 15 Hz), 30.5 (CCHMe$_2$), 29.3 (CH$_{2Cy}$), 29.1 (CH$_{2Cy}$), 28.8 (CCHMe$_2$), 28.5 (CH$_{2Cy}$), 28.0 – 27.9 (overlapping resonances, CH$_{2Cy}$), 27.8 – 27.5 (overlapping resonances, CH$_{2Cy}$), 27.1 (CH$_{2Cy}$), 26.3 (CCHMe_2), 24.5 (CCHMe_2), 7.4 (SiMe). $^{31}P\{^{1}H\}$ NMR (202.5 MHz, benzene-d_6): δ 56.2 (s with Pt satellites, $^{1}J_{PPt}$ = 3111 Hz). $^{29}Si\{^{1}H\}$ NMR (99.4 MHz, benzene-d_6): δ 35.5 (s with Pt satellites $^{1}J_{SiPt}$ = 790 Hz). Single crystals of **6-3** suitable for X-ray diffraction were obtained from Et_2O.

[Cy-PSiP]Pt{C(=N(2,6-Me$_2$C$_6$H$_3$))NHPh} (6-4) A solution of **6-1** (0.08 g, 0.10 mmol) in ca. 5 mL of benzene was treated with C≡N(2,6-Me$_2$C$_6$H$_3$) (0.013 g, 0.10 mmol). The resulting reaction mixture was allowed to stand at room temperature for 18 h. The volatile components of the reaction mixture were then removed under vacuum, and the residue was washed with ca. 3 mL of cold (-30 °C) pentane and dried under vacuum to afford **6-4** as a yellow solid (0.088 g, 82% yield). ^{1}H NMR (500 MHz, benzene-d_6): δ 8.23 (d, 2 H, H_{arom}, J = 7 Hz), 7.56 – 7.54 (overlapping resonances, 4 H, H_{arom} + NHPh_{meta}), 7.33 (t, 2 H, H_{arom} J = 7 Hz), 7.29 (d, 2 H, C=NAr_{meta}, J = 7 Hz), 7.21 (t, 2 H, H_{arom}, J = 7 Hz), 7.04 (t, 1 H, C=NAr_{para}), 6.96 (d, 2 H, NHPh_{ortho}, J = 7 Hz), 6.64 (t, 1 H, NHPh_{para}, J = 7 Hz), 3.73 (m, 2 H, PCH), 2.65 (s, 6 H, =NCCMe), 2.21 (m, 2 H, PCH), 2.13 – 2.05 (overlapping resonances, 5 H, PCy + NH; the NH resonance was identified at

2.5 ppm), 1.72 – 1.54 (overlapping resonances, 11 H, P*Cy*), 1.46 – 1.42 (overlapping resonances, 11 H, P*Cy*), 1.34 – 1.21 (overlapping resonances, 9 H, P*Cy*), 1.15 – 1.07 (overlapping resonances, 2 H, P*Cy*), 0.74 (s with Pt satellites, Si*Me*, $^{3}J_{HPt}$ = 11 Hz). $^{13}C\{^{1}H\}$ NMR (125.8 MHz, benzene-d_6): δ 195.4 (m, Pt*C*), 157.3 (apparent t, C_{arom}, J = 21 Hz), 152.7 (apparent t, NHPh_{ipso}, J = 31 Hz), 144.6 (s, C=NAr_{ipso}), 144.0 (apparent t, $C_{arom,}$ J = 18 Hz), 133.5 (apparent t, CH_{arom}, J = 10 Hz), 131.2 (apparent t, CH_{arom}, J = 20 Hz), 130.0 (CH_{arom}), 129.7 (s, C=NAr_{ortho}), 129.4 – 129.3 (overlapping resonances, CH_{arom} + NHPh_{meta} + NHPh_{ortho} + C=NAr_{meta}), 121.6 (C=NAr_{para}), 119.8 (NHPh_{para}), 37.8 (apparent t, CH_{Cy}, J = 14 Hz), 34.6 (apparent t, CH_{Cy}, J = 14 Hz), 31.8 (apparent t, CH_{2Cy}, J = 9 Hz), 28.8 (CH_{2Cy}), 28.5 (CH_{2Cy}), 27.6 (CH_{2Cy}), 27.4 (CH_{2Cy}), 27.2 – 26.9 (overlapping resonances, CH_{2Cy}), 25.9 (CH_{2Cy}), 22.6 (=NCC*Me*), 8.93 (apparent t, Si*Me*, J = 13 Hz). $^{31}P\{^{1}H\}$ NMR (202.5 MHz, benzene-d_6): δ 56.0 (s with Pt satellites, $^{1}J_{PPt}$ = 3043 Hz). $^{29}Si\{^{1}H\}$ NMR (99.4 MHz, benzene-d_6): δ 56.0 (s with Pt satellites $^{1}J_{SiPt}$ = 641 Hz). Single crystals of **6-4** suitable for X-ray diffraction were obtained from a concentrated benzene solution.

Generation of [Cy-PSiP]Pd(NHPh) (6-5). A solution of **3-2** (0.020 g, 0.027 mmol) in ca. 1 mL of benzene-d_6 was treated with LiNHPh (0.003 g, 0.027 mmol). Precipitation of LiCl from solution was observed and ^{31}P NMR analysis of the reaction mixture confirmed the complete consumption of **3-2** and quantitative formation of **6-5**, which was characterized immediately in solution. ^{1}H NMR (500 MHz, benzene-d_6): δ 8.03 (d, 2 H, H_{arom}, J = 7 Hz), 7.43 (d, 2 H, H_{arom}, J = 7 Hz), 7.32 (t, 2 H, H_{arom}, J = 7 Hz), 7.21 (t, 2 H, H_{arom}, J = 7 Hz), 7.14 (t, 2 H, NPh_{meta}, J = 7 Hz), 6.73 (d, 2 H, NPh_{ortho}, J = 7 Hz), 6.33 (t, 1 H, NPh_{para}, J = 7 Hz), 2.46 (m, 2 H, PC*H*), 2.19 (t, 2 H, PC*H*, J = 12 Hz),

2.12 – 2.10 (overlapping resonances, 3 H, P*Cy* + N*H*; the N*H* resonance was identified at 2.10 ppm), 1.93 (d, 2 H, P*Cy*, J = 13 Hz), 1.23 - 0.97 (overlapping resonances, 36 H, P*Cy*), 0.60 (s, 3 H, Si*Me*). $^{13}C\{^{1}H\}$ NMR (125.8 MHz, benzene-d_6): δ 164.6 (N*Ph*$_{ipso}$), 157.7 (apparent t, $C_{arom,}$ J = 26 Hz), 141.3 (apparent t, $C_{arom,}$ J = 20 Hz), 133.5 (apparent t, *C*H$_{arom}$, J = 9 Hz), 131.8 (*C*H$_{arom}$), 130.7 (*C*H$_{arom}$), 129.5 (N*Ph*$_{meta}$), 129.2 (*C*H$_{arom}$), 116.5 (N*Ph*$_{ortho}$), 108.3 (N*Ph*$_{para}$), 36.9 (apparent t, *C*H$_{Cy}$, J = 10 Hz), 36.6 (apparent t, *C*H$_{Cy}$, J = 11 Hz), 30.2 (*C*H$_{2Cy}$), 29.9 (*C*H$_{2Cy}$), 29.3 (*C*H$_{2Cy}$), 27.2 (*C*H$_{2Cy}$), 26.8 (*C*H$_{2Cy}$), 26.6 (*C*H$_{2Cy}$), 9.2 (Si*Me*). $^{31}P\{^{1}H\}$ NMR (202.5 MHz, benzene-d_6): δ 55.8. $^{29}Si\{^{1}H\}$ NMR (99.4 MHz, benzene-d_6): δ 55.6.

[κ^2-(2-Cy$_2$*P*C$_6$H$_4$)*Si*Me(NHPh)]Pd[(κ^2-(2-Cy$_2$*PC*$_6$H$_4$)] (6-6). A benzene solution of **6-5** (0.050 g, 0.064 mmol) was heated for 18 h at 70 °C, and was subsequently concentrated to dryness under vacuum to afford **(6-6** as an off white solid (0.042 g, 82% yield). ^{1}H NMR (500 MHz, benzene-d_6): δ 8.34 (m, 1 H, *H*$_{arom}$), 7.86 (d, 1 H, *H*$_{arom}$, J = 7 Hz), 7.41 – 7.37 (overlapping resonances, 2 H, *H*$_{arom}$), 7.21 – 7.17 (overlapping resonances, 2 H, *H*$_{arom}$), 7.15 – 7.12 (overlapping resonances, 2 H, *H*$_{arom}$), 7.04 (d, 2 H, N*Ph*$_{ortho}$, J = 7 Hz), 6.98 (t, 2 H, N*Ph*$_{meta}$, J = 7 Hz), 6.62 (t, 1 H, N*Ph*$_{para}$, J = 7 Hz), 4.20 (d, 1 H, N*H*, $^{4}J_{HP}$ = 3 Hz), 2.34 (m, 2 H, PC*H*), 2.23 – 2.10 (overlapping resonances, 6 H, PC*H* + P*Cy*), 1.98 – 1.95 (overlapping resonances, 3 H, P*Cy*), 1.83 – 1.00 (overlapping resonances, 33 H, P*Cy*), 0.85 (d, 3 H, Si*Me*, $^{4}J_{HP}$ = 2 Hz). $^{13}C\{^{1}H\}$ NMR (125.8 MHz, benzene-d_6): δ 167.9 (apparent d, $C_{arom,}$ J = 113 Hz), 162.7 (apparent d, $C_{arom,}$ J = 63 Hz), 149.7 – 149.5 (overlapping resonances, *C*$_{arom}$ + N*Ph*$_{ipso}$), 138.0 (apparent d, $C_{arom,}$ J = 44 Hz), 135.0 (d, *C*H$_{arom}$, J = 21 Hz), 134.1 (d, *C*H$_{arom}$, J = 24 Hz), 130.8 (*C*H$_{arom}$), 130.6 (*C*H$_{arom}$), 129.9 – 129.7 (overlapping resonances, *C*H$_{arom}$), 128.8 (*C*H$_{arom}$), 128.7

(N*Ph*$_{meta}$), 124.9 (apparent d, *C*H$_{arom}$, *J* = 4 Hz), 118.2 (N*Ph*$_{ortho}$), 117.3 (N*Ph*$_{para}$) 37.4 (apparent d, *C*H$_{Cy}$, *J* = 16 Hz), 34.4 (apparent d, *C*H$_{Cy}$, *J* = 18 Hz), 33.7 (*C*H$_{Cy}$), 32.0 (*C*H$_{Cy}$), 31.7 (apparent d, *C*H$_{2Cy}$, *J* = 8 Hz), 31.1 (apparent d, *C*H$_{2Cy}$, *J* = 8 Hz), 30.6 (apparent d, *C*H$_{2Cy}$, *J* = 6 Hz), 30.2 (*C*H$_{2Cy}$), 30.2 (*C*H$_{2Cy}$), 30.3 (*C*H$_{2Cy}$), 30.0 (apparent d, *C*H$_{2Cy}$, *J* = 5 Hz), 29.2 (*C*H$_{2Cy}$), 28.7 (*C*H$_{2Cy}$), 28.3 – 27.7 (overlapping resonances, *C*H$_{2Cy}$), 27.5 – 27.4 (overlapping resonances, *C*H$_{2Cy}$), 27.2 – 27.1 (overlapping resonances, *C*H$_{2Cy}$), 26.8 (*C*H$_{2Cy}$), 5.7 (d, Si*Me*, $^{3}J_{CP}$ = 8 Hz). ^{31}P{^{1}H} NMR (202.5 MHz, benzene-d_6): δ 69.2 (d, 1 P, $^{2}J_{PPcis}$ = 20 Hz), -39.6 (d,1 P, $^{2}J_{PPcis}$ = 20 Hz). ^{29}Si{^{1}H} NMR (99.4 MHz, benzene-d_6): δ 29.2 (d, $^{2}J_{SiP}$ = 152 Hz).

[κ^3-(2-Cy$_2$*P*C$_6$H$_4$)$_2$*Si*(NHPh)]NiMe (6-7b) + [κ^2-(2-Cy$_2$*P*C$_6$H$_4$)*Si*Me(NHPh)]Ni[κ^2-(2-Cy$_2$*PC*$_6$H$_4$)] (6-8). A solution of (0.10 g, 0.14 mmol) in ca 3 mL of THF was treated with LiNHPh (0.015 g, 0.14 mmol). The resulting dark red colored solution was allowed to stand at room temperature for 1 h and was subsequently concentrated to dryness under vacuum. The residue was re-dissolved in benzene and filtered through Celite. The filtrate was concentrated to dryness under vacuum to afford a 2:1 mixture (^{31}P NMR) of **6-7** and **6-8** (0.10 g, 98% yield). ^{1}H NMR (500 MHz, benzene-d_6; the integrations provided are relative to **(6-7,** whereby the high frequency resonance at 7.99 ppm is assigned an integral value of 2 H): δ 8.04 (m, 0.5 H, *H*$_{arom}$ in **6-8**), 7.99 (d, 2 H, *H*$_{arom}$ in **6-7**, *J* = 7 Hz), 7.81 (d, 0.5 H, *H*$_{arom}$ in **6-8**, *J* = 7 Hz), 7.39 – 7.38 (overlapping resonances, 4 H, *H*$_{arom}$ in **6-7** + **6-8**), 7.31 – 7.26 (overlapping resonances, 3 H, *H*$_{arom}$ in **6-7** + **6-8**), 7.20 – 7.15 (overlapping resonances, 2 H, *H*$_{arom}$ in **6-7** + **6-8**), 7.04 – 6.99 (overlapping resonances, 6 H, N*Ph*$_{ortho}$ and N*Ph*$_{meta}$ in **6-7** + **6-8**), 6.63 (t, 0.5 H, N*Ph*$_{para}$ in **6-8**, *J* = 7 Hz), 6.56 (t, 1 H, N*Ph*$_{para}$ in **6-7**, *J* = 7 Hz), 4.15 (s,

0.5 H, N*H* in **6-8**), 2.25 (m, 2 H, PC*H* in **6-8**), 2.32 (overlapping resonances, 4 H, PC*H* in **6-7** + **6-8**), 2.21 – 2.17 (overlapping resonances, 3 H, P*Cy* in **6-7** + **6-8**), 2.14 – 2.11 (overlapping resonances, 2 H, P*Cy* in **6-7** + **6-8**), 1.85 - 1.82 (overlapping resonances, 3 H, P*Cy* in **6-7** + **6-8**), 1.71 – 1.39 (overlapping resonances, 35 H, P*Cy* in **6-7** + **6-8**), 1.35 (s, 1 H, N*H* in **6-7**), 1.33 – 0.98 (overlapping resonances, 23 H, P*Cy* in **6-7** + **6-8**), 0.84 (s, 1.5 H, Si*Me* in **6-8**), 0.71 (s, 3 H, Ni*Me* in **6-7**). $^{13}C\{^{1}H\}$ NMR (125.8 MHz, benzene-d_6): δ 165.3 (d, C_{arom}, J = 66 Hz), 162.9 (C_{arom}), 162.2 (d, C_{arom}, J = 56 Hz), 158.1 (apparent t, $C_{arom,}$ J = 25 Hz), 149.8 (C_{arom}), 147.4 (d, C_{arom}, J = 28 Hz), 142.6 (apparent t, $C_{arom,}$ J = 21 Hz) 138.6 (d, C_{arom}, J = 21 Hz), 136.0 (apparent d, CH_{arom}, J = 21 Hz), 134.5 (apparent d, CH_{arom}, J = 19 Hz), 133.3 (apparent d, CH_{arom}, J = 23 Hz), 132.7 (apparent t, CH_{arom}, J = 10 Hz), 130.9 (CH_{arom}), 130.7 (CH_{arom}), 130.4 (CH_{arom}), 129.9 (CH_{arom}), 129.7 (CH_{arom}), 129.4(CH_{arom}), 129.1 – 128.9 (overlapping resonances, CH_{arom}), 125.7 (apparent d, CH_{arom}, J = 5 Hz), 118.1 (CH_{arom}), 117.0 (CH_{arom}), 116.9 (CH_{arom}), 109.8 (CH_{arom}), 37.1 – 36.6 (overlapping resonances, CH_{Cy}), 34.2 – 34.0 (overlapping resonances, CH_{Cy}), 32.0 (CH_{Cy}), 31.7 (apparent d, CH_{2Cy}, J = 9 Hz), 30.7 (CH_{2Cy}), 30.3 (CH_{2Cy}), 29.9 - 29.6 (overlapping resonances, CH_{2Cy}), 29.4 (CH_{2Cy}), 28.8 (apparent d, CH_{2Cy}, J = 4 Hz), 28.4 (CH_{2Cy}), 28.3 - 27.4 (overlapping resonances, CH_{2Cy}), 26.7 (CH_{2Cy}), 7.9 (Ni*Me* in **6-7**), 5.9 (d, Si*Me* in **6-8**, $^{3}J_{CP}$ = 5 Hz). $^{31}P\{^{1}H\}$ NMR (202.5 MHz, benzene-d_6): δ 68.6 (d, 1 P in **6-8**, $^{2}J_{PPcis}$ = 10 Hz), 49.1 (s, 4 P in **6-7**), -33.6 (d, 1 P in **6-8**, J = 10 Hz). $^{29}Si\{^{1}H\}$ NMR (99.4 MHz, benzene-d_6): δ 30.0 (d, **6-8**, $^{2}J_{SiP}$ = 145 Hz), 55.6 (**6-7**).

[Cy-PSiP]Pt(PHMes) (6-9). A pre-cooled (-30 °C) solution of **2-1** (0.10 g, 0.12 mmol) in ca. 5 mL of THF was treated with LiPHMes (0.012 g, 0.12 mmol) The resulting reaction mixture was allowed to stand at room temperature for 2 h. The volatile

components of the reaction mixture were then removed under vacuum, and the residue was extracted with ca. 10 mL of benzene. The benzene extracts were filtered through Celite and the filtrate was concentrated to dryness under vacuum. The remaining residue was washed with ca. 3 mL of cold (-30 °C) pentane and dried under vacuum to afford **6-9** as a yellow solid (0.10 g, 91% yield). ^{1}H NMR (500 MHz, benzene-d_6): δ 8.17 (d, 2 H, H_{arom}, J = 7 Hz), 7.53 (m, 2 H, H_{arom}, J = 7 Hz), 7.30 (d, 2 H, H_{arom}, J = 7 Hz), 7.18 (t, 2 H, H_{arom}, J = 7 Hz), 6.97 (s, 2 H, PAr_{meta}), 4.23 (dt with Pt satellites, 1 H, PH, $^{1}J_{PH}$ = 195 Hz, $^{3}J_{PH}$ = 7 Hz, $^{2}J_{PtH}$ = 47 Hz), 2.99 (s, 6 H, CMe_{ortho}), 2.65 (m, 2 H, PCH), 2.30 (s, 3 H, CMe_{para}), 2.22 - 1.95 (overlapping resonances, 9 H, PCH + PCy), 1.85 (m, 4 H, PCy), 1.60 - 1.19 (overlapping resonances, 29 H, PCy), 1.05 - 0.99 (overlapping resonances, 6 H, PCy), 0.71 (t with Pt satellites, 3 H, SiMe, $^{3}J_{HPt}$ = 13 Hz). ^{13}C{^{1}H} NMR (125.8 MHz, benzene-d_6): δ 157.7 (apparent t, C_{arom}, J = 22 Hz), 143.1 (m, C_{arom}), 133.5 (apparent t, CH$_{arom}$, J = 10 Hz), 131.6 (apparent t, CH$_{arom}$, J = 17 Hz), 130.5 (CH$_{arom}$), 128.7 (CH$_{arom}$), 128.6 (CH$_{Mes}$, found through correlation spectroscopy), 38.6 (apparent t, CH$_{Cy}$, J = 15 Hz), 37.3 (apparent t, CH$_{Cy}$, J = 13 Hz), 30.8 (CH$_{2Cy}$), 29.8 (CH$_{2Cy}$), 29.6 (CH$_{2Cy}$), 29.1 (CH$_{2Cy}$), 28.9 (CH$_{2Cy}$), 27.5 – 27.2 (overlapping resonances, CH$_{2Cy}$), 26.8 (CMe_{para}), 21.3 (CMe_{ortho}), 8.8 (SiMe, found through correlation spectroscopy). ^{31}P{^{1}H} NMR (202.5 MHz, benzene-d_6): δ 62.6 (s with Pt satellites, PCy$_2$, $^{1}J_{PPt}$ = 2906 Hz), -112.7 (s with Pt satellites, PtPHMes, $^{1}J_{PtP}$ = 536 Hz). ^{29}Si{^{1}H} NMR (99.4 MHz, benzene-d_6): δ 63.2 (d with Pt satellites, $^{1}J_{SiPt}$ = 851 Hz, $^{2}J_{SiP}$ = 60 Hz). X-ray quality crystals of **6-9** were obtained from a concentrated C_6H_6 solution.

[Cy-PSiP]Pt(P^{i}Pr$_2$) (6-10). A pre-cooled (-30 ºC) solution of **2-1** (0.075 g, 0.091 mmol) in ca. 5 mL of THF was treated with LiP^{i}Pr$_2$ (0.011 g, 0.091 mmol). The resulting

reaction mixture was allowed to stand at room temperature for 2 h. The volatile components of the reaction mixture were then removed under vacuum, and the residue was extracted with ca. 10 mL of benzene. The benzene extracts were filtered through Celite and the filtrate was concentrated to dryness under vacuum. The remaining residue was washed with ca. 3 mL of cold (-30 °C) pentane and dried under vacuum to afford **6-10** as an orange solid (0.055 g, 66% yield). ^{1}H NMR (500 MHz, benzene-d_6): δ 8.20 (d, 2 H, H_{arom}, J = 7 Hz), 7.61 (m, 2 H, H_{arom}, J = 7 Hz), 7.32 (t, 2 H, H_{arom}, J = 7 Hz), 7.22 (t, 2 H, H_{arom}, J = 7 Hz), 2.14 (m, 2 H, CH_{Cy}), 3.02 (m, 2 H, CHMe$_2$) 2.94 (m, 2 H, CH_{Cy}), 2.30 (d, 2 H, P*Cy*, J = 13 Hz), 2.03 - 1.82 (overlapping resonances, 8 H, P*Cy*), 1.63 (dd, 12 H, CH*Me*$_2$, $^{3}J_{CH}$ = 7 Hz, $^{3}J_{PH}$ = 12 Hz), 1.51 – 0.97 (overlapping resonances, 30 H, P*Cy*), 0.48 (s with Pt satellites, 3 H, Si*Me*, $^{3}J_{HPt}$ = 12 Hz). ^{13}C{^{1}H} NMR (125.8 MHz, benzene-d_6): δ 157.7 (apparent t, $C_{arom,}$ J = 22 Hz), 144.4 (apparent t, $C_{arom,}$ J = 26 Hz), 133.5 (apparent t, CH$_{arom}$, J = 10 Hz), 131.4 (apparent t, CH$_{arom}$, J = 17 Hz), 130.5 (CH$_{arom}$), 128.9 (CH$_{arom}$), 38.0 - 37.6 (overlapping resonances, CH$_{Cy}$), 30.9 (CH$_{2Cy}$), 30.3 (CH$_{2Cy}$), 29.8 (CH$_{2Cy}$), 29.4 (CH$_{2Cy}$), 29.6 (d, CHMe$_2$, $^{1}J_{CP}$ = 24 Hz), 28.9 (d, CH*Me*$_2$, $^{1}J_{CP}$ = 17 Hz), 28.1 (CH$_{2Cy}$), 27.7 – 27.5 (overlapping resonances, CH$_{2Cy}$), 27.2 – 26.9 (overlapping resonances, CH$_{2Cy}$), 8.5 (Si*Me*). ^{31}P{^{1}H} NMR (202.5 MHz, benzene-d_6): δ 56.2 (s with Pt satellites, 2 P, PCy$_2$, $^{1}J_{PPt}$ = 2948 Hz), -25.8 (s with Pt satellites, 1 P, P^{i}Pr$_2$, $^{1}J_{PPt}$ = 712 Hz). ^{29}Si{^{1}H} NMR (99.4 MHz, benzene-d_6): δ 65.8 (d with Pt satellites, $^{2}J_{SiP}$ = 72 Hz, $^{1}J_{SiPt}$ = 700 Hz).

[Cy-PSiP]Pd(PHMes) (6-11). A pre-cooled (-30 °C) solution of **3-2** (0.075 g, 0.10 mmol) in ca. 5 mL of THF was treated with LiPHMes (0.027 g, 0.10 mmol). The resulting reaction mixture was allowed to stand at room temperature for 2 h. The volatile

components of the reaction mixture were then removed under vacuum, and the residue was extracted with ca. 10 mL of benzene. The benzene extracts were filtered through Celite and the filtrate was concentrated to dryness under vacuum. The remaining residue was washed with ca. 3 mL of cold (-30 °C) pentane and dried under vacuum to afford **6-11** as a yellow solid (0.067 g, 75% yield). ^{1}H NMR (500 MHz, benzene-d_6): δ 8.10 (d, 2 H, H_{arom}, J = 7 Hz), 7.51 (m, 2 H, H_{arom}, J = 7 Hz), 7.31 (t, 2 H, H_{arom}, J = 7 Hz), 7.20 (t, 2 H, H_{arom}, J = 7 Hz), 6.95 (s, 2 H, P*Ar*$_{meta}$), 3.60 (dt, 1 H, P*H*, $^{1}J_{PH}$ = 188 Hz, $^{3}J_{PH}$ = 4 Hz), 2.86 (s, 6 H, C*Me*$_{ortho}$), 2.50 (m, 2 H, PC*H*), 2.30 (s, 3 H, C*Me*$_{para}$), 2.24 (m, 2 H, PC*H*), 2.02 - 1.99 (overlapping resonances, 6 H, P*Cy*), 1.83 - 1.76 (overlapping resonances, 6 H, P*Cy*), 1.60 – 1.06 (overlapping resonances, 28 H, P*Cy*), 0.70 (s, 3 H, Si*Me*). ^{13}C{^{1}H} NMR (125.8 MHz, benzene-d_6): δ 157.0 (apparent t, $C_{arom,}$ J = 28Hz), 143.5 (m, C_{arom}), 140.7 (P*Ar*), 140.6 (P*Ar*),133.5 (apparent t, *C*H$_{arom}$, J = 12 Hz), 131.9 (*C*H$_{arom}$), 130.6 (*C*H$_{arom}$), 131.5 (P*Ar*$_{ipso}$), 128.9 (*C*H$_{arom}$), 128.7 (P*Ar*$_{meta}$), 38.7 (apparent t, *C*H$_{Cy}$, J = 10 Hz) 36.8 (apparent t, *C*H$_{Cy}$, J = 10 Hz), 31.1 (*C*H$_{2Cy}$), 30.6 (*C*H$_{2Cy}$), 29.7 (*C*H$_{2Cy}$), 29.6 (*C*H$_{2Cy}$), 29.4 (*C*H$_{2Cy}$), 27.9 – 27.4 (overlapping resonances, *C*H$_{2Cy}$), 26.7 (*C*H$_{2Cy}$), 26.3 (*C*H$_{2Cy}$), 26.2 (C*Me*$_{ortho}$), 21.5 (*CMe*$_{para}$), 9.4 (Si*Me*). ^{31}P{^{1}H} NMR (202.5 MHz, benzene-d_6): δ 62.1 (s, 2 P, *P*Cy$_2$), -129.9 (s, 1 P, *P*HMes). ^{29}Si NMR (99.4 MHz, benzene-d_6): δ 66.1 (d, $^{2}J_{SiP}$ = 71 Hz).

[Cy-PSiP]Ni(PHMes) (6-12). A pre-cooled (-30 °C) solution of **3-1** (0.10 g, 0.15 mmol) in ca. 5 mL of THF was treated with LiPHMes (0.021 g, 0.15 mmol). The resulting reaction mixture was allowed to stand at room temperature for 2 h. The volatile components of the reaction mixture were then removed under vacuum, and the residue was extracted with ca. 10 mL of benzene. The benzene extracts were filtered through

Celite and the filtrate was concentrated to dryness under vacuum. The remaining residue was washed with ca. 3 mL of cold (-30 °C) pentane and dried under vacuum to afford **6-12** as an orange solid (0.11 g, 93% yield). ^{1}H NMR (500 MHz, benzene-d_6): δ 8.06 (d, 2 H, H_{arom}, J = 7 Hz), 7.44 (m, 2 H, H_{arom}, J = 7 Hz), 7.33 (t, 2 H, H_{arom}, J = 7 Hz), 7.19 (t, 2 H, H_{arom}, J = 7 Hz), 6.97 (s, 2 H, PAr_{meta}, J = 7 Hz), 4.35 (dt, 1 H, PH, $^{1}J_{PH}$ = 216 Hz, $^{3}J_{PH}$ = 9 Hz), 2.85 (s, 6 H, CMe_{ortho}), 2.42 - 2.30 (overlapping resonances, 4 H, PCH), 2.24 (s, 3 H, CMe_{para}), 2.21 - 1.24 (overlapping resonances, 40 H, PCy), 0.88 (s, 3 H, SiMe). ^{13}C{^{1}H} NMR (125.8 MHz, benzene-d_6): δ 157.5 (apparent t, $C_{arom,}$ J = 26 Hz), 144.5 (apparent t, $C_{arom,}$ J = 21 Hz), 142.3 - 142.1 (overlapping resonances, PAr_{para} + PAr_{ortho}), 134.0 (PAr_{ipso}), 132.8 (apparent t, CH$_{arom}$, J = 12 Hz), 130.9 (CH$_{arom}$), 130.3 (CH$_{arom}$), 129.2 (PAr_{meta}), 128.8 (CH$_{arom}$), 37.8 (apparent t, CH$_{Cy}$, J = 10 Hz), 36.5 (m, CH$_{Cy}$), 31.8 (CH$_{2Cy}$), 30.3 (CH$_{2Cy}$), 29.3 (CH$_{2Cy}$), 28.7 (CH$_{2Cy}$), 27.8 (CH$_{2Cy}$), 27.6 – 27.5 (overlapping resonances, CH$_{2Cy}$), 27.2 (CH$_{2Cy}$), 27.0 (CMe_{ortho}), 26.9 (CH$_{2Cy}$), 21.6 (CMe_{para}), 8.5 (SiMe). ^{31}P{^{1}H} NMR (202.5 MHz, benzene-d_6): δ 63.3 (s, 2 P, PCy$_2$), -55.5 (s, 1 P, PHMes). ^{29}Si{^{1}H} NMR (99.4 MHz, benzene-d_6): δ 66.4 (d, $^{2}J_{SiP}$ = 54 Hz). X-ray quality crystals of **6-12**•OEt$_2$ were obtained from a concentrated Et$_2$O solution at -30 ºC.

6.4.3 Crystallographic solution and refinement details

Crystallographic data for each of **6-3**, **6-4, 6-9, 6-12**•OEt$_2$ were obtained at 173(±2) K on a Bruker D8/APEX II CCD diffractometer using graphite-monochromated Mo Kα (λ = 0.71073 Å) radiation, employing a sample that was mounted in inert oil and transferred to a cold gas stream on the diffractometer. Programs for diffractometer

operation, data collection, and data reduction (including SAINT) were supplied by Bruker. Gaussian integration (face-indexed) was employed as the absorption correction method in each case except for **6-9**, where SADABS (Bruker) was used as the absorption correction method. All structures were solved by use of the Patterson search/structure expansion except for **6-9**, which was solved by direct methods. All structures were refined by use of full-matrix least-squares procedures (on F^2) with R_1 based on $F_o^2 \geq 2\sigma(F_o^2)$ and wR_2 based on $F_o^2 \geq -3\sigma(F_o^2)$. During the structure solution process for **6-12**•OEt_2, one equivalent of diethyl ether was located in the asymmetric unit and refined in a satisfactory manner. Anisotropic displacement parameters were employed throughout for all the non-hydrogen atoms. In the case of both **6-9** and **6-12**•OEt_2 the P-*H* was located in the difference map and refined isotropically. All remaining hydrogen-atoms were added at calculated positions and refined by use of a riding model employing isotropic displacement parameters based on the isotropic displacement parameter of the attached atom. All relevant crystal data for **6-3**, **6-4**, **6-9** and **6-12**•OEt_2 are provided in Appendix A.

CHAPTER 7: 'Hemilabile' Silyl Pincer Ligation: Group 10 PSiN Complexes

7.1 Introduction

Transition metal pincer complexes supported by LXL-type (L = neutral donor, X = anionic donor) ligands are of substantial interest due to the remarkable stoichiometric and catalytic reactivity exhibited by such complexes.[19,20c,129] While PCP, NCN, and PNP pincer ligation has been widely explored in this context, significant effort has also been devoted to the development of alternative pincer architectures. [19-20,24,129-130] In this regard, there has been increased interest in the chemistry of pincer complexes supported by PCN or PNN ligands that contain both hard (N) and soft (P) neutral donors.[22,34b,131] Upon complexation to electron-rich late metal centers, such ligands have been shown to exhibit hemilabile[132] coordination involving the L-donors due to the more labile amine donor, which has been demonstrated to lead to unique reactivity. Thus, Milstein and co-workers have shown that PCN- and PNN-ligated pincer complexes exhibit unprecedented reactivity,[22,34b,131] including the (PNN)Ru-catalyzed dehydrogenative synthesis of amides from alcohols and amines,[22] and water activation mediated by a rare (PCN)Pt=O complex.[34b]

Research in the Turculet group has focused on exploring the coordination chemistry and reactivity of new pincer complexes supported by bis(phosphino)silyl PSiP ligation.[25] These investigations have yielded rare examples of trigonal pyramidal Ru complexes, Ir species that undergo C-H and N-H activation, and Group 10 complexes that undergo reversible Si-C(sp^2) and Si-C(sp^3) bond cleavage. The synthesis and

reactivity of NSiN pincer species has been investigated by Tilley and co-workers, who have reported late metal complexes supported by a bis(quinolyl)silyl ligand.[51] However, no previous examples of PSiN pincer ligation has been reported. Given the unique reactivity properties and catalytic utility of PSiP and NSiN pincer species, hemilabile PSiN-ligated complexes are attractive targets of inquiry. In this context, the synthesis of PSiN-ligated Pd and Pt complexes derived from the new PSiN silyl pincer precursor [(2-$^{t}Bu_2PC_6H_4$)(2-$Me_2NC_6H_4$)SiMe]H ([^{t}Bu-PSiN-Me]H) is detailed in this chapter. These studies confirm that the amidio donor of the [^{t}Bu-PSiN-Me] ligand is indeed labile.

7.2 Results and Discussion

7.2.1 Synthesis and characterization of (^{t}Bu-PSiN-Me)M^{II} (M = Pd, Pt) complexes

The synthetic strategy for the preparation of PSiN-type ligands involved the synthesis of the hydridochlorosilane precursor [2-(NMe_2)C_6H_4]SiMeHCl, which was achieved by the reaction of [2-(NMe_2)C_6H_4]MgBr with excess $MeSiHCl_2$. The tertiary silane (^{t}Bu-PSiN-Me)H (**7-1**) was prepared in 78% yield by the reaction of [2-(NMe_2)C_6H_4]SiMeHCl with 2-($^{t}Bu_2P$)C_6H_4Li.

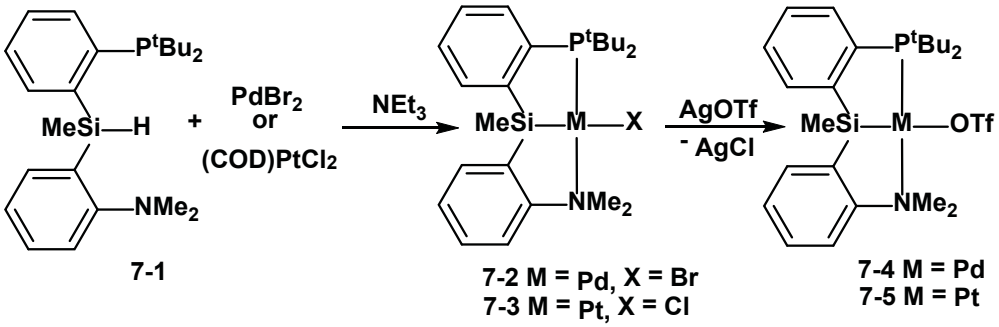

Scheme 7-1. Synthesis of (^{t}Bu-PSiN-Me)M^{II} (M = Pd, Pt) complexes.

Group 10 complexes of the type [^{t}Bu-PSiN-Me]MX (**7-2**, M = Pd, X = Br; **7-3**, M = Pt, X = Cl) were prepared by the reaction of **7-1** with either $PdBr_2$ or $(COD)PtCl_2$ (COD = 1,5-cyclooctadiene) in the presence of Et_3N (Scheme 7-1). The room temperature ^{1}H NMR (benzene-d_6) spectra of **7-2** and **7-3** each feature a broad singlet corresponding to the ligand N*Me*$_2$ protons (**7-2**: 3.17 ppm ; **7-3**: 3.22 ppm). At low temperature, this resonance decoalesces (toluene-d_8, 218 K: for **7-2**, 3.30 and 3.05 ppm; for **7-3**, 3.29 and 3.01 ppm), which is indicative of inequivalent N*Me* groups in square planar complexes of the type κ^3-[^{t}Bu-*PSiN*-Me)]MX. These lineshape changes are consistent with a dynamic process involving decomplexation of the amine arm and inversion and rotation at N, which renders the N*Me* groups equivalent at elevated temperatures ($\Delta G^{\ddagger}$ = 12 kcal mol^{-1} for **7-2**; $\Delta G^{\ddagger}$ = 13 kcal mol^{-1} for **7-3**). This phenomenon highlights the labile coordination of the amino donor arm of the ^{t}Bu-PSiN-Me ligand. Treatment of **7-2** and **7-3** with AgOTf led to the formation of [^{t}Bu-PSiN-Me]M(OTf) (M = Pd, **7-4**; M = Pt, **7-5**) species. The structure of **7-4** was confirmed by single-crystal X-ray diffraction analysis (Figure 7-1, Table 7-1) and indicates approximate square planar coordination geometry at Pd, with *trans*-disposed phosphino and amino donors. The Pd-Si distance of 2.2336(4) Å is short and falls outside the range

characteristic of Pd-Si bond distances (2.26–2.64 Å).[140] As well, the Pd-O distance of 2.3518(11) Å is longer than the Pd-O distance in [κ^3-(2-Me$_2$*N*C$_6$H$_4$)$_2$*N*]PdOTf (2.1067(16) Å),[141] which highlights the strong *trans*-influence of the silyl donor in **7-4**.

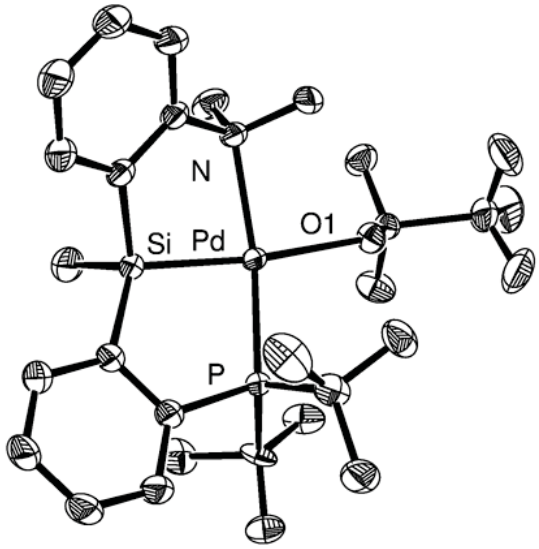

7-4

Figure 7-1. ORTEP diagram for **7-4** shown with 50% displacement ellipsoids; all H-atoms have been omitted for clarity.

Table 7-1. Selected interatomic distances (Å) and angles (º) for **7-4**.

Interatomic Distances (Å)			
Pd-P	2.2731(4)	Pd-Si	2.2336(4)
Pd-O1	2.3518(11)	Pd-N	2.2345(12)
Interatomic Angles (°)			
P-Pd-N	157.86(4)	P-Pd-Si	84.304(14)
Si-Pd-O1	168.92(3)	N-Pd-O1	91.12(4)

7.2.1 Reactivity of [^{t}Bu-PSiN-Me]M^{II} (M = Pd, Pt) complexes

Treatment of **7-2** and **7-3** with PMe_3 led to selective decomplexation of the amine arm of the PSiN ligand and the formation of complexes of the type κ^2-[^{t}Bu-*PSi*N-Me]MX(PMe_3) (**7-6**, M = Pd, X = Br; **7-7**, M = Pt, X = Cl; Scheme 7-2). The ^{1}H NMR spectra of **7-6** and **7-7** each feature a sharp singlet resonance corresponding to the six equivalent NMe_2 protons of the uncoordinated amino ligand arm. The coordination of PMe_3 to the metal center was confirmed in each case by use of ^{31}P NMR spectroscopy. The solid state structure of **7-7** was determined by single-crystal X-ray diffraction analysis (Figure 7-2, Table 7-2) and indicates approximate square planar coordination geometry at Pt, with the PMe_3 ligand coordinated *trans* to the phosphino ligand arm.

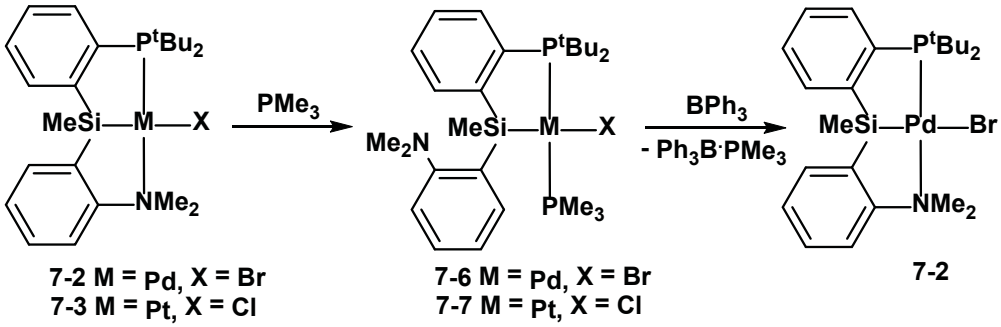

Scheme 7-2. Reaction of **7-2** and **7-3** with PMe_3, and subsequent reaction with BPh_3.

Treatment of complex **7-6** with an equivalent of BPh_3 in benzene solution led to precipitation of $Ph_3B{\cdot}PMe_3$[133] and quantitative regeneration of **7-2** (Scheme 7-2). This sequence of reactions involving complexation of PMe_3 to **7-2** to form **7-6** followed by reformation of **7-2** upon reaction with BPh_3 further illustrates the hemilabile character of [^{t}Bu-PSiN-Me] ligation.

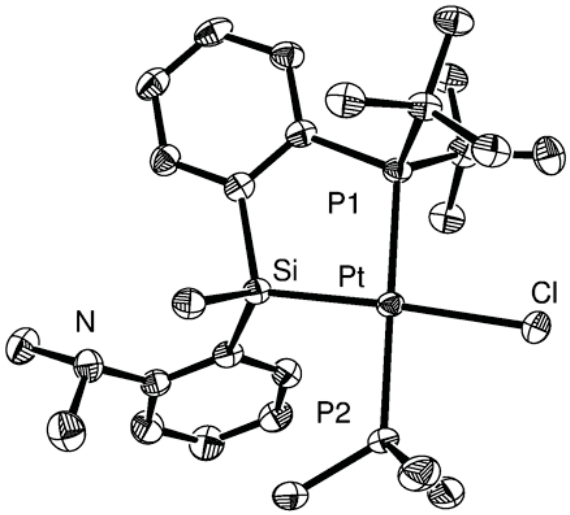

7-7

Figure 7-2. ORTEP diagram for **7-7** shown with 50% displacement ellipsoids; all H-atoms have been omitted for clarity.

Table 7-2. Selected interatomic distances (Å) and angles (º) for **7-7**.

Interatomic Distances (Å)			
Pt-P1	2.3188(8)	Pt-Si	2.3077(9)
Pt-Cl	2.4846(8)	Pt-P2	2.3026(8)
Interatomic Angles (°)			
P1-Pt-P2	179.36(3)	P1-Pt-Si	85.85(3)
Si-Pt-Cl	176.86(3)	P2-Pt-Cl	82.86(3)

7.3 Conclusions

In summary, the synthesis of the first examples of PSiN-ligated platinum group pincer complexes has been detailed. The amino donor of the [^{t}Bu-PSiN-Me] ligand is labile and is displaced from the metal coordination sphere by a better donor, such as PMe_3, to form κ^2-[^{t}Bu-*PSi*N-Me] species. The pincer structure is reformed upon abstraction of PMe_3 from the metal center. This reversible coordination of the amine pincer arm is anticipated to render PSiN-ligated complexes responsive to the changing electronic and coordinative requirements at a metal center that arise during substrate transformations, and may provide access to new and/or enhanced reactivity.

7.4 Experimental Section

7.4.1 General considerations

All experiments were conducted under argon or nitrogen in an MBraun glovebox or using standard Schlenk techniques. Tetrahydrofuran and diethyl ether were distilled from Na/benzophenone ketyl; while benzene, toluene, and pentane were purified over

one activated alumina column and one column packed with activated Q-5. All purified solvents were stored over 4 Å molecular sieves. Benzene-d_6 and toluene-d_8 were degassed via three freeze-pump-thaw cycles and stored over 4 Å molecular sieves. The compound (2-BrC_6H_4)P^tBu_2 was prepared according to a literature procedure.[134] All other reagents were purchased from Strem or Aldrich and used without further purification. Unless otherwise stated, ^1H, ^{13}C, ^{31}P and ^{29}Si NMR characterization data were collected at 300 K on a Bruker AV-500 spectrometer operating at 500.1, 125.8, 202.5, and 99.4 MHz (respectively) with chemical shifts reported in parts per million downfield of $SiMe_4$ (for ^1H, ^{13}C, and ^{29}Si) or 85% H_3PO_4 in D_2O (for ^{31}P). Variable-temperature NMR data were collected on a Bruker AC-250 spectrometer. ^1H and ^{13}C NMR chemical shift assignments are based on data obtained from ^{13}C-DEPTQ, ^1H-^1H COSY, ^1H-^{13}C HSQC, and ^1H-^{13}C HMBC NMR experiments. In some cases, fewer than expected ^{13}C NMR resonances were observed, despite prolonged acquisition times. ^{29}Si NMR assignments are based on ^1H-^{29}Si HMQC and ^1H-^{29}Si HMBC experiments. Elemental analyses were performed by Columbia Analytical Services of Tucson, Arizona and Midwest Microlab of Indianapolis, Indiana. Infrared spectra were recorded as thin films between NaCl plates using a Bruker VECTOR 22 FT-IR spectrometer at a resolution of 4 cm^{-1}.

7.4.2 Synthetic detail and characterization data

$C_6H_4(NMe_2)SiMeHCl$. A solution of 2-bromo-N,N-dimethylaniline (5.00 g, 25.0 mmol) in ca. 75 mL THF was added dropwise to flask containing Mg turnings (0.91 g, 37.5 mmol), and the reaction mixture was subsequently heated for 18 hours at 75 °C.

The resulting brown solution was allowed to cool to room temperature and was then added drop-wise to a solution of Cl_2SiMeH (14.34 g, 125 mmol) in ca. 50 mL of THF at -78 °C. A color change to orange was observed. The reaction mixture was allowed to warm to room temperature and stir for 18 h, at which point the volatile components were removed *in vacuo*, and the residue was extracted with benzene (ca. 30 mL). The benzene extract was filtered through Celite and the benzene was subsequently removed *in vacuo* to yield a red oil. This oil was then distilled under reduced pressure to afford $C_6H_4(NMe_2)SiMeHCl$ (bp = 39° C, <0.1 mm Hg) as a colorless oil (2.34 g, 47%). ^{1}H NMR (500 MHz, benzene-d_6): δ 7.89 (m, 1 H, H_{arom}), 7.15 (m, 1 H, H_{arom}), 7.06 (m, 1 H, H_{arom}), 6.84 (m, 1 H, H_{arom}), 5.55 (m, 1 H, Si-*H*), 2.20 (s, 6H, N*Me*$_2$), 0.60 (d, 3 H, J = 3 Hz, Si*Me*). $^{13}C\{^1H\}$ NMR (125.8 MHz, benzene-d_6): δ 160.65 (C_{arom}), 136.6 (CH_{arom}), 133.9 (C_{arom}), 132.9 (CH_{arom}), 127.3 (CH_{arom}), 121.4 (CH_{arom}), 46.6 (N*Me*$_2$), 2.4 (Si*Me*). ^{29}Si NMR (99.4 MHz, benzene-d_6): δ -21.0 ppm.

[^{t}Bu-PSiN-Me]H (7-1). ^{n}BuLi (1.6 M in hexanes, 0.69 mL, 1.1 mmol) was added to a cold (-78 °C) solution of $(2\text{-}BrC_6H_4)P^tBu_2$ (0.33 g, 1.1 mmol) in ca. 5 mL of pentane. The reaction mixture was allowed to warm to room temperature and after stirring for 2 h the volatile components were removed *in vacuo*. The remaining beige solid was dissolved in ca. 3 mL of THF and cooled to -30 °C. The cold THF solution was added drop-wise to a pre-cooled (-30 °C) solution of $C_6H_4NMe_2SiMeHCl$ (0.22 g, 1.1 mmol) in ca. 3 mL of THF. The reaction mixture was allowed to warm to room temperature and stired for 2 h. The volatile components were removed in vacuo, and the residue was extracted with ca. 10 mL of benzene. The benzene extracts were filtered through Celite and the filtrate solution was dried *in vacuo* to yield **7-1** as a pale yellow oil (0.33 g, 78%).

^{1}H NMR (500 MHz, benzene-d_6): δ 7.81 (m, 1 H, H_{arom}), 7.70 (m, 1 H, H_{arom}), 7.65 (m, 1 H, H_{arom}), 7.22 (m, 1 H, H_{arom}), 7.15 – 7.13 (overlapping resonances, 2 H, H_{arom}), 7.08 (m, 1 H, H_{arom}), 6.99 (m, 1 H, H_{arom}), 5.87 (m, 1 H, Si-*H*), 2.34 (s, 6 H, N*Me*$_2$), 1.16 (d, 9 H, PC*Me*$_3$, $^{3}J_{PH}$ = 11 Hz), 1.10 (d, 9 H, PC*Me*$_3$, $^{3}J_{PH}$ = 11 Hz), 0.83 (d, 3 H, Si*Me*, $^{3}J_{HP}$ = 4 Hz). ^{13}C{^{1}H} NMR (125.8 MHz, benzene-d_6): δ 161.6 (C_{arom}), 149.1 (d, C_{arom}, J_{CP} = 51 Hz), 144.7 (d, C_{arom}, J_{CP} = 21 Hz), 138.7 (*C*H$_{arom}$), 137.2 (d, *C*H$_{arom}$, J_{CP} = 17 Hz), 136.6 (C_{arom}), 135.1 (*C*H$_{arom}$), 131.5 (*C*H$_{arom}$), 128.9 (*C*H$_{arom}$), 128.6 (*C*H$_{arom}$), 125.3 (*C*H$_{arom}$), 121.5 (*C*H$_{arom}$), 46.6 (N*Me*$_2$), 33.6 (d, P*C*Me$_3$, J_{CP} = 8 Hz), 33.4 (d, P*C*Me$_3$, J_{CP} = 8 Hz), 31.5 – 31.3 (overlapping resonances, PC*Me*$_3$), -1.6 (d, Si*Me*, J_{CP} = 10 Hz). ^{31}P{^{1}H} NMR (202.5 MHz, benzene-d_6): δ 23.2. ^{29}Si NMR (99.4 MHz, benzene-d_6): δ -24.4 ppm ($^{1}J_{SiH}$ = 205 Hz). IR (cm^{-1}): 2128 (br, m, Si-H). Anal. Calcd for $C_{23}H_{36}NPSi$: C, 71.64; H, 9.41; N, 3.63. Found: C, 71.23; H, 9.18; N, 3.50.

κ^3-[^{t}Bu-*PSiN*-Me]PdBr (7-2). A solution of **7-1** (0.22 g, 0.57 mmol) and NEt_3 (0.095 mL, 0.68 mmol) in ca. 5 mL of benzene was added to a slurry of $PdBr_2$ (0.15 g, 0.57 mmol) in ca. 5 mL of benzene. The resulting reaction mixture was stirred at room temperature for 18 h. The pale yellow solution was filtered through Celite and the volatile components were removed *in vacuo*. The residue was triturated with pentane (3 × 2 mL) and dried *in vacuo* to yield **7-2** as a pale yellow solid (0.28 g, 86 % yield). ^{1}H NMR (500 MHz, benzene-d_6): δ 7.67 – 7.63 (overlapping resonances, 2 H, H_{arom}), 7.54 (m, 1 H, H_{arom}), 7.20-7.17 (overlapping resonances, 2 H, H_{arom}), 7.09 – 7.03 (overlapping resonances, 3 H, H_{arom}), 6.96 (d, 1 H, J = 7 Hz, H_{arom}), 3.17 (br s, 6 H, N*Me*$_2$), 1.43 (d, 9 H, PC*Me*$_3$, $^{3}J_{PH}$ = 14 Hz), 1.32 (d, 9 H, PC*Me*$_3$, $^{3}J_{PH}$ = 14 Hz), 0.59 (s, 3 H, Si*Me*). ^{13}C{^{1}H} NMR (300 K, 125.8 MHz, benzene-d_6): δ 162.0 (C_{arom}), 140.8 (C_{arom}) 133.9

(CH$_{arom}$), 133.5 (d, CH$_{arom}$, J_{CP} = 24 Hz), 133.2 (CH$_{arom}$), 131.1 (CH$_{arom}$), 130.8 (CH$_{arom}$), 128.9 (CH$_{arom}$), 127.6 (CH$_{arom}$), 122.0 (CH$_{arom}$), 52.0 (N*Me*), 37.6 (CMe$_3$), 38.0 (CMe$_3$), 31.9 (d, C*Me$_3$*, J_{CP} = 5 Hz), 31.1 (d, C*Me$_3$*, J_{CP} = 5 Hz), 7.5 (Si*Me*). ^{31}P{^{1}H} NMR (202.5 MHz, benzene-d_6): δ 99.4. ^{29}Si NMR (99.4 MHz, benzene-d_6): δ 54.0. Anal. Calcd for $C_{23}H_{35}BrNPPdSi$: C, 48.39; H, 6.18; N, 2.45. Found: C, 48.05; H, 6.33; N, 2.29.

κ^3-[^{t}Bu-*PSiN*-Me]PtCl (7-3). (COD)$PtCl_2$ (0.13 g, 0.36 mmol) was added to a solution of **7-1** (0.14 g, 0.36 mmol) and NEt_3 (0.060 mL, 0.43 mmol) in ca. 5 mL of benzene. The resulting reaction mixture was heated at 75 °C for 48 h. The solution was subsequently filtered through Celite and the volatile components were removed *in vacuo*. The residue was triturated with pentane (3 × 2 mL) and dried *in vacuo* to yield **7-3** as an off white solid (0.15 g, 68%). ^{1}H NMR (500 MHz, benzene-d_6): δ 7.82 (d, 1 H, J = 7 Hz, H_{arom}), 7.72 (m, 1 H, H_{arom}), 7.60 (m, 1 H, H_{arom}), 7.17 (m, 1 H, H_{arom}), 7.06 – 7.03 (overlapping resonances, 2 H, H_{arom}), 6.92 (m, 1 H, H_{arom}), 6.90 (d, 1H, J = 7 Hz, H_{arom}), 3.22 (br s, 6 H, N*Me$_2$*), 1.40 (d, 18 H, PC*Me$_3$*, $^3J_{PH}$ = 14 Hz), 0.52 (s, 3 H, Si*Me*). ^{13}C{^{1}H} NMR (300 K, 125.8 MHz, benzene-d_6): δ 133.5 (CH$_{arom}$), 133.1 (d, CH$_{arom}$, J_{CP} = 19 Hz), 132.9 (CH$_{arom}$), 130.6 (CH$_{arom}$), 130.5 (CH$_{arom}$), 128.7 (CH$_{arom}$), 127.9 (CH$_{arom}$), 121.8 (CH$_{arom}$), 36.8 (CMe$_3$), 31.5 (C*Me$_3$*), 30.8 (C*Me$_3$*), 8.69 (Si*Me*). ^{31}P{^{1}H} NMR (202.5 MHz, benzene-d_6): δ 74.7 (s with Pt satellites, $^1J_{PPt}$ = 4804 Hz) ^{29}Si NMR (99.4 MHz, benzene-d_6): δ 24.9. Anal. Calcd for $C_{23}H_{35}NPPtClSi$: C, 44.91; H, 5.76; N, 2.28. Found: C, 44.82; H, 6.12, N, 1.93.

κ^3-[^{t}Bu-*PSiN*-Me]Pd(OTf) (7-4). AgOTf (0.027 g, 0.11 mmol) was added to a solution of **7-2** (0.060 g, 0.11 mmol) in ca. 5 mL of benzene. The resulting reaction mixture was allowed to stir at room temperature for 30 minutes. The solution was subsequently filtered through Celite and the volatile components were removed *in vacuo*. The residue was triturated with pentane (3 × 2 mL) and dried *in vacuo* to yield **7-4** as a pale yellow solid (0.063 g, 89%). ^{1}H NMR (500 MHz, benzene-d_6): δ 7.52 (d, 1 H, H_{arom}, J = 7 Hz), 7.43 (m, 1 H, H_{arom}), 7.38 (m, 1 H, H_{arom}), 7.14 (m, 1 H, H_{arom}), 7.02 (m, 1 H, H_{arom}), 6.96 (m, 1 H, H_{arom}), 6.87 (d, 1 H, H_{arom}, J = 8 Hz), 3.13 (s, 3 H, N*Me*), 3.03 (s, 3 H, N*Me*), 1.26 (d, 9 H, PC*Me*$_3$, $^3J_{PH}$ = 15 Hz), 1.15 (d, 9 H, PC*Me*$_3$, $^3J_{PH}$ = 15 Hz), 0.43 (d, 3 H, Si*Me*, J = 2 Hz). ^{13}C{^{1}H} NMR (125.8 MHz, benzene-d_6): δ 161.5 (C_{arom}), 139.0 (C_{arom}), 133.4 – 133.2 (overlapping resonances, CH$_{arom}$), 132.6 (CH$_{arom}$), 131.7 (CH$_{arom}$), 131.1 (CH$_{arom}$), 129.6 (CH$_{arom}$), 121.5 (CH$_{arom}$), 49.6 (N*Me*), 37. 5 (CMe$_3$), 36.4 (CMe$_3$), 31.2 (C*Me*$_3$), 30.6 (C*Me*$_3$), 6.93 (Si*Me*). ^{31}P{^{1}H} NMR (202.5 MHz, benzene-d_6): δ 92.4. ^{29}Si NMR (99.4 MHz, benzene-d_6): δ 53.3. Anal. Calcd for $C_{24}H_{35}NPPdSiO_3SF_3$: C, 45.03; H, 5.51; N, 2.19. Found: C, 44.87; H, 5.94, N, 2.12.

κ^3-[^{t}Bu-*PSiN*-Me]Pt(OTf) (7-5). AgOTf (0.022 g, 0.086 mmol) was added to a solution of **7-3** (0.053 g, 0.086 mmol) in ca. 5 mL of benzene. The resulting reaction mixture was allowed to stir at room temperature for 30 minutes. The solution was subsequently filtered through Celite and the volatile components were removed *in vacuo*. The residue was triturated with pentane (3 × 2 mL) and dried *in vacuo* to yield **7-5** as a pale yellow solid (0.050 g, 80%). ^{1}H NMR (500 MHz, benzene-d_6): δ 7.61 (d, 1 H, H_{arom}, J = 7 Hz), 7.50 (m, 1 H, H_{arom}), 7.43 (m, 1 H, H_{arom}), 7.12 (m, 1 H, H_{arom}) 7.04 - 6.94 (overlapping resonances, 3 H, H_{arom}), 6.87 (d, 1 H, H_{arom}, J = 8 Hz), 3.19 (d, 6 H,

N*Me*, J = 2 Hz), 3.17 (d, 6 H, N*Me*, J = 2 Hz), 1.30 (d, 9 H, PC*Me*$_3$, $^3J_{PH}$ = 15 Hz), 1.22 (d, 9 H, PC*Me*$_3$, $^3J_{PH}$ = 15 Hz), 0.39 (s, 3 H, Si*Me*). $^{13}C\{^1H\}$ NMR (125.8 MHz, benzene-d_6): δ 162.1 (C_{arom}), 150.5 (C_{arom}), 142.1 (d, C_{arom}, J_{CP} = 55 Hz). 138.0 (C_{arom}), 133.1 (d, $CH_{arom,}$, J_{CP} = 5 Hz), 132.8 (d, CH_{arom}, J_{CP} = 18 Hz), 132.2 (CH_{arom}), 131.4 (CH_{arom}), 130.8 (CH_{arom}), 129.1 (d, CH_{arom}, J_{CP} = 7 Hz), 128.9 (CH_{arom}), 121.3 (CH_{arom}), 53.6 (N*Me*), 50.2 (N*Me*), 36.7 (CMe$_3$), 35.2 (CMe$_3$), 31.2 (d, C*Me*$_3$, J_{CP} = 5 Hz), 30.5 (d, C*Me*$_3$, J_{CP} = 5 Hz), 6.0 (Si*Me*). $^{31}P\{^1H\}$ NMR (202.5 MHz, benzene-d_6): δ 70.8 (s with Pt satellites, $^1J_{PtP}$ = 4611 Hz). ^{29}Si NMR (99.4 MHz, benzene-d_6): δ 14.6. Anal. Calcd for $C_{24}H_{35}NPPtSiO_3SF_3$: C, 39.56; H, 4.84; N, 1.92. Found: C, 39.19; H, 4.97, N, 2.06.

κ^2-[^{t}Bu-*PSi*N-Me]PdBr(PMe$_3$) (7-6). A solution of **7-2** (0.10 g, 0.18 mmol) in ca. 5 mL of benzene was treated with PMe$_3$ (0.04 mL, 0.39 mmol). The reaction mixture was allowed to stand at room temperature for 10 minutes. The volatile components of the reaction mixture were subsequently removed *in vacuo*. The residue was triturated with pentane (3 × 2 mL) and dried *in vacuo* to yield **7-6** as a pale yellow solid (0.10 g, 93%). ^1H NMR (500 MHz, benzene-d_6): δ 7.90 (d, 1 H, H_{arom}, J = 7 Hz), 7.66 (m, 1 H, H_{arom}), 7.50 (d, 1 H, H_{arom}, J = 7 Hz), 7.18 (m, 1 H, H_{arom}), 7.07 – 6.96 (overlapping resonances, 4 H, H_{arom}), 2.29 (s, 6 H, N*Me*$_2$), 1.60 (d, 9 H, PC*Me*$_3$, $^3J_{PH}$ = 14 Hz), 1.49 (d, 9 H, PC*Me*$_3$, $^3J_{PH}$ = 14 Hz), 1.20 (d, 9 H, J = 9 Hz, P*Me*$_3$), 0.81 (s, 3 H, Si*Me*). $^{13}C\{^1H\}$ NMR (125.8 MHz, benzene-d_6): δ 160.4 (C_{arom}), 138.5 (CH_{arom}), 134.3 (d, CH_{arom}, J_{CP} = 39 Hz), 133.8 (CH_{arom}), 131.0 (CH_{arom}), 130.3 (CH_{arom}), 127.6 (d, CH_{arom}, J_{CP} = 7 Hz), 125.3 (CH_{arom}), 122.8 (CH_{arom}), 47.4 (N*Me*$_2$), 37.5 (CMe$_3$), 32.3 (d, C*Me*$_3$, J_{CP} = 6 Hz), 31.8 (d, C*Me*$_3$, J_{CP} = 6 Hz), 17.0 (d, P*Me*$_3$, J_{CP} = 28 Hz), 6.6 (Si*Me*). $^{31}P\{^1H\}$ NMR (202.5 MHz, benzene-d_6): δ 95.2 (d, 1 P, P^tBu$_2$, $^2J_{PP}$ = 347 Hz), -20.4 (d, 1 P, PMe$_3$, $^2J_{PP}$ = 347 Hz).

^{29}Si NMR (99.4 MHz, benzene-d_6): δ 30.3. Anal. Calcd for $C_{26}H_{44}BrNP_2PdSi$: C, 48.27; H, 6.85; N, 2.16. Found: C, 48.06; H, 6.87, N, 1.85.

κ^2-[^{t}Bu-*PSi*N-Me]PtCl(PMe$_3$) (7-7). A solution of **7-3** (0.070 g, 0.11 mmol) in ca. 5 mL of benzene was treated with PMe_3 (0.02 mL, 0.24 mmol). The reaction mixture was allowed to stand at room temperature for 10 minutes. The volatile components of the reaction mixture were subsequently removed *in vacuo*. The residue was triturated with pentane (3 × 2 mL) and dried *in vacuo* to yield **7-7** as a pale yellow solid (0.021 g, 28%). ^{1}H NMR (500 MHz, benzene-d_6): δ 8.09 (d, 1 H, H_{arom}, J = 7 Hz), 7.69 - 7.67 (overlapping resonances, 2 H, H_{arom}), 7.19 (m, 1 H, H_{arom}, J = 7 Hz), 7.10-7.05 (overlapping resonances, 3 H, H_{arom}), 6.98 (m, 1 H, H_{arom}, J = 7 Hz), 2.37 (s, 6 H, N*Me$_2$*), 1.61 (d, 9 H, PC*Me$_3$*, $^3J_{PH}$ = 14 Hz), 1.50 (d, 9 H, PC*Me$_3$*, $^3J_{PH}$ = 14 Hz), 1.23 (dd, 9 H, P*Me$_3$*, $^2J_{HP}$ = 10 Hz, $^4J_{HP}$ = 2 Hz), 0.95 (s with Pt satellites, 3 H, Si*Me*, $^3J_{HPt}$ = 9 Hz). ^{13}C{^{1}H} NMR (125.8 MHz, benzene-d_6): δ 161.4 (C_{arom}), 141.3 (C_{arom}), 139.3 (CH$_{arom}$), 134.6 (CH$_{arom}$), 133.5 (CH$_{arom}$), 131.2 (CH$_{arom}$), 130.7 (CH$_{arom}$), 127.3 (CH$_{arom}$), 125.1 (CH$_{arom}$), 122.6 (CH$_{arom}$), 47.5 (N*Me$_2$*), 38.9 (CMe$_3$), 38.7 (CMe$_3$), 32.2 (d, C*Me$_3$*, J_{CP} = 6 Hz), 31.4 (d, C*Me$_3$*, J_{CP} = 6 Hz), 15.4 (d, P*Me$_3$*, J_{CP} = 36 Hz), 6.7 (Si*Me*). ^{31}P{^{1}H} NMR (202.5 MHz, benzene-d_6): δ 88.9 (d with Pt satellites, 1 P, P^tBu$_2$, $^2J_{PP}$ = 381 Hz, $^1J_{PtP}$ = 3013 Hz), -11.4 (d with Pt satellites, 1 P, P*Me$_3$*, $^2J_{PP}$ = 381 Hz, $^1J_{PtP}$ = 2692 Hz). ^{29}Si NMR (99.4 MHz, benzene-d_6): δ 6.5. $C_{26}H_{44}ClNP_2PtSi$: C, 45.18; H, 6.42; N, 2.03. Found: C, 44.82; H, 6.51, N, 2.37. A single crystal of **7** suitable for X-ray diffraction analysis was grown from benzene solution at room temperature.

7.4.2 Crystallographic solution and refinement details

Crystallographic data for each of **7-4**·0.5C_6H_6 and **7-7**, were obtained at 173(±2)K on a Bruker D8/APEX II CCD diffractometer using a graphite-monochromated Mo Kα (λ = 0.71073 Å) radiation, employing a sample that was mounted in inert oil and transferred to a cold gas stream on the diffractometer. Programs for diffractometer operation, data collection, and data reduction (including SAINT) were supplied by Bruker. Gaussian integration (face-indexed) was employed as the absorption correction method in each case. Both structures were solved by use of the Patterson search/structure expansion and were refined by use of full-matrix least-squares procedures (on F^2) with R_1 based on $F_o^2 \geq 2\sigma(F_o^2)$ and wR_2 based on $F_o^2 \geq -3\sigma(F_o^2)$. During the structure solution process for **7-4**·0.5C_6H_6 half an equivalent of disordered benzene was located in the asymmetric unit. The benzene carbon atoms (C1S-C3S) were modeled isotropically over two positions with occupancies of 0.5. Disorder involving the P^t*Bu*$_2$ substituents was also identified. The ^{t}Bu group carbon atoms (C31-C38) were modeled anisotropically over two positions with occupancy factors of 0.5. Anisotropic displacement parameters were employed for all remaining non-hydrogen atoms. All hydrogen atoms were added at calculated positions and refined by use of a riding model employing isotropic displacement parameters based on the isotropic displacement parameter of the attached atom. Additional crystallographic information for **7-4**·0.5C_6H_6 and **7-7** is provided in Appendix A.

CHAPTER 8: Conclusions

8.1 Summary and Conclusions

The synthesis and reactivity of Ni, Pd, and Pt complexes supported by (bisphosphino)silyl ligation have been detailed in this thesis. In Chapter 2, the synthesis and reactivity of [Cy-PSiP]Pt^{II} ([Cy-PSiP] = [κ^3-(2-$Cy_2PC_6H_4)_2SiMe$]$^-$) alkyl and cationic complexes was outlined. Terminal square planar alkyl and aryl derivatives were obtained via salt metathesis reactions of [Cy-PSiP]PtCl (**2-1**) with the corresponding Li alkyl and aryl reagents. The synthesis of a terminal Pt^{II} hydride complex was attempted by reacting **2-1** with $LiEt_3BH$; this reaction instead produced an η^2-Si-H complex (**2-7**), where the terminal hydride ligand has migrated to the silyl group in the ligand backbone. Such neutral Pt^{II} species proved unreactive towards sp^2-CH bonds in benzene. Potentially more reactive Pt^{II} cationic complexes were targeted by treatment of [Cy-PSiP]PtMe (**2-3**) with the Lewis acid $B(C_6F_5)_3$, which led to the formation of {[Cy-PSiP]Pt}$^+$[$MeB(C_6F_5)_3$]$^-$ (**2-5**). Despite the precedent for arene C-H activation by cationic Pt complexes, **2-5** did not exhibit reactivity with benzene C-H bonds. Rather, B-C bond cleavage in the [$MeB(C_6F_5)_3$]$^-$ counteranion was observed to produce [Cy-PSiP]Pt(C_6F_5) and $MeB(C_6F_5)_2$. Heating of [Cy-PSiP]PtX (X = Cl, OTf) complexes in benzene solution in the presence of amine bases also did not result in benzene C-H activation.

In an effort to further assess the reactivity of [Cy-PSiP]Pt(alkyl) species with respect to E-H bond activation, reactions with hydrosilanes were also carried out. The methyl complex **2-3** reacted readily with $PhSiH_3$ to form the corresponding bis(silyl) complex [Cy-PSiP]Pt(SiH_2Ph) (**2-8**) with loss of CH_4. By comparison, **2-3** reacted with

either Ph_2SiHCl, $^iPr_2SiHCl$, or Me_3SiCl to form **2-1** with concomitant evolution of Ph_2SiMeH, $^iPr_2SiMeH$, or Me_4Si, respectively. This reactivity is in stark contrast to that observed for analogous [Ph-PSiP]Pt(alkyl) complexes that reacted with hydridochlorosilanes to form the corresponding silyl complexes. Although the mechanism for the net Si-Cl bond cleavage reactions observed for **2-3** upon exposure to a chlorosilane has not been determined, the divergent reactivity observed for [Ph-PSiP]PtPh versus [Cy-PSiP]Pt(alkyl) species reveals that modification of the steric and electronic properties of the [R-PSiP] ligand directs the outcome of reactions with hydridochlorosilanes towards either Si-H or net Si-Cl bond cleavage. Interestingly, **2-7** reacted with Ph_2SiHCl to produce the corresponding Pt silyl complex [Cy-PSiP]Pt($SiClPh_2$) (**2-9**) with concomitant evolution of H_2.

Expanding on the scope of bond activation reactivity involving bis(phosphino)silyl Pt complexes, the potential for Si-C bond cleavage at a Pt center was also investigated. A modified ligand precursor, [Cy-PSiP]Me (**2-10**) reacted with $Pt(PPh_3)_4$ to afford [Cy-PSiP]PtMe as the product of net Si-Me oxidative addition. A similar reaction of **2-10** with $[(Me_2S)PtMe_2]_2$ also resulted in the formation of [Cy-PSiP]PtMe. Two intermediates were observed during the course of this latter reaction; one intermediate was tentatively identified as the bis(phosphino) Pt^{II} species (κ^2-Cy-PSiP)$PtMe_2$, which was crystallographically characterized, while the second was proposed to be a Pt^{IV} species of the type [Cy-PSiP]$PtMe_3$. Attempts to independently prepare a [Cy-PSiP]Pt^{IV} model complex were met with limited success. The reaction of [Cy-PSiP]H with a $PtMe_3I$ resulted in the elimination of methane and the formation of a short lived Pt^{IV} complex that has been tentatively assigned as [Cy-PSiP]$PtMe_2I$ (**2-14**).

Facile loss of ethane from **2-14** to form [Cy-PSiP]PtI was noted. Thus, [Cy-PSiP] ligation does not appear well-suited to support isolable Pt^{IV} species.

Square planar Ni^{II} and Pd^{II} chloride complexes of [Cy-PSiP] were also readily synthesized. Upon alkylation of [Cy-PSiP]PdCl with MeLi, a terminal methyl complex was formed, which after mild heating underwent a rearrangement involving Si-C(sp^2) bond cleavage in the PSiP ligand backbone and transfer of the Pd-*Me* group to Si. Interestingly, when the analogous alkylation of [Cy-PSiP]NiCl with MeMgBr was carried out, an equilibrium mixture containing the terminal Ni-*Me* complex (**3-6**) and the rearranged Si-C(sp^2) bond cleavage product (**3-7**) was obtained. ^{1}H-^{1}H and ^{31}P-^{31}P EXSY experiments were consistent with reversible Si-C(sp^2) and Si-C(sp^3) bond cleavage processes involving **3-6** and **3-7** on the NMR timescale. Such reversible Si-C bond cleavage steps are exceedingly rare. The coordination mode of the ligand *trans* to Si may have an important effect on the ability of square planar [Cy-PSiP] complexes to undergo ligand rearrangement processes involving Si-C bond cleavage. Thus, η^3-coordination of the allyl ligand in [Cy-PSiP]Ni(η^3-C_3H_5) prevented such rearrangement processes from occurring even after prolonged heating. By comparison the related Pd complex, which was spectroscopically identified as an η^1-allyl complex, underwent relatively facile Si-C(sp^2) bond cleavage in the ligand backbone and transfer of the allyl ligand to Si.

A Pd analogue of the η^2-Si-H complex **2-7** proved synthetically accessible. Both **2-7** and its Pd analogue (**4-1**) underwent insertion of CO_2 to give the corresponding formate complexes **3-6** and **3-7**, respectively. The formation of cationic Pd^{II} and Pt^{II} formato-borate complexes was achieved by reacting either **3-6** or **3-7** with BPh_3 or $B(C_6F_5)_3$. Alternatively, treatment of either **2-7** or **4-1** with $B(C_6F_5)_3$ followed by

exposure to CO_2 also produced Pt and Pd formato-borate complexes (**4-5** and **4-6**, respectively). Treatment of either **4-5** or **4-6** with four equiv. of Ph_2SiMeH resulted in the formation of methane, as well as the silyl ether $(Ph_2SiMe)_2O$ and the corresponding η^2-Si-H metal complex (**2-7** or **4-1**, respectively). This process for the hydrosilylation of CO_2 to form methane can be carried out in a catalytic fashion, using either **2-7** or **4-1** as the catalyst precursors in conjunction with $B(C_6F_5)_3$. TONs as high as 2156 were obtained when **2-7** was used at a loading of 0.016 mol%. A mechanism was proposed for this catalytic process, whereby the initial two reductions of CO_2 to form a bis(silylacetal) species are mediated by the metal complex, while the final two catalytic reduction steps are performed by $B(C_6F_5)_3$. Evidence for this mechanism was obtained by performing the catalytic reaction with BPh_3 as a co-catalyst rather than $B(C_6F_5)_3$, which resulted exclusively in formation of the bis(silyl)acetal $(Ph_2MeSiO)_2CH_2$ with no methane formation.

The synthesis of bis(phosphino)silyl supported Group 10 metal complexes featuring non-dative heteroatomic ligands (i.e. amido, alkoxo) was also described. Terminal, monomeric [Cy-PSiP]Pt(O^tBu) (**5-2**), [Cy-PSiP]Pt(OPh) (**5-3**) and [Cy-PSiP]Pt(OH) (**5-4**) proved readily accessible from treatment of [Cy-PSiP]Pt(NH^tBu) with the coresponding alcohol or with water. Such alkoxo and hydroxo complexes behave like strong Bronsted bases and can readily deprotonate the relatively acidic C-H bonds in phenylacetylene and acetonitrile to afford the corresponding acetylide and cyanomethyl Pt species. Interestingly, complexes **5-2** and **5-4** also underwent hydrogenolysis of the Pt-O linkage upon exposure to H_2. This represents a rare example of net H_2 addition across a late metal/alkoxo or hydroxo bond. Remarkably, treatment of **5-2, 5-3** or **5-4** with $PhSiH_3$

also resulted in Si-H addition across the Pt-O linkage to form the Pt bis(silyl) complex [Cy-PSiP]Pt(SiH_2Ph) with loss of either alcohol or water. No evidence for the formation of the corresponding siloxane and/or **2-7** was observed in these reactions, which is somewhat unusual given the potential to form strong Si-O bonds. DFT studies into the mechanism of H-H and Si-H addition to [Cy-PSiP]Pt(OH) are ongoing.

Terminal, monomeric Pt anilido complexes of the type [Cy-PSiP]Pt(NHAr) (Ar = Ph, 2,6-$Me_2C_6H_3$, 2,6-$^iPr_2C_6H_3$) were obtained through salt metathesis reactions of **2-1** with the corresponding LiNHAr species. The potential of such anilido complexes to undergo insertion chemistry was probed, and in this regard, [Cy-PSiP]Pt(NHPh) was shown to react with xylyl isocyanide to afford 1,1-insertion into the Pt-N bond**.** When analogous Pd^{II} complexes were targeted, initial formation of a Pd^{II} anilido complex of the type [Cy-PSiP]Pd(NHPh) (**6-5**) was observed. Upon mild heating **6-5** underwent a rearrangement involving Si-C(sp^2) bond cleavage in the PSiP backbone and transfer of the anilido ligand to Si, similar to the rearrangement previously observed for [Cy-PSiP]Pd(η^1-alkyl) complexes. When related Ni^{II} anilido complexes were targeted, spectroscopic evidence suggests that a mixture of products arising from related rearrangement processes involving Si-C cleavage in the PSiP backbone is formed.

Terminal, monomeric phosphido complexes of the type [Cy-PSiP]M(PRR') (M = Pt, R = R' = ^{i}Pr; M = Pt, Pd, Ni, R = Mes, R' = H) were prepared by reacting [Cy-PSiP]MCl with the corresponding lithium phosphido species. Remarkably, the Pd and Ni phosphido complexes are resistant to the rearrangement processes observed for related anilido derivatives. X-ray crystallographic characterization of [Cy-PSiP]Ni(PHMes) indicated a less pyramidal P donor in this complex than was noted for the Pt analogue,

which suggests that some π-type interaction may be involved in the Ni-phosphido bonding. Such an interaction may impart added stability to the terminal Ni phosphido complex (and potentially to the Pd analogue), thereby preventing rearrangement processes involving Si-C cleavage in the pincer ligand backbone.

Finally, the potential for silyl pincer complexes featuring a hemilabile pincer arm was explored. The PSiN ligand precursor [(2-^{t}Bu$_2$*P*C$_6$H$_4$)(2-Me$_2$*N*C$_6$H$_4$)*Si*Me]H ([^{t}Bu-PSiN-Me]H) was readily metalated to Pd and Pt to afford square planar PSiN complexes of the type [^{t}Bu-PSiN-Me]MX (M = Pd, X = Br; M = Pt, X = Cl). The presence of an amino pincer arm opens the possibility for "hemilabile" reactivity, where the amine donor could de-chelate and open a coordination site at the metal. Indeed, variable temperature ^{1}H NMR analysis of [^{t}Bu-PSiN-Me]MX revealed lineshape changes consistent with a dynamic process involving decomplexation of the amino ligand arm and inversion and rotation at N, which highlights the labile coordination of the amino donor arm of the [^{t}Bu-PSiN-Me] ligand. Furthermore, reaction of [^{t}Bu-PSiN-Me]MX with PMe_3 led to selective displacement of the amino pincer arm from the metal center to afford complexes of the type κ^2-(^{t}Bu-*PSi*N-Me)MX(PMe_3). Treatment of the Pt analogue κ^2-(^{t}Bu-*PSi*N-Me)PtCl(PMe_3) with BPh_3 resulted in abstraction of the PMe_3 ligand and re-formation of the κ^3-PSiN Pt complex, thus demonstrating the potential 'hemilability' of the amino donor.

8.2 Future Work

Having thoroughly explored the coordination chemistry of [Cy-PSiP]M Group 10 species, future work in this area could further explore the potential catalytic activity of

such complexes. For instance, the reactivity of [Cy-PSiP]Ni species towards arene C-F bond cleavage processes may be pursued. There has been great interest in recent years in the ability of transition metal complexes to activate C-F bonds, both stoichiometrically and catalytically.[135] Fluorocarbons are generally reluctant to coordinate to metal centers and are resistant to chemical attack as a consequence of the great strength of the C-F bond and the high electronegativity of fluorine. However, bis(phosphine) Ni^0 complexes have exhibited an aptitude for C-F bond activation in aromatic fluorocarbons,[135b,136] and computational studies have indicated that the activation of aromatic C-F bonds by such Ni complexes is thermodynamically favorable.[137] Given that [Cy-PSiP]Ni(alkyl) complexes are proposed to provide access to Ni^0 species via Si-alkyl reductive elimination, it may be possible for such *in situ* generated [Cy-PSiP]Ni^0 species to undergo C-F bond cleavage processes. The reactivity of [Cy-PSiP]Ni(alkyl) complexes with fluorinated aromatic substrates should therefore be investigated. The potential for such C-F bond cleavage steps to be incorporated into catalytic cycles for the formation of C-C bonds may also be pursued (Scheme 8-1), as catalytic C-F bond activation processes are quite rare.[135c,135d]

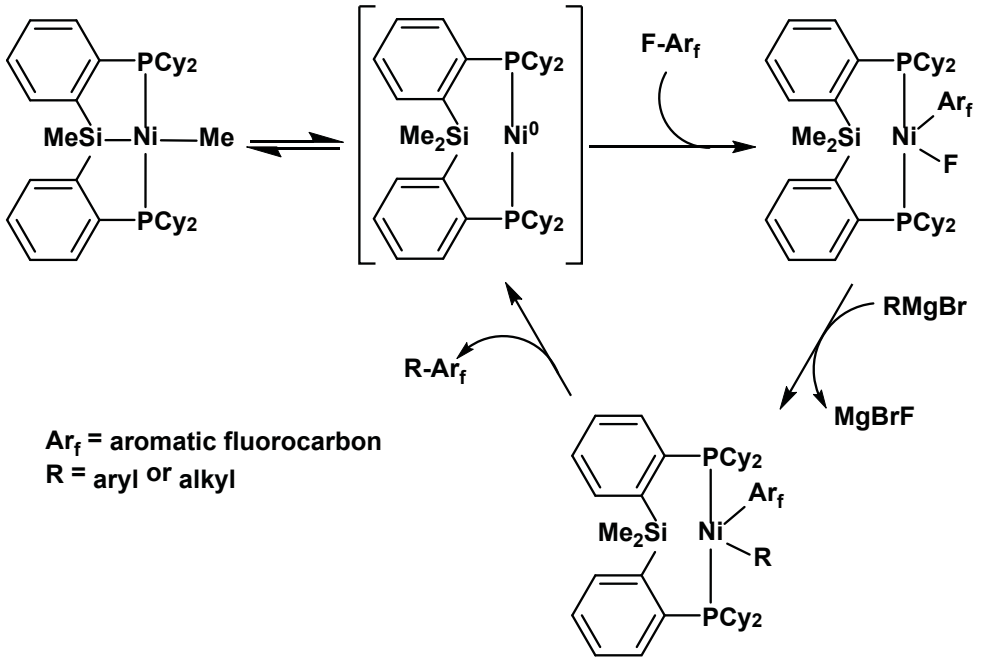

Scheme 8-1. Proposed catalytic cycle for the [Cy-PSiP]Ni-catalyzed Kumada coupling of aromatic fluorocarbons with Grignard reagents.

In Chapter 4, the reduction of CO_2 using hydrosilanes was described. While these methods are effective, the ideal reducing agent for such chemistry is hydrogen. High pressure experiments using [Cy-P*Si*(μ-H)P]*M* (M = Pd, Pt) species as a catalyst to reduce CO_2 with H_2 should be explored (Scheme 8-2). In an effort the circumvent the use of high pressure gases, the use of a co-catalyst that could cleave H_2 under ambient pressure and transfer the hydrides to the [Cy-PSiP]M^{II} (M = Pd, Pt) formate complexes may prove effective. Main group catalyst, such as frustrated Lewis pairs, are suited for such transformations as some combinations are able to cleave H_2 without inserting CO_2.[138]

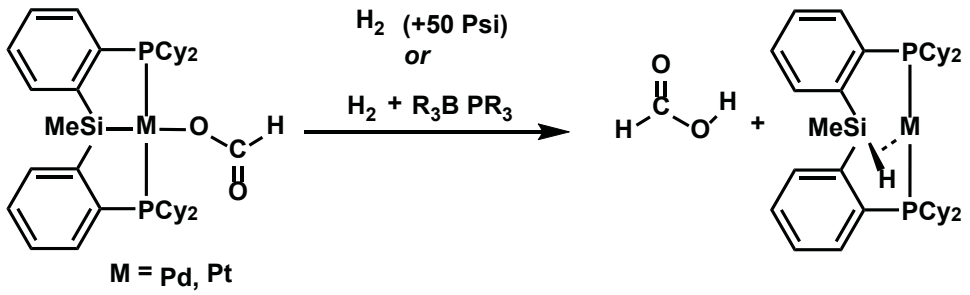

Scheme 8-2. Possible reduction of [Cy-PSiP]M(CO_2H) (M = Pd, Pt) using high pressure of hydrogen or 'pre-activation' using frustrated Lewis pairs.

Throughout such catalytic studies, it would be of interest to vary substitution at phosphorus, as well as at the silicon, in order to study the effects of such steric and electronic changes on catalytic activity, for example, the introduction of an aryl group at Si (rather then Me) could be particularly informative as both electron-withdrawing, and electron-donating aryl substituents could be utilized in order to study electronic effects. Ligand derivatives featuring *p*-tolyl, *p*-methoxyphenyl, *p*-dimethylaminophenyl and *p*-fluorophenyl should all be synthetically accessible.[139]

References

1. R. H. Crabtree, *The Organometallic Chemistry of the Transition Metals, Fourth Edition*, Wiley, Hoboken, 2005.

2. T. W. Dekleva and D. Forster, in *Advances in Catalysis*, eds. H. P. D.D. Eley and B. W. Paul, Academic Press, 1986, vol. Volume 34, pp. 81.

3. F. D. A. de Meijere, *Metal-Catalyzed Cross-Coupling Reactions*, Wiley-VCH, Weinheim, 2004.

4. W. S. Knowles, *Angew. Chem. Int. Ed.*, **2002**, *41*, 1998.

5. R. Noyori, *Angew. Chem. Int. Ed.*, **2002**, *41*, 2008.

6. K. B. Sharpless, *Angew. Chem. Int. Ed.*, **2002**, *41*, 2024.

7. (a) Y. Chauvin, *Angew. Chem. Int. Ed.*, **2006**, *45*, 3740; (b) R. R. Schrock, *Angew. Chem. Int. Ed.*, **2006**, *45*, 3748; (c) R. H. Grubbs, *Angew. Chem. Int. Ed.*, **2006**, *45*, 3760.

8. (a) C. C. C. Johansson Seechurn, M. O. Kitching, T. J. Colacot and V. Snieckus, *Angew. Chem. Int. Ed.*, **2012**, *51*, 5062; (b) A. Suzuki, *Angew. Chem. Int. Ed.*, **2011**, *50*, 6722; (c) E.-i. Negishi, *Angew. Chem. Int. Ed.*, **2011**, *50*, 6738.

9. (a) C. F. Bender and R. A. Widenhoefer, *J. Am. Chem. Soc.*, **2005**, *127*, 1070; (b) B. M. Cochran and F. E. Michael, *J. Am. Chem. Soc.*, **2008**, *130*, 2786; (c) M. A. Brook, *Silicon in Organic Organometallic and Polymer Chemistry*, Wiley, New York, 2000; (d) S. P. I. Ojima, Z. Rappoport, *The Chemistry of Organic Sillicon Compounds*, Wiley, Chichester UK, 1989; (e) J. A. Labinger and J. E. Bercaw, *Nature*, **2002**, *417*, 507; (f) U. Fekl and K. I. Goldberg, *Adv. Inorg. Chem.*, **2003**, *54*, 259; (g) M. Lersch and M. Tilset, *Chem. Rev.*, **2005**, *105*, 2471.

10. A. S. G. B. Shul'pin, *Activation and Catalytic Reactions of Saturated Hydrocarbons,* Kluwer, New York, 2000.

11. (a) J. C. Saam and J. L. Speier, *J. Am. Chem. Soc.*, **1958**, *80*, 4104; (b) J. L. Speier, J. A. Webster and G. H. Barnes, *J. Am. Chem. Soc.*, **1957**, *79*, 974.

12. (a) P. B. Hitchcock, M. F. Lappert and N. J. W. Warhurst, *Angew. Chem. Int. Ed.*, **1991**, *30*, 438; (b) G. Chandra, P. Y. Lo, P. B. Hitchcock and M. F. Lappert, *Organometallics*, **1987**, *6*, 191.

13. A. F. Littke and G. C. Fu, *Angew. Chem. Int. Ed.*, **2002**, *41*, 4176.

14. (a) B. Schlummer and U. Scholz, *Adv. Synth. Catal.*, **2004**, *346*, 1599; (b) S. L. B. A. R. Muci, *Top. Curr. Chem.*, **2002**, *219*, 131.

15. (a) R. J. Lundgren, B. D. Peters, P. G. Alsabeh and M. Stradiotto, *Angew. Chem. Int. Ed.*, **2010**, *49*, 4071; (b) G. D. Vo and J. F. Hartwig, *J. Am. Chem. Soc.*, **2009**, *131*, 11049.

16. (a) S. E. Denmark and C. R. Butler, *Chem. Commun.*, **2009**, 20; (b) M. R. Netherton and G. C. Fu, *Adv. Synth. Catal.*, **2004**, *346*, 1525.

17. (a) R. J. P. Corriu and J. P. Masse, *J. Chem. Soc., Chem. Commun.*, **1972**, 144a; (b) K. Tamao, K. Sumitani and M. Kumada, *J. Am. Chem. Soc.*, **1972**, *94*, 4374.

18. M. Peuckert and W. Keim, *Organometallics*, **1983**, *2*, 594.

19. D. Morales-Morales and C. M. Jensen, *The Chemistry of Pincer Compounds*, Elsevier, Oxford, 2007.

20. (a) W. Leis, H. A. Mayer and W. C. Kaska, *Coord. Chem. Rev.*, **2008**, *252*, 1787; (b) M. E. van der Boom and D. Milstein, *Chem. Rev.*, **2003**, *103*, 1759; (c) M. Albrecht and G. van Koten, *Angew. Chem., Int. Ed.*, **2001**, *40*, 3750; (d) L.-C. Liang, *Coord. Chem. Rev.*, **2006**, *250*, 1152.

21. C. M. Jensen, *Chem. Commun.*, **1999**, 2443.

22. C. Gunanathan, Y. Ben-David and D. Milstein, *Science*, **2007**, *317*, 790.

23. (a) N. A. Al-Salem, H. D. Empsall, R. Markham, B. L. Shaw and B. Weeks, *J. Chem. Soc., Dalton Trans.*, **1979**, 1972; (b) C. Crocker, R. J. Errington, R. Markham, C. J. Moulton, K. J. Odell and B. L. Shaw, *J. Am. Chem. Soc.*, **1980**, *102*, 4373; (c) C. J. Moulton and B. L. Shaw, *J. Chem. Soc., Dalton Trans.*, **1976**, 1020; (d) C. Crocker, R. J. Errington, W. S. McDonald, K. J. Odell, B. L. Shaw and R. J. Goodfellow, *J. Chem. Soc., Chem. Commun.*, **1979**, 498; (e) H. D. Empsall, E. M. Hyde, R. Markham, W. S. McDonald, M. C. Norton, B. L. Shaw and B. Weeks, *J. Chem. Soc., Chem. Commun.*, **1977**, 589.

24. Y. Segawa, M. Yamashita and K. Nozaki, *J. Am. Chem. Soc.*, **2009**, *131*, 9201.

25. (a) M. C. MacInnis, D. F. MacLean, R. J. Lundgren, R. McDonald and L. Turculet, *Organometallics*, **2007**, *26*, 6522; (b) D. F. MacLean, R. McDonald, M. J. Ferguson, A. J. Caddell and L. Turculet, *Chem. Commun.*, **2008**, 5146; (c) M. C. MacInnis, R. McDonald, M. J. Ferguson, S. Tobisch and L. Turculet, *J. Am. Chem. Soc.*, **2011**, *133*, 13622; (d) E. Morgan, D. F. MacLean, R. McDonald and L. Turculet, *J. Am. Chem. Soc.*, **2009**, *131*, 14234; (e) S. J. Mitton, R. McDonald and L. Turculet, *Organometallics*, **2009**, *28*, 5122; (f) S. J. Mitton, R. McDonald

and L. Turculet, *Angew. Chem., Int. Ed.*, **2009**, *48*, 8568; (g) S. J. Mitton, R. McDonald and L. Turculet, *Polyhedron*, **2013**, *52*, 750; (h) S. J. Mitton and L. Turculet, *Chem. Eur. J.*, **2012**, *18*, 15258.

26. B. A. Arndtsen, R. G. Bergman, T. A. Mobley and T. H. Peterson, *Acc. Chem. Res.*, **1995**, *28*, 154.

27. S. B. Harkins and J. C. Peters, *Organometallics*, **2002**, *21*, 1753.

28. L.-C. Liang, J.-M. Lin and W.-Y. Lee, *Chem. Commun.*, **2005**, 2462.

29. J. C. DeMott, N. Bhuvanesh and O. V. Ozerov, *Chem. Sci.*, **2013**, *4*, 642.

30. R. H. Holm, *Chem. Rev.*, **1987**, *87*, 1401.

31. C. E. MacBeth, A. P. Golombek, V. G. Young, C. Yang, K. Kuczera, M. P. Hendrich and A. S. Borovik, *Science*, **2000**, *289*, 938.

32. E. Spaltenstein, R. R. Conry, S. C. Critchlow and J. M. Mayer, *J. Am. Chem. Soc.*, **1989**, *111*, 8741.

33. (a) R. Cao, T. M. Anderson, P. M. B. Piccoli, A. J. Schultz, T. F. Koetzle, Y. V. Geletii, E. Slonkina, B. Hedman, K. O. Hodgson, K. I. Hardcastle, X. Fang, M. L. Kirk, S. Knottenbelt, P. Kögerler, D. G. Musaev, K. Morokuma, M. Takahashi and C. L. Hill, *J. Am. Chem. Soc.*, **2007**, *129*, 11118; (b) T. M. Anderson, W. A. Neiwert, M. L. Kirk, P. M. B. Piccoli, A. J. Schultz, T. F. Koetzle, D. G. Musaev, K. Morokuma, R. Cao and C. L. Hill, *Science*, **2004**, *306*, 2074.

34. (a) C. Limberg, *Angew. Chem. Int. Ed.*, **2009**, *48*, 2270; (b) E. Poverenov, I. Efremenko, A. I. Frenkel, Y. Ben-David, L. J. W. Shimon, G. Leitus, L. Konstantinovski, J. M. L. Martin and D. Milstein, *Nature*, **2008**, *455*, 1093.

35. (a) N. S. Lewis and D. G. Nocera, *Proceedings of the National Academy of Sciences*, **2006**, *103*, 15729; (b) J. H. Alstrum-Acevedo, M. K. Brennaman and T. J. Meyer, *Inorg. Chem.*, **2005**, *44*, 6802; (c) M. Yagi and M. Kaneko, *Chem. Rev.*, **2000**, *101*, 21; (d) W. Rüttinger and G. C. Dismukes, *Chem. Rev.*, **1997**, *97*, 1; (e) J. K. Hurst, *Coord. Chem. Rev.*, **2005**, *249*, 313; (f) X. Yang and M.-H. Baik, *J. Am. Chem. Soc.*, **2006**, *128*, 7476.

36. V. V. Rostovtsev, J. A. Labinger, J. E. Bercaw, T. L. Lasseter and K. I. Goldberg, *Organometallics*, **1998**, *17*, 4530.

37. (a) L.-C. Liang, J.-M. Lin and C.-H. Hung, *Organometallics*, **2003**, *22*, 3007; (b) L.-C. Liang, P.-S. Chien, J.-M. Lin, M.-H. Huang, Y.-L. Huang and J.-H. Liao, *Organometallics*, **2006**, *25*, 1399.

38. L.-C. Liang, P.-S. Chien and Y.-L. Huang, *J. Am. Chem. Soc.*, **2006**, *128*, 15562.

39. (a) T. E. Müller and M. Beller, *Chem. Rev.*, **1998**, *98*, 675; (b) F. Pohlki and S. Doye, *Chem. Soc. Rev.*, **2003**, *32*, 104; (c) F. Alonso, I. P. Beletskaya and M. Yus, *Chem. Rev.*, **2004**, *104*, 3079; (d) R. Severin and S. Doye, *Chem. Soc. Rev.*, **2007**, *36*, 1407; (e) J. F. Hartwig, *Nature*, **2008**, *455*, 314; (f) T. E. Müller, K. C. Hultzsch, M. Yus, F. Foubelo and M. Tada, *Chem. Rev.*, **2008**, *108*, 3795.

40. S. D. Gray, K. J. Weller, M. A. Bruck, P. M. Briggs and D. E. Wigley, *J. Am. Chem. Soc.*, **1995**, *117*, 10678.

41. (a) A. C. Sykes, P. White and M. Brookhart, *Organometallics*, **2006**, *25*, 1664; (b) J. Zhao, A. S. Goldman and J. F. Hartwig, *Science*, **2005**, *307*, 1080; (c) M. Kanzelberger, X. Zhang, T. J. Emge, A. S. Goldman, J. Zhao, C. Incarvito and J. F. Hartwig, *J. Am. Chem. Soc.*, **2003**, *125*, 13644; (d) R. Koelliker and D. Milstein, *Angew. Chem. Int. Ed.*, **1991**, *30*, 707; (e) A. L. Casalnuovo, J. C. Calabrese and D. Milstein, *Inorg. Chem.*, **1987**, *26*, 971.

42. (a) M. Gandelman and D. Milstein, *Chem. Commun.*, **2000**, 1603; (b) Y. W. Chan, M. W. Renner and A. L. Balch, *Organometallics*, **1983**, *2*, 1888; (c) J. B. Bonanno, T. P. Henry, D. R. Neithamer, P. T. Wolczanski and E. B. Lobkovsky, *J. Am. Chem. Soc.*, **1996**, *118*, 5132; (d) M. Tayebani, S. Gambarotta and G. Yap, *Organometallics*, **1998**, *17*, 3639; (e) M. Torrent, D. G. Musaev and K. Morokuma, *Organometallics*, **2000**, *19*, 4402; (f) B. L. Lin, C. R. Clough and G. L. Hillhouse, *J. Am. Chem. Soc.*, **2002**, *124*, 2890.

43. (a) O. V. Ozerov, C. Guo, L. Fan and B. M. Foxman, *Organometallics*, **2004**, *23*, 5573; (b) L. Fan, L. Yang, C. Guo, B. M. Foxman and O. V. Ozerov, *Organometallics*, **2004**, *23*, 4778; (c) L. Fan, B. M. Foxman and O. V. Ozerov, *Organometallics*, **2004**, *23*, 326.

44. T. T. Wenzel, in *Stud. Surf. Sci. Catal.*, ed. L. I. Simándi, Elsevier, 1991, vol. Volume 66, pp. 545.

45. O. V. Ozerov, *Chem. Soc. Rev.*, **2009**, *38*, 83.

46. (a) G. V. Goeden and K. G. Caulton, *J. Am. Chem. Soc.*, **1981**, *103*, 7354; (b) C. Deutsch, N. Krause and B. H. Lipshutz, *Chem. Rev.*, **2008**, *108*, 2916.

47. P. G. Jessop, T. Ikariya and R. Noyori, *Chem. Rev.*, **1995**, *95*, 259.

48. (a) G. R. Fulmer, R. P. Muller, R. A. Kemp and K. I. Goldberg, *J. Am. Chem. Soc.*, **2009**, *131*, 1346; (b) G. R. Fulmer, A. N. Herndon, W. Kaminsky, R. A. Kemp and K. I. Goldberg, *J. Am. Chem. Soc.*, **2011**, *133*, 17713.

49. R. Gerber, T. Fox and C. M. Frech, *Chem. Eur. J.*, **2010**, *16*, 6771.

50. (a) X. Zhou and S. R. Stobart, *Organometallics*, **2001**, *20*, 1898; (b) R. D. Brost, G. C. Bruce, F. L. Joslin and S. R. Stobart, *Organometallics*, **1997**, *16*, 5669; (c) R. A. Gossage, G. D. McLennan and S. R. Stobart, *Inorg. Chem.*, **1996**, *35*, 1729; (d) M. J. Auburn, R. D. Holmes-Smith, S. R. Stobart, P. K. Bakshi and T. S. Cameron, *Organometallics*, **1996**, *15*, 3032; (e) F. L. Joslin and S. R. Stobart, *J. Chem. Soc., Chem. Commun.*, **1989**, 504; (f) M. J. Auburn and S. R. Stobart, *Inorg. Chem.*, **1985**, *24*, 318.

51. P. Sangtrirutnugul and T. D. Tilley, *Organometallics*, **2008**, *27*, 2223.

52. (a) S. M. Kloek and K. I. Goldberg, *J. Am. Chem. Soc.*, **2007**, *129*, 3460; (b) U. Fekl, W. Kaminsky and K. I. Goldberg, *J. Am. Chem. Soc.*, **2001**, *123*, 6423; (c) S. Reinartz, P. S. White, M. Brookhart and J. L. Templeton, *J. Am. Chem. Soc.*, **2001**, *123*, 6425.

53. J. Takaya and N. Iwasawa, *J. Am. Chem. Soc.*, **2008**, *130*, 15254.

54. (a) J. Takaya, N. Kirai and N. Iwasawa, *J. Am. Chem. Soc.*, **2011**, *133*, 12980; (b) J. Takaya, K. Sasano and N. Iwasawa, *Org. Lett.*, **2011**, *13*, 1698.

55. B. Qian, D. L. Ward and M. R. Smith, III, *Organometallics*, **1998**, *17*, 3070.

56. X. Yang, C. L. Stern and T. J. Marks, *J. Am. Chem. Soc.*, **1994**, *116*, 10015.

57. (a) M. G. Thorn, Z. C. Etheridge, P. E. Fanwick and I. P. Rothwell, *Organometallics*, **1998**, *17*, 3636; (b) F. Guerin, J. C. Stewart, C. Beddie and D. W. Stephan, *Organometallics*, **2000**, *19*, 2994; (c) J. D. Scollard, D. H. McConville and S. J. Rettig, *Organometallics*, **1997**, *16*, 1810; (d) T. J. Woodman, M. Bochmann and M. Thornton-Pett, *Chem. Commun.*, **2001**, 329; (e) R. A. Metcalfe, D. I. Kreller, J. Tian, H. Kim, N. J. Taylor, J. F. Corrigan and S. Collins, *Organometallics*, **2002**, *21*, 1719.

58. G. K. Barlow, J. D. Boyle, N. A. Cooley, T. Ghaffar and D. F. Wass, *Organometallics*, **2000**, *19*, 1470.

59. J. Y. Corey and J. Braddock-Wilking, *Chem. Rev.*, **1999**, *99*, 175.

60. (a) G. J. Kubas, *Metal Dihydrogen and σ-Bond Complexes*, Kluwer Academic, New York, 2001; (b) G. I. Nikonov, *Adv. Organomet. Chem.*, **2005**, *53*, 217; (c) S. Lachaize and S. Sabo-Etienne, *Eur. J. Inorg. Chem.*, **2006**, 2115; (d) Z. Lin, *Chem. Soc. Rev.*, **2002**, *31*, 239.

61. (a) S. R. Dubberley, S. K. Ignatov, N. H. Rees, A. G. Razuvaev, P. Mountford and G. I. Nikonov, *J. Am. Chem. Soc.*, **2003**, *125*, 642; (b) S. K. Ignatov, N. H. Rees, B. R. Tyrrell, S. R. Dubberley, A. G. Razuvaev, P. Mountford and G. I. Nikonov, *Chem. Eur. J.*, **2004**, *10*, 4991.

62. (a) Y. Levchinsky, N. P. Rath and J. Braddock-Wilking, *Organometallics*, **1999**, *18*, 2583; (b) J. Braddock-Wilking, Y. Levchinsky and N. P. Rath, *Organometallics*, **2000**, *19*, 5500; (c) J. Braddock-Wilking, J. Y. Corey, K. A. Trankler, H. Xu, L. M. French, N. Praingam, C. White and N. P. Rath, *Organometallics*, **2006**, *25*, 2859; (d) M. Ciriano, M. Green, J. A. K. Howard, J. Proud, J. L. Spencer, F. G. A. Stone and C. A. Tsipis, *J. Chem. Soc., Dalton Trans.*, **1978**, 801; (e) L. M. Sanow, M. Chai, D. B. McConnville, K. J. Galat, R. S. Simons, P. L. Rinaldi, W. J. Youngs and C. A. Tessier, *Organometallics*, **2000**, *19*, 192.

63. J. Takaya and N. Iwasawa, *Organometallics*, **2009**, *28*, 6636.

64. U. Schubert, *Adv. Organomet. Chem.*, **1990**, *30*, 151.

65. Y. Obora, Y. Tsuji, K. Nishiyama, M. Ebihara and T. Kawamura, *J. Am. Chem. Soc.*, **1996**, *118*, 10922.

66. Y.-J. Kim, J.-I. Park, S.-C. Lee, K. Osakada, M. Tanabe, J.-C. Choi, T.-a. Koizumi and T. Yamamoto, *Organometallics*, **1999**, *18*, 1349.

67. (a) H. Yamashita, T. Hayashi, T. Kobayashi, M. Tanaka and M. Goto, *J. Am. Chem. Soc.*, **1988**, *110*, 4417; (b) B. J. Rappoli, T. S. Janik, M. R. Churchill, J. S. Thompson and J. D. Atwood, *Organometallics*, **1988**, *7*, 1939; (c) A. A. Zlota, F. Frolow and D. Milstein, *J. Chem. Soc., Chem. Commun.*, **1989**, 1826; (d) C. J. Levy, J. J. Vittal and R. J. Puddephatt, *Organometallics*, **1996**, *15*, 2108; (e) C. J. Levy, R. J. Puddephatt and J. J. Vittal, *Organometallics*, **1994**, *13*, 1559; (f) C. J. Levy and R. J. Puddephatt, *J. Am. Chem. Soc.*, **1997**, *119*, 10127; (g) Y. Tanaka, H. Yamashita, S. Shimada and M. Tanaka, *Organometallics*, **1997**, *16*, 3246; (h) F. Stohr, D. Sturmayr, G. Kickelbick and U. Schubert, *Eur. J. Inorg. Chem.*, **2002**, 2305; (i) H. Yoo, P. J. Carroll and D. H. Berry, *J. Am. Chem. Soc.*, **2006**, *128*, 6038; (j) S. Gatard, C.-H. Chen, B. M. Foxman and O. V. Ozerov, *Organometallics*, **2008**, *27*, 6257.

68. P. Hofmann, H. Heiss, P. Neiteler, G. Mueller and J. Lachmann, *Angew. Chem.*, **1990**, *102*, 935.

69. C. M. Ong, T. J. Burchell and R. J. Puddephatt, *Organometallics*, **2004**, *23*, 1493.

70. M. Safa, M. C. Jennings and R. J. Puddephatt, *Organometallics*, **2012**, *31*, 3539.

71. A. F. Heyduk, J. A. Labinger and J. E. Bercaw, *J. Am. Chem. Soc.*, **2003**, *125*, 6366.

72. (a) M. P. Brown, R. J. Puddephatt and C. E. E. Upton, *J. Chem. Soc., Dalton Trans.*, **1974**, 2457; (b) K. I. Goldberg, J. Yan and E. M. Breitung, *J. Am. Chem. Soc.*, **1995**, *117*, 6889; (c) D. M. Crumpton-Bregel and K. I. Goldberg, *J. Am. Chem. Soc.*, **2003**, *125*, 9442.

73. (a) P. Steenwinkel, R. A. Gossage, T. Maunula, D. M. Grove and G. van Koten, *Chem. Eur. J.*, **1998**, *4*, 763; (b) K. Temple, A. J. Lough, J. B. Sheridan and I. Manners, *J. Chem. Soc., Dalton Trans.*, **1998**, 2799; (c) H. Gilges and U. Schubert, *Organometallics*, **1998**, *17*, 4760; (d) N. Mintcheva, Y. Nishihara, M. Tanabe, K. Hirabayashi, A. Mori and K. Osakada, *Organometallics*, **2001**, *20*, 1243.

74. (a) D. E. Hendriksen, A. A. Oswald, G. B. Ansell, S. Leta and R. V. Kastrup, *Organometallics*, **1989**, *8*, 1153; (b) S. K. Thomson and G. B. Young, *Organometallics*, **1989**, *8*, 2068; (c) P. Burger and R. G. Bergman, *J. Am. Chem. Soc.*, **1993**, *115*, 10462.

75. (a) B. L. Edelbach, R. J. Lachicotte and W. D. Jones, *Organometallics*, **1999**, *18*, 4660; (b) E. E. Korshin, G. Leitus, L. J. W. Shimon, L. Konstantinovski and D. Milstein, *Inorg. Chem.*, **2008**, *47*, 7177.

76. W. Lin, S. R. Wilson and G. S. Girolami, *Organometallics*, **1994**, *13*, 2309.

77. A. Rufinska, R. Goddard, C. Weidenthaler, M. Buehl and K.-R. Poerschke, *Organometallics*, **2006**, *25*, 2308.

78. (a) J. Hansen, L. Nazarenko, R. Ruedy, M. Sato, J. Willis, G. A. Del, D. Koch, A. Lacis, K. Lo, S. Menon, T. Novakov, J. Perlwitz, G. Russell, G. A. Schmidt and N. Tausnev, *Science*, **2005**, *308*, 1431; (b) A. G. G. A. Olah, G. K. Surya Prakash, *Beyond Oil and Gas: The Methanol Economyy*, Wiley-VCH, Weinheim, 2006.

79. (a) R. Lal, *Energy Environ. Sci.*, **2008**, *1*, 86; (b) D. M. D'Alessandro, B. Smit and J. R. Long, *Angew. Chem., Int. Ed.*, **2010**, *49*, 6058; (c) C. M. White, B. R. Strazisar, E. J. Granite, J. S. Hoffman and H. W. Pennline, *J. Air Waste Manage. Assoc.*, **2003**, *53*, 645; (d) K. Z. House, C. F. Harvey, M. J. Aziz and D. P. Schrag, *Energy Environ. Sci.*, **2009**, *2*, 193.

80. (a) Z. Jiang, T. Xiao, V. L. Kuznetsov and P. P. Edwards, *Philos. Trans. R. Soc., A*, **2010**, *368*, 3343; (b) G. A. Olah, G. K. S. Prakash and A. Goeppert, *J. Am. Chem. Soc.*, **2011**, *133*, 12881; (c) G. Centi and S. Perathoner, *Catal. Today*, **2009**, *148*, 191; (d) H. Arakawa, M. Aresta, J. N. Armor, M. A. Barteau, E. J. Beckman, A. T. Bell, J. E. Bercaw, C. Creutz, E. Dinjus, D. A. Dixon, K. Domen,

D. L. DuBois, J. Eckert, E. Fujita, D. H. Gibson, W. A. Goddard, D. W. Goodman, J. Keller, G. J. Kubas, H. H. Kung, J. E. Lyons, L. E. Manzer, T. J. Marks, K. Morokuma, K. M. Nicholas, R. Periana, L. Que, J. Rostrup-Nielson, W. M. H. Sachtler, L. D. Schmidt, A. Sen, G. A. Somorjai, P. C. Stair, B. R. Stults and W. Tumas, *Chem. Rev.*, **2001**, *101*, 953.

81. (a) M. Aresta and A. Dibenedetto, *Dalton Trans*, **2007**, 2975; (b) T. Sakakura, J.-C. Choi and H. Yasuda, *Chem. Rev.*, **2007**, *107*, 2365; (c) M. Cokoja, C. Bruckmeier, B. Rieger, W. A. Herrmann and F. E. Kuehn, *Angew. Chem., Int. Ed.*, **2011**, *50*, 8510.

82. (a) W. Leitner, *Angew. Chem., Int. Ed. Engl.*, **1995**, *34*, 2207; (b) P. G. Jessop, F. Joo and C.-C. Tai, *Coord. Chem. Rev.*, **2004**, *248*, 2425; (c) R. Tanaka, M. Yamashita and K. Nozaki, *J. Am. Chem. Soc.*, **2009**, *131*, 14168; (d) C. Federsel, R. Jackstell and M. Beller, *Angew. Chem., Int. Ed.*, **2010**, *49*, 6254; (e) T. Schaub and R. A. Paciello, *Angew. Chem., Int. Ed.*, **2011**, *50*, 7278; (f) R. Langer, Y. Diskin-Posner, G. Leitus, L. J. W. Shimon, Y. Ben-David and D. Milstein, *Angew. Chem., Int. Ed.*, **2011**, *50*, 9948; (g) C. Federsel, A. Boddien, R. Jackstell, R. Jennerjahn, P. J. Dyson, R. Scopelliti, G. Laurenczy and M. Beller, *Angew. Chem., Int. Ed.*, **2010**, *49*, 9777.

83. (a) U. Kestel, G. Froehlich, D. Borgmann and G. Wedler, *Chem. Eng. Technol.*, **1994**, *17*, 390; (b) A. Baiker, *Appl. Organomet. Chem.*, **2000**, *14*, 751; (c) H. Sakurai and M. Haruta, *Appl. Catal., A*, **1995**, *127*, 93; (d) J. Ma, N. Sun, X. Zhang, N. Zhao, F. Xiao, W. Wei and Y. Sun, *Catal. Today*, **2009**, *148*, 221; (e) I. A. Fisher and A. T. Bell, *J. Catal.*, **1997**, *172*, 222; (f) L. C. Grabow and M. Mavrikakis, *ACS Catal.*, **2011**, *1*, 365.

84. (a) C. Finn, S. Schnittger, L. J. Yellowlees and J. B. Love, *Chem. Commun.*, **2012**, *48*, 1392; (b) E. E. Benson, C. P. Kubiak, A. J. Sathrum and J. M. Smieja, *Chem. Soc. Rev.*, **2009**, *38*, 89; (c) J.-M. Saveant, *Chem. Rev.*, **2008**, *108*, 2348.

85. (a) T. Inoue, A. Fujishima, S. Konishi and K. Honda, *Nature*, **1979**, *277*, 637; (b) S. C. Roy, O. K. Varghese, M. Paulose and C. A. Grimes, *ACS Nano*, **2010**, *4*, 1259; (c) A. J. Morris, G. J. Meyer and E. Fujita, *Acc. Chem. Res.*, **2009**, *42*, 1983.

86. (a) B. Denise and R. P. A. Sneeden, *J. Organomet. Chem.*, **1981**, *221*, 111; (b) K. Tominaga, Y. Sasaki, M. Kawai, T. Watanabe and M. Saito, *J. Chem. Soc., Chem. Commun.*, **1993**, 629; (c) L. Vaska, S. Schreiner, R. A. Felty and J. Y. Yu, *J. Mol. Catal.*, **1989**, *52*, L11; (d) C. A. Huff and M. S. Sanford, *J. Am. Chem. Soc.*, **2011**, *133*, 18122; (e) S. Wesselbaum, S. T. vom, J. Klankermayer and W. Leitner, *Angew. Chem., Int. Ed.*, **2012**, *51*, 7499.

87. E. Balaraman, C. Gunanathan, J. Zhang, L. J. W. Shimon and D. Milstein, *Nat. Chem.*, **2011**, *3*, 609.

88. (a) G. Menard and D. W. Stephan, *J. Am. Chem. Soc.*, **2010**, *132*, 1796; (b) A. Schäfer, W. Saak, D. Haase and T. Müller, *Angew. Chem. Int. Ed.*, **2012**, *51*, 2981; (c) A. E. Ashley, A. L. Thompson and D. O'Hare, *Angew. Chem., Int. Ed.*, **2009**, *48*, 9839.

89. (a) S. Chakraborty, J. Zhang, J. A. Krause and H. Guan, *J. Am. Chem. Soc.*, **2010**, *132*, 8872; (b) F. Huang, C. Zhang, J. Jiang, Z.-X. Wang and H. Guan, *Inorg. Chem.*, **2011**, *50*, 3816; (c) S. Chakraborty, Y. J. Patel, J. A. Krause and H. Guan, *Polyhedron*, **2012**, *32*, 30.

90. (a) T. C. Eisenschmid and R. Eisenberg, *Organometallics*, **1989**, *8*, 1822; (b) S. N. Riduan, Y. Zhang and J. Y. Ying, *Angew. Chem., Int. Ed.*, **2009**, *48*, 3322; (c) F. Huang, G. Lu, L. Zhao, H. Li and Z.-X. Wang, *J. Am. Chem. Soc.*, **2010**, *132*, 12388.

91. (a) T. Matsuo and H. Kawaguchi, *J. Am. Chem. Soc.*, **2006**, *128*, 12362; (b) S. Park, D. Bezier and M. Brookhart, *J. Am. Chem. Soc.*, **2012**, *134*, 11404; (c) A. Berkefeld, W. E. Piers and M. Parvez, *J. Am. Chem. Soc.*, **2010**, *132*, 10660; (d) M. Khandelwal and R. J. Wehmschulte, *Angew. Chem., Int. Ed.*, **2012**, *51*, 7323.

92. A. J. M. Miller, J. A. Labinger and J. E. Bercaw, *Organometallics*, **2011**, *30*, 4308.

93. (a) D. J. Parks and W. E. Piers, *J. Am. Chem. Soc.*, **1996**, *118*, 9440; (b) D. J. Parks, J. M. Blackwell and W. E. Piers, *J. Org. Chem.*, **2000**, *65*, 3090; (c) V. Gevorgyan, M. Rubin, S. Benson, J.-X. Liu and Y. Yamamoto, *J. Org. Chem.*, **2000**, *65*, 6179; (d) D. B. Thompson and M. A. Brook, *J. Am. Chem. Soc.*, **2008**, *130*, 32.

94. (a) H. E. Bryndza and W. Tam, *Chem. Rev.*, **1988**, *88*, 1163; (b) J. P. Wolfe, S. Wagaw, J.-F. Marcoux and S. L. Buchwald, *Acc. Chem. Res.*, **1998**, *31*, 805; (c) D. M. Roundhill, *Catal. Today*, **1997**, *37*, 155.

95. (a) R. G. Bergman, *Polyhedron*, **1995**, *14*, 3227; (b) J. R. Fulton, A. W. Holland, D. J. Fox and R. G. Bergman, *Acc. Chem. Res.*, **2001**, *35*, 44; (c) P. L. Holland, R. A. Andersen and R. G. Bergman, *Comments Inorg. Chem.*, **1999**, *21*, 115.

96. (a) T. B. Gunnoe, *Eur. J. Inorg. Chem.*, **2007**, *2007*, 1185; (b) J. E. Bercaw, N. Hazari, J. A. Labinger and P. F. Oblad, *Angew. Chem. Int. Ed.*, **2008**, *47*, 9941.

97. (a) J. Oxgaard, W. J. Tenn, R. J. Nielsen, R. A. Periana and W. A. Goddard, *Organometallics*, **2007**, *26*, 1565; (b) W. J. Tenn, K. J. H. Young, G. Bhalla, J.

Oxgaard, W. A. Goddard and R. A. Periana, *J. Am. Chem. Soc.*, **2005**, *127*, 14172; (c) W. J. Tenn, K. J. H. Young, J. Oxgaard, R. J. Nielsen, W. A. Goddard and R. A. Periana, *Organometallics*, **2006**, *25*, 5173.

98. (a) Y. Feng, M. Lail, K. A. Barakat, T. R. Cundari, T. B. Gunnoe and J. L. Petersen, *J. Am. Chem. Soc.*, **2005**, *127*, 14174; (b) Y. Feng, M. Lail, N. A. Foley, T. B. Gunnoe, K. A. Barakat, T. R. Cundari and J. L. Petersen, *J. Am. Chem. Soc.*, **2006**, *128*, 7982.

99. S. M. Kloek, D. M. Heinekey and K. I. Goldberg, *Angew. Chem. Int. Ed.*, **2007**, *46*, 4736.

100. (a) R. C. Mehrotra, S. K. Agarwal and Y. P. Singh, *Coord. Chem. Rev.*, **1985**, *68*, 101; (b) H. W. Roesky, S. Singh, K. K. M. Yusuff, J. A. Maguire and N. S. Hosmane, *Chem. Rev.*, **2006**, *106*, 3813; (c) A. Singh, U. Anandhi, M. A. Cinellu and P. R. Sharp, *Dalton Trans.*, **2008**, 2314; (d) U. Anandhi and P. R. Sharp, *Inorg. Chem.*, **2004**, *43*, 6780; (e) U. Anandhi, T. Holbert, D. Lueng and P. R. Sharp, *Inorg. Chem.*, **2003**, *42*, 1282.

101. J. R. Webb, C. Munro-Leighton, A. W. Pierpont, J. T. Gurkin, T. B. Gunnoe, T. R. Cundari, M. Sabat, J. L. Petersen and P. D. Boyle, *Inorg. Chem.*, **2011**, *50*, 4195.

102. (a) T. L. Lohr, W. E. Piers and M. Parvez, *Inorg. Chem.*, **2012**, *51*, 4900; (b) B. F. Straub, F. Rominger and P. Hofmann, *Inorg. Chem. Commun.*, **2000**, *3*, 214; (c) G. S. Hill, L. Manojlovic-Muir, K. W. Muir and R. J. Puddephatt, *Organometallics*, **1997**, *16*, 525; (d) A. Klein, K.-W. Klinkhammer and T. Scheiring, *J. Organomet. Chem.*, **1999**, *592*, 128.

103. (a) M. A. Bennett, G. B. Robertson, P. O. Whimp and T. Yoshida, *J. Am. Chem. Soc.*, **1973**, *95*, 3028; (b) J. F. Britten, B. Lippert, C. J. L. Lock and P. Pilon, *Inorg. Chem.*, **1982**, *21*, 1936.

104. (a) T. G. Appleton and M. A. Bennett, *Inorg. Chem.*, **1978**, *17*, 738; (b) R. Ross, R. A. Michelin, R. Bataillard and R. Roulet, *J. Organomet. Chem.*, **1978**, *161*, 75; (c) R. A. Michelin, M. Napoli and R. Ros, *J. Organomet. Chem.*, **1979**, *175*, 239; (d) D. P. Arnold and M. A. Bennett, *J. Organomet. Chem.*, **1980**, *199*, 119; (e) M. A. Cairns, K. R. Dixon and M. A. R. Smith, *J. Organomet. Chem.*, **1977**, *135*, C33; (f) T. Yoshida, T. Okano and S. Otsuka, *J. Chem. Soc., Dalton Trans.*, **1976**, 993.

105. W. S. Matthews, J. E. Bares, J. E. Bartmess, F. G. Bordwell, F. J. Cornforth, G. E. Drucker, Z. Margolin, R. J. McCallum, G. J. McCollum and N. R. Vanier, *J. Am. Chem. Soc.*, **1975**, *97*, 7006.

106. (a) U. Siemeling, K. Bausch, H. Fink, C. Bruhn, M. Baldus, B. Angerstein, R. Plessow and A. Brockhinke, *Dalton Transactions*, **2005**, 2365; (b) S.-C. Chan, M. C. W. Chan, Y. Wang, C.-M. Che, K.-K. Cheung and N. Zhu, *Chem. Eur. J.*, **2001**, *7*, 4180; (c) M. Hissler, W. B. Connick, D. K. Geiger, J. E. McGarrah, D. Lipa, R. J. Lachicotte and R. Eisenberg, *Inorg. Chem.*, **2000**, *39*, 447; (d) W. Lu, M. C. W. Chan, N. Zhu, C.-M. Che, Z. He and K.-Y. Wong, *Chem. Eur. J.*, **2003**, *9*, 6155.

107. R. J. Keaton, J. M. Blacquiere and R. T. Baker, *J. Am. Chem. Soc.*, **2007**, *129*, 1844.

108. C. A. Sandoval, T. Ohkuma, K. Muñiz and R. Noyori, *J. Am. Chem. Soc.*, **2003**, *125*, 13490.

109. (a) A. Milet, A. Dedieu, G. Kapteijn and G. van Koten, *Inorg. Chem.*, **1997**, *36*, 3223; (b) F. Hutschka, A. Dedieu, M. Eichberger, R. Fornika and W. Leitner, *J. Am. Chem. Soc.*, **1997**, *119*, 4432; (c) F. Hutschka, A. Dedieu and W. Leitner, *Angew. Chem. Int. Ed.*, **1995**, *34*, 1742; (d) T. R. Cundari, T. V. Grimes and T. B. Gunnoe, *J. Am. Chem. Soc.*, **2007**, *129*, 13172.

110. P. L. Holland, R. A. Andersen, R. G. Bergman, J. Huang and S. P. Nolan, *J. Am. Chem. Soc.*, **1997**, *119*, 12800.

111. (a) X. Yu, L. A. Morton and Z.-L. Xue, *Organometallics*, **2004**, *23*, 2210; (b) J. Y. Corey, *Chem. Rev.*, **2011**, *111*, 863; (c) N. P. Mankad, D. S. Laitar and J. P. Sadighi, *Organometallics*, **2004**, *23*, 3369; (d) H. Kaur, F. K. Zinn, E. D. Stevens and S. P. Nolan, *Organometallics*, **2004**, *23*, 1157; (e) J. B. Diminnie, X. Liu, H. Cai, Z. Wu, J. R. Blanton, T. Chen, A. A. Tuinman, K. T. Quisenberry, C. E. Vallet, R. A. Zuhr, D. B. Beach, Z. Peng, Y.-D. Wu, T. E. Concolino, A. L. Rheingold and Z. Xue, *Pure Appl. Chem.*, **2001**, *73*, 331.

112. (a) G. Korogodsky, M. Bendikov, D. Bravo-Zhivotovskii and Y. Apeloig, *Organometallics*, **2002**, *21*, 3157; (b) E. Buncel and T. K. Venkatachalam, *J. Organomet. Chem.*, **2000**, *604*, 208.

113. (a) J. F. Hartwig, *Inorg. Chem.*, **2007**, *46*, 1936; (b) D. S. Glueck, *Dalton Trans.*, **2008**, 5276.

114. D. S. Glueck, *Synlett*, **2007**, *2007*, 2627.

115. (a) J. R. Fulton, A. W. Holland, D. J. Fox and R. G. Bergman, *Acc. Chem. Res.*, **2002**, *35*, 44; (b) P. R. Sharp, *Dalton Trans.*, **2000**, 2647.

116. S. L. Marquard, D. C. Rosenfeld and J. F. Hartwig, *Angew. Chem. Int. Ed.*, **2010**, *49*, 793.

117. L.-C. Liang, C.-W. Li, P.-Y. Lee, C.-H. Chang and H. Man Lee, *Dalton Trans.*, **2011**, *40*, 9004.

118. (a) R. Waterman, *Dalton Trans.*, **2009**, *0*, 18; (b) P. Mastrorilli, *Eur. J. Inorg. Chem.*, **2008**, *2008*, 4835.

119. F. Maassarani, M. F. Davidson, I. C. M. Wehman-Ooyevaar, D. M. Grove, M. A. van Koten, W. J. J. Smeets, A. L. Spek and G. van Koten, *Inorg. Chim. Acta*, **1995**, *235*, 327.

120. R. Melenkivitz, D. J. Mindiola and G. L. Hillhouse, *J. Am. Chem. Soc.*, **2002**, *124*, 3846.

121. R. L. Cowan and W. C. Trogler, *J. Am. Chem. Soc.*, **1989**, *111*, 4750.

122. D. P. Klein, J. C. Hayes and R. G. Bergman, *J. Am. Chem. Soc.*, **1988**, *110*, 3704.

123. D. Rais and R. G. Bergman, *Chem. Eur. J.*, **2004**, *10*, 3970.

124. L. Rosenberg, *Coord. Chem. Rev.*, **2012**, *256*, 606.

125. C. Scriban, D. K. Wicht, D. S. Glueck, L. N. Zakharov, J. A. Golen and A. L. Rheingold, *Organometallics*, **2006**, *25*, 3370.

126. D. K. Wicht, S. N. Paisner, B. M. Lew, D. S. Glueck, G. P. A. Yap, L. M. Liable-Sands, A. L. Rheingold, C. M. Haar and S. P. Nolan, *Organometallics*, **1998**, *17*, 652.

127. M. A. Zhuravel, J. R. Moncarz, D. S. Glueck, K.-C. Lam and A. L. Rheingold, *Organometallics*, **2000**, *19*, 3447.

128. M. A. Zhuravel, D. S. Glueck, L. N. Zakharov and A. L. Rheingold, *Organometallics*, **2002**, *21*, 3208.

129. M. E. van der Boom and D. Milstein, *Chem. Rev.*, **2003**, *103*, 1759.

130. (a) R. Gerber, O. Blacque and C. M. Frech, *Dalton Trans.*, **2011**, *40*, 8996; (b) M. Mazzeo, M. Strianese, O. Kuehl and J. C. Peters, *Dalton Trans.*, **2011**, *40*, 9026.

131. (a) C. Gunanathan and D. Milstein, *Acc. Chem. Res.*, **2011**, *44*, 588; (b) E. Poverenov, M. Gandelman, L. J. W. Shimon, H. Rozenberg, Y. Ben-David and D. Milstein, *Chem. Eur. J.*, **2004**, *10*, 4673.

132. C. S. Slone, D. A. Weinberger and C. A. Mirkin, *Prog. Inorg. Chem.*, **1999**, *48*, 233.

133. V. K. Dioumaev, K. Ploessl, P. J. Carroll and D. H. Berry, *Organometallics*, **2000**, *19*, 3374.

134. H. Fang, Y.-K. Choe, Y. Li and S. Shimada, *Chem. Asian J.*, **2011**, *6*, 2512.

135. (a) J. L. Kiplinger, T. G. Richmond and C. E. Osterberg, *Chem. Rev.*, **1994**, *94*, 373; (b) T. Braun and R. N. Perutz, *Chem. Commun.*, **2002**, *0*, 2749; (c) V. P. W. Böhm, C. W. K. Gstöttmayr, T. Weskamp and W. A. Herrmann, *Angew. Chem. Int. Ed.*, **2001**, *40*, 3387; (d) R. J. Young and V. V. Grushin, *Organometallics*, **1999**, *18*, 294.

136. (a) T. Braun, S. P. Foxon, R. N. Perutz and P. H. Walton, *Angew. Chem. Int. Ed.*, **1999**, *38*, 3326; (b) D. R. Fahey and J. E. Mahan, *J. Am. Chem. Soc.*, **1977**, *99*, 2501; (c) T. Braun, L. Cronin, C. L. Higgitt, J. E. McGrady, R. N. Perutz and M. Reinhold, *New J. Chem.*, **2001**, *25*, 19; (d) M. I. Sladek, T. Braun, B. Neumann and H.-G. Stammler, *J. Chem. Soc., Dalton Trans.*, **2002**, *0*, 297; (e) L. Cronin, C. L. Higgitt, R. Karch and R. N. Perutz, *Organometallics*, **1997**, *16*, 4920.

137. M. Reinhold, J. E. McGrady and R. N. Perutz, *J. Am. Chem. Soc.*, **2004**, *126*, 5268.

138. (a) D. W. Stephan, *Org. Biomol. Chem.*, **2012**, *10*, 5740; (b) D. W. Stephan, *Chem. Commun.*, **2010**, *46*, 8526; (c) D. W. Stephan and G. Erker, *Angew. Chem., Int. Ed.*, **2010**, *49*, 46.

139. H. Kanew, S. Ishii, H. and H. Nakazawa, *Dalton Trans.*, **2013**, *42*, 4663.

140. J. Y. Corey, *Chem. Rev.*, **2011**, *111*, 863.

141. P. Ren, O. Wechorkin, Z. Csok, I. Salihu, R. Scopelliti and X. Hu, *Dalton Trans*., **2011**, *40*, 8906.

142. H.-W. Suh, T. J. Schmeier, N. Hazari, R.A. Kemp, M. K. Takase, *Organometallics*, **2012**, *31*, 8225.

Appendix A: Crystallographic Experimental Details

Table A-1. Crystallographic experimental details for [Cy-PSiP]PtPh (**2-4**)·OEt_2

A. Crystal Data	
formula	$C_{47}H_{70}OP_2PtSi$
formula weight	936.15
crystal dimensions (mm)	0.45 × 0.39 × 0.15
crystal system	triclinic
space group	*P* (No. 2)
unit cell parameters[a]	
a (Å)	13.506 (5)
b (Å)	14.057 (5)
c (Å)	14.950 (6)
α (deg)	116.378 (4)
β (deg)	93.480 (4)
γ (deg)	112.518 (4)
V (Å^3)	2255.8 (15)
Z	2
ρ_{calcd} (g cm^{-3})	1.378
μ (mm^{-1})	3.240
B. Data Collection and Refinement Conditions	
diffractometer	Bruker D8/APEX II CCD[b]
radiation (λ [Å])	graphite-monochromated Mo Kα (0.71073)
temperature (°C)	–100
scan type	ω scans (0.3°) (20 s exposures)
data collection 2θ limit (deg)	55.06
total data collected	19714 (-17 ≤ *h* ≤ 17, -17 ≤ *k* ≤ 17, -19 ≤ *l* ≤ 19)
independent reflections	10198 (R_{int} = 0.0133)
number of observed reflections (*NO*)	9813 [$F_o^2 \geq 2\sigma(F_o^2)$]
structure solution method	Patterson/structure expansion (*DIRDIF–2008*[c])
refinement method	full-matrix least-squares on F^2 (*SHELXL–97*[d])
absorption correction method	Gaussian integration (face-indexed)
range of transmission factors	0.6387–0.3209
data/restraints/parameters	10198 [$F_o^2 \geq -3\sigma(F_o^2)$] / 0 / 469
goodness-of-fit (*S*)[e]	1.030 [$F_o^2 \geq -3\sigma(F_o^2)$]
final *R* indices[f]	
R_1 [$F_o^2 \geq 2\sigma(F_o^2)$]	0.0157
wR_2 [$F_o^2 \geq -3\sigma(F_o^2)$]	0.0412
largest difference peak and hole	0.836 and –0.471 e Å^{-3}

[a]Obtained from least-squares refinement of 9996 reflections with $5.40° < 2\theta < 55.06°$.

[b]Programs for diffractometer operation, data collection, data reduction and absorption correction were those supplied by Bruker.

[c]Beurskens, P. T.; Beurskens, G.; de Gelder, R.; Smits, J. M. M; Garcia-Granda, S.; Gould, R. O. (2008). The *DIRDIF-2008* program system. Crystallography Laboratory, Radboud University Nijmegen, The Netherlands.

[d]Sheldrick, G. M. *Acta Crystallogr.* **2008**, *A64*, 112–122.

[e]$S = [\Sigma w(F_o^2 - F_c^2)^2/(n-p)]^{1/2}$ (n = number of data; p = number of parameters varied; $w = [\sigma^2(F_o^2) + (0.0235P)^2 + 0.6339P]^{-1}$ where $P = [\mathrm{Max}(F_o^2, 0) + 2F_c^2]/3$).

[f]$R_1 = \Sigma||F_o| - |F_c||/\Sigma|F_o|$; $wR_2 = [\Sigma w(F_o^2 - F_c^2)^2/\Sigma w(F_o^4)]^{1/2}$.

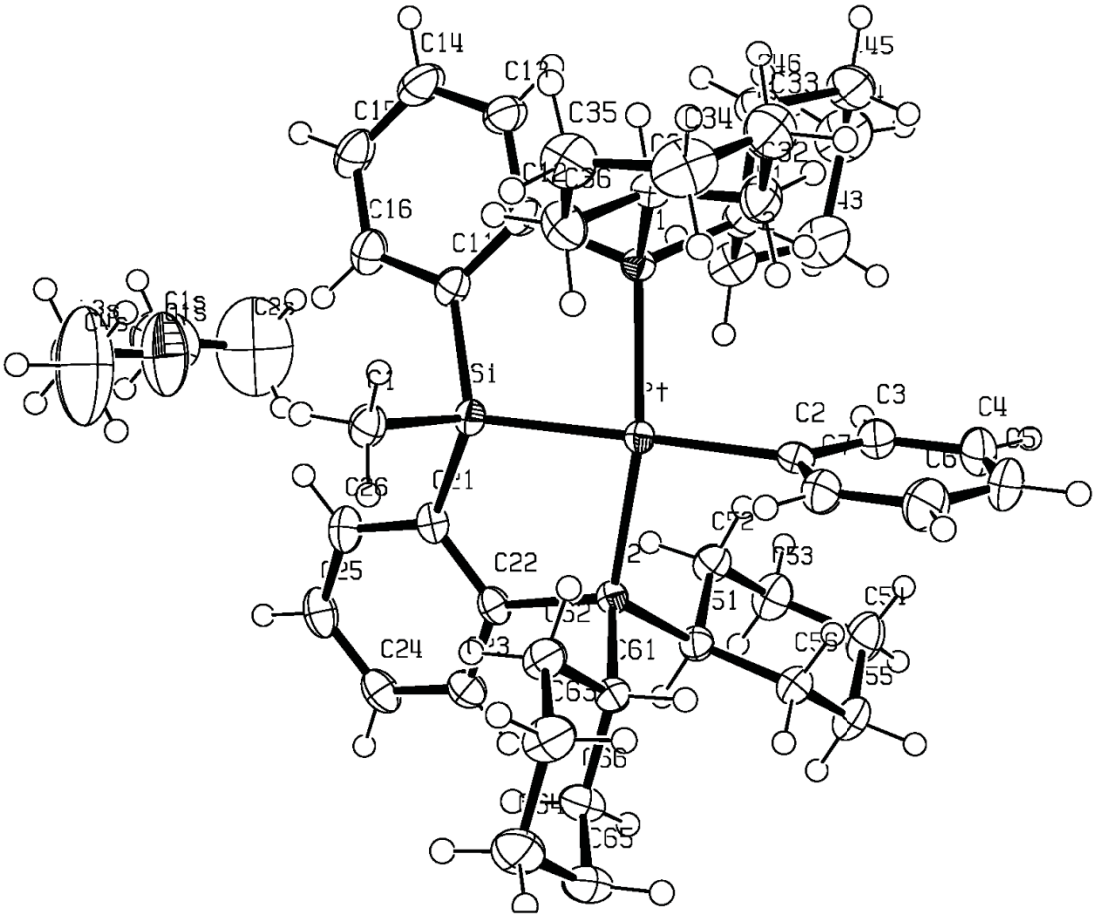

Figure A-1. ORTEP diagram for [Cy-PSiP]PtPh (**2-4**·OEt_2)

Table A-2. Crystallographic experimental details for κ^2-{$Me_2Si(C_6H_4PCy_2)_2$}$PtMe_2$ (**2-11**)

A. Crystal Data	
formula	$C_{40}H_{64}P_2PtSi$
formula weight	830.03
crystal dimensions (mm)	0.63 × 0.44 × 0.31
crystal system	monoclinic
space group	*C*2/*c* (No. 15)
unit cell parameters[a]	
a (Å)	38.7504 (13)
b (Å)	9.3925 (3)
c (Å)	20.8598 (7)
β (deg)	96.2086 (4)
V (Å^3)	7547.7 (4)
Z	8
ρ_{calcd} (g cm^{-3})	1.461
μ (mm^{-1})	3.861
B. Data Collection and Refinement Conditions	
diffractometer	Bruker D8/APEX II CCD[b]
radiation (λ [Å])	graphite-monochromated Mo Kα (0.71073)
temperature (°C)	–100
scan type	ω scans (0.3°) (15 s exposures)
data collection 2θ limit (deg)	55.12
total data collected	32378 (-49 ≤ *h* ≤ 50, -12 ≤ *k* ≤ 12, -26 ≤ *l* ≤ 27)
independent reflections	8699 (R_{int} = 0.0123)
number of observed reflections (*NO*)	7991 [$F_o^2 \geq 2\sigma(F_o^2)$]
structure solution method	Patterson/structure expansion (*DIRDIF–2008*[c])
refinement method	full-matrix least-squares on F^2 (*SHELXL–97*[d])
absorption correction method	Gaussian integration (face-indexed)
range of transmission factors	0.3759–0.1940
data/restraints/parameters	8699 [$F_o^2 \geq -3\sigma(F_o^2)$] / 0 / 401
goodness-of-fit (*S*)[e]	1.053 [$F_o^2 \geq -3\sigma(F_o^2)$]
final *R* indices[f]	
R_1 [$F_o^2 \geq 2\sigma(F_o^2)$]	0.0154
wR_2 [$F_o^2 \geq -3\sigma(F_o^2)$]	0.0400
largest difference peak and hole	0.684 and –0.723 e Å^{-3}

[a]Obtained from least-squares refinement of 9896 reflections with 4.66° < 2θ < 55.10°.
[b]Programs for diffractometer operation, data collection, data reduction and absorption correction were those supplied by Bruker.

[c]Beurskens, P. T.; Beurskens, G.; de Gelder, R.; Smits, J. M. M; Garcia-Granda, S.; Gould, R. O. (2008). The *DIRDIF-2008* program system. Crystallography Laboratory, Radboud University Nijmegen, The Netherlands.

[d]Sheldrick, G. M. *Acta Crystallogr.* **2008**, *A64*, 112–122.

[e]$S = [\Sigma w(F_o^2 - F_c^2)^2/(n-p)]^{1/2}$ (n = number of data; p = number of parameters varied; $w = [\sigma^2(F_o^2) + (0.0196P)^2 + 9.0454P]^{-1}$ where $P = [\text{Max}(F_o^2, 0) + 2F_c^2]/3$).

[f]$R_1 = \Sigma||F_o| - |F_c||/\Sigma|F_o|$; $wR_2 = [\Sigma w(F_o^2 - F_c^2)^2/\Sigma w(F_o^4)]^{1/2}$.

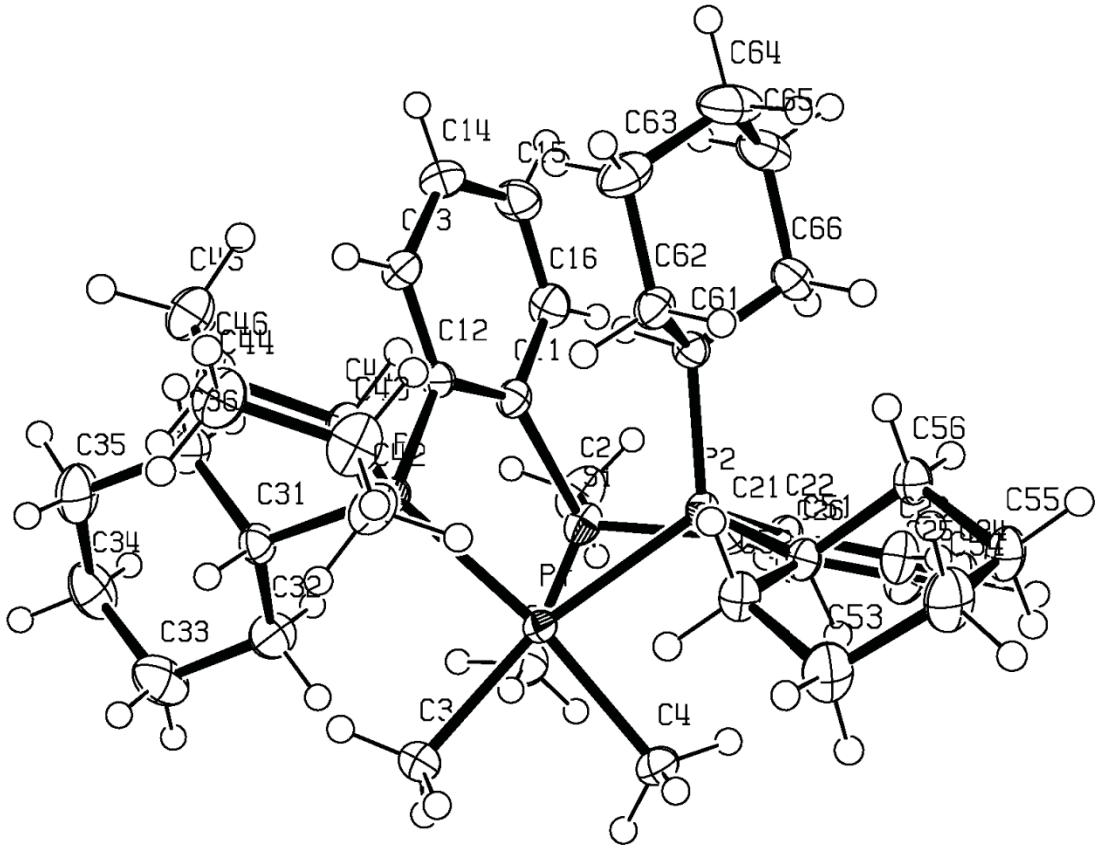

Figure A-2. ORTEP structure for κ^2-{$Me_2Si(C_6H_4PCy_2)_2$}$PtMe_2$ (**2-11**).

Table A-3. Crystallographic experimental details for [Cy-PSiP]NiCl (**3-1**).

A. Crystal Data	
formula	$C_{37}H_{55}ClNiP_2Si$
formula weight	684.00
crystal dimensions (mm)	0.28 × 0.19 × 0.12
crystal system	monoclinic
space group	$P2_1/c$ (No. 14)
unit cell parameters[a]	
a (Å)	12.784 (3)
b (Å)	13.988 (3)
c (Å)	20.774 (5)
β (deg)	99.109 (3)
V (Å^3)	3668.1 (15)
Z	4
ρ_{calcd} (g cm^{-3})	1.239
μ (mm^{-1})	0.746
B. Data Collection and Refinement Conditions	
diffractometer	Bruker D8/APEX II CCD[b]
radiation (λ [Å])	graphite-monochromated Mo Kα (0.71073)
temperature (°C)	–100
scan type	ω scans (0.3°) (20 s exposures)
data collection 2θ limit (deg)	51.56
total data collected	26268 ($-15 \le h \le 15$, $-17 \le k \le 17$, $-25 \le l \le 25$)
independent reflections	7025 (R_{int} = 0.0869)
number of observed reflections (*NO*)	4494 [$F_o^2 \ge 2\sigma(F_o^2)$]
structure solution method	Patterson/structure expansion (*DIRDIF–2008*[c])
refinement method	full-matrix least-squares on F^2 (*SHELXL–97*[d])
absorption correction method	Gaussian integration (face-indexed)
range of transmission factors	0.9172–0.8173
data/restraints/parameters	7025 [$F_o^2 \ge -3\sigma(F_o^2)$] / 0 / 379
goodness-of-fit (S)[e]	1.017 [$F_o^2 \ge -3\sigma(F_o^2)$]
final R indices[f]	
R_1 [$F_o^2 \ge 2\sigma(F_o^2)$]	0.0465
wR_2 [$F_o^2 \ge -3\sigma(F_o^2)$]	0.1176
largest difference peak and hole	0.714 and –0.488 e Å^{-3}

[a]Obtained from least-squares refinement of 5888 reflections with $4.34° < 2\theta < 50.08°$.
[b]Programs for diffractometer operation, data collection, data reduction and absorption correction were those supplied by Bruker.
[c]Beurskens, P. T.; Beurskens, G.; de Gelder, R.; Smits, J. M. M; Garcia-Granda, S.; Gould, R. O. (2008). The *DIRDIF-2008* program system. Crystallography

Laboratory, Radboud University Nijmegen, The Netherlands.

[d]Sheldrick, G. M. *Acta Crystallogr.* **2008**, *A64*, 112–122.

[e]$S = [\Sigma w(F_o^2 - F_c^2)^2/(n-p)]^{1/2}$ (n = number of data; p = number of parameters varied; $w = [\sigma^2(F_o^2) + (0.0287P)^2 + 7.8903P]^{-1}$ where $P = [\text{Max}(F_o^2, 0) + 2F_c^2]/3$).

[f]$R_1 = \Sigma||F_o| - |F_c||/\Sigma|F_o|$; $wR_2 = [\Sigma w(F_o^2 - F_c^2)^2/\Sigma w(F_o^4)]^{1/2}$.

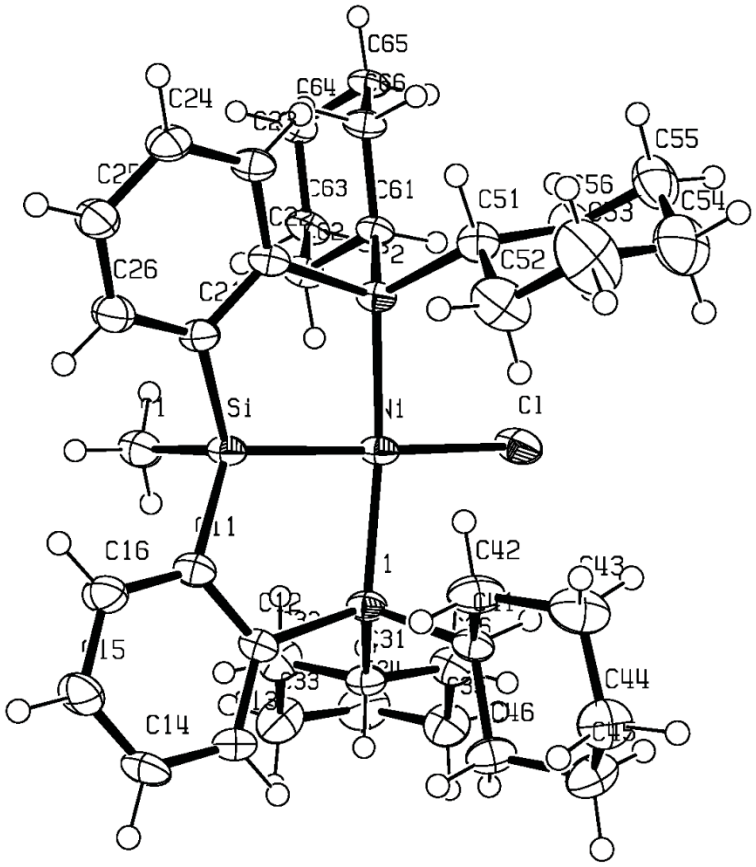

Figure A-3. ORTEP diagram for [Cy-PSiP]NiCl (**3-1**).

Table A-4. Crystallographic experimental details for [(κ^2–$Cy_2PC_6H_4SiMe_2$)Pd(κ^2–$Cy_2PC_6H_4$)] (**3-4**).

A. Crystal Data	
formula	$C_{38}H_{58}P_2PdSi$
formula weight	711.27
crystal dimensions (mm)	0.41 × 0.29 × 0.28
crystal system	monoclinic
space group	$P2_1/c$ (No. 14)
unit cell parameters[a]	
a (Å)	9.4296 (6)
b (Å)	17.1349 (10)
c (Å)	22.9209 (13)
β (deg)	100.3475 (6)
V (Å^3)	3643.2 (4)
Z	4
ρ_{calcd} (g cm^{-3})	1.297
μ (mm^{-1})	0.655
B. Data Collection and Refinement Conditions	
diffractometer	Bruker D8/APEX II CCD[b]
radiation (λ [Å])	graphite-monochromated Mo Kα (0.71073)
temperature (°C)	–100
scan type	ω scans (0.4°) (10 s exposures)
data collection 2θ limit (deg)	55.06
total data collected	31380 (-12 ≤ h ≤ 12, -22 ≤ k ≤ 22, -29 ≤ l ≤ 29)
independent reflections	8366 (R_{int} = 0.0185)
number of observed reflections (*NO*)	7645 [$F_o^2 \geq 2\sigma(F_o^2)$]
structure solution method	Patterson/structure expansion (*DIRDIF–2008*[c])
refinement method	full-matrix least-squares on F^2 (*SHELXL–97*[d])
absorption correction method	Gaussian integration (face-indexed)
range of transmission factors	0.8405–0.7737
data/restraints/parameters	8366 [$F_o^2 \geq -3\sigma(F_o^2)$] / 0 / 379
goodness-of-fit (S)[e]	1.032 [$F_o^2 \geq -3\sigma(F_o^2)$]
final R indices[f]	
R_1 [$F_o^2 \geq 2\sigma(F_o^2)$]	0.0213
wR_2 [$F_o^2 \geq -3\sigma(F_o^2)$]	0.0566
largest difference peak and hole	0.537 and –0.283 e Å^{-3}

[a]Obtained from least-squares refinement of 9886 reflections with 5.00° < 2θ < 55.04°.
[b]Programs for diffractometer operation, data collection, data reduction and absorption

correction were those supplied by Bruker.

[c]Beurskens, P. T.; Beurskens, G.; de Gelder, R.; Smits, J. M. M; Garcia-Granda, S.; Gould, R. O. (2008). The *DIRDIF-2008* program system. Crystallography Laboratory, Radboud University Nijmegen, The Netherlands.

[d]Sheldrick, G. M. *Acta Crystallogr.* **2008**, *A64*, 112–122.

[e]$S = [\Sigma w(F_o^2 - F_c^2)^2/(n-p)]^{1/2}$ (n = number of data; p = number of parameters varied; $w = [\sigma^2(F_o^2) + (0.0292P)^2 + 1.5060P]^{-1}$ where $P = [\text{Max}(F_o^2, 0) + 2F_c^2]/3$).

[f]$R_1 = \Sigma||F_o| - |F_c||/\Sigma|F_o|$; $wR_2 = [\Sigma w(F_o^2 - F_c^2)^2/\Sigma w(F_o^4)]^{1/2}$.

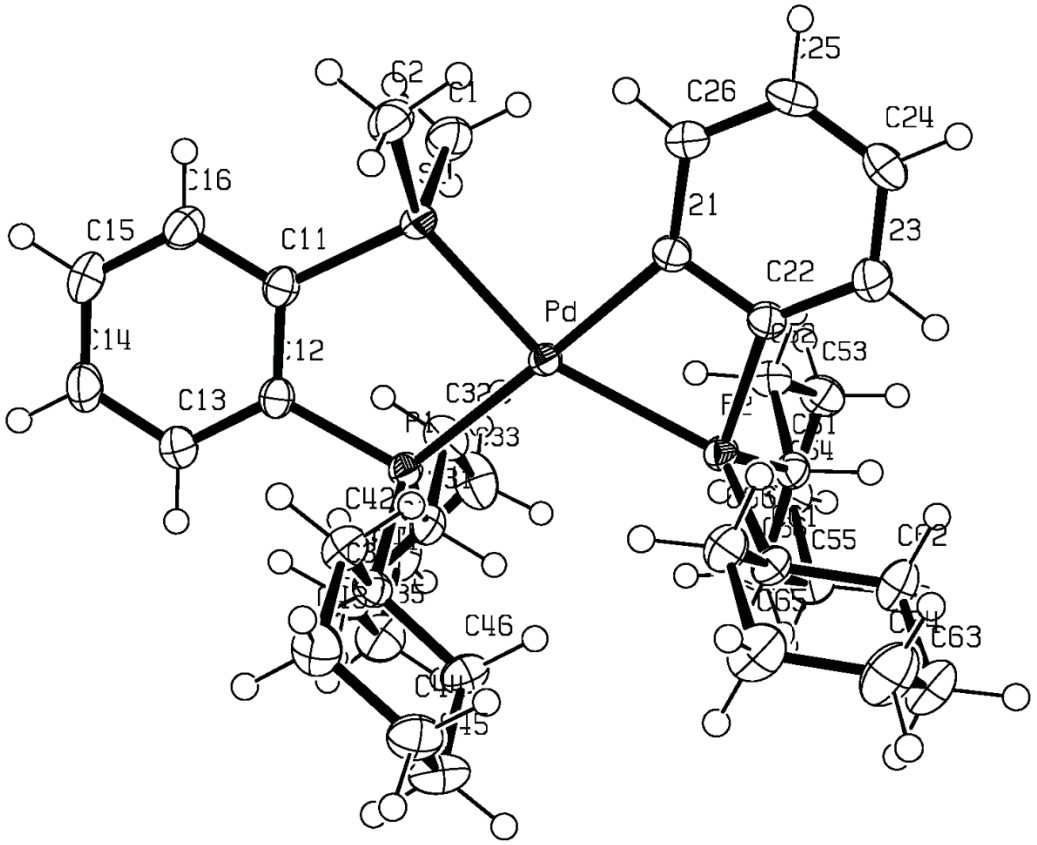

Figure A-4. ORTEP diagram for [(κ^2–$Cy_2PC_6H_4SiMe_2$)Pd(κ^2–$Cy_2PC_6H_4$)] (**3-4**).

Table A-5. Crystallographic experimental details for [Cy-PSiP]Pd($SiPhH_2$) **(3-9)**.

A. Crystal Data	
formula	$C_{49}H_{66}P_2PdSi_2$
formula weight	879.54
crystal dimensions (mm)	0.56 × 0.19 × 0.11
crystal system	orthorhombic
space group	*Pbca* (No. 61)
unit cell parameters[a]	
a (Å)	19.6885 (6)
b (Å)	18.6292 (5)
c (Å)	24.7147 (7)
V (Å^3)	9064.9 (4)
Z	8
ρ_{calcd} (g cm^{-3})	1.289
μ (mm^{-1})	0.565
B. Data Collection and Refinement Conditions	
diffractometer	Bruker D8/APEX II CCD[b]
radiation (λ [Å])	graphite-monochromated Mo Kα (0.71073)
temperature (°C)	–100
scan type	ω scans (0.3°) (15 s exposures)
data collection 2θ limit (deg)	55.00
total data collected	76745 (-25 ≤ *h* ≤ 25, -24 ≤ *k* ≤ 24, -32 ≤ *l* ≤ 32)
independent reflections	10417 (R_{int} = 0.0249)
number of observed reflections (*NO*)	9216 [$F_o^2 \geq 2\sigma(F_o^2)$]
structure solution method	Patterson/structure expansion (*DIRDIF–2008*[c])
refinement method	full-matrix least-squares on F^2 (*SHELXL–97*[d])
absorption correction method	Gaussian integration (face-indexed)
range of transmission factors	0.9415–0.7440
data/restraints/parameters	10417 [$F_o^2 \geq -3\sigma(F_o^2)$] / 0 / 491
goodness-of-fit (*S*)[e]	1.037 [$F_o^2 \geq -3\sigma(F_o^2)$]
final *R* indices[f]	
R_1 [$F_o^2 \geq 2\sigma(F_o^2)$]	0.0216
wR_2 [$F_o^2 \geq -3\sigma(F_o^2)$]	0.0583
largest difference peak and hole	0.361 and –0.284 e Å^{-3}

[a]Obtained from least-squares refinement of 9671 reflections with 4.46° < 2θ < 55.00°.

[b]Programs for diffractometer operation, data collection, data reduction and absorption correction were those supplied by Bruker.

[c]Beurskens, P. T.; Beurskens, G.; de Gelder, R.; Smits, J. M. M; Garcia-Granda, S.;

Gould, R. O. (2008). The *DIRDIF-2008* program system. Crystallography Laboratory, Radboud University Nijmegen, The Netherlands.

[d]Sheldrick, G. M. *Acta Crystallogr.* **2008**, *A64*, 112–122.

[e]$S = [\Sigma w(F_o^2 - F_c^2)^2/(n-p)]^{1/2}$ (n = number of data; p = number of parameters varied; $w = [\sigma^2(F_o^2) + (0.0277P)^2 + 4.6618P]^{-1}$ where $P = [\text{Max}(F_o^2, 0) + 2F_c^2]/3$).

[f]$R_1 = \Sigma||F_o| - |F_c||/\Sigma|F_o|$; $wR_2 = [\Sigma w(F_o^2 - F_c^2)^2/\Sigma w(F_o^4)]^{1/2}$.

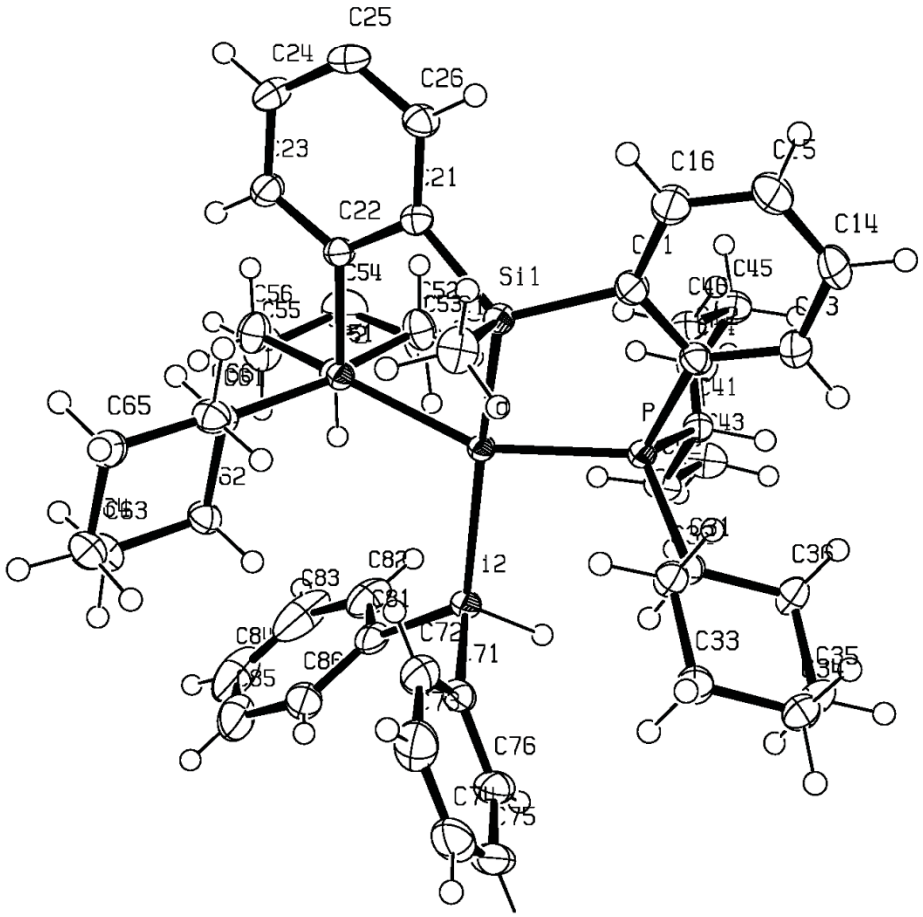

Figure A-5. ORTEP diagram for [Cy-PSiP]Pd(SiPhH$_2$) (**3-9**).

Table A-6. Crystallographic experiment detail for [Cy-PSiP]Ni(η^3-C_3H_5) (**3-10**·OEt_2).

A. Crystal Data	
formula	$C_{44}H_{70}NiOP_2Si$
formula weight	763.74
crystal dimensions (mm)	0.53 × 0.30 × 0.21
crystal system	monoclinic
space group	$P2_1/c$ (No. 14)
unit cell parameters[a]	
a (Å)	13.4523 (4)
b (Å)	11.6440 (4)
c (Å)	26.4702 (9)
β (deg)	93.6025 (4)
V (Å^3)	4138.1 (2)
Z	4
ρ_{calcd} (g cm^{-3})	1.226
μ (mm^{-1})	0.607
B. Data Collection and Refinement Conditions	
diffractometer	Bruker D8/APEX II CCD[b]
radiation (λ [Å])	graphite-monochromated Mo Kα (0.71073)
temperature (°C)	–100
scan type	ω scans (0.3°) (20 s exposures)
data collection 2θ limit (deg)	54.94
total data collected	35538 (-17 ≤ h ≤ 17, -15 ≤ k ≤ 15, -34 ≤ l ≤ 34)
independent reflections	9455 (R_{int} = 0.0208)
number of observed reflections (*NO*)	8453 [$F_o^2 \geq 2\sigma(F_o^2)$]
structure solution method	Patterson/structure expansion (*DIRDIF–2008*[c])
refinement method	full-matrix least-squares on F^2 (*SHELXL–97*[d])
absorption correction method	Gaussian integration (face-indexed)
range of transmission factors	0.8831–0.7379
data/restraints/parameters	9455 [$F_o^2 \geq -3\sigma(F_o^2)$] / 0 / 462
goodness-of-fit (*S*)[e]	1.036 [$F_o^2 \geq -3\sigma(F_o^2)$]
final R indices[f]	
R_1 [$F_o^2 \geq 2\sigma(F_o^2)$]	0.0270
wR_2 [$F_o^2 \geq -3\sigma(F_o^2)$]	0.0734
largest difference peak and hole	0.421 and –0.299 e Å^{-3}

[a]Obtained from least-squares refinement of 9937 reflections with 4.64° < 2θ < 54.84°.

[b]Programs for diffractometer operation, data collection, data reduction and absorption correction were those supplied by Bruker.

[c]Beurskens, P. T.; Beurskens, G.; de Gelder, R.; Smits, J. M. M; Garcia-Granda, S.; Gould, R. O. (2008). The *DIRDIF-2008* program system. Crystallography Laboratory, Radboud University Nijmegen, The Netherlands.

[d]Sheldrick, G. M. *Acta Crystallogr.* **2008**, *A64*, 112–122.

[e]$S = [\Sigma w(F_o^2 - F_c^2)^2/(n-p)]^{1/2}$ (n = number of data; p = number of parameters varied; $w = [\sigma^2(F_o^2) + (0.0392P)^2 + 1.4900P]^{-1}$ where $P = [\text{Max}(F_o^2, 0) + 2F_c^2]/3$).

[f]$R_1 = \Sigma||F_o| - |F_c||/\Sigma|F_o|$; $wR_2 = [\Sigma w(F_o^2 - F_c^2)^2/\Sigma w(F_o^4)]^{1/2}$.

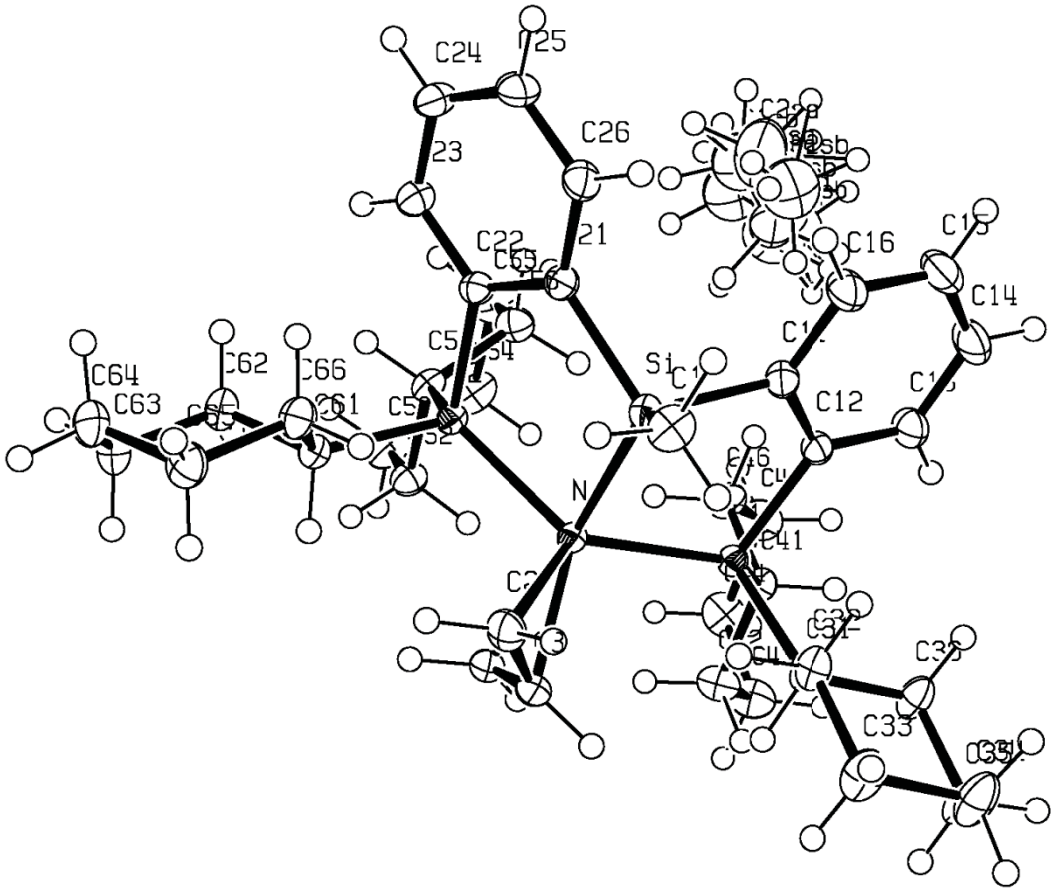

Figure A-6. ORTEP diagram for [Cy-PSiP]Ni(η^3-C_3H_5) (**3-11**).

Table A-7. Crystallographic experimental details for [Cy-PSiP]Pt(O^{t}Bu) (**5-2**·OEt_2)

A. Crystal Data	
formula	$C_{45}H_{74}O_2P_2PtSi$
formula weight	932.16
crystal dimensions (mm)	0.33 × 0.12 × 0.12
crystal system	orthorhombic
space group	$Pca2_1$ (No. 29)
unit cell parameters[a]	
a (Å)	19.0627 (13)
b (Å)	13.7399 (10)
c (Å)	17.7189 (12)
V (Å^3)	4640.9 (6)
Z	4
ρ_{calcd} (g cm^{-3})	1.334
μ (mm^{-1})	3.151
B. Data Collection and Refinement Conditions	
diffractometer	Bruker PLATFORM/APEX II CCD[b]
radiation (λ [Å])	graphite-monochromated Mo Kα (0.71073)
temperature (°C)	–50
scan type	ω scans (0.3°) (15 s exposures)
data collection 2θ limit (deg)	55.04
total data collected	40068 ($-24 \le h \le 24$, $-17 \le k \le 17$, $-22 \le l \le 23$)
independent reflections	10642 (R_{int} = 0.0503)
number of observed reflections (*NO*)	9119 [$F_o^2 \ge 2\sigma(F_o^2)$]
structure solution method	Patterson/structure expansion (*DIRDIF–2008*[c])
refinement method	full-matrix least-squares on F^2 (*SHELXL–97*[d])
absorption correction method	Gaussian integration (face-indexed)
range of transmission factors	0.7133–0.4192
data/restraints/parameters	10642 / 14[e] / 447
Flack absolute structure parameter[f]	0.006(4)
goodness-of-fit (*S*)[g] [all data]	1.027
final *R* indices[h]	
R_1 [$F_o^2 \ge 2\sigma(F_o^2)$]	0.0253
wR_2 [all data]	0.0584
largest difference peak and hole	0.659 and –0.386 e Å^{-3}

[a]Obtained from least-squares refinement of 7690 reflections with $4.32° < 2\theta < 38.20°$.

[b]Programs for diffractometer operation, data collection, data reduction and absorption correction were those supplied by Bruker.

[c]Beurskens, P. T.; Beurskens, G.; de Gelder, R.; Smits, J. M. M.; Garcia-Granda, S.; Gould, R. O. (2008). The *DIRDIF-2008* program system. Crystallography

Laboratory, Radboud University Nijmegen, The Netherlands.

[d]Sheldrick, G. M. *Acta Crystallogr.* **2008**, *A64*, 112–122.

[e]Restraints were applied to the following interatomic distances within the disordered solvent diethyl ether molecule: d(O1SA–C1SA) = d(O1SA–C3SA) = d(O1SB–C1SB) = d(O1SB–C3SB) = 1.46 (2) Å; d(C1SA–C2SA) = d(C3SA–C4SA) = d(C1SB–C2SB) = d(C3SB–C4SB) = 1.54(2) Å; d(O1SA···C2SA) = d(O1SA···C4SA) = d(O1SB···C2SB) = d(O1SB···C4SB) = 2.45(2) Å; d(C1SA···C3SA) = d(C1SB···C3SB) = 2.38(2) Å.

[f]Flack, H. D. *Acta Crystallogr.* **1983**, *A39*, 876–881; Flack, H. D.; Bernardinelli, G. *Acta Crystallogr.* **1999**, *A55*, 908–915; Flack, H. D.; Bernardinelli, G. *J. Appl. Cryst.* **2000**, *33*, 1143–1148. The Flack parameter will refine to a value near zero if the structure is in the correct configuration and will refine to a value near one for the inverted configuration.

[g]$S = [\Sigma w(F_o^2 - F_c^2)^2/(n-p)]^{1/2}$ (n = number of data; p = number of parameters varied; $w = [\sigma^2(F_o^2) + (0.0176P)^2]^{-1}$ where $P = [\mathrm{Max}(F_o^2, 0) + 2F_c^2]/3$).

[h]$R_1 = \Sigma||F_o| - |F_c||/\Sigma|F_o|$; $wR_2 = [\Sigma w(F_o^2 - F_c^2)^2/\Sigma w(F_o^4)]^{1/2}$

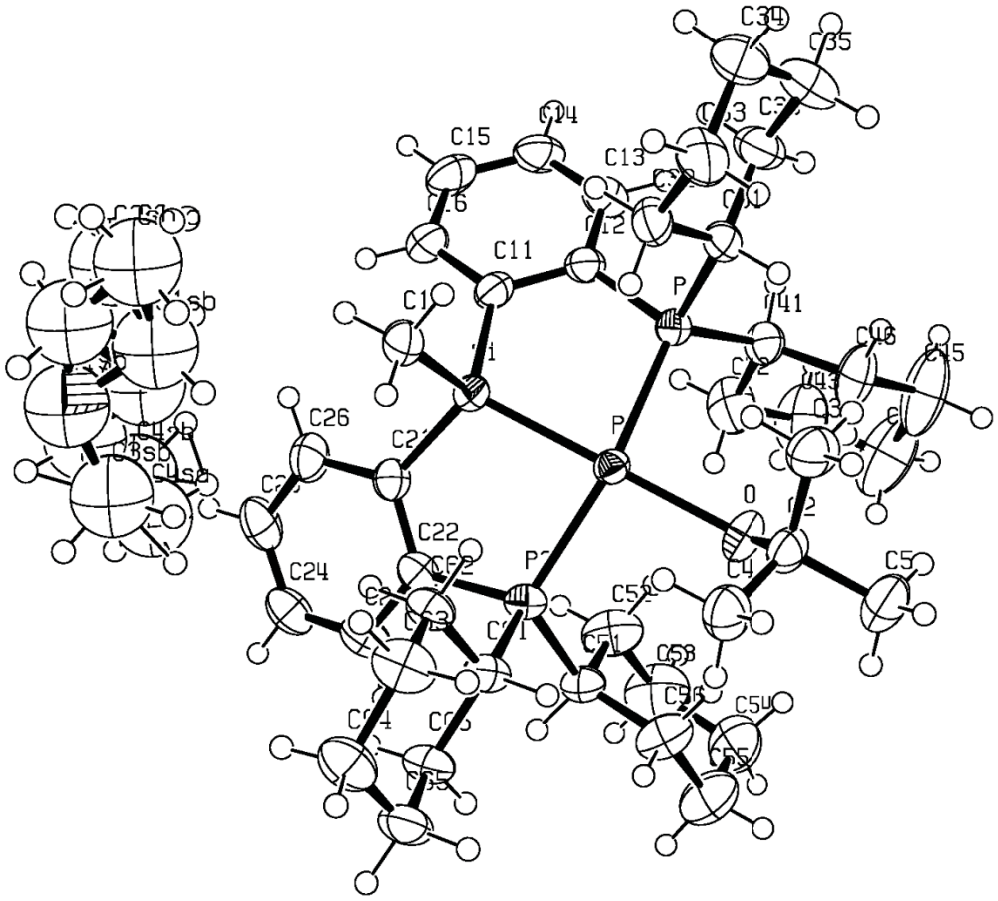

Figure A-7. ORTEP diagram for [Cy-PSiP]Pt(OtBu) (**5-2**·OEt_2).

Table A-8. Crystallographic experimental details for [Cy-PSiP]Pt(OH) (**5-4**).

A. Crystal Data	
formula	$C_{41}H_{66}O_2P_2PtSi$
formula weight	876.06
crystal dimensions (mm)	0.36 × 0.17 × 0.14
crystal system	monoclinic
space group	$P2_1/c$ (No. 14)
unit cell parameters[a]	
a (Å)	16.8126 (8)
b (Å)	14.8200 (7)
c (Å)	18.2039 (9)
β (deg)	114.6110 (10)
V (Å^3)	4123.7 (3)
Z	4
ρ_{calcd} (g cm^{-3})	1.411
μ (mm^{-1})	3.541
B. Data Collection and Refinement Conditions	
diffractometer	Bruker D8/APEX II CCD[b]
radiation (λ [Å])	graphite-monochromated Mo Kα (0.71073)
temperature (°C)	–100
scan type	ω scans (0.3°) (20 s exposures)
data collection 2θ limit (deg)	55.04
total data collected	35716 ($-21 \le h \le 21$, $-19 \le k \le 19$, $-23 \le l \le 23$)
independent reflections	9465 (R_{int} = 0.0432)
number of observed reflections (*NO*)	7619 [$F_o^2 \ge 2\sigma(F_o^2)$]
structure solution method	direct methods (*SHELXS–97*[c])
refinement method	full-matrix least-squares on F^2 (*SHELXL–97*[c])
absorption correction method	Gaussian integration (face-indexed)
range of transmission factors	0.6314–0.3637
data/restraints/parameters	9465 [$F_o^2 \ge -3\sigma(F_o^2)$] / 0 / 425
goodness-of-fit (*S*)[d]	1.084 [$F_o^2 \ge -3\sigma(F_o^2)$]
final R indices[e]	
R_1 [$F_o^2 \ge 2\sigma(F_o^2)$]	0.0281
wR_2 [$F_o^2 \ge -3\sigma(F_o^2)$]	0.0775
largest difference peak and hole	1.698 and –0.65 e Å^{-3}

[a]Obtained from least-squares refinement of 9835 reflections with $4.52° < 2\theta < 53.58°$.

[b]Programs for diffractometer operation, data collection, data reduction and absorption correction were those supplied by Bruker.

[c]Sheldrick, G. M. *Acta Crystallogr.* **2008**, *A64*, 112–122.

[d]$S = [\Sigma w(F_o^2 - F_c^2)^2/(n-p)]^{1/2}$ (n = number of data; p = number of parameters varied; w

$= [\sigma^2(F_o^2) + (0.0416P)^2 + 1.0791P]^{-1}$ where $P = [\text{Max}(F_o^2, 0) + 2F_c^2]/3)$.
[e] $R_1 = \Sigma||F_o| - |F_c||/\Sigma|F_o|$; $wR_2 = [\Sigma w(F_o^2 - F_c^2)^2/\Sigma w(F_o^4)]^{1/2}$.

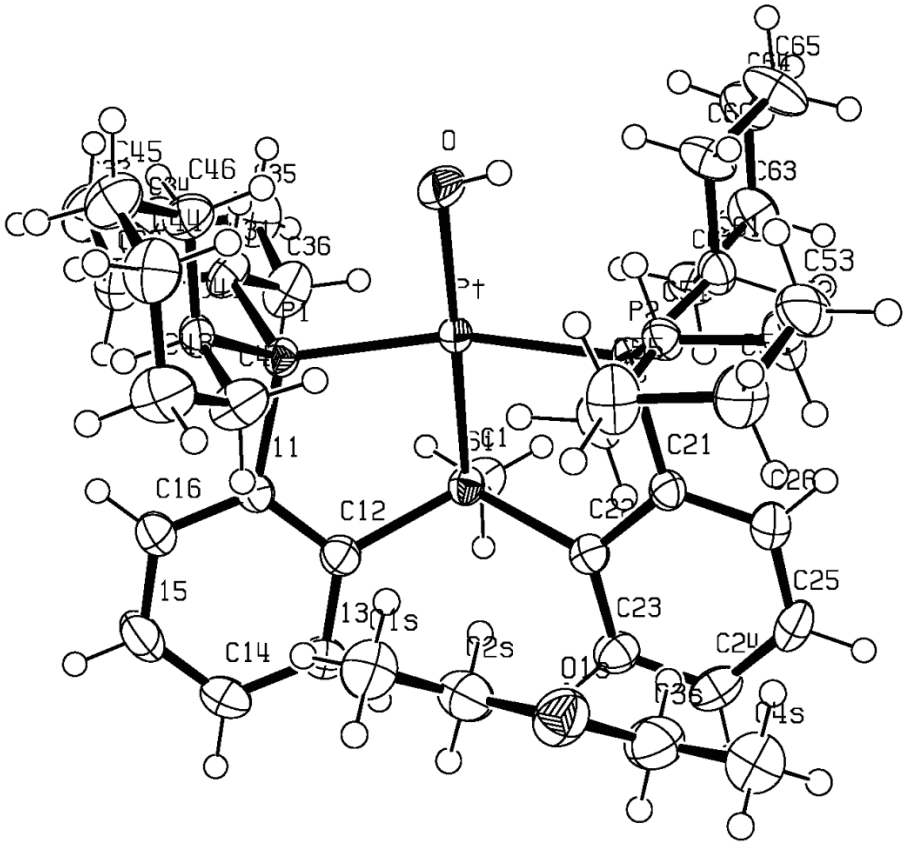

Figure A-8. ORTEP diagram for [Cy-PSiP]Pt(OH) (**5-4**).

Table A-9. Crystallographic experimental details for [Cy-PSiP]P(C≡CPh) (**5-5**·C_6H_6)

A. Crystal Data	
formula	$C_{51}H_{66}P_2PtSi$
formula weight	964.16
crystal dimensions (mm)	0.43 × 0.34 × 0.28
crystal system	monoclinic
space group	$P2_1/c$ (No. 14)
unit cell parameters[a]	
a (Å)	21.1273 (12)
b (Å)	12.1245 (7)
c (Å)	17.7081 (10)
β (deg)	95.8512 (9)
V (Å^3)	4512.4 (4)
Z	4
ρ_{calcd} (g cm^{-3})	1.419
μ (mm^{-1})	3.241
B. Data Collection and Refinement Conditions	
diffractometer	Bruker D8/APEX II CCD[b]
radiation (λ [Å])	graphite-monochromated Mo Kα (0.71073)
temperature (°C)	–100
scan type	ω scans (0.4°) (10 s exposures)
data collection 2θ limit (deg)	55.04
total data collected	34571 ($-27 \le h \le 26$, $-15 \le k \le 15$, $-23 \le l \le 23$)
independent reflections	10342 (R_{int} = 0.0341)
number of observed reflections (*NO*)	8941 [$F_o^2 \ge 2\sigma(F_o^2)$]
structure solution method	Patterson/structure expansion (*DIRDIF–2008*[c])
refinement method	full-matrix least-squares on F^2 (*SHELXL–97*[d])
absorption correction method	Gaussian integration (face-indexed)
range of transmission factors	0.4639–0.3390
data/restraints/parameters	10342 / 0 / 497
goodness-of-fit (*S*)[e] [all data]	1.025
final *R* indices[f]	
R_1 [$F_o^2 \ge 2\sigma(F_o^2)$]	0.0218
wR_2 [all data]	0.0507
largest difference peak and hole	0.602 and –0.635 e Å^{-3}

[a]Obtained from least-squares refinement of 4750 reflections with $4.42° < 2\theta < 41.28°$.

[b]Programs for diffractometer operation, data collection, data reduction and absorption correction were those supplied by Bruker.

[c]Beurskens, P. T.; Beurskens, G.; de Gelder, R.; Smits, J. M. M.; Garcia-Granda, S.; Gould, R. O. (2008). The *DIRDIF-2008* program system. Crystallography

Laboratory, Radboud University Nijmegen, The Netherlands.

[d]Sheldrick, G. M. *Acta Crystallogr.* **2008**, *A64*, 112–122.

[e]$S = [\Sigma w(F_o^2 - F_c^2)^2/(n-p)]^{1/2}$ (n = number of data; p = number of parameters varied; $w = [\sigma^2(F_o^2) + (0.0213P)^2 + 1.1352P]^{-1}$ where $P = [\text{Max}(F_o^2, 0) + 2F_c^2]/3$).

[f]$R_1 = \Sigma||F_o| - |F_c||/\Sigma|F_o|$; $wR_2 = [\Sigma w(F_o^2 - F_c^2)^2/\Sigma w(F_o^4)]^{1/2}$.

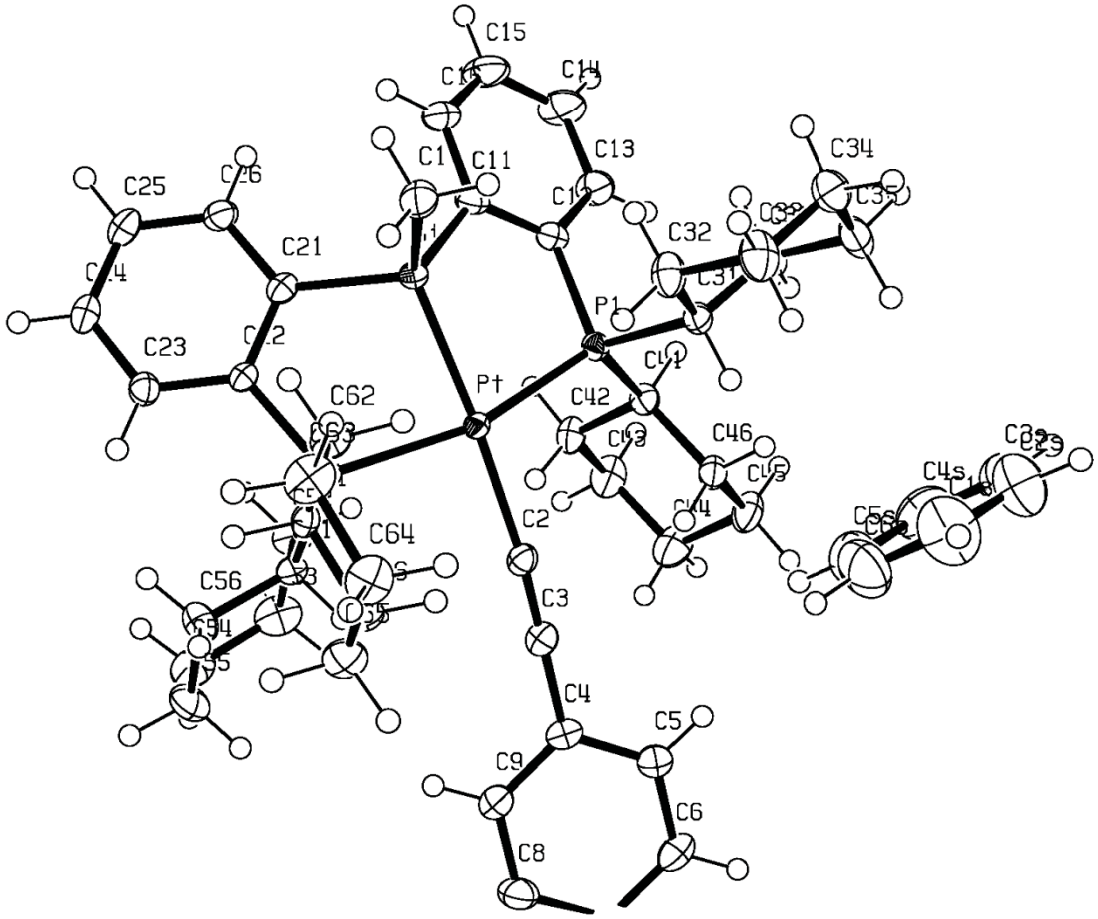

Figure A-9. ORTEP diagram for [Cy-PSiP]PtC≡CPh (**5-5**·C_6H_6).

Table A-10. Crystallographic experimental details for [Cy-PSiP]Pt(CH_2CN) (**5-6**).

A. Crystal Data	
formula	$C_{38.3}H_{56.3}Cl_{0.35}N_{0.65}P_2PtSi$
formula weight	823.37
crystal dimensions (mm)	0.15 × 0.12 × 0.04
crystal system	monoclinic
space group	$P2_1/c$ (No. 14)
unit cell parameters[a]	
a (Å)	12.8511 (6)
b (Å)	14.0995 (6)
c (Å)	20.9009 (9)
β (deg)	100.4342 (6)
V (Å^3)	3724.5 (3)
Z	4
ρ_{calcd} (g cm^{-3})	1.468
μ (mm^{-1})	3.937
B. Data Collection and Refinement Conditions	
diffractometer	Bruker PLATFORM/APEX II CCD[b]
radiation (λ [Å])	graphite-monochromated Mo Kα (0.71073)
temperature (°C)	–100
scan type	ω scans (0.3°) (20 s exposures)
data collection 2θ limit (deg)	52.74
total data collected	29371 ($-16 \le h \le 16$, $-17 \le k \le 17$, $-26 \le l \le 26$)
independent reflections	7610 (R_{int} = 0.0671)
number of observed reflections (*NO*)	5841 [$F_o^2 \ge 2\sigma(F_o^2)$]
structure solution method	Patterson/structure expansion (*DIRDIF–2008*[c])
refinement method	full-matrix least-squares on F^2 (*SHELXL–97*[d])
absorption correction method	Gaussian integration (face-indexed)
range of transmission factors	0.8680–0.5879
data/restraints/parameters	7610 / 0 / 402
goodness-of-fit (*S*)[e] [all data]	1.015
final *R* indices[f]	
R_1 [$F_o^2 \ge 2\sigma(F_o^2)$]	0.0294
wR_2 [all data]	0.0619
largest difference peak and hole	0.619 and –0.582 e Å^{-3}

[a]Obtained from least-squares refinement of 7015 reflections with $4.32° < 2\theta < 41.10°$.

[b]Programs for diffractometer operation, data collection, data reduction and absorption correction were those supplied by Bruker.

[c]Beurskens, P. T.; Beurskens, G.; de Gelder, R.; Smits, J. M. M.; Garcia-Granda, S.; Gould, R. O. (2008). The *DIRDIF-2008* program system. Crystallography

Laboratory, Radboud University Nijmegen, The Netherlands.

[d]Sheldrick, G. M. *Acta Crystallogr.* **2008**, *A64*, 112–122.

[e]$S = [\Sigma w(F_o^2 - F_c^2)^2/(n-p)]^{1/2}$ (n = number of data; p = number of parameters varied; $w = [\sigma^2(F_o^2) + (0.0213P)^2 + 2.1028P]^{-1}$ where $P = [\text{Max}(F_o^2, 0) + 2F_c^2]/3$).

[f]$R_1 = \Sigma||F_o| - |F_c||/\Sigma|F_o|$; $wR_2 = [\Sigma w(F_o^2 - F_c^2)^2/\Sigma w(F_o^4)]^{1/2}$.

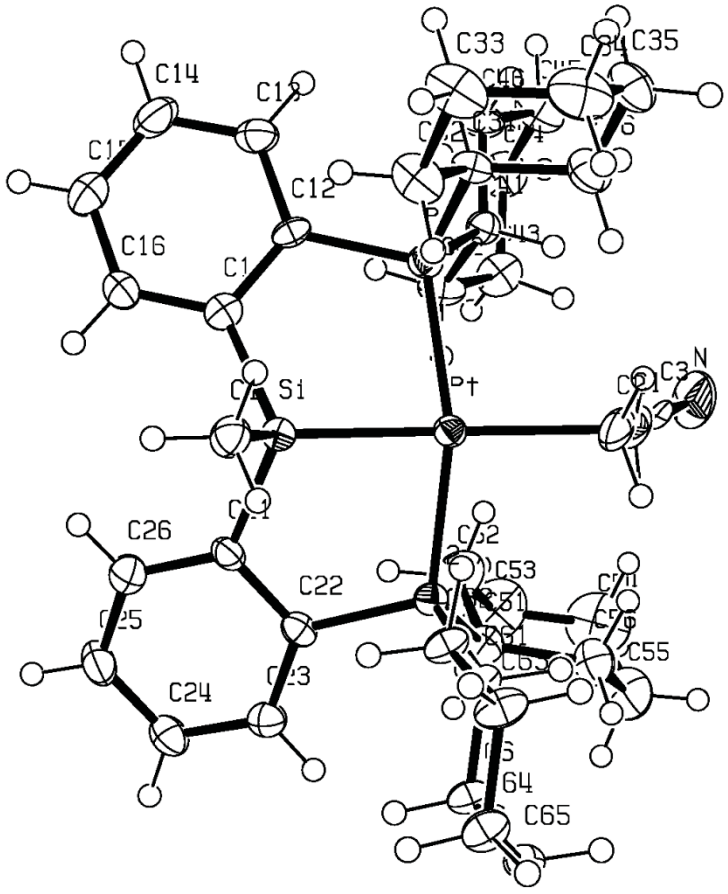

Figure A-10. ORTEP diagram for [Cy-PSiP]Pt(CH_2CN) (**5-6**).

Table A-11. Crystallographic experiment detail for [Cy-PSiP]Pt{NH(2,6-$^{i}Pr_2C_6H_3$} (**6-3**).

A. Crystal Data	
formula	$C_{49}H_{73}NP_2PtSi$
formula weight	961.20
crystal dimensions (mm)	0.33 × 0.20 × 0.06
crystal system	monoclinic
space group	$P2_1/c$ (No. 14)
unit cell parameters[a]	
a (Å)	12.0014 (4)
b (Å)	17.3287 (5)
c (Å)	21.4647 (6)
β (deg)	90.0895 (4)
V (Å^3)	4464.0 (2)
Z	4
ρ_{calcd} (g cm^{-3})	1.430
μ (mm^{-1})	3.276
B. Data Collection and Refinement Conditions	
diffractometer	Bruker D8/APEX II CCD[b]
radiation (λ [Å])	graphite-monochromated Mo Kα (0.71073)
temperature (°C)	–100
scan type	ω scans (0.3°) (15 s exposures)
data collection 2θ limit (deg)	52.84
total data collected	35664 (-15 ≤ h ≤ 15, -21 ≤ k ≤ 21, -26 ≤ l ≤ 26)
independent reflections	9170 (R_{int} = 0.0281)
number of observed reflections (*NO*)	8153 [$F_o^2 \geq 2\sigma(F_o^2)$]
structure solution method	Patterson/structure expansion (*DIRDIF–2008*[c])
refinement method	full-matrix least-squares on F^2 (*SHELXL–97*[d])
absorption correction method	Gaussian integration (face-indexed)
range of transmission factors	0.8277–0.4075
data/restraints/parameters	9170 / 0 / 487
goodness-of-fit (S)[e] [all data]	1.056
final R indices[f]	
R_1 [$F_o^2 \geq 2\sigma(F_o^2)$]	0.0211
wR_2 [all data]	0.0488
largest difference peak and hole	1.416 and –1.031 e Å^{-3}

[a]Obtained from least-squares refinement of 8175 reflections with $4.46° < 2\theta < 46.34°$.
[b]Programs for diffractometer operation, data collection, data reduction and absorption correction were those supplied by Bruker.

[c]Beurskens, P. T.; Beurskens, G.; de Gelder, R.; Smits, J. M. M; Garcia-Granda, S.; Gould, R. O. (2008). The *DIRDIF-2008* program system. Crystallography Laboratory, Radboud University Nijmegen, The Netherlands.
[d]Sheldrick, G. M. *Acta Crystallogr.* **2008**, *A64*, 112–122.
[e]$S = [\Sigma w(F_o^2 - F_c^2)^2/(n - p)]^{1/2}$ (n = number of data; p = number of parameters varied; $w = [\sigma^2(F_o^2) + (0.0201P)^2 + 3.7611P]^{-1}$ where $P = [\text{Max}(F_o^2, 0) + 2F_c^2]/3$).
[f]$R_1 = \Sigma||F_o| - |F_c||/\Sigma|F_o|$; $wR_2 = [\Sigma w(F_o^2 - F_c^2)^2/\Sigma w(F_o^4)]^{1/2}$.

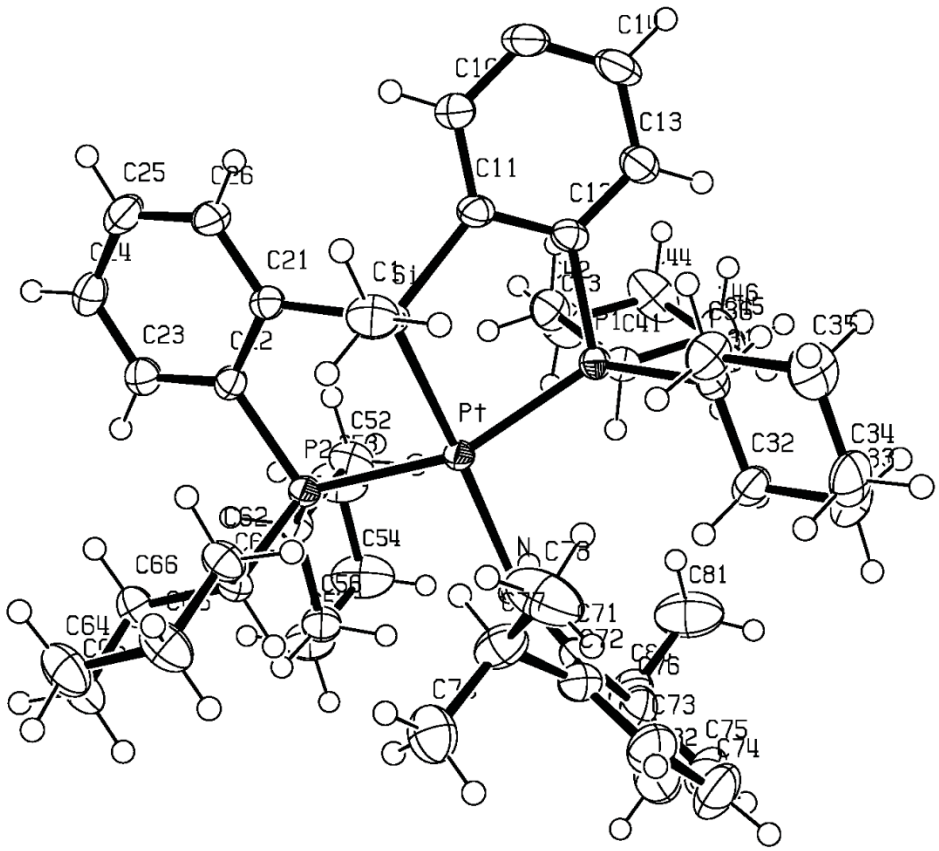

Figure A-11. ORTEP diagram for [Cy-PSiP]Pt{NH(2,6-$^{i}Pr_2C_6H_3$)} (**6-3**).

Table A-12. Crystallographic experimental details for [Cy-PSiP]Pt{C(=N(2,6,-$Me_2C_6H_3$))NHPh} (**6-4**).

A. Crystal Data	
formula	$C_{52}H_{70}N_2P_2PtSi$
formula weight	1008.22
crystal dimensions (mm)	0.30 × 0.22 × 0.08
crystal system	monoclinic
space group	$P2_1/n$ (an alternate setting of $P2_1/c$ [No. 14])
unit cell parameters[a]	
a (Å)	12.1123 (9)
b (Å)	19.1494 (14)
c (Å)	21.0603 (16)
β (deg)	104.9805 (9)
V (Å^3)	4718.8 (6)
Z	4
ρ_{calcd} (g cm^{-3})	1.419
μ (mm^{-1})	3.103
B. Data Collection and Refinement Conditions	
diffractometer	Bruker PLATFORM/APEX II CCD[b]
radiation (λ [Å])	graphite-monochromated Mo Kα (0.71073)
temperature (°C)	–100
scan type	ω scans (0.3°) (20 s exposures)
data collection 2θ limit (deg)	51.00
total data collected	34303 (-14 ≤ h ≤ 14, -23 ≤ k ≤ 23, -25 ≤ l ≤ 25)
independent reflections	8797 (R_{int} = 0.0699)
number of observed reflections (*NO*)	6399 [$F_o^2 \geq 2\sigma(F_o^2)$]
structure solution method	Patterson/structure expansion (*DIRDIF–2008*[c])
refinement method	full-matrix least-squares on F^2 (*SHELXL–97*[d])
absorption correction method	Gaussian integration (face-indexed)
range of transmission factors	0.7849–0.4602
data/restraints/parameters	8797 / 0 / 525
goodness-of-fit (S)[e] [all data]	1.025
final R indices[f]	
R_1 [$F_o^2 \geq 2\sigma(F_o^2)$]	0.0423
wR_2 [all data]	0.1167
largest difference peak and hole	4.088 and –1.495 e Å^{-3}

[a]Obtained from least-squares refinement of 9955 reflections with 4.44° < 2θ < 45.26°.
[b]Programs for diffractometer operation, data collection, data reduction and absorption correction were those supplied by Bruker.
[c]Beurskens, P. T.; Beurskens, G.; de Gelder, R.; Smits, J. M. M; Garcia-Granda, S.;

Gould, R. O. (2008). The *DIRDIF-2008* program system. Crystallography Laboratory, Radboud University Nijmegen, The Netherlands.

[d]Sheldrick, G. M. *Acta Crystallogr.* **2008**, *A64*, 112–122.

[e]$S = [\Sigma w(F_o^2 - F_c^2)^2/(n-p)]^{1/2}$ (n = number of data; p = number of parameters varied; $w = [\sigma^2(F_o^2) + (0.0636P)^2 + 9.2650P]^{-1}$ where $P = [\text{Max}(F_o^2, 0) + 2F_c^2]/3$).

[f]$R_1 = \Sigma||F_o| - |F_c||/\Sigma|F_o|$; $wR_2 = [\Sigma w(F_o^2 - F_c^2)^2/\Sigma w(F_o^4)]^{1/2}$.

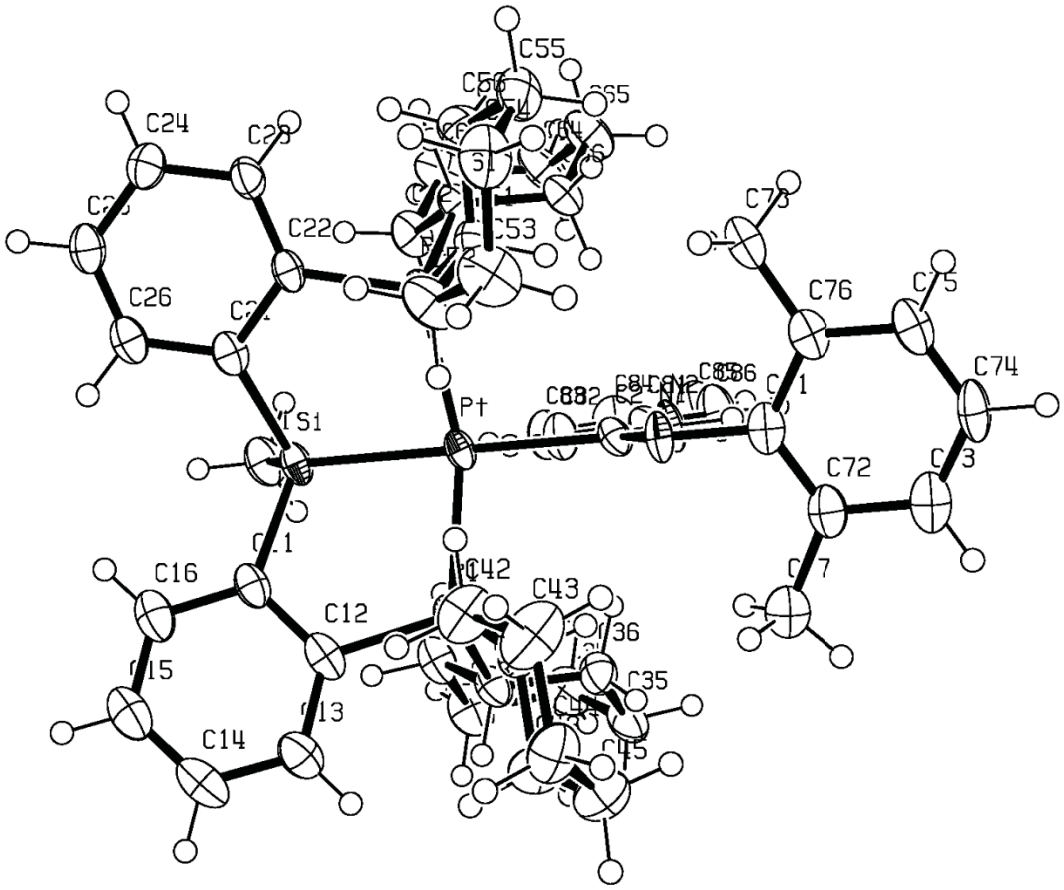

Figure A-12. ORTEP diagram [Cy-PSiP]Pt{C(=N(2,6,-$Me_2C_6H_3$))NHPh} (**6-4**).

Table A-13. Crystallographic experimental details for [Cy-PSiP]Pt(PHMes) (**6-9**·C_6H_6).

A. Crystal Data	
formula	$C_{46}H_{67}P_3PtSi$
formula weight	936.09
crystal dimensions (mm)	0.48 × 0.43 × 0.13
crystal system	orthorhombic
space group	*Pbca* (No. 61)
unit cell parameters[a]	
a (Å)	20.7804 (16)
b (Å)	17.4945 (13)
c (Å)	24.1880 (18)
V (Å^3)	8793.4 (11)
Z	8
ρ_{calcd} (g cm^{-3})	1.414
μ (mm^{-1})	3.358
B. Data Collection and Refinement Conditions	
diffractometer	Bruker D8/APEX II CCD[b]
radiation (λ [Å])	graphite-monochromated Mo Kα (0.71073)
temperature (°C)	–100
scan type	ω scans (0.3°) (20 s exposures)
data collection 2θ limit (deg)	55.08
total data collected	74528 (-26 ≤ *h* ≤ 26, -22 ≤ *k* ≤ 22, -31 ≤ *l* ≤ 31)
independent reflections	10123 (R_{int} = 0.0317)
number of observed reflections (*NO*)	8634 [$F_o^2 \geq 2\sigma(F_o^2)$]
structure solution method	direct methods (*SIR*97[c])
refinement method	full-matrix least-squares on F^2 (*SHELXL–97*[d])
absorption correction method	multi-scan (*SADABS*)
range of transmission factors	0.6770–0.2955
data/restraints/parameters	10123 [$F_o^2 \geq -3\sigma(F_o^2)$] / 0 / 464
goodness-of-fit (*S*)[e]	1.037 [$F_o^2 \geq -3\sigma(F_o^2)$]
final *R* indices[f]	
R_1 [$F_o^2 \geq 2\sigma(F_o^2)$]	0.0270
wR_2 [$F_o^2 \geq -3\sigma(F_o^2)$]	0.0665
largest difference peak and hole	2.925 and –1.610 e Å^{-3}

[a]Obtained from least-squares refinement of 9610 reflections with 4.54° < 2θ < 55.02°.

[b]Programs for diffractometer operation, data collection, data reduction and absorption correction were those supplied by Bruker.

[c]Altomare, A.; Burla, M. C.; Camalli, M.; Cascarano, G. L.; Giacovazzo, C.; Guagliardi, A.; Moliterni, A. G. G.; Polidori, G.; Spagna, R. *J. Appl. Cryst.* **1999**, *32*, 115–119.

[d]Sheldrick, G. M. *Acta Crystallogr.* **2008**, *A64*, 112–122.

[e]$S = [\Sigma w(F_o^2 - F_c^2)^2/(n-p)]^{1/2}$ (n = number of data; p = number of parameters varied; $w = [\sigma^2(F_o^2) + (0.0261P)^2 + 15.9773P]^{-1}$ where $P = [\text{Max}(F_o^2, 0) + 2F_c^2]/3$).

[f]$R_1 = \Sigma||F_o| - |F_c||/\Sigma|F_o|$; $wR_2 = [\Sigma w(F_o^2 - F_c^2)^2/\Sigma w(F_o^4)]^{1/2}$

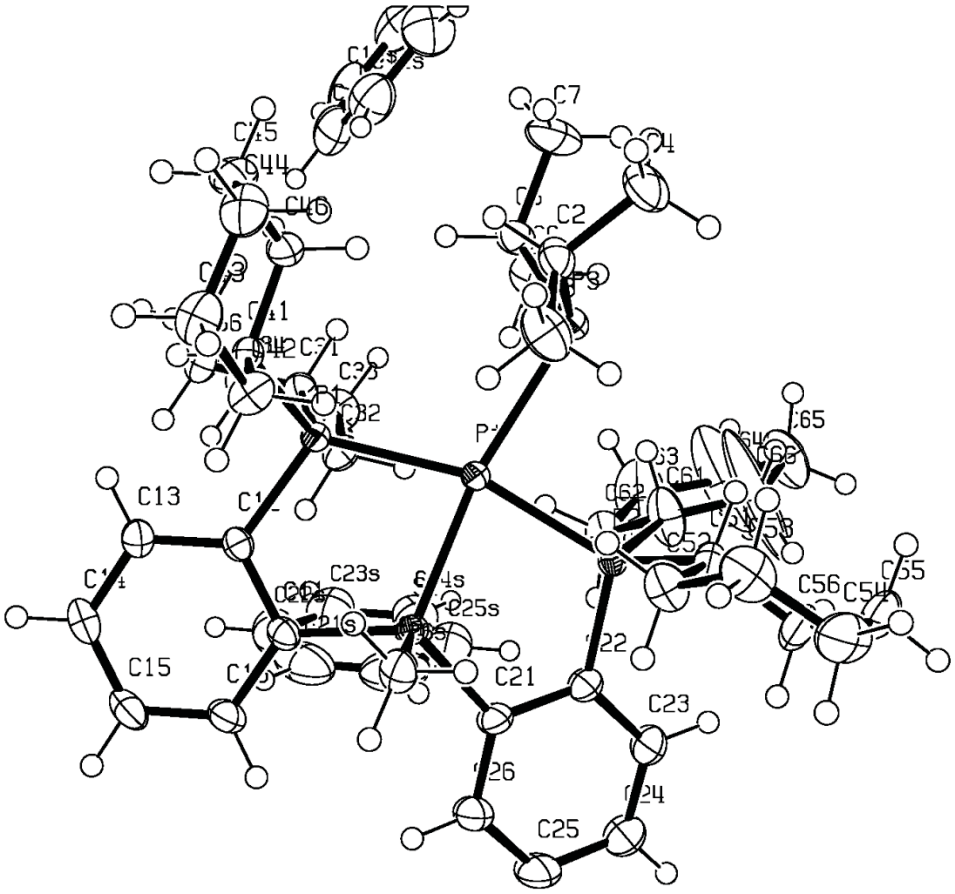

Figure A-13. ORTEP diagram for [Cy-PSiP]Pt(PHMes) (**6-9**·C_6H_6).

Table A-14. Crystallographic experimental details for [Cy-PSiP]Ni(PHMes) (**6-12**·OEt_2).

A. Crystal Data	
formula	$C_{50}H_{77}NiOP_3Si$
formula weight	873.83
crystal dimensions (mm)	0.47 × 0.29 × 0.04
crystal system	orthorhombic
space group	$P2_12_12_1$ (No. 19)
unit cell parameters[a]	
a (Å)	11.7120 (4)
b (Å)	17.6960 (5)
c (Å)	23.5657 (7)
V (Å^3)	4884.1 (3)
Z	4
ρ_{calcd} (g cm^{-3})	1.188
μ (mm^{-1})	0.554
B. Data Collection and Refinement Conditions	
diffractometer	Bruker D8/APEX II CCD[b]
radiation (λ [Å])	graphite-monochromated Mo Kα (0.71073)
temperature (°C)	–100
scan type	ω scans (0.3°) (20 s exposures)
data collection 2θ limit (deg)	55.18
total data collected	43747 ($-15 \le h \le 15$, $-23 \le k \le 23$, $-30 \le l \le 30$)
independent reflections	11258 (R_{int} = 0.0385)
number of observed reflections (*NO*)	10178 [$F_o^2 \ge 2\sigma(F_o^2)$]
structure solution method	Patterson/structure expansion (*DIRDIF–2008*[c])
refinement method	full-matrix least-squares on F^2 (*SHELXL–97*[d])
absorption correction method	Gaussian integration (face-indexed)
range of transmission factors	0.9803–0.7823
data/restraints/parameters	11258 / 0 / 512
Flack absolute structure parameter[e]	-0.008(6)
goodness-of-fit (S)[f] [all data]	1.033
final R indices[g]	
R_1 [$F_o^2 \ge 2\sigma(F_o^2)$]	0.0267
wR_2 [all data]	0.0627
largest difference peak and hole	0.266 and –0.177 e Å^{-3}

[a]Obtained from least-squares refinement of 5592 reflections with $4.52° < 2\theta < 33.50°$.

[b]Programs for diffractometer operation, data collection, data reduction and absorption correction were those supplied by Bruker.

[c]Beurskens, P. T.; Beurskens, G.; de Gelder, R.; Smits, J. M. M.; Garcia-Granda, S.;

Gould, R. O. (2008). The *DIRDIF-2008* program system. Crystallography Laboratory, Radboud University Nijmegen, The Netherlands.

[d]Sheldrick, G. M. *Acta Crystallogr.* **2008**, *A64*, 112–122.

[e]Flack, H. D. *Acta Crystallogr.* **1983**, *A39*, 876–881; Flack, H. D.; Bernardinelli, G. *Acta Crystallogr.* **1999**, *A55*, 908–915; Flack, H. D.; Bernardinelli, G. *J. Appl. Cryst.* **2000**, *33*, 1143–1148. The Flack parameter will refine to a value near zero if the structure is in the correct configuration and will refine to a value near one for the inverted configuration.

[f]$S = [\Sigma w(F_o^2 - F_c^2)^2/(n-p)]^{1/2}$ (n = number of data; p = number of parameters varied; $w = [\sigma^2(F_o^2) + (0.0305P)^2 + 0.3795P]^{-1}$ where $P = [\mathrm{Max}(F_o^2, 0) + 2F_c^2]/3$).

[g]$R_1 = \Sigma||F_o| - |F_c||/\Sigma|F_o|$; $wR_2 = [\Sigma w(F_o^2 - F_c^2)^2/\Sigma w(F_o^4)]^{1/2}$.

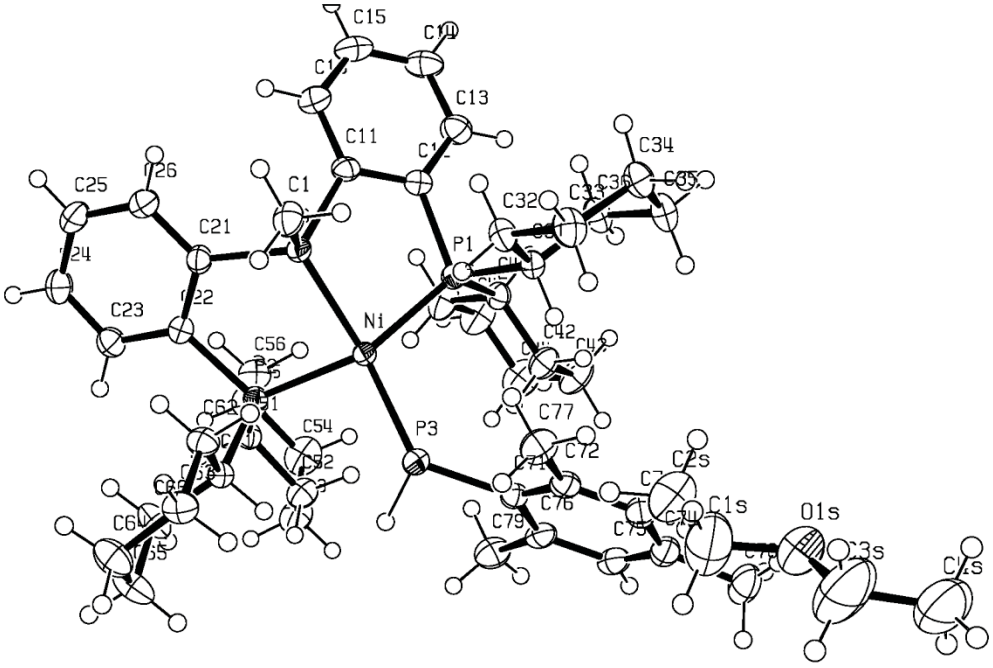

Figure A-14. ORTEP diagram for [Cy-PSiP]Ni(PHMes) (**6-12**·OEt_2).

Table A-15. Crystallographic experimental details for (^{t}Bu-PSiN-Me)Pd(OTf) (**7-4**·0.5C_6H_6).

A. Crystal Data	
formula	$C_{27}H_{38}F_3NO_3PPdSSi$
formula weight	679.10
crystal dimensions (mm)	0.45 × 0.36 × 0.20
crystal system	orthorhombic
space group	*Pbca* (No. 61)
unit cell parameters[a]	
a (Å)	14.8703 (4)
b (Å)	15.7929 (4)
c (Å)	26.5312 (7)
V (Å^3)	6230.7 (3)
Z	8
ρ_{calcd} (g cm^{-3})	1.448
μ (mm^{-1})	0.798
B. Data Collection and Refinement Conditions	
diffractometer	Bruker D8/APEX II CCD[b]
radiation (λ [Å])	graphite-monochromated Mo Kα (0.71073)
temperature (°C)	–100
scan type	ω scans (0.3°) (15 s exposures)
data collection 2θ limit (deg)	55.06
total data collected	52762 ($-19 \le h \le 19$, $-20 \le k \le 20$, $-34 \le l \le 34$)
independent reflections	7180 (R_{int} = 0.0241)
number of observed reflections (*NO*)	6450 [$F_o^2 \ge 2\sigma(F_o^2)$]
structure solution method	Patterson/structure expansion (*DIRDIF–2008*[c])
refinement method	full-matrix least-squares on F^2 (*SHELXL–97*[d])
absorption correction method	Gaussian integration (face-indexed)
range of transmission factors	0.8534–0.7132
data/restraints/parameters	7180 / 0 / 412
goodness-of-fit (*S*)[e] [all data]	1.056
final *R* indices[f]	
R_1 [$F_o^2 \ge 2\sigma(F_o^2)$]	0.0208
wR_2 [all data]	0.0556
largest difference peak and hole	0.447 and –0.321 e Å^{-3}

[a]Obtained from least-squares refinement of 9963 reflections with $4.86° < 2\theta < 53.50°$.

[b]Programs for diffractometer operation, data collection, data reduction and absorption correction were those supplied by Bruker.

[c]Beurskens, P. T.; Beurskens, G.; de Gelder, R.; Smits, J. M. M; Garcia-Granda, S.; Gould, R. O. (2008). The *DIRDIF-2008* program system. Crystallography

Laboratory, Radboud University Nijmegen, The Netherlands.

[d]Sheldrick, G. M. *Acta Crystallogr.* **2008**, *A64*, 112–122.

[e]$S = [\Sigma w(F_o^2 - F_c^2)^2/(n-p)]^{1/2}$ (n = number of data; p = number of parameters varied; $w = [\sigma^2(F_o^2) + (0.0257P)^2 + 3.1481P]^{-1}$ where $P = [\text{Max}(F_o^2, 0) + 2F_c^2]/3$).

[f]$R_1 = \Sigma||F_o| - |F_c||/\Sigma|F_o|$; $wR_2 = [\Sigma w(F_o^2 - F_c^2)^2/\Sigma w(F_o^4)]^{1/2}$.

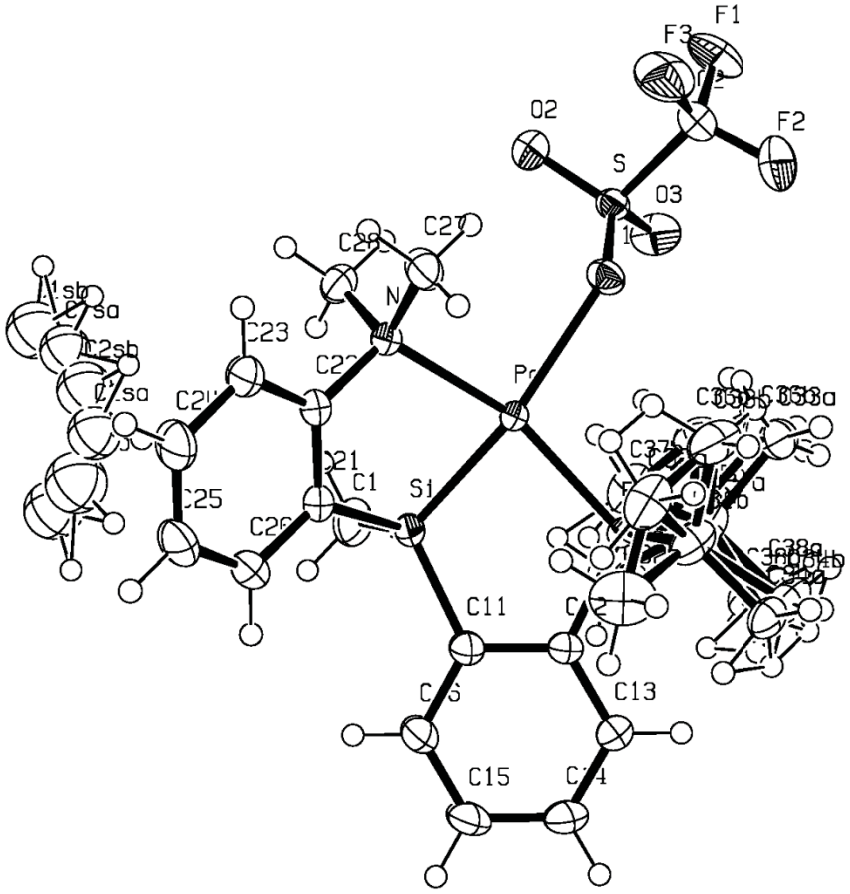

Figure A-15. ORTEP diagram for ([t]Bu-PSiN-Me)Pd(OTf)(**7-4**·0.5C_6H_6).

Table A-16. Crystallographic experimental details for (^{t}Bu-PSiN-Me)Pt(Cl)(PMe_3) (**7-7**)

A. Crystal Data	
formula	$C_{26}H_{44}ClNP_2PtSi$
formula weight	691.19
crystal dimensions (mm)	0.37 × 0.23 × 0.17
crystal system	orthorhombic
space group	*Pbca* (No. 61)
unit cell parameters[a]	
a (Å)	18.097 (3)
b (Å)	16.248 (2)
c (Å)	19.608 (3)
V (Å^3)	5765.4 (14)
Z	8
ρ_{calcd} (g cm^{-3})	1.593
μ (mm^{-1})	5.128
B. Data Collection and Refinement Conditions	
diffractometer	Bruker D8/APEX II CCD[b]
radiation (λ [Å])	graphite-monochromated Mo Kα (0.71073)
temperature (°C)	–100
scan type	ω scans (0.3°) (15 s exposures)
data collection 2θ limit (deg)	55.20
total data collected	48604 ($-23 \le h \le 23$, $-21 \le k \le 21$, $-25 \le l \le 25$)
independent reflections	6654 (R_{int} = 0.0359)
number of observed reflections (*NO*)	5930 [$F_o^2 \ge 2\sigma(F_o^2)$]
structure solution method	Patterson/structure expansion (*DIRDIF–2008*[c])
refinement method	full-matrix least-squares on F^2 (*SHELXL–97*[d])
absorption correction method	Gaussian integration (face-indexed)
range of transmission factors	0.4743–0.2555
data/restraints/parameters	6654 / 0 / 289
goodness-of-fit (*S*)[e] [all data]	1.116
final *R* indices[f]	
R_1 [$F_o^2 \ge 2\sigma(F_o^2)$]	0.0241
wR_2 [all data]	0.0543
largest difference peak and hole	1.049 and –1.263 e Å^{-3}

[a]Obtained from least-squares refinement of 9042 reflections with $4.50° < 2\theta < 48.00°$.

[b]Programs for diffractometer operation, data collection, data reduction and absorption correction were those supplied by Bruker.

[c]Beurskens, P. T.; Beurskens, G.; de Gelder, R.; Smits, J. M. M; Garcia-Granda, S.; Gould, R. O. (2008). The *DIRDIF-2008* program system. Crystallography

Laboratory, Radboud University Nijmegen, The Netherlands.

[d]Sheldrick, G. M. *Acta Crystallogr.* **2008**, *A64*, 112–122.

[e]$S = [\Sigma w(F_o^2 - F_c^2)^2/(n-p)]^{1/2}$ (n = number of data; p = number of parameters varied; $w = [\sigma^2(F_o^2) + (0.0164P)^2 + 11.5037P]^{-1}$ where $P = [\text{Max}(F_o^2, 0) + 2F_c^2]/3$).

[f]$R_1 = \Sigma||F_o| - |F_c||/\Sigma|F_o|$; $wR_2 = [\Sigma w(F_o^2 - F_c^2)^2/\Sigma w(F_o^4)]^{1/2}$.

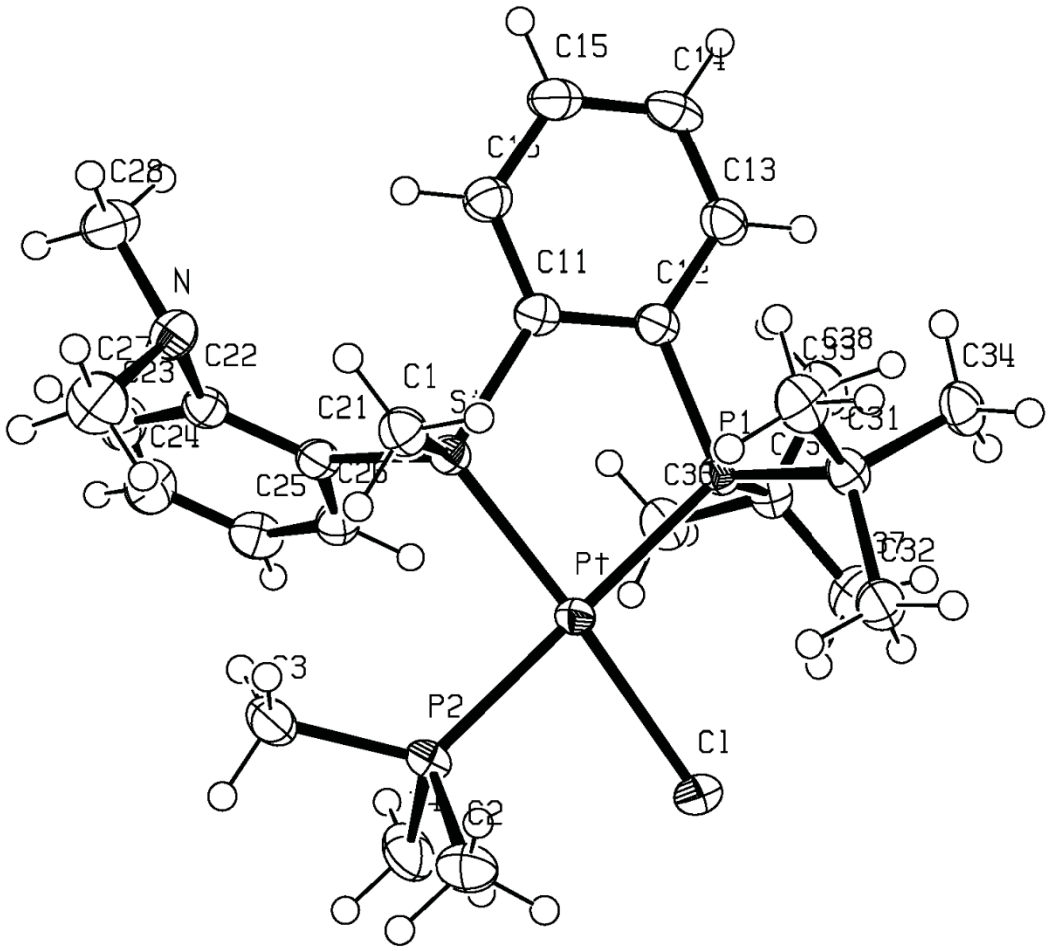

Figure A-16. ORTEP diagram for (^{t}Bu-PSiN-Me)Pt(Cl)(PMe$_3$) (**7-7**).